

Separation and Recovery of Phosphorus from Steelmaking Slag with High P₂O₅ Content by Leaching

著者	DU CHUANMING
学位授与機関	Tohoku University
学位授与番号	11301甲第18118号
URL	http://hdl.handle.net/10097/00125236

Ph.D Dissertation

**Separation and Recovery of Phosphorus from
Steelmaking Slag with High P₂O₅ Content by Leaching**

高 P₂O₅ 含有製鋼スラグからの浸出によるリンの分離
回収

Chuan-ming Du

杜 传明

Department of Metallurgy

Graduate School of Engineering

Tohoku University

2018

Contents

1	Introduction	1
1.1	Phosphorus resources and high-P iron ores	1
1.2	Hot metal dephosphorization	5
1.3	P recovery from steelmaking slag	10
1.4	Selective leaching of P-condensed solid solution from slag.....	14
1.5	Purposes and contents of the present study.....	19
	References	23
2	Dissolution behavior of P from the C₂S-C₃P solid solution with high P₂O₅ content	27
2.1	Experimental method	27
2.1.1	Synthesis of solid solution and Na ₂ O modification.....	27
2.1.2	Leaching experiment	29
2.2	Experimental results	30
2.2.1	Effect of leaching agent on the dissolution of C ₂ S-C ₃ P solid solution.....	31
2.2.2	Modification of C ₂ S-C ₃ P by Na ₂ SiO ₃	34
2.2.3	Dissolution behavior of the modified solid solution	38
2.2.4	Dissolution behavior of the modified solid solution at various pH	43
2.3	Discussion.....	47
2.3.1	Effect of acid (leaching agent)	47
2.3.2	Effect of Na ₂ SiO ₃ modification.....	51
2.3.3	Effect of pH.....	54
2.4	Summary	56

References	58
3 Dissolution behavior of P from modified steelmaking slag with Na₂O addition	59
3.1 Experimental method	60
3.1.1 Synthesis of slags	60
3.1.2 Leaching of slags	61
3.1.3 Chemical analysis of slag and residue.....	62
3.2 Results and discussion.....	63
3.2.1 Effect of the cooling rate on the dissolution behavior of slag.....	63
3.2.2 Effect of Na ₂ O content on the dissolution behavior of slag	76
3.2.3 Effect of pH on the dissolution behavior of the modified slag	90
3.2.4 Effect of the valency of Fe on the dissolution behavior of slag	99
3.3 Summary.....	111
References	113
4 Dissolution behavior of P from modified steelmaking slag with K₂O addition.....	115
4.1 Experimental method	115
4.2 Experimental results	116
4.2.1 Mineralogical composition of slags	116
4.2.2 Dissolution behavior of slags at different pH conditions	121
4.2.3 Residue composition	130
4.3 Discussion on K₂O addition.....	134
4.4 Summary.....	141
References	143

5	Distribution of P_2O_5 and Na_2O between the solid solution and liquid phase in slag with high P_2O_5 content	144
5.1	Experimental method	144
5.2	Experimental results	146
5.2.1	Effect of P_2O_5 and Na_2O contents	148
5.2.2	Effect of Fe_2O_3 content	154
5.2.3	Effect of slag basicity (CaO/SiO_2)	158
5.3	Discussion	160
5.3.1	Na_2O in the solid solution	160
5.3.2	Activity coefficient of P_2O_5	163
5.4	Summary	167
	References	169
6	P recovery from the leachate by precipitation	170
6.1	Experimental method	170
6.2	Experimental results and discussion	172
6.2.1	Effect of alkaline solution on P precipitation	172
6.2.2	Effect of pH on P precipitation	180
6.3	Overall process outline	186
6.4	Summary	188
	References	190
7	Conclusions and future works	191
7.1	Conclusions	191
7.1.1	Conclusions of the dissolution of solid solution	191
7.1.2	Conclusions of the dissolution of slag with high P_2O_5 content	192

7.1.3	Conclusions of the distribution of P_2O_5 and Na_2O	193
7.1.4	Conclusions of P recovery from the leachate	194
7.2	Future works	195
Achievements	198
Acknowledgement	202

1 Introduction

1.1 Phosphorus resources and high-P iron ores

Because phosphorus (P) is essential for the growth of animals and plants, it is considered an important element, playing a great role in the agricultural and industrial development. P, together with nitrogen and potassium, are the three major elements present in fertilizers. P supply is a major constraint on the quantity and quality of food production. The main raw material for industrial phosphorus is phosphate rock. Approximately 242 million tons of phosphate ores was mined in the world during 2015. China (120 million tons), Morocco (29.0 million tons), and the United States (27.4 million tons) are the leading producing countries, accounting for 73% of the world total production [1]. However, in Japan, there are no deposits of phosphate ore, and all phosphate ore is imported. Figure 1.1 shows the amounts of P resources imported into Japan, mainly in the form of phosphate rock, fertilizers, and concentrated superphosphate [2].

Phosphate fertilizer is generally produced from phosphate rock, in which the main mineral is fluorapatite ($\text{Ca}_{10}(\text{PO}_4)_6\text{F}_2$). In this form, P is not readily available for plants and requires further industrial processing to make it accessible for them. The processes used for this transformation include: the thermal route and the wet route. In the thermal route, fluorapatite's crystalline structure is modified by a thermal action, producing a soluble phosphate compound known as fused magnesium phosphate. In the wet route, the phosphate rock is digested by sulfuric acid yielding single superphosphate or phosphoric acid as main products, an intermediate used for the manufacturing of triple superphosphate and ammonium phosphates [3].

With the increase in world population, the demand for food and biofuel has been increasing. As a result, a large amount of phosphate fertilizer is needed to increase the growth and production

of crop and sugarcane. However, the phosphate rock is a non-renewable resource and current global reserves may be depleted in 50-100 years [4]. The fertilizer industry recognizes that the quality of reserves is declining and the cost of extraction and processing is increasing [5]. Consequently, the price of phosphate ores and phosphate fertilizer has been increasing, as shown in Fig. 1.1. With the depletion of high-grade phosphate ore, utilization of low-grade phosphate ores is gaining considerable attention; however, some heavy and radioactive metals exist in the low-grade phosphate ores [6]. There are currently no commercial measures of removing these pollutants completely during fertilizer manufacturing process. To secure a sustainable supply of phosphate, it is urgent to find and develop an alternative source of P. Therefore, recycling of P from waste materials by chemical or thermal processes is becoming increasingly important. A lot of efforts have been made to evaluate the effectiveness of recycled P products from sewage sludge and animal wastes as phosphate fertilizer [7].

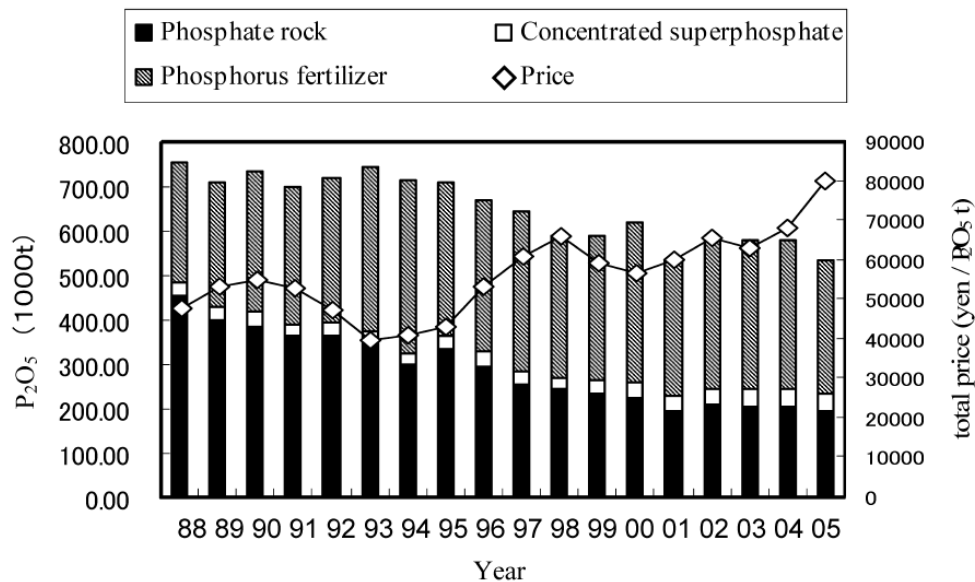






Fig. 1.1 Trends in the amounts and the prices of P resources imported into Japan

Iron ores are essential raw materials for the production of iron and steel, and they contain some P. In contrast to its nature as a strategic resource, described above, P is one of the most detrimental impurities in steels as it reduces the low-temperature toughness of steel products. Most of the P that contained in iron ore or hot metal should be removed during ironmaking and steelmaking process. Therefore, it is desirable to have a low P level in iron ore. Market specifications for P in iron ore exported from Australia are around 0.075 mass% P [8]. Over the past decade, the crude steel production in the world increased significantly, reaching 1.6 billion tones in 2016 [9]. In particular, China is the largest producer of steel product, which accounts for nearly half of the whole world production. Such huge steel production consumed a large amount of high-grade iron ore that mainly imported from Australia and Brazil. With the gradual decrease of the reserves of high-grade iron ore around the world, the price of high-grade iron ores consistently increases, and its supply has become the bottleneck to restrict the development of iron and steel industry.

To solve the crisis of resources, utilization of the low-grade iron ore is in an urgent need, such as high-P iron ore. High-P iron ore is a typical complex resource, which contains a high content of iron, but it is hard to be used due to the presence of a large amount of P [10]. Table 1.1 shows high-P and low-P deposits in Brockman mine in Brazil; low-grade and high-P layer contiguous with high-grade and low-P layer [11]. As the high-grade layer has already mined, the mining of low-grade layer has started from 2000. The reserves of high-P iron ore are large all over the world. For instance, more than 80% of Western Australian iron ores contains an average of 0.15 mass% P [8]; China has a large deposit of high-P iron ore with existing reserves of 10 billion tones which is unexploited in any large scale [12]. Therefore, exploring an efficient way of dephosphorization to fully utilize high-P iron ore could be a possible way to alleviate the shortage of high-grade iron ore. From another perspective, the P separated from iron and steel

industry is considered as a great potential P source because of the huge reserves and consumption of high-P iron ore [13]. Overall, the utilization of high-P iron ore would have a significant effect on the sustainable development of iron and steel industry and phosphate industry.

Table 1.1 High-P and low-P deposits in Brockman mine

		Brockman mine	
		Low P deposit	High P deposit
Composition (mass%)	Fe	63-64	56-62
	P	<0.07	>0.10
	Al ₂ O ₃	2.0-2.2	2.0-2.2
	Bonding water	2.0-3.0	5.0-7.0
Production (Year)	1965-2000		
	2000-2040		

Although methods for removing P from molten iron exist, a number of factors such as financial penalties and market access make it attractive to ensure that P is removed from the iron ore prior to its use in smelting [14]. Considerable attention has been focused on developing methods for the dephosphorization of high-P iron ore. Two different approaches are generally used for decreasing the P content of iron ore. The first approach is suitable if the iron ore is used as pellets. In this route, the ore is extensively ground until the P bearing mineral (apatite) is completely liberated from the iron minerals. The separation is then carried out using physical methods, such as magnetic separation and flotation [15, 16]. The second approach is a wet chemical method and is suitable for the treatment of iron ore sinters. In this treatment, iron ore is leached with a suitable solution (mineral acid) for removal of the P by the dissolution of apatite [17-19].

Recently, some other approaches were proposed to remove P with respect to various kinds of high-P iron ore. Fisher-White *et al.* [14] studied the effects of a heat treatment with sodium hydroxide followed by leaching with water and a caustic leach on the removal of P from goethitic iron ores. Guo *et al.* [20] proposed a process with acid leaching followed by hydrogen-based fluidized reduction and melt separation to recover DRI (direct reduced iron) from high-P oolitic hematite. Matinde and Hino [21, 22] investigated the possibility of dephosphorization by using pre-reduction and screening methods combined with mechanical crushing or air jet milling. However, due to the large amount of iron ores, enormous processing capacity is required and the treatment cost was considered to be huge.

1.2 Hot metal dephosphorization

During ironmaking process, the P was reduced and concentrated in hot metal. In the case of utilization of high-P iron ore, hot metal with high P content will be generated. In India, iron ore containing 0.1% or more P has already been mined and used, and the P content in hot metal has been 0.25% or more [23]. To meet the demand for low P steel and to ease the environmental burden, a highly efficient dephosphorization process with less slag is necessary to remove P from hot metal as much as possible. Hot metal dephosphorization is well developed in Japan [24]. Since the 1990 s, most of the companies in Japan have improved and restructured the hot metal treatment facilities, aiming at not only improvement of refining efficiency so as to achieve a higher degree of purity steel with higher productivity at lower cost, but also reduction in slag volume with the environmental problems taken into consideration [25]. Figure 1.2 shows a method of hot metal pretreatment using converters developed by Nippon Steel Corporation [26]: the multi-refining converter process, whereby hot metal is dephosphorized and decarburized sequentially in the same converter vessel with de-slagging in between. The advantages of this

process, besides those of the converter-type pretreatment, are that the loss of time and heat due to vessel change is avoided, and that decarburization slag can be left in the vessel and used for the following charge, which lowers lime consumption.

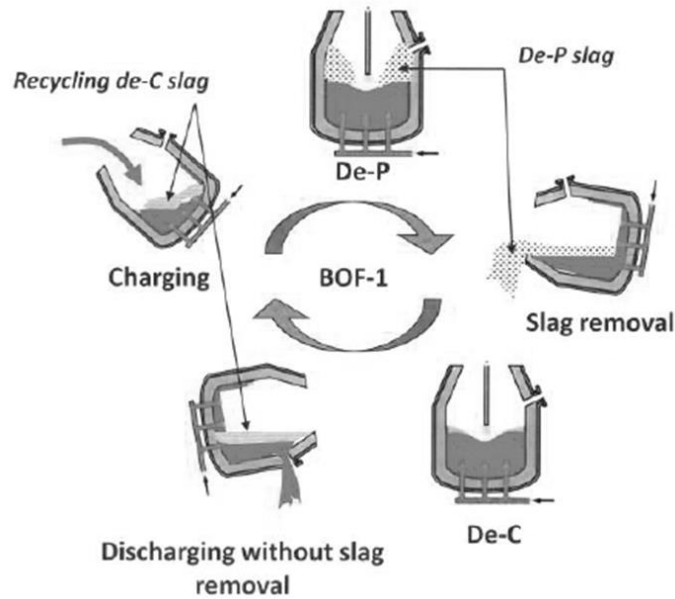
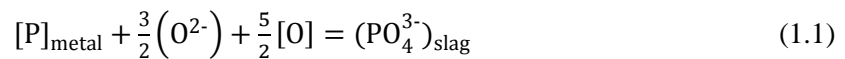


Fig. 1.2 Hot metal dephosphorization process (multi-refining converter)



In the hot metal dephosphorization reaction, as described in Eq. (1.1), the P in hot metal is oxidized to P_2O_5 , which is then transferred into slag and reacts with CaO to form tricalcium phosphate ($3CaO \cdot P_2O_5$, C_3P). To improve the efficiency of dephosphorization, the distribution ratio of P between different slag systems and hot metal have been investigated by many researchers. Suito *et al.* [27] studied the P distribution between liquid iron and the CaO-SiO₂-Fe_tO slag equilibrated in a magnesia crucible in the temperature range 1823 K to 1923 K. The P distribution ratio $(P_2O_5)_{\text{slag}}/[P]_{\text{metal}}$ increased with increasing CaO content and decreasing temperature. The maximum value of the distribution ratio was found to be present near the slag composition saturated with the tricalcium silicate and magnesio wustite phases. Im

et al. [28] assessed the possibility of hot metal dephosphorization by CaO-SiO₂-Fe_tO slags of low CaO content. They found that P distribution ratio strongly depended on CaO content but not so much on Fe_tO content of the slag. It increased with an increase in CaO content when Fe_tO content was kept constant, while it slightly decreased when total Fe content was increased at the (%CaO)/(%SiO₂) ratio of around unity. Muraki *et al.* [29] measured the P partition ratio for the CaO-Na₂O-SiO₂-CaF₂ slag doubly saturated with CaO and 3CaO·SiO₂ at 1573 K. They found that the distribution ratio of P between slag and C-saturated iron increased significantly with a small Na₂O addition. Pak *et al.* [30] reported that Na₂O addition to CaO-SiO₂ slags significantly increased the P distribution ratio and phosphate capacity. In steelmaking slag containing 40 mass% of Fe_tO, the addition of 6 mass% Na₂O increased the P distribution ratio by a factor of 5. Kunisada *et al.* [31] investigated the dephosphorization of liquid iron by CaO-FeO-SiO₂ slag and that containing Na₂O. The effect of Na₂O on P distribution was evaluated as a CaO-equivalence, and the following Eq. (1.2) was obtained.

$$\log \left\{ \frac{(\%P)_{\text{slag}}}{(\%P)_{\text{metal}}} \right\} = 0.071\{(\%CaO)+0.1(\%MgO)+[1.5(\%Na_2O)+4.4]\}+2.5\log(\%T.Fe)+\frac{8260}{T}-8.56 \quad (1.2)$$

In the hot metal dephosphorization with multi-phase slag, the slag is normally consisted in the CaO-SiO₂-Fe_tO-P₂O₅-MgO system, and the industrial operation is mainly carried out in the dicalcium silicate (2CaO·SiO₂, C₂S) saturated region. It is well known that 2CaO·SiO₂ forms a solid solution with the dephosphorization product (3CaO·P₂O₅) at the treatment temperature over a wide composition range [32, 33]. Consequently, a 2CaO·SiO₂-3CaO·P₂O₅ solid solution (C₂S-C₃P) forms and it coexists with the liquid slag in the dephosphorization process. This implies that the product of the dephosphorization reaction can be dissolved into the solid phase in slag. Inoue *et al.* [34] studied the P transfer behavior from P₂O₅-containing CaO-SiO₂-Fe_tO slag to 2CaO·SiO₂ particles homogeneously dispersed in slag. The transfer rate of P from slag to

a $2\text{CaO}\cdot\text{SiO}_2$ particle was considerably fast and a $2\text{CaO}\cdot\text{SiO}_2$ particle changed to the particle with the composition of $2\text{CaO}\cdot\text{SiO}_2\text{-}3\text{CaO}\cdot\text{P}_2\text{O}_5$ solid solution within 5 s. Hamano *et al.* [35] and Yang *et al.* [36, 37] systematically investigated the formation reaction of phosphate compound in multi-phase flux and the mass transfer processes between CaO or $2\text{CaO}\cdot\text{SiO}_2$ particles and molten slag. Measurements of the equilibrium distribution ratio of P_2O_5 between the solid solution and liquid phase revealed that P_2O_5 is concentrated in the solid solution with a high distribution ratio [38]. On the basis of these results, the solid solution plays an important role in efficient dephosphorization-by acting as a sink for phosphorus and lowering the phosphorus content in the liquid phase-as pointed out by Kitamura *et al.* [39].

In order to increase the efficiency of dephosphorization and to use the P-condensed $\text{C}_2\text{S}\text{-}\text{C}_3\text{P}$ solid solution as an alternative source of phosphate ores, many researches have been conducted to investigate the distribution ratio of P_2O_5 between the solid solution and liquid phase. Ito *et al.* [38] determined the equilibrium distribution ratio of P_2O_5 ($L_{\text{P}_2\text{O}_5}$) between solid $2\text{CaO}\cdot\text{SiO}_2$ and molten $\text{CaO}\text{-}\text{SiO}_2\text{-}\text{Fe}_2\text{O}_3$ and $\text{CaO}\text{-}\text{SiO}_2\text{-}\text{FeO}$ slags. It was found that $L_{\text{P}_2\text{O}_5}$ increased with increasing total Fe content, regardless of the valency of Fe. No dependence of $L_{\text{P}_2\text{O}_5}$ on temperature and $(\% \text{CaO})/(\% \text{SiO}_2)$ ratio in slags was observed.

Pahlevani *et al.* [40] investigated the influences of MgO, MnO, and Al_2O_3 on the distribution of P_2O_5 between $\text{C}_2\text{S}\text{-}\text{C}_3\text{P}$ solid solution and liquid phase in the case of FeO or Fe_2O_3 as the iron oxide. They found that the distribution ratio of P_2O_5 decreased with the addition of MgO and MnO, but it did not change with the addition of Al_2O_3 . They also reported that the CaO content in the liquid phase and the activity coefficient of P_2O_5 in the solid solution are the ruling factors on distribution ratio of P_2O_5 .

Lin *et al.* [41, 42] systematically studied the effects of Na_2O and SiO_2 modification on P_2O_5 enrichment and existence form in steelmaking slag. Their results showed that the melting point

of slag decreased obviously with the increasing of Na₂O content in slag, and high-P₂O₅ solid solution (Ca₂SiO₄-Ca₃(PO₄)₂ and Na₂Ca₄(PO₄)₂SiO₄) are generated. Ca₂SiO₄ in the solid solution reduced with increasing SiO₂; hence, the P₂O₅ content in the solid solution increased. If the addition of SiO₂ was excessive, the amount of Ca₂SiO₄ precipitation in the slag decreased remarkably (and even disappeared), and the generation of C₂S-C₃P solid solution reduced, which was not favorable for P₂O₅ enrichment.

Xie *et al.* [43] investigated the effects of Na₂O and B₂O₃ on the distribution ratio of P₂O₅ and morphologies of corresponding solid solutions in CaO-SiO₂-Fe₂O₃-P₂O₅ slag system. It was found that the distribution ratio of P₂O₅ would be improved with the increase of Na₂O content due to the formation of Na₂O-containing solid solution with a similar morphology as that of C₂S-C₃P solid solution. However, B₂O₃ played an opposite role, and it would reduce the P₂O₅ distribution ratio.

Jiang *et al.* [44] investigated the effect of Al₂O₃ modification on the P₂O₅ enrichment behavior in dephosphorization slag. The results showed that P₂O₅ was mainly existed in C₂S-C₃P solid solution and Al₂O₃ modification was beneficial to the P₂O₅ enrichment. Al₂O₃ could react with the initially precipitated solid solution with low P₂O₅ content and decomposed to high-P₂O₅ containing C₂S-C₃P solid solution and Ca₂Al₂SiO₇.

With the deterioration of iron ore quality caused by the increased utilization of high-P iron ores, the P content in hot metal is gradually increasing. Kitamura *et al.* [45] studied the dephosphorization treatment of hot metal with high P content on the basis of a simulation model developed by the ISIJ research group-“Process Simulation for Dephosphorization of Pig Iron by Multi-Phases”. It showed that when the P content in steel decreased to 0.015% from 0.3% by hot metal pretreatment process, P₂O₅ content in slag increased to about 12 mass%. These results indicated the high potential of the hot metal dephosphorization process for the treatment of hot

metal with high P content. Through efficient dephosphorization, most of the P in hot metal was eliminated and concentrated in slag, and a slag with high P_2O_5 content will generate.

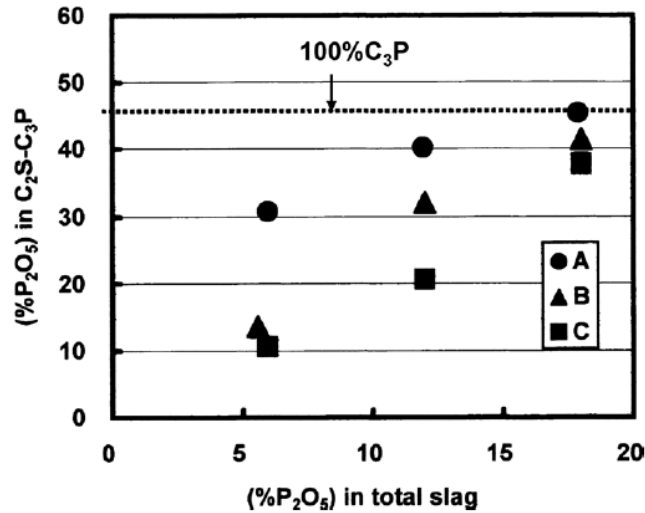


Fig. 1.3 Influence of slag composition on P_2O_5 content in the C_2S-C_3P solid solution

Figure 1.3 shows the relationship between the P_2O_5 content in slag and in the solid solution [46]. It shows that the P_2O_5 content in the solid solution increased with the P_2O_5 content in slag. When the P_2O_5 content in slag reached 18 mass%, the precipitated solid solution was found be nearly pure $3CaO \cdot P_2O_5$. Therefore, in the case of slag with high P_2O_5 content, P_2O_5 was still concentrated in the solid solution, and a solid solution with high P_2O_5 content will precipitate.

1.3 P recovery from steelmaking slag

The recycling of industrial by-product has attracted widespread attention because of resource exhaustion and environment protection. Steelmaking slag, including dephosphorization slag, is produced in an enormous quantity annually. Although steelmaking slag contains many valuable components, such as Fe_2O_3 , MnO , and P_2O_5 , it mainly used as roadbed and civil engineering materials [47]; the value of some useful elements in slag has not been exploited well. One of the

desired methods is to recycle the steelmaking slag inside ironmaking and steelmaking process, and to recover some valuable elements. However, the existence of P_2O_5 restricts the recycling of slag, because it will result in a high P content in hot metal and increase dephosphorization burden. Therefore, the key point of the effective utilization of steelmaking slag depends on how to separate and remove P_2O_5 from slag efficiently. Because the supply of phosphate ore is currently becoming very tight, and Japan has no domestic P resources, the P separated from steelmaking slag, especially slag with high P_2O_5 content, was considered to be a potential phosphate source to produce phosphate fertilizer [48].

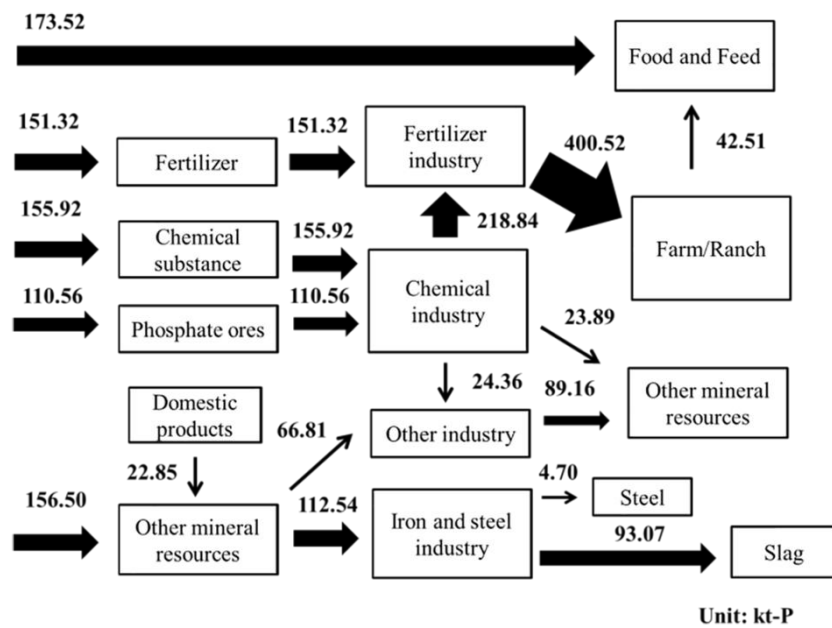


Fig. 1.4 Domestic material flows of P in Japan (kt-P)

Based on the statistical data for the material flow of P in Japan [48], as shown in Fig. 1.4, the P quantity in steelmaking slag is almost equal to that in imported phosphate ore. It means that the efficient recovery of P from steelmaking slag not only maintains a sustainable supply of P, but also lowers production costs of steelmaking and save resources. Therefore, it is urgent to develop an effective method to recover P from steelmaking slag. On the basis of the difference

in properties between the P_2O_5 or the P-condensed solid solution and other components, a great deal of efforts has been made to separate and recover P from slag by physical or chemical separation.

Ono *et al.* [49] proposed removal of P from steelmaking slag by floating of the P-concentrated dicalcium silicate during solidification. Dicalcium silicate is crystallized primarily and floats up owing to the difference of density between dicalcium silicate and residual liquid. As a result of slow cooling, CaO , SiO_2 , and P_2O_5 were enriched in the top layer; Fe_2O and MnO were concentrated in the bottom layer. Dicalcium silicate was found to be apt to separate more efficiently with higher total Fe content in slag, and at higher start temperature of cooling.

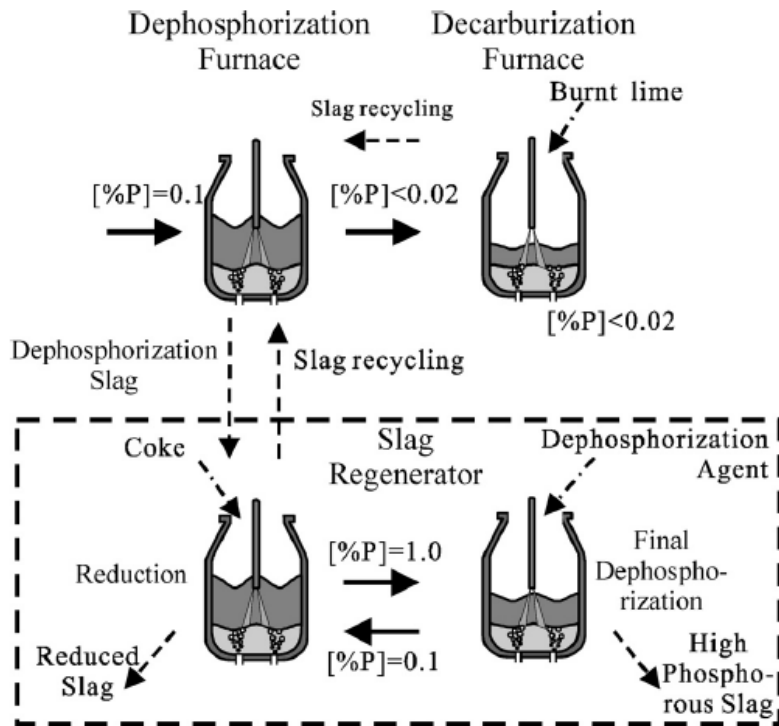


Fig. 1.5 Outline of the slag regeneration process

A waste-free steelmaking process, in which slags are recycled inside the steelmaking process itself by using a so-called slag regenerator, has been proposed by Li and Suito [50], and its

possibility was investigated by means of computer simulations. Ishikawa [51] studied the reduction behavior of dephosphorization slag on the iron bath in the reduction furnace of the slag regeneration process by test converter experiments. Figure 1.5 illustrates the slag regeneration process. Hot metal dephosphorization slag is charged to the slag regenerator to be reduced with carbon from coke and with hot metal. P_2O_5 , MnO and FeO in the dephosphorization slag are recovered in the hot metal. The reduced dephosphorization slag can be used for high grade applications or be used as a recycled slag in a dephosphorization furnace. The hot metal in the slag regenerator can be used several times repeatedly as P and Mn contents in the metal bath gradually increased by the reduction of the dephosphorization slag.

Yokoyama *et al.* [52] and Kubo *et al.* [53] studied the separation of the P-condensed solid solution from steelmaking slag with the aid of a strong magnetic field. P exists mainly in the form of C_2S-C_3P solid solution rather than the FeO -rich liquid phase in slag and exhibits remarkable segregation in the solidified slag. Through measurements of magnetic properties of these phases, different behaviors in a magnetic field have been found. By their experiment, about 65% of the P enriched phase can be recovered with less than 10% of FeO matrix phase contamination. To further promote the magnetic separation of the P-condensed phase from dephosphorization slag, Diao *et al.* [54] and Lin *et al.* [55] investigated the effect of slag modification on the P recovery ratio. It was found that the addition of SiO_2 , Al_2O_3 and TiO_2 had a positive influence on the P recovery ratio. However, the P recovery ratio and the concentration of P_2O_5 in unmagnetized slag showed a reciprocal relationship with increasing SiO_2 and Al_2O_3 content. The P recovery ratio was little affected by the addition of FeO and MnO.

Miki *et al.* [56] studied the recoverability of FeO and P from steelmaking slag using a novel mechanical approach involving capillary action. To improve the efficiency of the separation of the solid $2CaO \cdot SiO_2$ phase and the FeO -rich liquid phase in steelmaking slag, capillary action

was used to facilitate penetration into sintered CaO. Once the liquid phase had penetrated the CaO sinter, it was found that the solid $2\text{CaO}\cdot\text{SiO}_2$ phase and the FeO-rich phase could be effectively separated. It was possible to recover 87% of the P_2O_5 and 90% of the FeO from steelmaking slag.

Morita *et al.* [57] investigated the carbothermal reduction behavior of steelmaking slag in microwave irradiation. The slags were mixed with graphite powder and heated to 1873 K to precipitate a lump of Fe-C alloy. An increase in the SiO_2 content of slag led to a considerable improvement in the reduction for both Fe and P because of the improvement in the fluidity of the slags and an increase in the activity coefficient of P_2O_5 in the slags. The extraction behavior of P from Fe-P- C_{satd} alloy was also investigated at 1473 K by Na_2CO_3 treatment. The P_2O_5 in the fluxes could be concentrated to more than 9 mass% showing that it could be used as a P resource.

Li *et al.* [58] studied the enrichment of P-concentrating phase from CaO- SiO_2 -FeO-MgO- P_2O_5 melt with super gravity. The results show that there was an obvious stratification appearing in the sample after centrifugal enrichment. The upper part of the sample was loose and porous, while the lower part was smooth and compact. It was found that the P-concentrating phase gathered in the upper part, while it was hard to find any P-concentrating phase in the lower part of the sample. In this case, the recovery ratio of P_2O_5 in the concentrate reached 72.6%.

These methods were possible to separate P_2O_5 or $\text{C}_2\text{S}\text{-C}_3\text{P}$ solid solution from steelmaking slag. However, these trials on P recovery had not been successfully applied to steelmaking industry.

1.4 Selective leaching of P-condensed solid solution from slag

Compared with the above methods, leaching has an advantage in recovering P from steelmaking slag, because it is effective, energy-saving, and easily controlled [59]. Some attempts have been

made to dissolve dephosphorization slag to form aqueous phosphate, which can be used as a raw material for various phosphate-containing compounds. Sugiyama *et al.* [60] investigated the elution of aqueous phosphate from dephosphorization slag using nitric acid (HNO_3). It was found that 82% of the dephosphorization slag could be dissolved, but all components contained in the slag were unselectively dissolved. To remove the Fe-species in the aqueous solution, which has been referred to as the “slag solution”, calcium hydroxyapatite was added, and then a P-concentrating and Fe-free solution was obtained.

The solubility of slag in 2% citric acid is an important index to evaluate the applicability of dephosphorization slag to phosphate fertilizer. Diao *et al.* [61] studied the effect of slag composition on P_2O_5 solubility of dephosphorization slag in the citric solution. It was shown that more than 80% of P_2O_5 was dissolved. The P_2O_5 solubility increased with the increase of $(\% \text{CaO})/(\% \text{SiO}_2)$ ratio, and decreased with the increase of both Fe_2O_3 and P_2O_5 content. Lin *et al.* [62] found the addition of CaF_2 into dephosphorization slag deteriorated the P_2O_5 solubility of slag in the citric solution because of the formation of fluorapatite ($\text{Ca}_5(\text{PO}_4)_2\text{F}$). The P_2O_5 solubility could increase to 96% when Na_2CO_3 was added during slag synthesis, which resulted from the formation of $\text{Na}_2\text{Ca}_4(\text{PO}_4)_2\text{SiO}_4$ and Na_3PO_4 . However, dissolution behaviors of other elements, especially Fe, from the slag were not investigated in their studies.

The majority of the P_2O_5 in dephosphorization slag was concentrated in the C_2S - C_3P solid solution. If the solid solution was selectively dissolved in the aqueous solution, the soluble P in the leachate would be a suitable raw material for phosphate fertilizer production because it is similar with that in the production of phosphate fertilizer in a wet process [63]; the remaining P-poor mineralogical phase (Fe-rich phase) could be recycled for further use in the steelmaking process.

Previously, a series of etch tests have demonstrated that dicalcium silicates can be selectively removed from iron ore sinter using weak acids [64]. On the basis of different solubility between the solid solution and other phases in aqueous solutions, Kitamura *et al.* [65] proposed selective leaching of the P-concentrated solid solution from steelmaking slag. It was shown that at a constant pH, the solubility of elements from the matrix phase, in the HNO₃ solution, was lower than that from the solid solution. It was possible to dissolve a solid solution containing P without dissolving the matrix phase [65]. Figure 1.6 shows the surface of steelmaking slag after leaching [66]. Many holes were observed on the slag surface. The composition of the plateau area was almost the same as the matrix phase before leaching. There were no solid solution particles. This result confirmed that the solid solution in steelmaking slag was selectively dissolved.

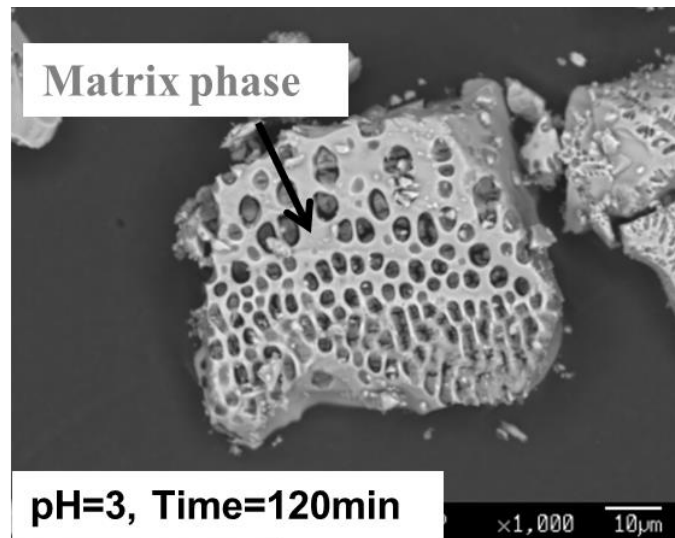


Fig. 1.6 Surface of steelmaking slag (quenched) after leaching in the nitric solution at pH 3

Some studies on selective leaching of P have been conducted in our laboratory. Teratoko *et al.* [65] investigated the dissolution behavior of a solid solution with various compositions in the aqueous solution, as shown in Fig. 1.7. They clarified that the dissolution ratio of Ca is close to

1.0 in the case of pure C_2S , but it decreased greatly as the C_3P content in the solid solution increased. However, the dissolution ratio of P was about 0.1 and did not change with the C_3P content. It means that in the case of slag with high P_2O_5 content, the solid solution with high P_2O_5 content is difficult to be dissolved. In addition, the dissolution ratio of P increased for 30 min, but after it reached the maximum value, it began to decrease owing to precipitation of hydroxyapatite ($Ca_{10}(PO_4)_6(OH)_2$, HAP). In this experiment, the dissolution behavior of a solid solution with a matrix phase in the $CaO-SiO_2-P_2O_5-Fe_2O_3$ slag system was also investigated. It was found that when FeO was used as an iron oxide, the dissolution ratio of P was much lower than when Fe_2O_3 was used. In the case of Fe_2O_3 -containing slag, the dissolution ratios of each element in the matrix phase were lower than that in the solid solution at various pH conditions.

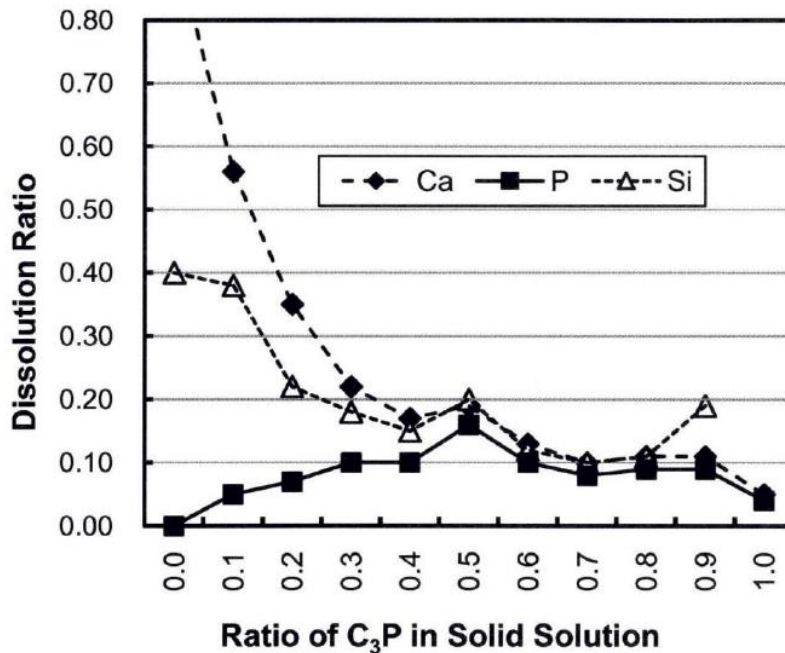


Fig. 1.7 Change in the maximum dissolution ratio of each element with the composition of the solid solution

Numuta *et al.* [66] clarified the possibility of selective extraction of the solid solution from the quenched steelmaking slag. Figure 1.8 shows the dissolution ratios of each element from slag in

the nitric solution. For both conditions, a selective dissolution of the solid solution occurred since the dissolution ratio of Fe was small. The dissolution ratios of each element from slag were much greater at pH 3 than at pH 7. At pH 3, most of the Ca and Si in the solid solution dissolved after 120 min; however, the dissolution ratio of P was approximately 65% smaller than that of Ca. XRD analysis revealed that the peak corresponding to the solid solution disappeared in the residue. The mass ratio of the residue to the dissolved slag was close to the ratio of the matrix to the solid solution before leaching. These results confirmed that the solid solution of the initial slag was selectively dissolved in the aqueous solution. However, the dissolution ratio of P from slag was not high because of phosphate precipitation in these cases.

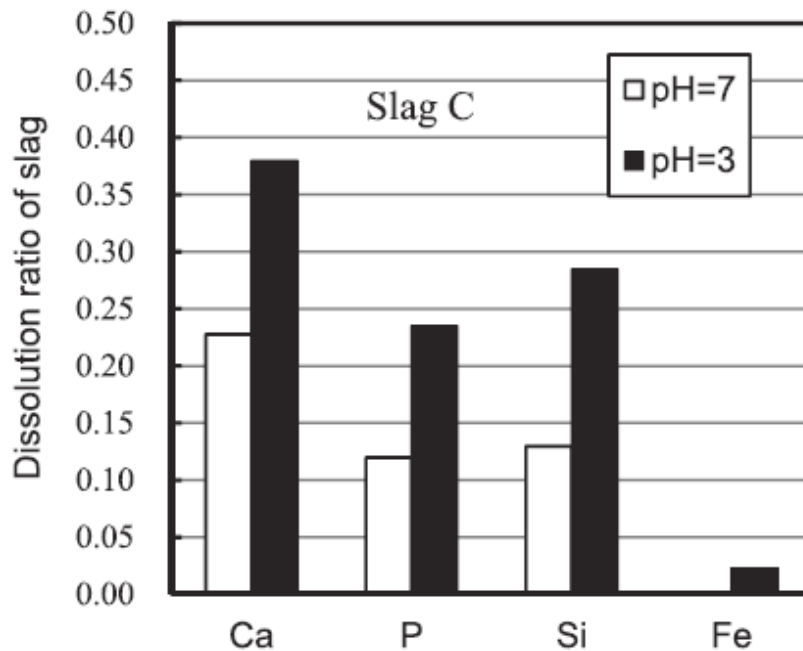


Fig. 1.8 Dissolution ratios of each element from steelmaking slag in the nitric solution

Qiao *et al.* [67] investigated the dephosphorization of steelmaking slag by leaching with acidic aqueous solution composed of citric acid, sodium hydroxide, hydrochloric acid and ion-exchanged water. Their results showed that temperature had no obvious effect on the dissolution ratio of P. However, it had a significant effect on the dissolution ratio of Fe. The

dephosphorization rate increased with the decrease of slag particle size and the pH value of the solution. More than 90% of the P can be dissolved in the solution while the dissolution ratio of Fe was only 30% below the optimal condition. Because of a higher dissolution ratio of Fe in this case, a better selective leaching of P from slag did not achieve.

1.5 Purposes and contents of the present study

The steelmaking slag with high P_2O_5 content generated from the utilization of high-P iron ore is considered as a great potential source of P. Because the majority of the P_2O_5 in slag was concentrated in the solid solution, selective leaching of C_2S-C_3P solid solution was adopted to recover P from slag with high P_2O_5 content as a phosphate fertilizer and recycle the undissolved slag inside steelmaking process. The previous studies [65] revealed that the C_2S-C_3P solid solution with high P_2O_5 content was difficult to be dissolved and the dissolution ratio of P was very low because of phosphate precipitation. Therefore, the first purpose of the present study was to suppress phosphate precipitation in the aqueous solution and promote P dissolution from the solid solution with high P_2O_5 content. Although a large amount of P could dissolve from steelmaking slag in some case, the significant dissolution of Fe occurred simultaneously [66, 67]. Therefore, the second purpose of the present study was to suppress dissolution of Fe-containing phases and achieve an excellent selective leaching of P from slag with high P_2O_5 content. Following leaching of steelmaking slag, a leachate containing soluble P was obtained, and there were no studies on P recovery from such solution. The third purpose of the present study was to explore an effective method to extract a phosphate product from the leachate.

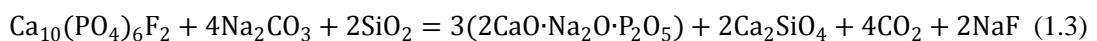
To achieve these goals, some innovations were proposed in the present study:

- (1) Organic acid (oxalic acid and citric acid) was selected as the leaching agent:

Leaching agents (acid) have a significant effect in metal extraction from mineral ores because of their different properties and dissolution mechanism [68, 69]. For selective leaching of P from slag by nitric acid, the dissolved phosphate ions in the aqueous solution was easy to react with Ca^{2+} and precipitate in the form of hydroxyapatite ($\text{Ca}_{10}(\text{PO}_4)_6(\text{OH})_2$), resulting in a lower dissolution ratio of P [66]. In the oxalic acid ($\text{H}_2\text{C}_2\text{O}_4$) solution, Ca^{2+} and $\text{C}_2\text{O}_4^{2-}$ ions can form CaC_2O_4 sediment [70]. In the citric acid ($\text{H}_3\text{C}_6\text{H}_5\text{O}_7$) solution, $\text{C}_6\text{H}_5\text{O}_7^{3-}$ species have a strong capacity to react with Ca^{2+} and form a $\text{CaC}_6\text{H}_5\text{O}_7^-$ complex [71]. In these cases, the Ca^{2+} was “fixed” by organic ions, and then its effect on P precipitation may be weakened. Therefore, oxalic acid and citric acid were selected as leaching agents and their effects on P dissolution from the $\text{C}_2\text{S}-\text{C}_3\text{P}$ solid solution were investigated.

(2) Na_2O (and K_2O) modification of slag with high P_2O_5 content:

The Rhenania phosphate fertilizer with an ammonium citrate solubility of 98% was produced by the reaction of fluorine apatite ($\text{Ca}_{10}(\text{PO}_4)_6\text{F}_2$), soda, and quartz sand at high temperatures, as shown in Reaction (1.3) [72]. An alkali-dicalcium phosphate is formed and calcium is displaced by alkali, and the excess lime is bound by silica as orthosilicate. The stable existence of $2\text{CaO}\cdot\text{Na}_2\text{O}\cdot\text{P}_2\text{O}_5$ has been confirmed by the phase diagram of $\text{Ca}_3(\text{PO}_4)_2-\text{CaNaPO}_4$ [73]. Because $2\text{CaO}\cdot\text{Na}_2\text{O}\cdot\text{P}_2\text{O}_5$ shows a higher solubility than $3\text{CaO}\cdot\text{P}_2\text{O}_5$ in the 2% citric acid solution [74], if Na_2O could be introduced into $2\text{CaO}\cdot\text{SiO}_2-3\text{CaO}\cdot\text{P}_2\text{O}_5$ solid solution to substitute for CaO , the solubility of solid solution would be significantly improved, and the dissolution of P from slag would be promoted. Therefore, modification of $\text{C}_2\text{S}-\text{C}_3\text{P}$ with Na_2SiO_3 at high temperatures was proposed. The effect of Na_2O (and K_2O) modification on dissolution behavior of slag was investigated.



(3) Slow cooling of the molten slag:

Cooling rate of the molten slag significantly affects not only the size of the crystals but also the fraction of each mineralogical phase. Slow cooling promoted the formation of dicalcium silicate with high P_2O_5 content in steelmaking slag, and some phases could be crystallized from the matrix phase (glassy phase) [75]. For the silicate glassy phase, decreasing cooling could also change its structure [76]. In addition, some studies have clarified that some elements were easier to dissolve from amorphous slag than from crystalline slag [77, 78]. Consequently, it is concluded that decreasing cooling rate of the molten slag would affect the dissolution behavior of each phase in the aqueous solution, and then the effect of the cooling rate on slag dissolution was investigated.

(4) P precipitation by adding alkaline solution

The process of P recovery from the leachate was similar with the P removal technologies in wastewater treatment which have been widely investigated [79]. Chemical precipitation comprises the addition of a divalent or trivalent metal salt to wastewater. It caused the precipitation of an insoluble metal phosphate that is settled out by sedimentation. Calcium phosphates are the major component of phosphate fertilizer, and can precipitate at high pH condition [80]. To offer a more valuable and consistent product for recycling P to agriculture, Ca is considered the most suitable metal to precipitate phosphate. In addition, alkaline solution can adjust the pH of the leachate easily to control the formation of phosphate precipitate. Therefore, $Ca(OH)_2$ solution was selected, and the effect of pH on P precipitation by $Ca(OH)_2$ addition was investigated.

The contents of this thesis are as follows:

- Chapter 1 presents the background and purposes of this thesis;

- Chapter 2 presents the dissolution behavior of the P-concentrated C_2S-C_3P solid solution. The effects of leaching agent (acid), Na_2O modification, and pH on the dissolution of P from the solid solution were investigated.
- Chapter 3 presents the dissolution behavior of P from modified steelmaking slag with Na_2O addition. The effects of the cooling rate of molten slag, Na_2O content, pH, and the valency of Fe in slag on the dissolution of P from slag were investigated.
- Chapter 4 presents the dissolution behavior of P from modified steelmaking slag with K_2O addition. The effects of K_2O content and pH on the dissolution of P from slag were investigated.
- Chapter 5 presents the distribution of P_2O_5 and Na_2O between the solid solution and liquid phase in slag with high P_2O_5 content. The effects of slag composition on the distribution ratio of P_2O_5 and mass fraction of the solid solution were investigated.
- Chapter 6 represents P recovery from the leachate by precipitation. The effects of alkaline solution and pH on the P precipitation in the leachate were investigated. A process for the comprehensive utilization of slag with high P_2O_5 content was proposed.
- Chapter 7 represents the conclusions of the present thesis.

References

1. https://minerals.usgs.gov/minerals/pubs/commodity/phosphate_rock/, Phosphate Rock Statistics and Information, U.S. Geological Survey, 2017.
2. <http://www.customs.go.jp/toukei/info/index.htm>, Trade Statistics of Japan, Ministry of Finance, 2006.
3. G.A. da Silva, L.A. Kulay: *Journal of Cleaner Production*, 13(2005), pp. 1321-1325.
4. P.H. Abelson: *Science*, 283(1999), p 2015.
5. D. Cordell, J. Drangert, S. White: *Global Environmental Change*, 19(2009), pp. 292-305.
6. Sabiha-Javied, T. Mehmood, M.M. Chaudhry, M. Tufail, N. Irfan: *Microchemical Journal*, 91(2009), pp. 94-99.
7. R. Cabeza, B. Steingrobe, W. Römer, N. Claassen: *Nutrient Cycling in Agroecosystems*, 91(2011), pp. 173-184.
8. C.Y. Cheng, V.N. Misra, J. Clough, R. Mun: *Minerals Engineering*, 12(1999), pp.1083-1092.
9. <http://www.worldsteel.org/>, Total Production of Crude Steel, World Steel Association, 2016.
10. J. Gao, L. Guo, Z. Guo: *Metallurgical and Materials Transactions B*, 46B(2015), pp. 2180-2189.
11. Y. Matui: *Proceedings of the Symposium on the Contribution of Iron and Steel Industry to Phosphorus Resource Security*, ISIJ, Tokyo, (2013), p 26
12. J. Yu, Z. Guo, H. Tang: *ISIJ International*, 53(2013), pp. 2056-2064.
13. K. Matsubae, E. Yamasue, T. Inazumi, E. Webeck, T. Miki, T. Nagasaka: *Science of the Total Environment*, 542(2016), pp. 1162-1168.
14. M.J. Fisher-white, R.R. Lovel, G. J. Sparrow: *ISIJ International*, 52(2012), pp. 797-803.
15. A.P.L. Nunes, C.L.L. Pinto, G.E.S. Valadao, P.R.M. Viana: *Minerals Engineering*, 39 (2012), pp. 206-212.
16. G.W. Qi, A. Parentich, L.H. Little, L.J. Warren: *International Journal of Mineral Processing*, 34(1992), pp. 83-102.
17. M. Muhammed, Y. Zhang: *Hydrometallurgy*, 21(1989), pp. 277-292.
18. W.T. Xia, Z.D. Ren, Y.F. Gao: *Journal of Iron and Steel Research, International*, 18 (2011), pp. 1-4.
19. Y. Zhang, M. Muhammed: *Hydrometallurgy*, 21 (1989), pp. 255-275.
20. L. Guo, J. Gao, Y. Zhong, H. Gao, Z. Guo: *ISIJ International*, 55(2015), pp. 1806-1815.
21. E. Matinde, M. Hino: *ISIJ International*, 51 (2011), pp. 220-227.
22. E. Matinde, M. Hino: *ISIJ International*, 51 (2011), pp. 544-551.

23. P.K.Tripathy, A.Banerjee, B.Singh, D.Das, K.Das: ISIJ International, 48(2008), pp. 578-583.
24. T. Emi: ISIJ International, 55(2015), pp. 36-66.
25. Y. Ogawa, N. Maruoka: Tetsu-to-Hagané, 100(2014), pp. 434-444.
26. N. Sasaki, Y. Ogawa, S. Mukawa, K. Miyamoto: Nippon Steel Technical Report, 104(2013), pp. 27-32.
27. H. Suito, R. Inoue, M. Takada: Transactions ISIJ, 21(1981), pp. 250-259.
28. J. Im, K. Morita, N. Sano: ISIJ International, 36(1996), pp. 517-521.
29. M. Muraki, H. Fukushima, N. Sano: Transactions ISIJ, 25(1985), pp. 1025-1030.
30. J.J. Park, R. J. Frunhan: Metallurgical and Materials Transactions B, 22B(1991), pp. 39-46.
31. K. Kunisada, H. Iwai: Transactions ISIJ, 27(1987), pp. 263-269.
32. H. Suito, Y. Hayashida, Y. Takahashi: Tetsu-to-Hagané, 63(1977), pp. 1252-1259.
33. W. Fix, H. Heyman, R. Heinke: Journal of the American Ceramic Society, 52(1969), pp. 346-347.
34. R. Inoue, H. Suito: ISIJ International, 46(2006), pp. 174-179.
35. T. Hamano, S. Fukagai, F. Tsukihashi: ISIJ International, 46 (2006), pp. 490-495.
36. X. Yang, H. Matsuura, F. Tsukihashi: ISIJ International, 49 (2009), pp. 1298-1307.
37. X. Yang, H. Matsuura, F. Tsukihashi: ISIJ International, 50 (2010), pp. 702-711.
38. K. Ito, M. Yanagisawa, N. Sano: Tetsu-to-Hagané, 68 (1982), pp. 342-344.
39. S. Kitamura, H. Shibata, N. Maruoka: Steel Research International, 79(2008), pp. 586-590.
40. F. Pahlevani, S. Kitamura, H. Shibata, N. Maruoka: ISIJ International, 50(2010), pp. 822-829.
41. L. Lin, Y. Bao, W. Jiang, Q. Wu: ISIJ International, 55(2015), pp. 552-558.
42. L. Lin, Y.P. Bao, M. Wang, H.M. Zhou, L.Q. Zhang: Ironmaking and Steelmaking, 40(2013), pp. 521-527.
43. S. Xie, W. Wang, Y. Liu, H. Matsuura: ISIJ International, 54(2014), pp. 766-773.
44. L. Jiang, J. Diao, X. Yan, B. Xie, Y. Ren, T. Zhang, G. Fan: ISIJ International, 55(2015), pp. 564-569.
45. S. Kitamura, F. Pahlevani: Tetsu-to-Hagané, 100(2014), pp. 500-508.
46. K. Shimauchi, S. Kitamura, H. Shibata: ISIJ International, 49(2009), pp. 505-511.
47. <http://www.slg.jp/e/index.htm>, Nippon Slag Association, 2017.
48. K. Yokoyama, H. Kubo, K. Nakajima, T. Nagasaka: Journal of Industrial Ecology, 13(2009), pp. 687-705.
49. H. Ono, A. Inagaki, T. Masui, H. Narita, T. Mitsuo, S. Nosaka, S. Gohda: Tetsu-to-Hagané, 66(1980), pp.1317-1326.
50. H.-J. Li, H. Suito, M. Tokuda: ISIJ International, 35(1995), pp. 1079-1088.

51. M. Ishikawa: ISIJ International, 46(2006), pp. 530-538.
52. K. Yokoyama, H. Kubo, K. Mori, H. Okada, S. Takeuchi, T. Nagasaka: ISIJ International, 47(2007), pp. 1541-1548.
53. H. Kubo, T. Nagasaka, K. Yokoyama: ISIJ International, 50(2010), pp. 59-64.
54. J. Diao, B. Xie, Y. Wang, X. Guo: ISIJ International, 52(2012), pp. 955-959.
55. L. Lin, Y. Bao, M. Wang, W. Jiang, H. Zhou: Journal of Iron and Steel Research, International, 21(2014), 496-502.
56. T. Miki, S. Kaneko: ISIJ International, 55(2015), pp. 142-148.
57. K. Morita, M. Guo, N. Oka, N. Sano: Journal of Material Cycles and Waste Management, 4(2002), pp. 93-101.
58. C. Li, J. Gao, Z. Guo: ISIJ International, 56(2016), pp. 759-764.
59. L.P. James, W.H. Cooksey, M.E. Park, K.Y. Sung: Korean Journal of Chemical Engineering, 18(2001), pp. 948-954.
60. S. Sugiyama, I. Shinomiya, R. Kitora, K. Nakagawa, M. Katoh: Journal of Chemical Engineering of Japan, 47(2014), pp. 483-487.
61. J. Diao, L. Jiang, Y. H. Wang, B. Xie: Phosphorus, Sulfur, and Silicon, 190 (2015), pp. 387-395.
62. L. Lin, Y. P. Bao, M. Wang, W. Jiang, H. M. Zhou: ISIJ International, 54(2014), pp. 2746-2753.
63. F.T. Nielsson: Manual of fertilizer processing. Marcel Dekker New York, NY, USA, 1987.
64. T.R.C. Patrick, R.R. Lovel: ISIJ International, 41(2001), pp.128-135.
65. T. Teratoko, N. Maruoka, H. Shibata, S. Kitamura: High Temperature Material Process, 31(2012), pp. 329-338.
66. M. Numata, N. Maruoka, S.J. Kim, S. Kitamura: ISIJ International, 54(2014), pp. 1983-1990.
67. Y. Qiao, J. Diao, X. Liu, X. Li, T. Zhang, B. Xie: JOM, 68(2016), pp. 2511-2519.
68. W.P. Miller, L.W. Zelazny, D.C. Martens: Geoderma, 37(1986), pp. 1-13.
69. W. Astuti, T. Hirajima, K. Sasaki, N. Okibe: Minerals Engineering, 85(2016), pp. 1-16.
70. R. W. Clark, J. M. Bonicamp: Journal of Chemical Education, 75 (1998), pp. 1182-1185.
71. J. Muus, H. Lebel: Mathematisk-fysiske Meddelelser Danske Videnskabernes Selskab, 13 (1936), pp. 1-16.
72. H. Jantzen, K. Schugerl, H. Helmrich: Powder Technology, 23 (1979), pp. 1-14.
73. J. Ando: Bulletin of the Chemical Society of Japan, 1958, pp. 201-205.
74. R.P. Gunawardane, F.P. Glasser: Journal of Materials Science, 14(1979), pp. 2797-2810.
75. M. Gautier, J. Poirier, F. Bodénan, G. Franceschini, E. Véron: International Journal of Mineral Processing, 123 (2013), pp. 94-101.

76. J. Tan, S. Zhao, W. Wang, G. Davies and X. Mo: *Materials Science and Engineering: B*, 106(2004), pp. 295-299.
77. K. Maweja, T. Mukongo, R. K. Mbaya, E.A. Mochubele: *Journal of Hazardous Materials*, 183(2010), pp. 294-300.
78. H. Mizukami, M. Ishikawa, T. Hirata, T. Kamiyama, K. Ichikawa: *ISIJ International*, 44(2004), pp. 623-629.
79. G.K. Morse, S.W. Brett, J.A. Guy, J.N. Lester: *The Science of the Total Environment*, 212(1998), pp. 69-81.
80. E. Valsami-Jones: *Mineralogical Magazine*, 65(2001), pp. 611-620.

2 Dissolution behavior of P from the C₂S-C₃P solid solution with high P₂O₅ content

The key to selective leaching of P from slag was to promote the dissolution of P from the P-condensed solid solution. In this chapter, the dissolution behavior of P from the C₂S-C₃P solid solution with high P₂O₅ content was studied. To suppress precipitation of the dissolved P during leaching, oxalic acid (H₂C₂O₄) and citric acid (H₃C₆H₅O₇) were selected as leaching agents. This is because the dissolved Ca²⁺ ions can form precipitation or complex in the oxalic and citric solutions [1, 2], respectively, and then the effect of Ca²⁺ ions on phosphate precipitation is possible to be weakened. To improve the solubility of C₂S-C₃P solid solution, modification of C₂S-C₃P with Na₂SiO₃ at high temperatures was proposed. It has been reported that the addition of Na₂O to slag promoted the dissolution of P from dephosphorization slag in 2% citric acid solution, which resulted from the formation of Na₂Ca₄(PO₄)₂SiO₄ (However, the dissolution behavior of Fe from slag were not investigated) [3]. Because 2CaO·Na₂O·P₂O₅ shows a higher solubility than 3CaO·P₂O₅ in 2% citric acid solution [4], if Na₂O could be introduced into the C₂S-C₃P solid solution, its solubility would increase, and a higher dissolution ratio of P may achieve. Consequently, the effect of Na₂O addition on the dissolution of solid solution was investigated at various pH conditions controlled by the addition of either oxalic acid or citric acid.

2.1 Experimental method

2.1.1 Synthesis of solid solution and Na₂O modification

Reagent-grade SiO₂ and Ca₃(PO₄)₂ as well as synthetic CaO were utilized to synthesize C₂S-C₃P solid solution. Synthetic CaO was prepared by heating reagent-grade CaCO₃ at 1273 K for at least 12 h under air atmosphere. For the preparation of C₂S, a mixture of CaO and SiO₂ with a target

composition of CaO-34.9 mass% SiO₂ was pressed to form a disc of 13 mm in diameter, and then heated at 1773 K for 24 h. After cooling, γ -C₂S powder was obtained, since the disc disintegrated due to the volume expansion caused by phase transformation. The formation of dicalcium silicate was confirmed using X-ray diffraction analysis (XRD). To prepare C₂S-C₃P solid solution, the synthesized C₂S powder was fully mixed with Ca₃(PO₄)₂ powder, pressed into a disc of 13 mm in diameter, and annealed in a Pt boat at 1773 K for 48 h under air atmosphere. After cooling, the phase of the solid solution was determined by XRD.

Table 2.1 Compositions of the solid solution samples before and after Na₂SiO₃ addition (mass%)

Sample	before modification			after Na ₂ SiO ₃ addition			
	CaO	SiO ₂	P ₂ O ₅	CaO	SiO ₂	P ₂ O ₅	Na ₂ SiO ₃
0% Na ₂ SiO ₃	60.4	19.6	20.0	60.4	19.6	20.0	0
10% Na ₂ SiO ₃	59.8	18.0	22.2	53.9	16.2	20.0	9.8
20% Na ₂ SiO ₃	59.2	15.9	24.9	47.5	12.8	20.0	19.7
30% Na ₂ SiO ₃	58.4	13.3	28.4	41.1	9.4	20.0	29.5

For the Na₂O modification procedure, Na₂SiO₃ was selected as the modifier because it was more stable than Na₂CO₃. Reagent-grade Na₂SiO₃ powder was mixed with the synthesized C₂S-C₃P powder at a target mass ratio, pressed into tablets, and annealed in a Pt boat at 1773 K under air atmosphere. To promote this reaction which occurs between solid and liquid phase, the holding time at 1773 K was set as 2 h. In each case, the pellets were crashed into powder after being cooled down in air to confirm their crystalline structure using XRD and electron probe microanalysis (EPMA).

Steelmaking slag generally contains about 3 mass% of P₂O₅. In the case of utilization of high-P iron ores, P₂O₅ content in steelmaking slag can increase to about 8 mass%. Assuming that the mass fraction of solid solution in slag is about 0.3 and the distribution ratio of P₂O₅ between solid solution and liquid phase is 5, P₂O₅ content in the solid solution can reach about 20 mass%. Therefore, P₂O₅ content in the samples were fixed at 20 mass% in all cases. Table 2.1 shows the

compositions of the solid solution samples before and after Na_2SiO_3 addition. For the solid solution samples, the $3\text{CaO}\cdot\text{P}_2\text{O}_5$ content was the same because of the same P_2O_5 content. When different mass ratios of Na_2SiO_3 were added, the $2\text{CaO}\cdot\text{SiO}_2$ content would be changed correspondingly, and thus the ratio between C_2S and C_3P was different in each sample. For the modified sample containing 19.7 mass% of Na_2SiO_3 , the molar ratio of P_2O_5 to Na_2O was equal to approximately 1:1. In this study, the solid solution samples containing 9.8, 19.7, and 29.5 mass% of Na_2SiO_3 are named as 10% Na_2SiO_3 , 20% Na_2SiO_3 , and 30% Na_2SiO_3 , respectively.

2.1.2 Leaching experiment

The prepared $\text{C}_2\text{S}\text{-C}_3\text{P}$ samples and that after Na_2SiO_3 addition were ground into fine particles with sizes smaller than $53\ \mu\text{m}$ (270 mesh). The schematic of the leaching apparatus is shown in Figure 2.1. One gram of the powdered sample was added to 400 mL of deionized water. A Teflon container with a 500 mL capacity was used as a vessel, and the temperature was kept constant at 298 K using an isothermal water bath. The aqueous solution was agitated using a semicircular-shaped rotating stirrer of 60 mm in width at 200 rpm. Because the dissolution of Ca from solid solution increased the pH of the aqueous solution, to keep the pH at a constant value, a pH meter was attached to the system, and an acid was automatically supplied into the solution by a PC-controlled system. In this study, nitric acid (HNO_3 , 0.1 mol/L), oxalic acid ($\text{H}_2\text{C}_2\text{O}_4$, 0.1 mol/L) and citric acid ($\text{H}_3\text{C}_6\text{H}_5\text{O}_7$, 0.1 mol/L) were used as leaching agents, respectively. According to the previous studies [5, 6], the dissolution of each element from slag was difficult at a higher pH ($\text{pH} \geq 9$), while a large amount of slag, including Fe, was dissolved at a lower pH ($\text{pH} \leq 5$). Consequently, to achieve selective leaching of P, the pH was set within this range ($5 \leq \text{pH} \leq 9$). About 5 mL of the aqueous solution was periodically sampled at certain

intervals (1, 3, 5, 10, 20, 30, 60, 120 min) followed by filtration using syringe filters (< 0.45 μm). The leaching time was set as 120 min.

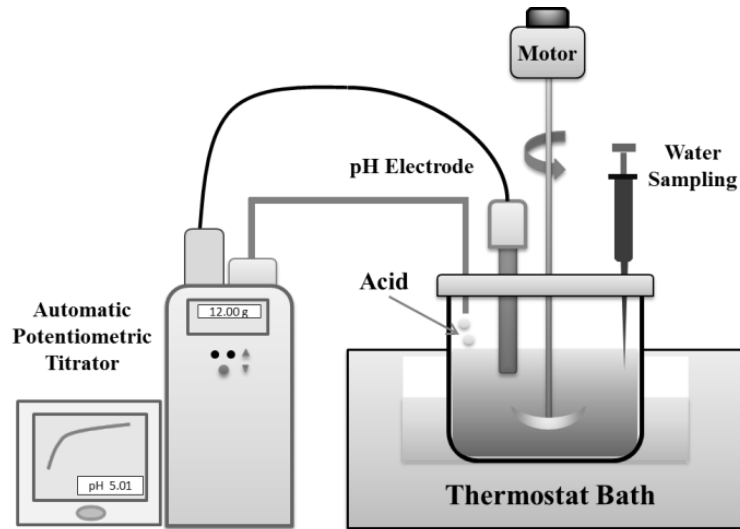


Fig. 2.1 Schematic of leaching apparatus

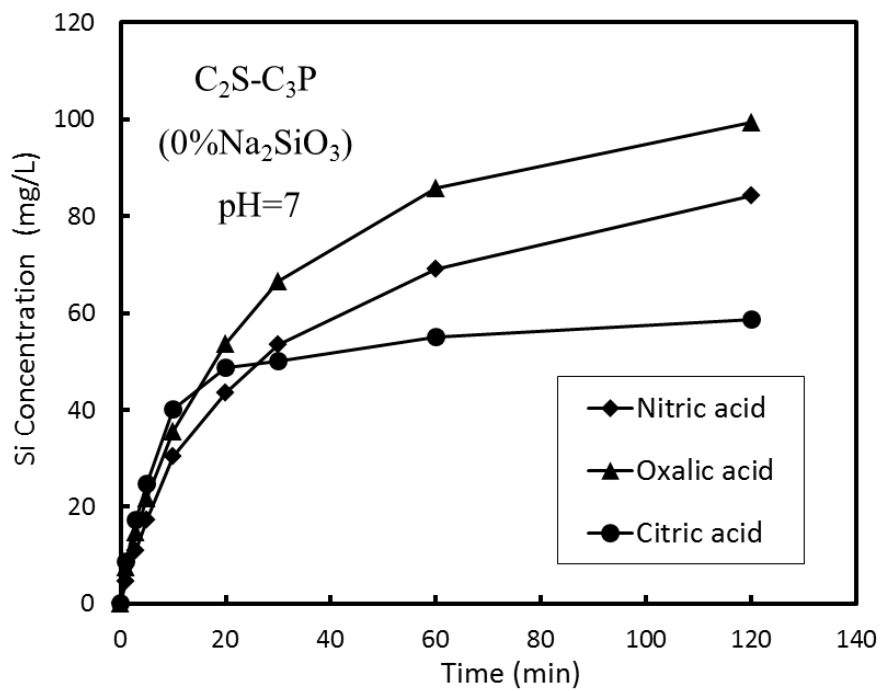
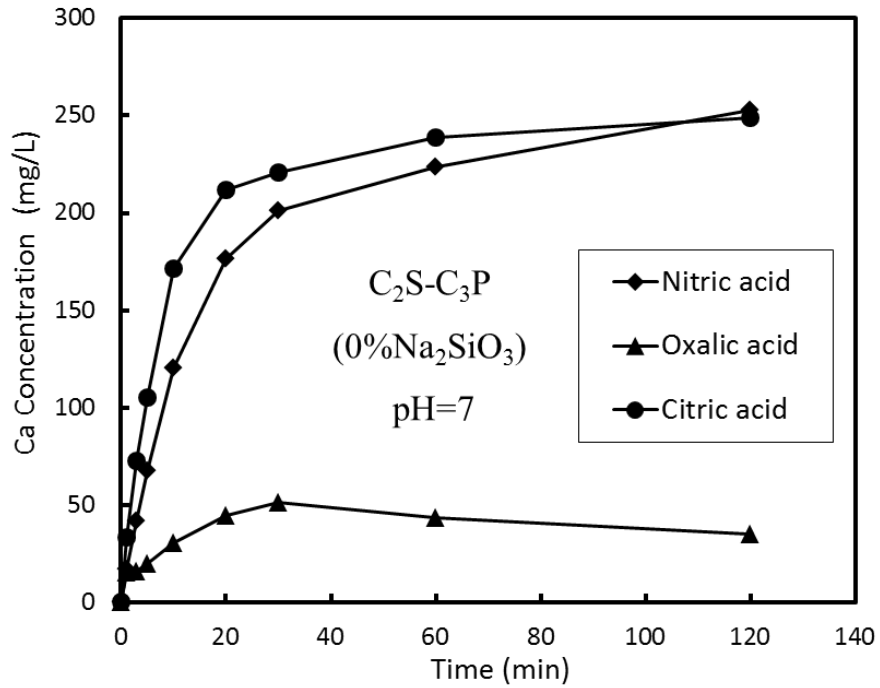
After leaching, the remaining aqueous solution was filtered, and the residue was collected from the filter. The concentrations of each element in the sampled aqueous solution were determined using inductively coupled plasma emission spectroscopy (ICP-AES). The residue was analyzed using XRD and EPMA. In order to investigate the effects of leaching agent and Na_2SiO_3 modification at different pH values, 16 sets of leaching experiments were conducted (shown in Table 2.2).

Table 2.2 Leaching experiments at various pH conditions (pH)

Sample Acid	0% Na_2SiO_3	10% Na_2SiO_3	20% Na_2SiO_3	30% Na_2SiO_3
Nitric acid	7	-	5, 7, 9	-
Oxalic acid	7	7	5, 7, 9	7
Citric acid	7	7	5, 7, 9	7

2.2 Experimental results

2.2.1 Effect of leaching agent on the dissolution of C₂S-C₃P solid solution



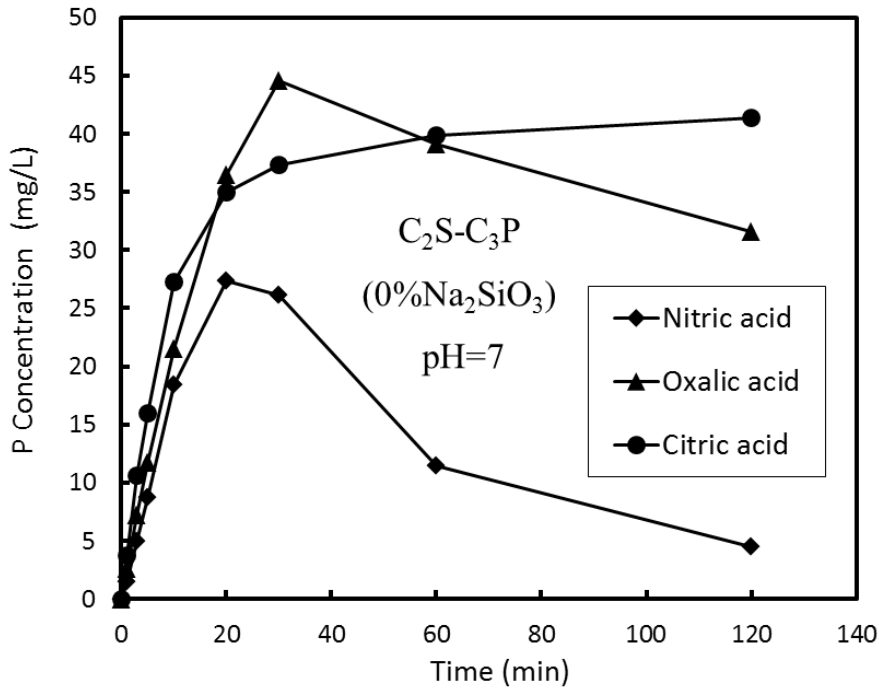


Fig 2.2 Change in the Ca and P concentrations in different acid solutions at pH 7

To investigate the effect of the leaching agent, unmodified C_2S-C_3P sample was leached by nitric acid, oxalic acid, and citric acid at pH 7. Figure 2.2 shows the change in the concentrations of Ca, Si, and P with leaching time in different leaching agents. In the beginning, the C_2S-C_3P dissolution was fast due to low ion concentrations in the aqueous solution, and the concentrations of each element increased rapidly. In the nitric solution, the Ca and Si concentrations increased continuously, reaching 252.9 mg/L and 84.2 mg/L, respectively, after 120 min. The dissolved P was not stable; its concentration first increased, and then decreased to 4.5 mg/L after 120 min. When oxalic acid was used as a leaching agent, the Ca concentration in the aqueous solution was very low, and the P concentration significantly increased compared to that in the nitric solution, although it slightly decreased after the maximum value. In the citric solution, the Ca concentration was as high as that in the nitric solution, and the P concentration increased continuously, reaching 41.3 mg/L after 120 min.

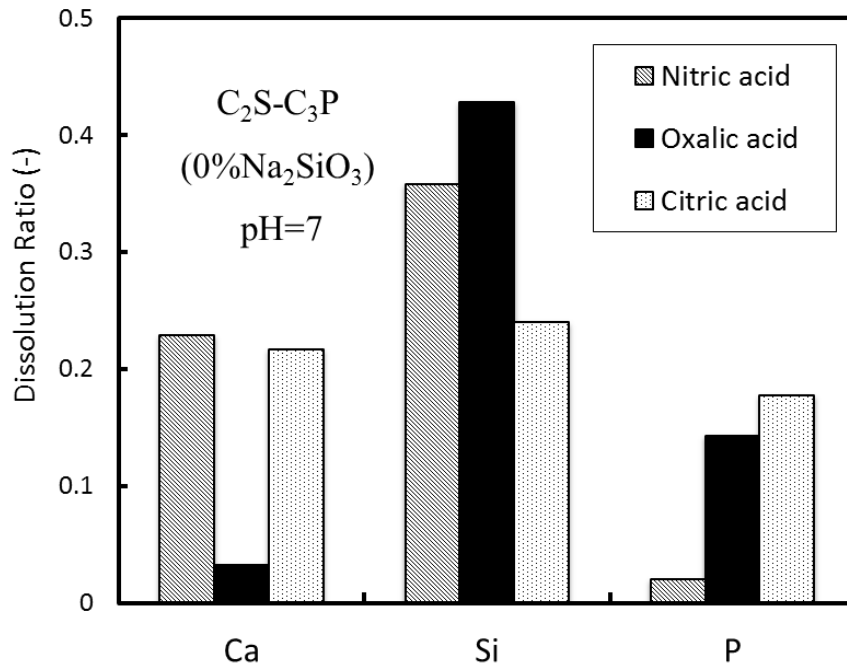


Fig 2.3 Dissolution ratios of each element from C_2S-C_3P in different acid solutions at pH 7

From the obtained concentrations of each element in the aqueous solution, the dissolution ratios were calculated for Ca, Si, and P using Eq. (2.1), where R_M is the dissolution ratio of element M; C_M is the concentration of element M in the aqueous solution after 120 min (mg/L); V is the final volume of the aqueous solution (L); and m_M is the original mass of element M in 1 g of the C_2S-C_3P sample (mg).

$$R_M = \frac{C_M \cdot V}{m_M} \quad (2.1)$$

The dissolution ratios of Ca, Si, and P from the C_2S-C_3P solid solution in different leaching agents at pH 7 are shown in Fig. 2.3. The dissolution ratio of Ca exceeded 22% in the nitric and citric solutions, but was very low in the oxalic solution. The dissolution ratio of Si was higher than that of other elements in each case. Approximately 43% of Si was dissolved from C_2S-C_3P in the oxalic solution. In the nitric solution, the dissolution of P was difficult; only a small fraction of the P was dissolved. However, the dissolution ratio of P in the oxalic and citric

solutions significantly increased reaching 14.3% and 17.8%, respectively. Therefore, organic acid (oxalic acid and citric acid) were more efficient than nitric acid at extracting P from the C₂S-C₃P solid solution in the aqueous solution at pH 7.

2.2.2 Modification of C₂S-C₃P by Na₂SiO₃

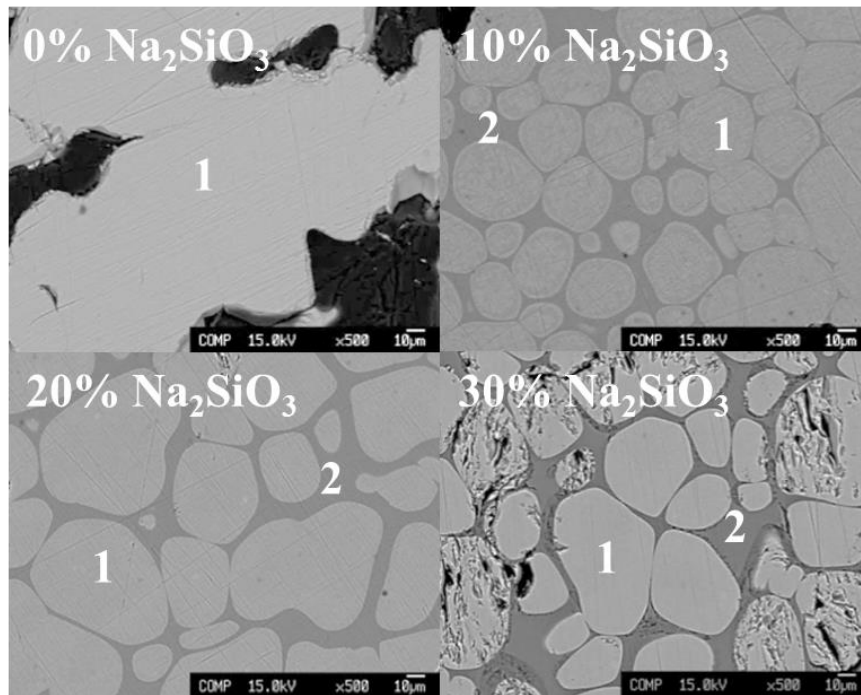


Fig 2.4 Cross section of the solid solution samples with different mass fractions of Na₂SiO₃

Table 2.3 Compositions of each phase in the solid solution samples with different mass fractions of Na₂SiO₃ (mass%)

Sample		CaO	SiO ₂	P ₂ O ₅	Na ₂ O	Phase
0% Na ₂ SiO ₃	1	59.7	18.5	21.9	-	Solid solution
10% Na ₂ SiO ₃	1	54.8	17.2	23.6	4.5	Solid solution
	2	47.3	43.3	6.1	3.3	CS phase
20% Na ₂ SiO ₃	1	49.9	15.5	25.7	8.9	Solid solution
	2	41.1	45.9	4.9	8.1	CS phase
30% Na ₂ SiO ₃	1	45.5	12.8	30.1	11.6	Solid solution
	2	30.7	51.7	4.8	12.8	CS phase

Figure 2.4 and Table 2.3 show the cross section and compositions of the samples with different mass fractions of Na_2SiO_3 . After Na_2SiO_3 modification, the obtained samples consist of two phases. The major phase was considered the solid solution modified with Na_2O . The other phase, mainly contains CaO and SiO_2 , was considered the $\text{CaO}\cdot\text{SiO}_2$ (CS) phase. The P_2O_5 content in the new CS phase was far lower than that in the modified solid solution. The Na_2O content in the modified solid solution was almost the same as that in the CS phase. The compositions of each phase in the samples with and without modification were plotted in a $(\text{CaO}+\text{Na}_2\text{O})\text{-SiO}_2\text{-P}_2\text{O}_5$ pseudo-phase diagram, as shown in Fig. 2.5. The Na_2O content in the solid solution was taken into consideration. The compositions of solid solution in this study are nearly located on the line between $2(\text{CaO}, \text{Na}_2\text{O})\cdot\text{SiO}_2$ and $3(\text{CaO}, \text{Na}_2\text{O})\cdot\text{P}_2\text{O}_5$. This would indicate that a part of CaO in the $\text{C}_2\text{S}\text{-C}_3\text{P}$ solid solution was replaced by Na_2O in the newly formed solid solution. The observed compositions of the other phase were located near the composition of CS phase. It illustrates that the replaced CaO would be combined with SiO_2 and formed $\text{CaO}\cdot\text{SiO}_2$ phase.

Compared with the compositions of $\text{C}_2\text{S}\text{-C}_3\text{P}$, the SiO_2 and P_2O_5 contents in the modified solid solution changed little, but the CaO content decreased since it was replaced by Na_2O . As shown in Fig 2.6, with an increase in Na_2SiO_3 content, the Na_2O content in the modified solid solution increased, but the CaO content decreased. In the case of sample with about 20 mass% of Na_2SiO_3 , the Na_2O content in the modified solid solution reached 11.6 mass%.

To estimate the mass ratio of each element distributed to the solid solution, the phase fraction was calculated. The mass balance of each oxide can be represented using Eqs. (2.2) and (2.3):

$$N_{\text{MO}_n} = \alpha N_{\text{MO}_n}^{\alpha} + \beta N_{\text{MO}_n}^{\beta} \quad (2.2)$$

$$\alpha + \beta = 1 \quad (2.3)$$

where α and β are the mass fractions of the solid solution and the other phase, respectively, N_{MO_n} is the MO_n content in slag, and $N_{MO_n}^\alpha$ is the MO_n content in the solid solution. The mass fraction of solid solution was defined as the average of the calculated mass fractions using the mass balance of CaO, SiO_2 and P_2O_5 . The results, shown in Fig. 2.7, indicated that most of the added Na_2O and P_2O_5 were distributed in the modified solid solution. With an increase in the Na_2SiO_3 content, the mass ratio of Na_2O distributed in the modified solid solution decreased, but the distribution of P_2O_5 had a little change. When about 20 mass% of Na_2SiO_3 was added, about 94% of the P and 76% of the Na were distributed in the modified solid solution.

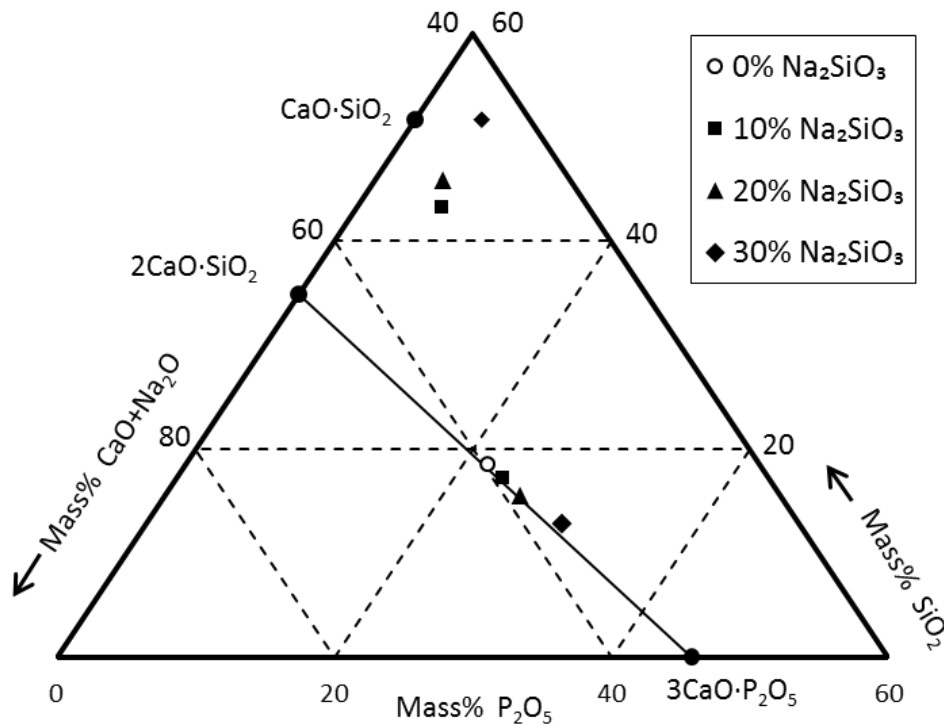
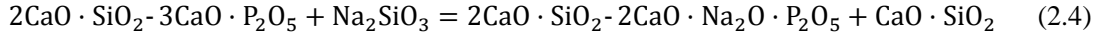


Fig. 2.5 Compositions of each phase in the $(CaO+Na_2O)-SiO_2-P_2O_5$ pseudo-phase diagram

Figure 2.8 shows the XRD patterns of the solid solution samples with different mass ratios of Na_2SiO_3 . Without the Na_2SiO_3 modification, the main phase corresponds to C_2S-C_3P . If more than 20 mass% of Na_2SiO_3 was added to the C_2S-C_3P sample, a new solid solution phase was

observed, which can be characterized as $2\text{CaO}\cdot\text{SiO}_2\text{-}2\text{CaO}\cdot\text{Na}_2\text{O}\cdot\text{P}_2\text{O}_5$ ($\text{C}_2\text{S-C}_2\text{NP}$). This newly formed $2\text{CaO}\cdot\text{Na}_2\text{O}\cdot\text{P}_2\text{O}_5$ compound was previously confirmed to exist in the phase diagram of a $\text{Ca}_3(\text{PO}_4)_3\text{-CaNaPO}_4$ system [7].



According to the EPMA and XRD results, the reaction between the $\text{C}_2\text{S-C}_3\text{P}$ solid solution and Na_2SiO_3 at high temperatures can be described by Eq. (2.4). As a result of the Na_2SiO_3 modification, $\text{C}_2\text{S-C}_2\text{NP}$ solid solution and a $\text{CaO}\cdot\text{SiO}_2$ phase were formed. The P-condensed phase changed from the original $\text{C}_2\text{S-C}_3\text{P}$ to $\text{C}_2\text{S-C}_2\text{NP}$.

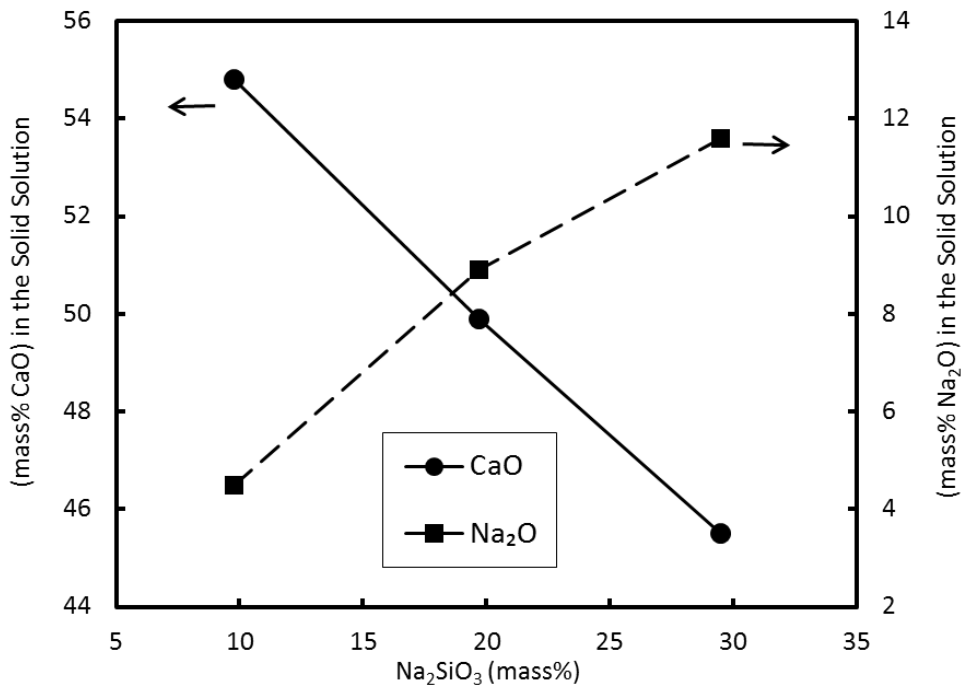


Fig. 2.6 Change in CaO and Na_2O contents in the modified solid solution with Na_2SiO_3 addition

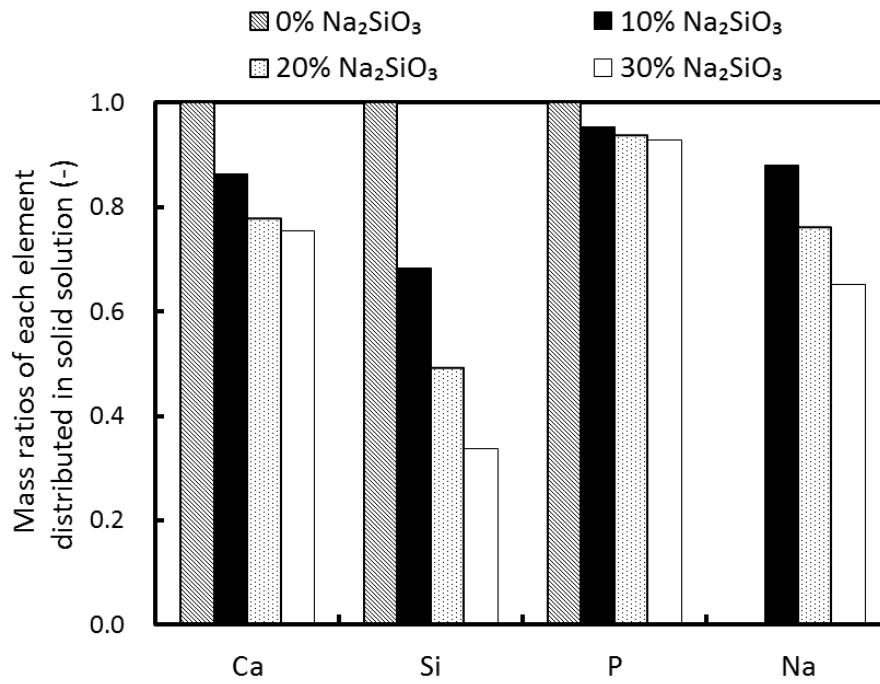


Fig. 2.7 Mass ratios of each element distributed in the modified solid solution

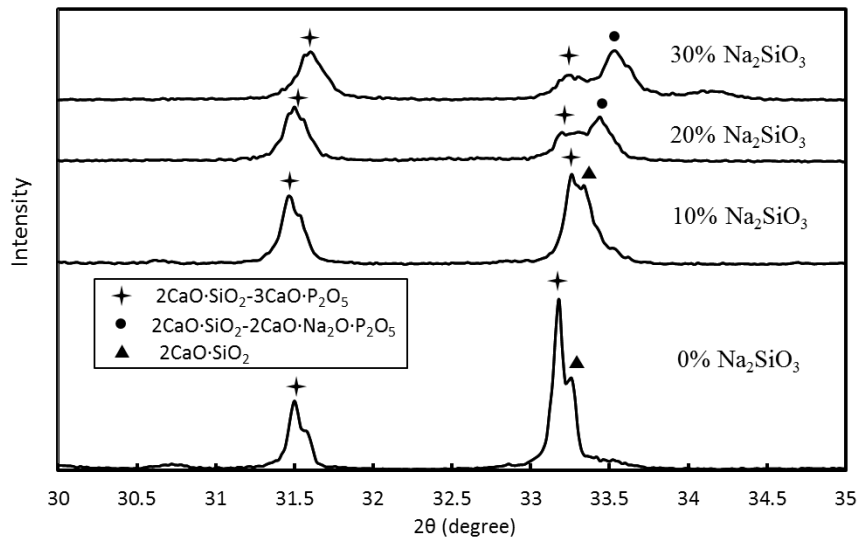


Fig. 2.8 XRD patterns of the solid solution samples with different mass ratios of Na₂SiO₃

2.2.3 Dissolution behavior of the modified solid solution

To examine the effect of the Na₂SiO₃ modification on the dissolution of P, the samples with different mass fractions of Na₂SiO₃ were leached by oxalic acid and citric acid at pH 7. Figure

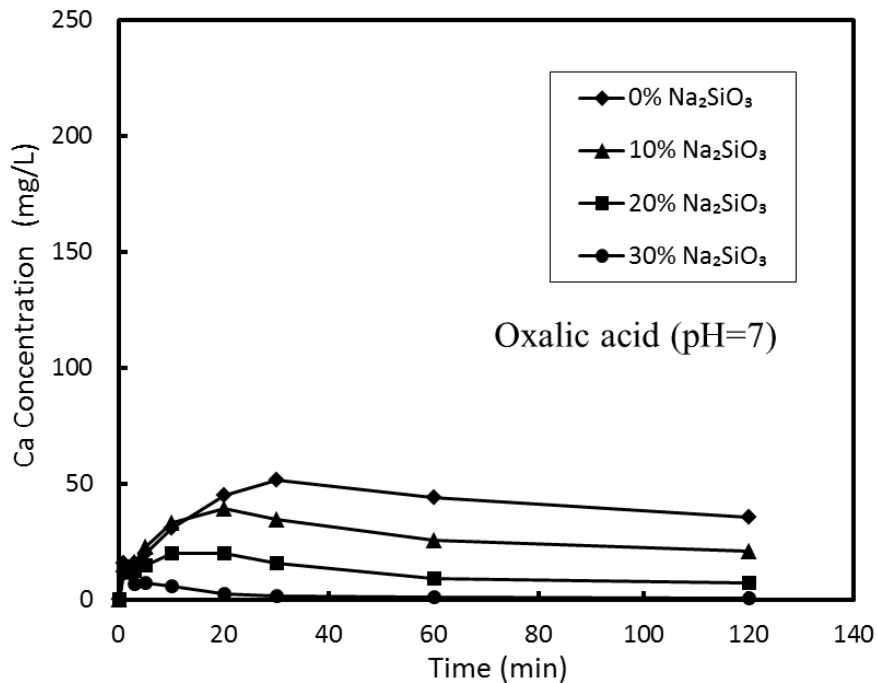
2.9 shows the change in the Ca and P concentrations in the oxalic solution at pH 7. The Ca concentration in the aqueous solution further decreased with an increase in the Na_2SiO_3 content in the sample. When the Na_2SiO_3 content exceeded 19.7 mass%, the Ca concentration was less than 10 mg/L after 120 min. Without modification, the P concentration had a little decrease after 20 min, reaching 31.6 mg/L. After Na_2SiO_3 modification, the P concentration in the aqueous solution increased significantly, with a larger addition of Na_2SiO_3 leading to better P dissolution. For the sample containing about 20 mass% of Na_2SiO_3 , the P concentration increased almost three times compared with the unmodified $\text{C}_2\text{S-C}_3\text{P}$. It indicates that Na_2SiO_3 modification could promote the dissolution of P from solid solution by oxalic acid.

The dissolution ratios of each element from the samples with different mass fractions of Na_2SiO_3 were calculated using Eq. 2.1, as shown in Fig. 2.10. The dissolution ratio of Ca was very low in each case, less than 3%. The differences between the dissolution ratios of Si and Na from each sample were small. Na_2SiO_3 modification caused a significant improvement in P dissolution. Compared with the $\text{C}_2\text{S-C}_3\text{P}$ solid solution, in the case of the solid solution containing about 20 mass% of Na_2SiO_3 , the dissolution ratio of P increased from 14.1% to 43.9%. However, further increase in the Na_2SiO_3 content did not result in a significant improvement in the P dissolution.

Figure 2.11 shows the changes in the Ca and P concentrations in the citric solution at pH 7. The Ca and P concentrations increased continuously with leaching time. In the beginning, the dissolution rate of solid solution was high, resulting in higher Ca and P concentrations after 20 min. Contrary to the dissolution behavior in the oxalic solution, the Ca concentration in the citric solution increases with an increase in the Na_2SiO_3 content. Although the Ca concentration was high, the P concentration in the citric solution was also high. With the increase in the

Na_2SiO_3 content, the P concentration increased as well. For the sample containing about 30 mass% of Na_2SiO_3 , the P concentration almost doubled, reaching 76.2 mg/L.

The dissolution ratios of each element from solid solution with different mass fractions of Na_2SiO_3 in the citric solution are shown in Figure 2.12. With an increase in the Na_2SiO_3 content, the dissolution ratios of Ca, P, and Na in the citric solution increased at pH 7. In the case of solid solution containing about 10 mass% of Na_2SiO_3 , the dissolution ratio of P increased slightly, however, a further addition of Na_2SiO_3 resulted in a significant improvement in P dissolution. For the solid solution containing about 30 mass% of Na_2SiO_3 , the dissolution ratio of P increased to 33.8%. Overall, Na_2SiO_3 modification promoted the dissolution of P from solid solution, but the dissolution ratio of P was lower in the citric solution than in the oxalic solution at pH 7.



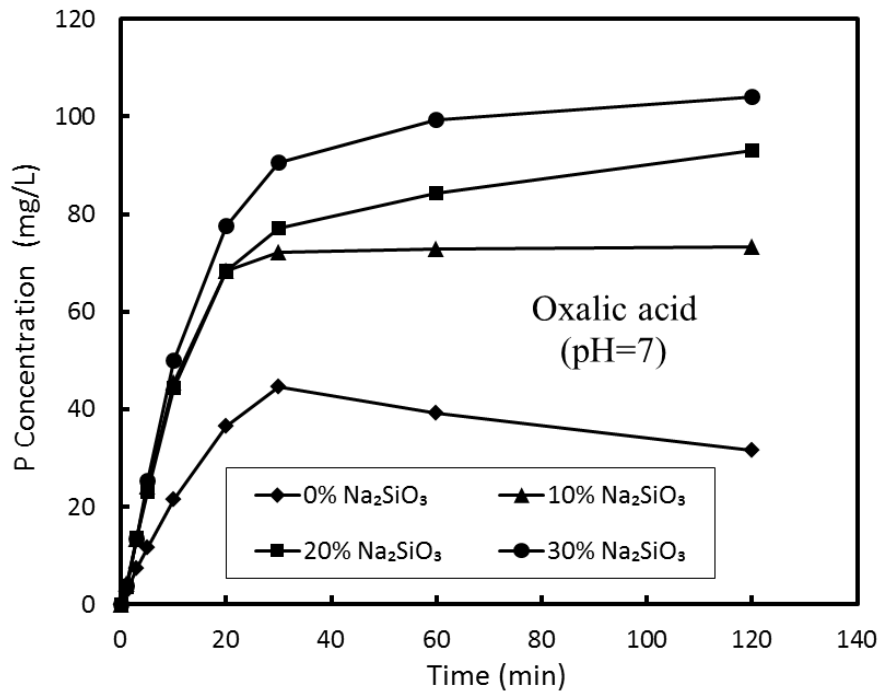


Fig. 2.9 Change in the Ca and P concentrations in the oxalic solution at pH 7

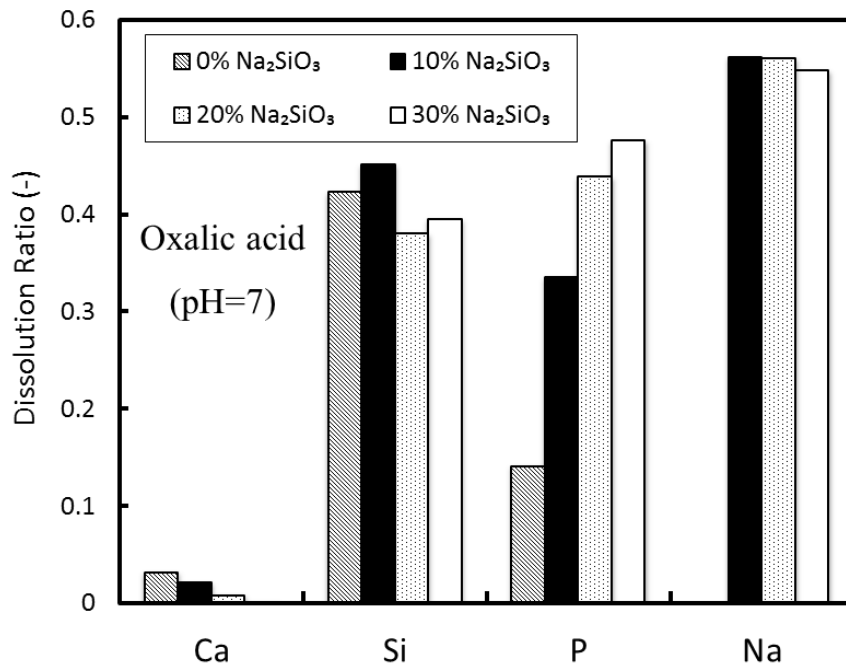


Fig. 2.10 Dissolution ratios of each element from the solid solution samples in the oxalic solution at pH 7

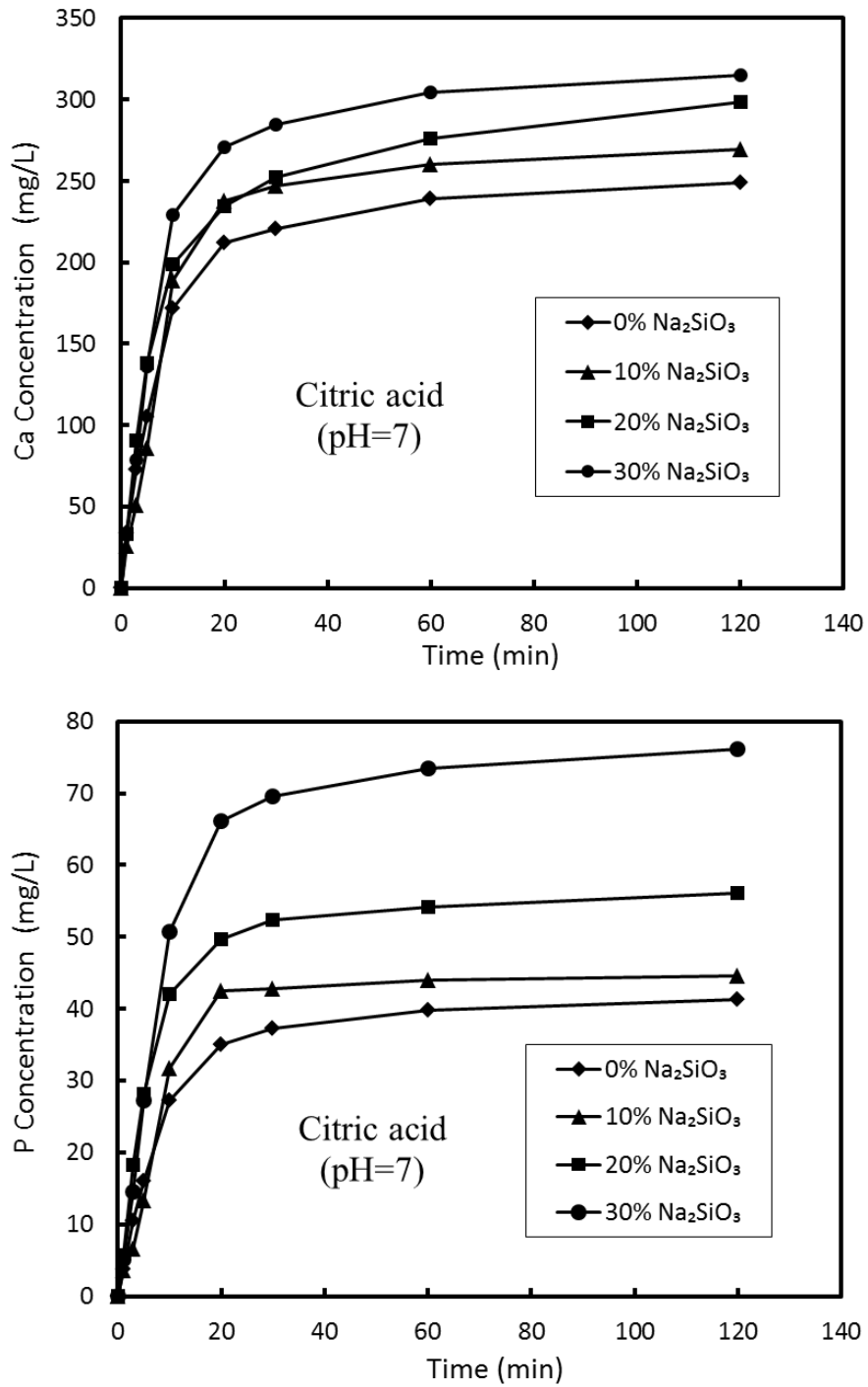


Fig. 2.11 Change in the Ca and P concentrations in the citric solution at pH 7

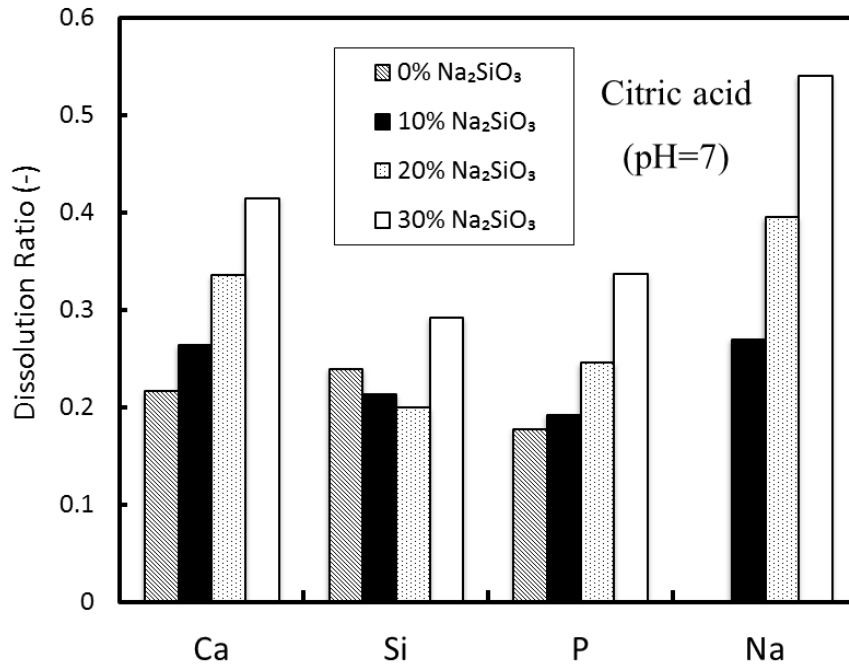
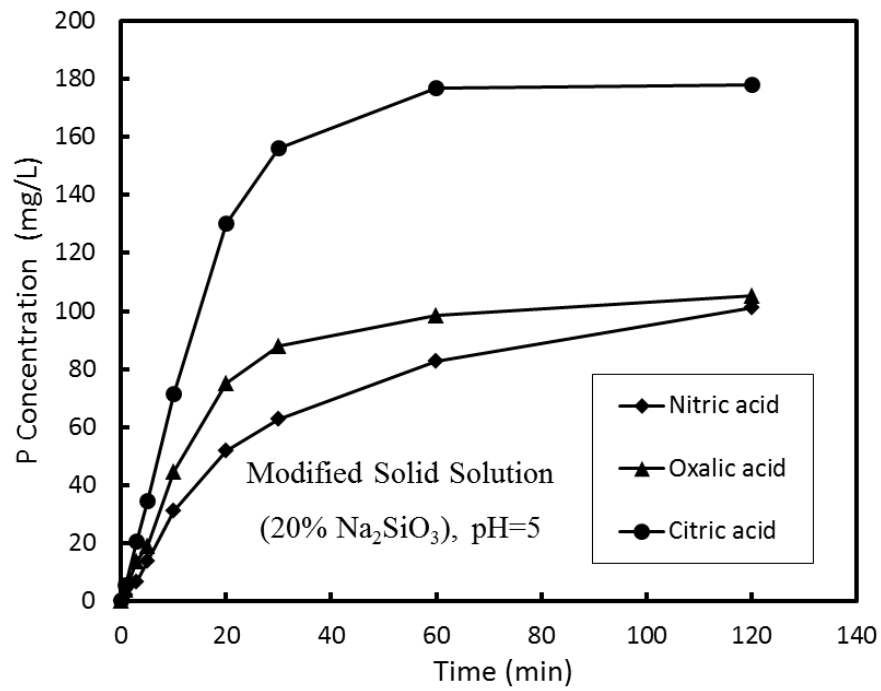
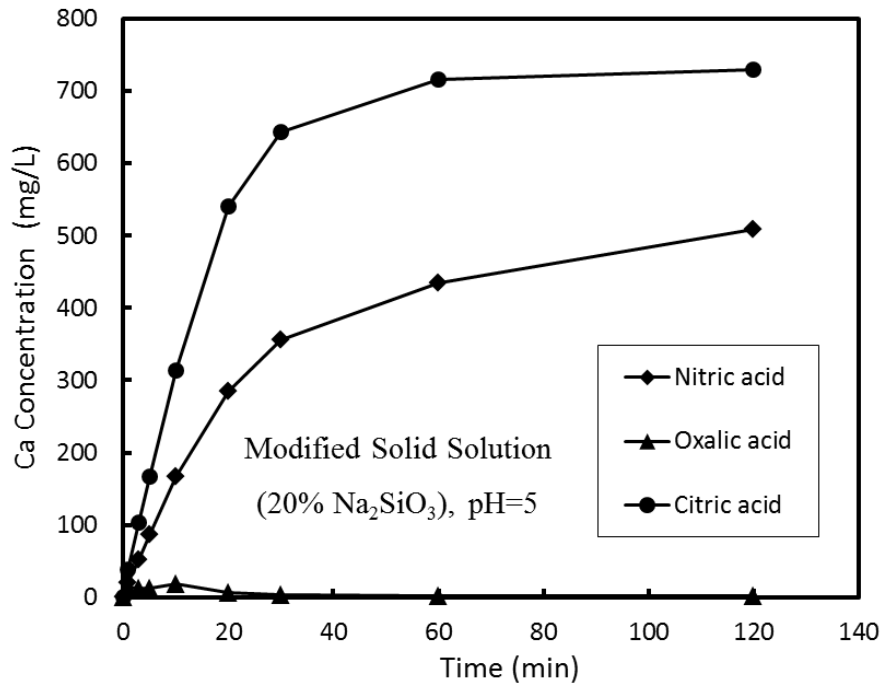


Fig. 2.12 Dissolution ratios of each element from the solid solution samples in the citric solution at pH 7

2.2.4 Dissolution behavior of the modified solid solution at various pH

In order to obtain the optimum leaching condition, the dissolution behavior of the solid solution containing about 20 mass% of Na₂SiO₃ was investigated at various pH. Figure 2.13 shows the change in the Ca, P, and Na concentrations in different acid solutions at pH 5. The Ca concentration in the nitric and citric solutions was relatively high (508.3 mg/L and 729.9 mg/L, respectively), while the Ca concentration in the oxalic solution was very low, only several mg/L. As the leaching progressed, the P concentration increased in each case, but after 60 min, they exhibited a little change. The P concentration in the nitric solution was almost equal to that in the oxalic solution (over 100 mg/L). In the citric solution, the P concentration was far higher than that in the nitric and oxalic solutions, reaching 178.2 mg/L. The Na concentration in the

citric solution was the highest, reaching 168.4 mg/L. Compared with Ca concentration, Na concentration was far lower in the citric and nitric solutions.



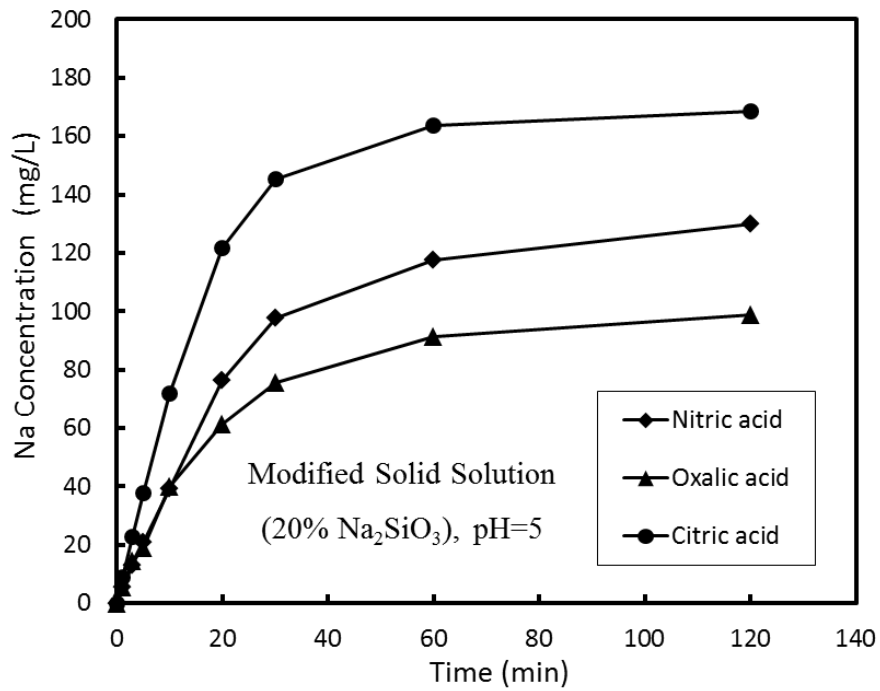


Fig. 2.13 Change in the Ca, P, and Na concentrations in different acid solutions at pH 5

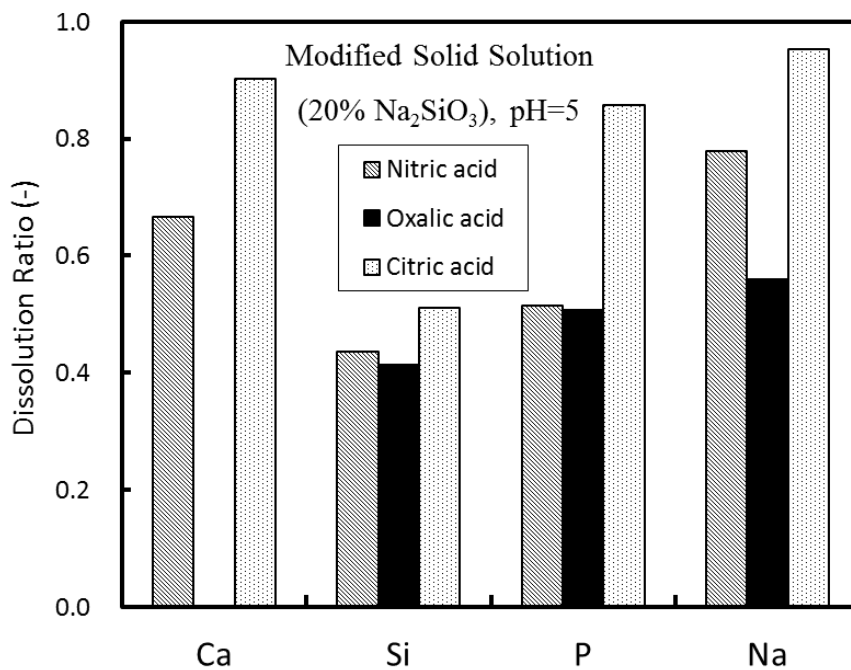


Fig. 2.14 Dissolution ratios of each element from the solid solution containing about 20 mass% of Na₂SiO₃ at pH 5

The dissolution ratios of each element in different acid solutions at pH 5 are shown in Fig. 2.14. In the nitric solution, approximately 66.7% of the Ca and 51.5% of the P was dissolved from the modified solid solution. In the oxalic solution, Ca did not dissolve and the dissolution ratio of P was 50.7%. In the citric solution, almost all of the Ca and P were dissolved; the dissolution ratio of P reached 85.7%. The dissolution ratio of Si had a little difference in different acid solutions.

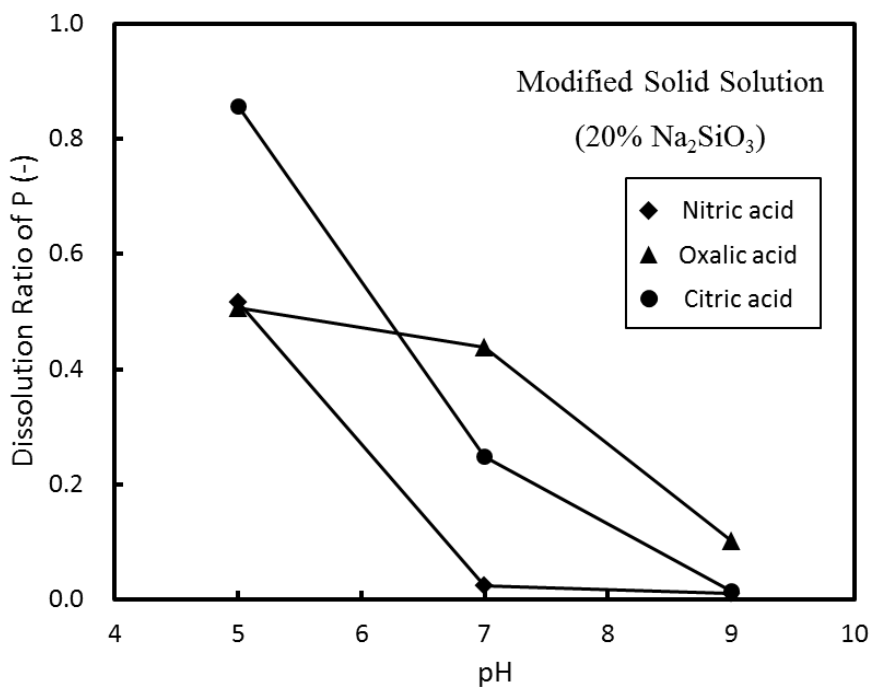


Fig. 2.15 Relationship between the dissolution ratio of P from the modified solid solution and pH in different acid solutions

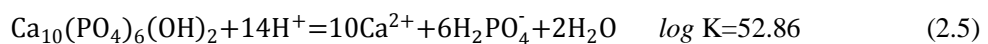
The relationship between the dissolution ratio of P from the modified solid solution and pH in different acid solutions is shown in Figure 2.15. The dissolution ratio of P increased with a decrease in the pH regardless of the leaching agent, but the observed trends varied depending on the pH range. In the nitric solution, the dissolution ratio of P was very low at higher pH ($\text{pH} \geq 7$), but when the pH decreased to 5, it increased to 51.5%. At higher pH, the dissolution ratio of P in the oxalic solution was the highest; however, it was difficult to further improve it by

decreasing the pH. At higher pH, the dissolution ratio of P was lower in the citric solution than in the oxalic solution. When the pH decreased to 5, a significant improvement in the P dissolution was observed: 85.7% of the total P could be dissolved in the citric solution. In summary, oxalic acid was beneficial for the dissolution of P in the aqueous solution at pH 7, but the dissolution ratio was far lower than unity; citric acid was the optimum leaching agent for extracting soluble P from the modified solid solution at pH 5.

2.3 Discussion

2.3.1 Effect of acid (leaching agent)

When Ca^{2+} and phosphate ions coexist in the aqueous solution, hydroxyapatite (HAP: $\text{Ca}_{10}(\text{PO}_4)_6(\text{OH})_2$) is easily formed at higher pH [8]. Therefore, there is a high possibility that P concentration in the aqueous solution is controlled by the presence of HAP. At pH 7, the predominant phosphate specie in the aqueous solution is H_2PO_4^- [9, 10]. The dissolution reaction of HAP and its equilibrium constant are described by Eq. (2.5). The thermodynamic data of each species are listed in Table 2.4 [11, 12]. The activity coefficients of dissolved substances were estimated using Debye-Hückel theory (described in Eq. (2.6)) [11], where A and B are constants which depends on temperature and solvent, z is valency of dissolved substances, α^0 is ion-size parameter, and I is ionic strength of the solvent. The values of A , B , and I applied in the present work were 0.509, 0.329, and 0.676, respectively [13, 14]. The values for ion-size parameter reported by Klotz [15] were used in the present work. Because the solution system was simple and the highest ionic strength was only 0.031 (when the modified solid solution was dissolved in the citric solution at pH 5), the ionic strength has little effect on the activity coefficient and the activity coefficient of all ions can be assumed as 1 in this study.



$$\log \gamma_i = -\frac{Az_i^2\sqrt{I}}{1+B\alpha^0\sqrt{I}} \quad (2.6)$$

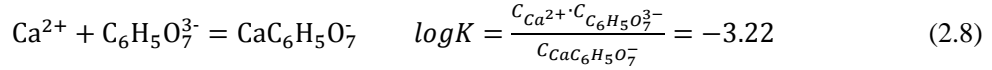
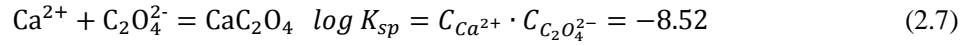
Table 2.4 Thermodynamic data of each species in the aqueous solution

Species	H ⁺	Ca ²⁺	H ₂ PO ₄ ⁻	HPO ₄ ²⁻	PO ₄ ³⁻	Ca ₁₀ (PO ₄) ₆ (OH) ₂	H ₂ O
ΔG J/mol	0	-553067	-1135173	-1094168	-1025547	-12514370	-237141

During C₂S-C₃P dissolution in the nitric solution, both Ca and P species dissolved simultaneously, but the Ca concentration was higher due to a higher CaO content in the C₂S-C₃P sample. With a continuous increase in the Ca concentration, the P concentration in the aqueous solution was near the saturation level determined by Eq. (2.5); as a result, the dissolved P precipitated in the form of HAP by the further increase in Ca concentration. Then, P concentration eventually decreased as the increase in Ca concentration. As shown in Fig. 2.16 and Table 2.5, the residue surface was mainly composed of Ca, P, and O elements after leaching in the nitric solution, which corresponds to precipitated phosphates. The relationship between the Ca and P concentrations in the aqueous solution was calculated using Eq. (2.5) at pH 7, as shown in Fig. 2.17. With the decrease in the Ca concentration, the P concentration in the aqueous solution increased. The observed point for the Ca and P concentrations in the nitric solution was located near the HAP solubility line indicating that the P concentration in the nitric solution reached saturation, and the high Ca concentration prevented the dissolution of P.

According to Eq. (2.7) [1], the dissolved Ca²⁺ in the oxalic solution easily reacts with C₂O₄²⁻ ions resulting in a CaC₂O₄ sediment. In Fig. 2.16 and Table 2.5, the residue surface mainly contained Ca, C, and O elements, but the P content was low indicating that the obtained residue was wrapped by the precipitated CaC₂O₄ after leaching. Due to the decrease in Ca concentration resulting from the formation of CaC₂O₄, a precipitation of phosphates was suppressed, and the P concentration increased dramatically. In Fig. 2.17, the observed Ca and P concentrations in the

oxalic solution was located below the HAP solubility line, which showed that such a low Ca concentration would not affect the dissolution of P.



$$C_{\text{Ca}^{2+}} = \frac{\sqrt{4K \cdot C_{\text{T.Ca}} + (C_{\text{T.Cit}} - C_{\text{T.Ca}} + K)^2} - C_{\text{T.Cit}} + C_{\text{T.Ca}} - K}{2} \quad (2.9)$$

In the citric solution, $\text{C}_6\text{H}_5\text{O}_7^{3-}$ species have a strong capacity to react with Ca^{2+} and form a $\text{CaC}_6\text{H}_5\text{O}_7^-$ complex, as shown by Eq. (2.8) [2]. The Ca^{2+} and $\text{CaC}_6\text{H}_5\text{O}_7^-$ concentrations in Eq. (2.8) can be calculated using Eq. (2.9) [16], where $C_{\text{T.Ca}}$ and $C_{\text{T.Cit}}$ (mol/L) are the total Ca^{2+} and $\text{C}_6\text{H}_5\text{O}_7^{3-}$ concentrations in the aqueous solution, respectively. The $\text{C}_6\text{H}_5\text{O}_7^{3-}$ concentration was determined by the final volume of the aqueous solution and the mass of the added citric acid. The remaining Ca^{2+} species, which did not react with the $\text{C}_6\text{H}_5\text{O}_7^{3-}$ ions, were identified as free Ca^{2+} in the aqueous solution. The calculated free Ca^{2+} concentrations are listed in Table 2.8. Although the total Ca^{2+} concentration was high, more than half of the Ca^{2+} existed in the form of $\text{CaC}_6\text{H}_5\text{O}_7^-$ complex, and the free Ca^{2+} concentration was only 3.09 mmol/L (123.6 mg/L). In Fig. 2.17, the concentration of free Ca^{2+} and P was located above the HAP solubility line. Allowing for the complexity of $\text{CaC}_6\text{H}_5\text{O}_7^-$ formation, it was considered that the P concentration reached saturation in the citric solution. In Table 2.5, the residue surface was mainly composed of Ca and P elements confirming the HAP formation. These results indicate that in the case of citric acid, the concentration of Ca^{2+} ions decreased by the formation of $\text{C}_6\text{H}_5\text{O}_7^{3-}$ complex and the P concentration in the aqueous solution increased which controlled by the solubility product of HAP. In summary, using oxalic acid or citric acid as the leaching agent could weaken the effect of dissolved Ca^{2+} on P precipitation thus improving the dissolution of P from the $\text{C}_2\text{S-C}_3\text{P}$.

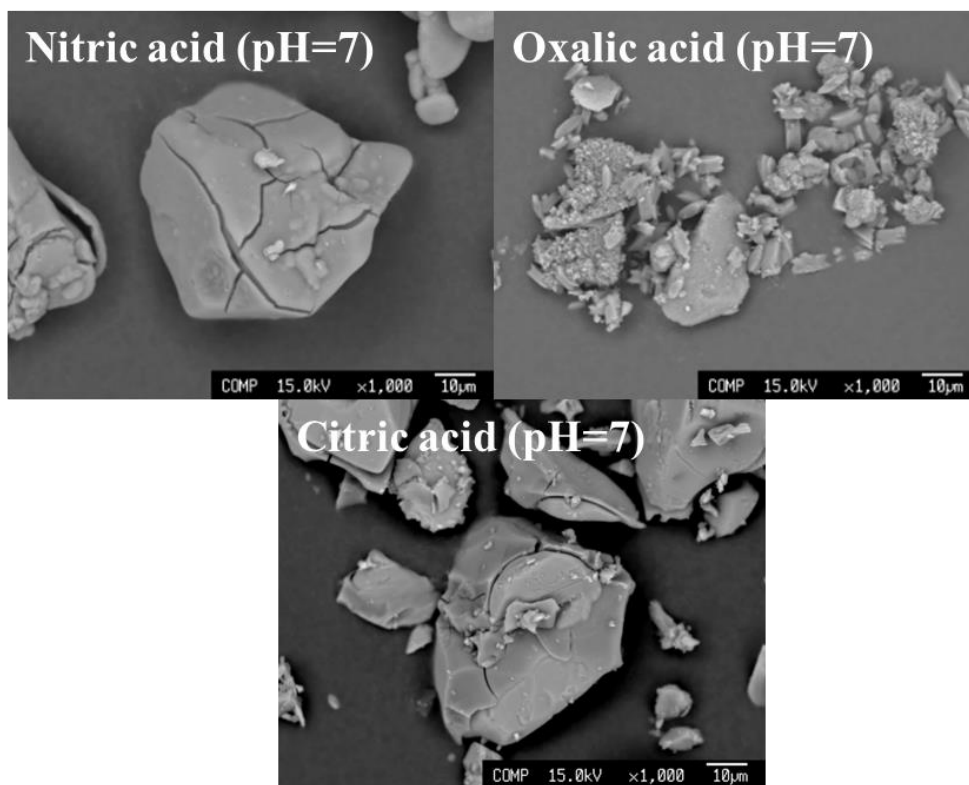


Fig. 2.16 Surface of the residues ($\times 1000$) after leaching in different acid solutions at pH 7.

Table 2.5 Compositions of residue surface after leaching in different acid solutions at pH 7 (mass%)

Sample	C	Ca	Si	O	P
Nitric acid	1.4	34.0	4.8	43.5	13.0
Oxalic acid	6.1	36.7	0.5	39.8	2.1
Citric acid	0.8	28.0	6.2	42.8	10.8

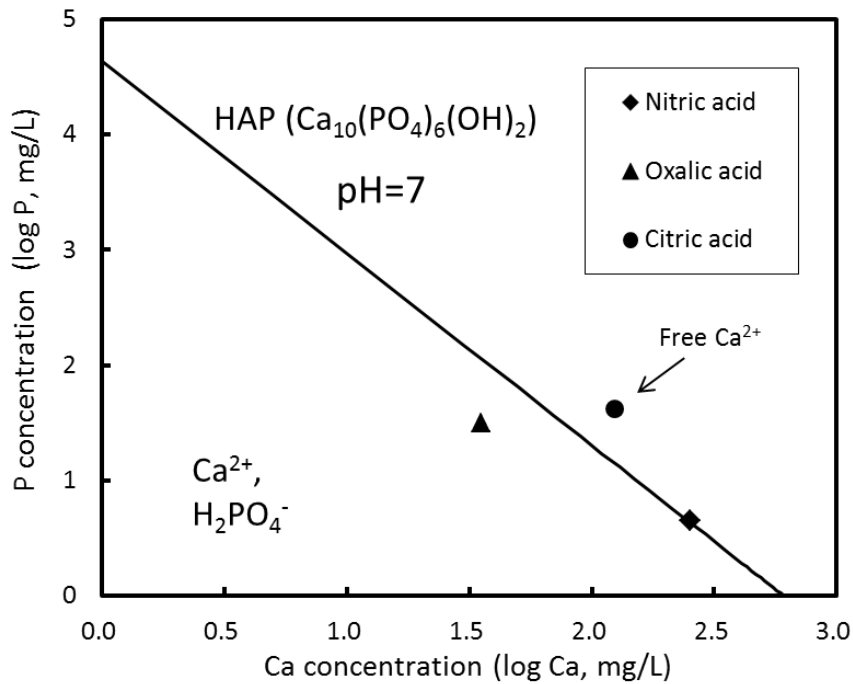


Fig. 2.17 HAP solubility line and leaching results for the C₂S-C₃P at pH 7

2.3.2 Effect of Na₂SiO₃ modification

In silicate or phosphate minerals, silicon and phosphorus form a tetrahedral unit with four oxygen atoms, SiO₄⁴⁻ and PO₄³⁻. Metal cations share the oxygen atoms on the corners of the tetrahedral structure [17]. Metal cations and silicon or phosphorus are combined by the bonds of Metal-O-Si or Metal-O-P. The electrical charge and cation size determines the bond strength of Cation-O. Shorter bond lengths and higher electric charges of the metal ion result in higher bond strengths [18]. To consider both the electric charge and the ionic radius simultaneously, the ionization potential (Z/r^2) is often utilized, as presented in Table 2.6 [19]. It shows that silicon and phosphorus can form strong bonds of Si-O and P-O. In the C₂S-C₃P sample, Ca-O-P bond exists. By Na₂SiO₃ modification, a part of Na₂O entered into the solid solution and combined with P₂O₅, and thus Na-O-P bond formed.

Table 2.6 Effective ionic radius for cations and anions and their coordination number and ionization potential

Ion	Coordination number	Ionic radius (nm)	Z/r^2 (nm ⁻²)
Na ⁺	6	0.102	96.1
Ca ²⁺	6	0.100	200.0
Si ⁴⁺	4	0.026	5917.1
P ⁵⁺	4	0.017	17301.0
O ²⁻	-	0.140	102.0

The dissolution of silicate or phosphate minerals in acid solutions depends on the breaking of the weaker bond in structure. Because the bond strength of P–O is significantly higher than that of Metal–O, dissolution would favor the breaking of the Metal–O bond. Thus, the metal dissolves to form metal cations and the phosphorus dissolves to form phosphate, PO₄³⁻ [17]. As listed in Table 2.6, the bond strength of Na–O is lower than that of Ca–O. Therefore, for the modified solid solution, Na–O–P bond is easier to be broken during leaching compared to Ca–O–P bond in the C₂S–C₃P, which promotes the dissolution of PO₄³⁻. This is the reason that 2CaO·Na₂O·P₂O₅ shows a higher solubility than Ca₃(PO₄)₂ in 2% citric acid solution.

The breaking of mineral structure and dissolution of metal cations requires the H⁺ cations from the added acid. Therefore, the acid consumption can reflect the dissolution behavior of the solid solution samples. Table 2.7 lists the amount of acid consumption during leaching. In both cases of oxalic and citric acid, with the increase in the additional amount of Na₂SiO₃, the acid consumption increased. This result demonstrates that the dissolution of solid solution was enhanced by Na₂SiO₃ modification.

For the modified solid solution, not only Ca but also Na was dissolved as cations in the aqueous solution. However, Na⁺ and phosphate ions are difficult to form phosphate precipitation in this condition [20], and the Na⁺ concentration was much lower than the Ca²⁺ concentration in each case. Therefore, the effect of the dissolved Na⁺ ions on phosphate precipitation is negligible.

Figure 2.18 shows the concentrations of (free) Ca and P for the modified solid solution comparing with the solubility of HAP. In the case of oxalic acid, the observed concentrations were located below the HAP solubility line indicating that the most of the dissolved Ca was precipitated as CaC_2O_4 and the effect on the dissolution of P can be ignored. After the Na_2SiO_3 modification, the dissolution ratio of P from the modified sample in the oxalic solution significantly increased due to a transformation from the $\text{C}_2\text{S-C}_3\text{P}$ to $\text{C}_2\text{S-C}_2\text{NP}$ with higher water solubility [4]. However, with an increase in the Na_2SiO_3 content, the dissolution ratio of P was difficult to improve further. The precipitated $\text{Ca}_2\text{C}_2\text{O}_4$ wrapped the unreacted solid solution particles, as shown in Fig. 2.16, and thus prevented continuous dissolution of the modified sample.

In the case of citric acid, the dissolution of the modified solid solution at pH 7 was also promoted, and the dissolution of Ca increased. Using Eq. (2.9), free Ca^{2+} concentrations were calculated (see Table 2.8). Most of the dissolved Ca^{2+} reacts with the citrate ions. With the increase in the Na_2SiO_3 content in the modified sample, the total Ca concentration in the aqueous solution increased, but the free Ca^{2+} concentration decreased. In Fig. 2.18, the calculated concentration of the free Ca^{2+} and the observed concentration of P were located near the solubility line of HAP. This result indicates that although the solubility of the modified solid solution increased, the P concentration at pH 7 was still determined by the solubility of HAP. Higher concentration of the free Ca^{2+} suppressed the P dissolution. Therefore, the dissolution ratio of P from the modified solid solution was lower in the citric solution than in the oxalic solution at pH 7.

Table 2.7 Consumptions of oxalic acid and citric acid during leaching at pH 7 (mL)

Acid	Sample	0%	10%	20%	30%
		Na ₂ SiO ₃	Na ₂ SiO ₃	Na ₂ SiO ₃	Na ₂ SiO ₃
Oxalic acid (0.1mol/L)		34.8	48.7	52.5	47.9
Citric acid (0.1 mol/L)		14.8	17.1	21.8	26.8

Table 2.8 Concentrations of free Ca²⁺ and complex in the citric solution (mmol/L)

Sample	pH	T. Cit	T. Ca	CaC ₆ H ₅ O ₇ ⁻	free Ca ²⁺
0% Na ₂ SiO ₃	7	3.75	6.23	3.14	3.09
10% Na ₂ SiO ₃		4.28	6.74	3.59	3.15
20% Na ₂ SiO ₃		5.46	7.46	4.53	2.93
30% Na ₂ SiO ₃		6.67	7.87	5.37	2.50
20% Na ₂ SiO ₃	5	15.96	18.24	13.99	4.25

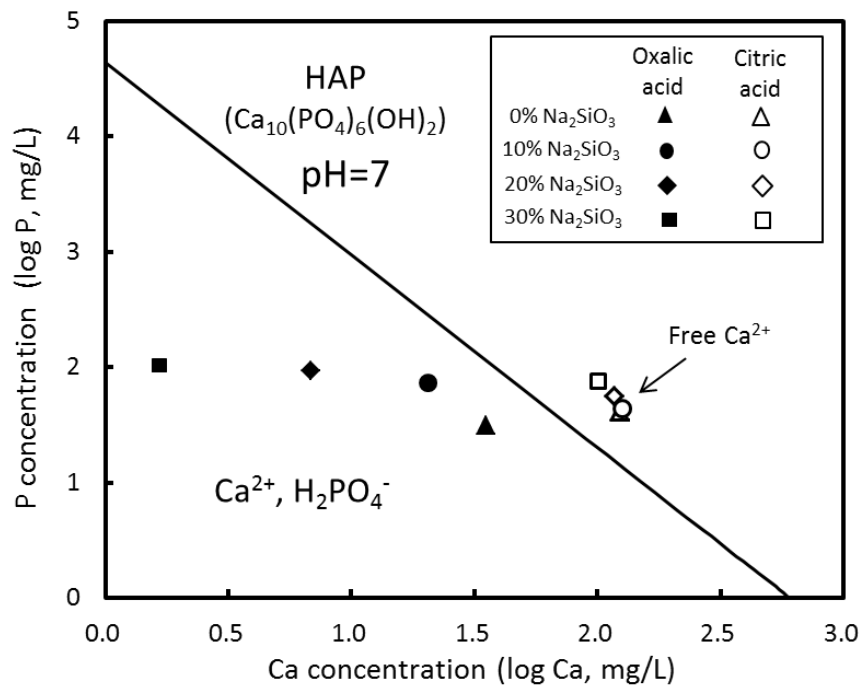


Fig. 2.18 HAP solubility line and leaching results for the modified solid solution at pH 7

2.3.3 Effect of pH

The solubility of HAP in the aqueous solution is greatly influenced by pH. Figure 2.19 shows the solubility line of HAP at pH 5 and 7, respectively. Compared with the conditions at pH 7, the solubility of HAP increased, and P and Ca can be dissolved in the higher concentration region at pH 5. The concentrations of Ca and P observed by the experiments at pH 5 are shown in Fig. 2.19. In the case of oxalic acid, as mentioned above, the precipitated CaC_2O_4 prevented the further dissolution of the solid solution. Therefore, it was difficult to further promote the dissolution of P in the oxalic solution by decreasing the pH.

In the nitric and citric solutions, the observed concentrations of P and Ca were located below the solubility line of HAP at pH 5. It indicates that the dissolution of P was not influenced by the Ca concentration at pH 5. However, higher Ca and P concentrations were obtained in the citric solution, showing that the dissolution of the modified solid solution was promoted. This is because the dissolution mechanism of minerals by citric acid is different from those by inorganic acid (nitric acid) [21]. Although citric acid is a weak acid, it is an excellent chelating agent and metal binder. Ligands or chelating agents aid mineral dissolution by specifically adsorbing on mineral surfaces and forming highly soluble complexes with metal cations. The formation of ligand–metal complexes at the mineral surface shifts the electron density toward the metal cations, which destabilizes the Metal–O lattice bonds and facilitates detachment of Metal–O–P bond into the aqueous solution [22]. In addition, ligands also enhance the dissolution of minerals by forming complexes with leached cations in the aqueous solution, thereby lowering the apparent solubilization of the mineral [23]. In summary, citric acid can dissolve minerals via two possible mechanisms: displacement of metal cations from the mineral matrix by H^+ ions, and the formation of soluble metal complexes and chelates. These beneficial mechanisms led to the effectiveness of citric acid in dissolving the modified solid solution.

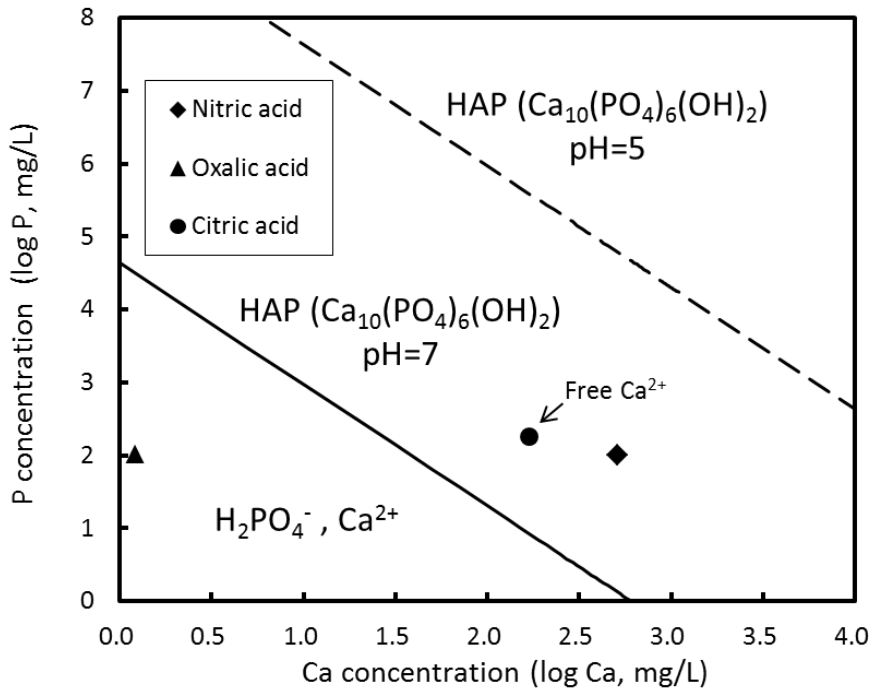


Fig. 2.19 HAP solubility line and leaching results for the modified solid solution (20% Na_2SiO_3) at pH 5

2.4 Summary

The effects of acid (leaching agent), Na_2SiO_3 modification, and pH on the dissolution behavior of the solid solution were investigated. The obtained results are summarized as follows:

- (1) When nitric acid was used as leaching agent, the dissolution ratio of P was not high at pH 7 because of phosphate precipitation. When oxalic acid or citric acid was used as leaching agent, Ca^{2+} ions were removed by the formation of CaC_2O_4 precipitate or $\text{CaC}_6\text{H}_5\text{O}_7^-$ complex, respectively. Phosphate precipitation in the aqueous solution was suppressed, and thus the dissolution ratio of P from the $\text{C}_2\text{S-C}_3\text{P}$ sample increased significantly.
- (2) When the $\text{C}_2\text{S-C}_3\text{P}$ sample was modified by adding Na_2SiO_3 at high temperatures, the solid solution containing Na_2O was formed. The composition located on the line between $2(\text{CaO}$,

$\text{Na}_2\text{O}\cdot\text{SiO}_2$ and $3(\text{CaO}, \text{Na}_2\text{O})\cdot\text{P}_2\text{O}_5$. By XRD analysis, $2\text{CaO}\cdot\text{SiO}_2\text{-}2\text{CaO}\cdot\text{Na}_2\text{O}\cdot\text{P}_2\text{O}_5$ phase was detected, which indicated that Na_2O substituted for the CaO in C_3P .

- (3) By Na_2SiO_3 modification, the dissolution of P in the oxalic and citric solutions was promoted. With an increase in the Na_2SiO_3 content, the dissolution ratio of P increased. As the acid consumption to keep pH was increased by the Na_2SiO_3 modification, the solid solution of $2\text{CaO}\cdot\text{SiO}_2\text{-}2\text{CaO}\cdot\text{Na}_2\text{O}\cdot\text{P}_2\text{O}_5$ would have better water solubility than $\text{C}_2\text{S}\text{-}\text{C}_3\text{P}$. However, at pH 7, the dissolution ratio of P from the modified solid solution containing about 20 mass% of Na_2SiO_3 reached only 43.9% in the oxalic solution.
- (4) As the pH decreased, the dissolution ratio of P significantly increased in the citric solution. At pH 5, the dissolution ratio of P from the modified solid solution containing about 20 mass% of Na_2SiO_3 reached 85.7%. However, in the oxalic solution, the precipitated CaC_2O_4 prevented the further dissolution of P by decreasing the pH. Therefore, citric acid was an optimal leaching agent for extracting soluble P from solid solution at pH 5.

References

1. R. W. Clark, J. M. Bonicamp: *Journal of Chemical Education*, 75 (1998), pp. 1182-1185.
2. J. Muus, H. Lebel: *Mathematisk-fysiske Meddelelser Danske Videnskabernes Selskab*, 13 (1936), pp. 1-16.
3. L. Lin, Y. P. Bao, M. Wang, W. Jiang, H. M. Zhou: *ISIJ International*, 54(2014), pp. 2746-2753.
4. R.P. Gunawardane, F.P. Glasser: *Journal of Materials Science*, 14(1979), pp. 2797-2810.
5. T. Teratoko, N. Maruoka, H. Shibata, S. Kitamura: *High Temperature Material Process*, 31(2012), pp. 329-338.
6. M. Numata, N. Maruoka, S.J. Kim, S. Kitamura: *ISIJ International*, 54(2014), pp. 1983-1990.
7. J. Ando: *Bulletin of the Chemical Society of Japan*, 1958, pp. 201-205.
8. M. Bohner, J. Lemaitre, T. A. Ring: *Journal of Colloid and Interface Science*, 190(1997), pp. 37-48.
9. S. Recillas, V. Rodríguez-Lugo, M.L. Montero, S. Viquez-Canoc, L. Hernandez, V.M. Castaño: *Journal of Ceramic Processing Research*, 13 (2012), pp. 5-10.
10. Kagakubinran, Kisohen, ed. by The Chemical Society of Japan, Maruzen Publishing, Tokyo, 1984.
11. T. Futatsuka, K. Shitogiden, T. Miki, T. Nagasaka and M. Hino: *ISIJ International*, 44 (2004), pp. 753-761.
12. A. L. Iglesia: *Estudios Geológicos*, 65 (2009), pp. 109-119.
13. S. Okabe, I. Hirota, K. Shimizu: *Chemistry of Ocean*, Tokai University Press, Tokyo, 1980.
14. S. Okabe, S. Kanamori, Y. Kitano, K. Saruhashi, Y. Sugiyura, Y. Sugimura, M. Tsuchiya, H. Tsubota, Y. Horibe, S. Matsuo, Y. Miyake: *Chemistry of Seawater*, Tokai University Press, Tokyo, 1970.
15. I. M. Klotz: *Chemical Thermodynamics*, W. A. Benjamin, NY, 1964.
16. A. B. Hastings, F. C. McLean, L. Eichelberger: *Journal of Biological Chemistry*, 107 (1934), pp. 351-370.
17. F.K. Crundwell: *Hydrometallurgy*, 149(2014), pp. 265-275.
18. I. Sohn, D.J. Min: *Steel Research International*, 83(2012), pp. 611-630.
19. R.D. Shannon: *Acta Crystallographica Section A*, A32(1976), pp. 751-767.
20. S.J. Markich, P.L. Brown: *Thermochemical Data for Environmentally-relevant Elements*, ANSTO Environment Division, NSW, 1999.
21. W. Astuti, T. Hirajima, K. Sasaki, N. Okibe: *Minerals Engineering*, 85(2016), pp. 1-16.
22. W. Stumm: *Chemistry of the Solid-Water Interface*, John Wiley and Sons Inc., New York, 1992.
23. V. Prigiobbe, M. Mazzotti: *Chemical Engineering Science*, 66(2011), pp. 6544-6

3 Dissolution behavior of P from modified steelmaking slag with Na₂O addition

In the previous chapter, we determined that Na₂O modification and using citric acid as the leaching agent promoted the dissolution of P from the C₂S-C₃P solid solution. On the basis of these results, the dissolution behavior of the synthesized steelmaking slag was studied in this chapter. The slag with high P₂O₅ content was modified by Na₂SiO₃ addition, and then leached by citric acid. To obtain the optimum conditions for selective leaching of P, the effects of Na₂O content and pH on the dissolution behavior of the modified slag were investigated.

Cooling rate of the molten slag significantly affects not only the size of the crystals but also the fraction of each mineralogical phase. Slow cooling promoted the formation of dicalcium silicate with high P₂O₅ content in steelmaking slag, and some phases could be crystallized from the glassy phase [1]. It was clarified that some elements were easier to dissolve from amorphous slag than from crystalline slag [2, 3]. Consequently, it is expected that decreasing cooling rate of the molten slag would affect the dissolution behavior of each phase in the aqueous solution, and then the effect of the cooling rate on the dissolution behavior of the modified slag was investigated.

The practical steelmaking slag mainly consists of CaO-SiO₂-Fe₂O₃ system, and some of the iron oxide exists in the form of FeO. It has been reported that when FeO was used as iron oxide, the dissolution ratio of P from slag in the aqueous solution was much lower than when Fe₂O₃ was used [4]. However, in the case of Na₂O modification, the dissolution behavior of the modified slag containing FeO was not clear. Therefore, the effect of the valency of Fe on the dissolution behavior of the modified slag was also investigated.

3.1 Experimental method

3.1.1 Synthesis of slags

To prepare the slag of CaO-SiO₂-Fe₂O₃ system, reagent-grade CaCO₃, SiO₂, Ca₃(PO)₄, Fe₂O₃, Fe, MgO, and Na₂SiO₃ were used. CaO was produced by calcining CaCO₃ in an Al₂O₃ crucible at 1273 K for at least 10 h. To synthesis FeO, electrolytic Fe powder and Fe₂O₃ was fully mixed in the molar ratio of 1: 1, and then heated to 1723 K in a Fe crucible under Ar atmosphere. After melting, the sample was taken out of furnace and quenched by water. The sample was crushed and the Fe particles were removed by magnetic separation. Table 3.1 lists the initial compositions of different slags. In the case of utilization of high-P iron ore, the P content in hot metal will increase, and a slag with high P₂O₅ content will be generated by efficient dephosphorization [5]. Therefore, the P₂O₅ content in each slag was fixed as 8.0 mass%. To increase dephosphorization efficiency and fluidity of slag, a relatively lower basicity slag saturated with 2CaO·SiO₂ is generally used in dephosphorization process [6]. Consequently, the basicity of the synthesized slag (mass% CaO)/(mass% SiO₂) was set as about 1.6. Because the total Fe content in the practical steelmaking slag was about 20 mass%, the Fe₂O₃ content in these synthesized slags was fixed about 30 mass%. Slag F and Slag G contain the different valency of Fe, but the total Fe content is same. The existence of MgO in slag was also taken into consideration because steelmaking slag contains MgO which mainly originates from the added flux and refractory corrosion.

According to slag composition, 10 g of the reagents were thoroughly mixed and first heated to form a homogeneous liquid phase. The heating pattern for synthesizing slag is shown in Fig. 3.1. In the case of slag contains Fe₂O₃, the mixed reagents was put in a Pt crucible and heated to 1823 K under air atmosphere. In the case of slag containing FeO, the mixed reagents was put in a Fe crucible and heated to 1723 K under Ar atmosphere. Then, the sample was cooled to 1623

K at a cooling rate of 3 K/min and held at this temperature for 20 min to precipitate solid solution. After heating, Slag A was cooled quickly by water; other slags were cooled in the furnace at a cooling rate of 5 K/min and withdrawn from the furnace at 1323 K, because the change in the mineralogical structural at temperatures below 1373 K is negligible [1]. Finally, the mineralogical composition of slag sample was analyzed by electron probe microanalysis (EPMA) and X-ray diffraction (XRD) analysis.

3.1.2 Leaching of slags

Table 3.1 Compositions of the synthesized slags and cooling method

Sample	CaO	SiO ₂	Fe ₂ O ₃	FeO	P ₂ O ₅	MgO	Na ₂ O	Cooling method
Slag A	34.5	21.5	29.0	-	8.0	3.0	4.0	Quenching
Slag B	34.5	21.5	29.0	-	8.0	3.0	4.0	Furnace cooling
Slag C	37.0	23.0	29.0	-	8.0	3.0	0	
Slag D	35.7	22.2	30.0	-	8.0	3.1	1.0	
Slag E	32.1	19.9	29.0	-	8.0	3.0	8.0	
Slag F	33.5	22.3	32.2	-	8.0	-	4.0	
Slag G	35.4	23.6	-	29.0	8.0	-	4.0	

The leaching apparatus is the same as that used in Chapter 2 (Fig. 2.1). The synthesized slag was ground into particles smaller than 53 μm (270 mesh). One gram of slag was added to 400 mL of distilled water which was agitated using a rotating stirrer at 200 rpm. The temperature of the aqueous solution was maintained at 298 K using an isothermal water bath. During slag dissolution, Ca²⁺ ions dissolved into the aqueous solution, which increased the pH. To keep the pH at a constant value, citric acid (0.1 mol/L) was used as the leaching agent and automatically added to the aqueous solution using a PC control system. In the previous studies [7], the concentrations of each element had little change after 120 min. Therefore, the leaching time was set as 120 min. About 5 mL of aqueous solution was sampled at adequate intervals and filtered

using a syringe filter ($< 0.45 \mu\text{m}$). The concentrations of each element in filtered water were analyzed using inductively coupled plasma atomic emission spectroscopy (ICP-AES). After leaching, the dissolved slag was collected by filtering all the aqueous solution. The dried residue was weighed and analyzed by XRD and EPMA. The conducted leaching experiments are summarized in Table 3.2.

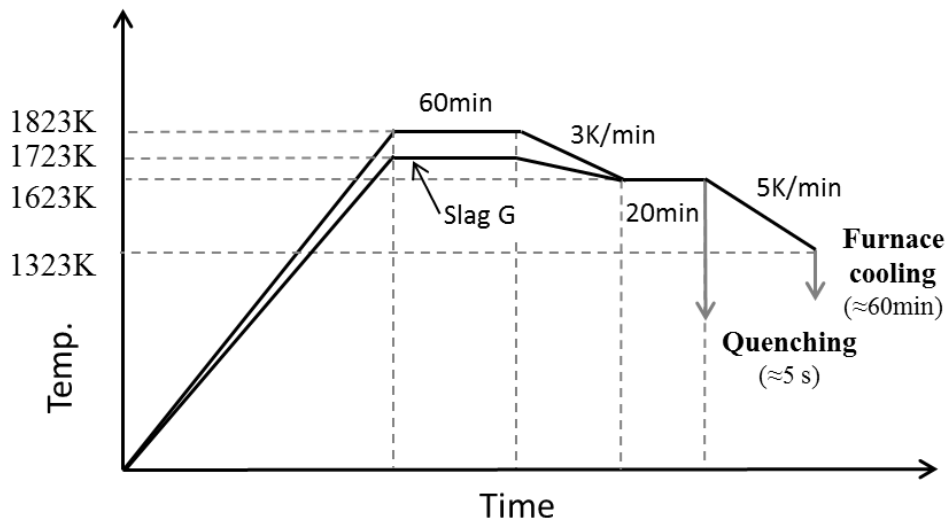


Fig. 3.1 Experimental condition for synthesizing slag

Table 3.2 Leaching condition of the synthesized slags

Sample	Leaching condition	
	pH	Leaching agent
Slag A	5, 6	Citric acid (0.1 mol/L)
Slag B	4, 5, 6, 7	
Slag C	6	
Slag D		
Slag E		
Slag F		
Slag G		

3.1.3 Chemical analysis of slag and residue

The concentrations of Ca, Fe, P, Mg, and Na were analyzed using ICP-AES. Deionized water was used throughout for sample preparation. The reagent-grade HCl, HNO₃, HF, HClO₄, and H₂O₂ were used as acid solutions. About 0.15 g of slag or residue powder (270 mesh) for ICP-AES analysis was prepared by grinding samples. Slag sample was placed in 100 mL Teflon beaker. After adding the H₂O (10 mL), HCl (3 mL), and HNO₃ (1 mL) to the Teflon beaker, the sample was heated at 423 K for 5 h. Si in the solution was eliminated by adding HF (1 mL), and then the excessive HF in the solution was removed by HClO₄ (1 mL). After the solution to dissolve the slag sample was dried thoroughly, residues in the Teflon beaker were re-dissolved by adding H₂O, HCl, and HNO₃ (10:3:1). Finally, the dissolution of metallic ions in the solution was conducted by the addition of H₂O (1 mL). Assuming that CaO, Fe₂O₃, MgO, P₂O₅, and Na₂O are the oxide components, the SiO₂ content was calculated by subtracting the sum of these components from 100 mass%.

3.2 Results and discussion

3.2.1 Effect of the cooling rate on the dissolution behavior of slag

3.2.1.1 Mineralogical composition of slags with different cooling rates

Typical cross sections of the modified slags which were cooled at different cooling rates are shown in Fig. 3.2. Table 3.3 lists the average compositions of each phase in different slags. The quenched slag consisted mainly of two phases. The black phase, which contains about 26 mass% of P₂O₅, was the solid solution. The other phase of the CaO-SiO₂-Fe₂O₃ system was considered the matrix phase. The Na₂O content in the solid solution was nearly twice as much as that in the matrix phase. The high distribution ratio of P₂O₅ between the solid solution and the matrix phase indicated that most of the P was concentrated in the solid solution. In addition to some large solid solution particles, many fine solid solution particles were also precipitated and

distributed in the matrix phases. In the case of furnace cooling, another phase formed, and the slag consisted mainly of three phases. The white phase that was rich in Fe_2O_3 and MgO was considered the magnesioferrite phase. Because the composition of the solid solution differed little from that observed in the quenched slag, the magnesioferrite phase was thought to be formed by decomposition of the matrix phase, which resulted in a decrease in the Fe_2O_3 content in the matrix phase. No fine solid solution particles were observed in the furnace-cooled slag, indicating that slow cooling was beneficial for the aggregation of solid solution. The results obtained by Numata *et al.* [7] also demonstrated this point: a coarsening of the precipitated solid solution occurred during slow cooling and holding at 1673 K for a long time period. For the furnace-cooled slag, the P_2O_5 content in the matrix phase was lower than that in the quenched slag.

Table 3.3 Compositions of each phase in the modified slags with different cooling rates (mass%)

Sample	Phase	CaO	SiO ₂	Fe ₂ O ₃	P ₂ O ₅	MgO	Na ₂ O
Slag A (Quenching)	1. Matrix phase	29.6	21.6	38.3	3.0	3.4	3.5
	2. Solid solution	50.9	14.3	0.9	25.9	1.1	6.8
Slag B (Furnace cooling)	1. Matrix phase	34.4	33.1	25.9	1.1	1.5	3.9
	2. Solid solution	51.4	15.6	0.9	25.4	0.3	6.4
	3. Magnesioferrite	1.8	0	86.8	0	11.1	0.3

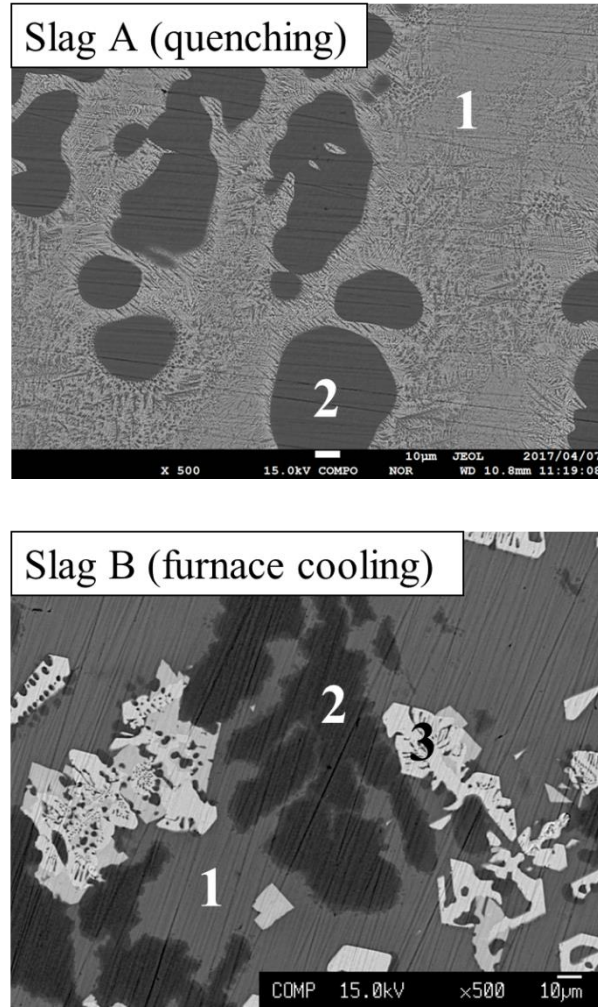


Fig. 3.2 Cross sections ($\times 500$) of the modified slags with different cooling rates

On the basis of the above EPMA results, the mass fractions of each phase in the slags with different cooling rates were estimated using Eqs. (3.1) and (3.2):

$$\sum(\text{mass\% MO})^i \times X^i = (\text{mass\% MO})_{\text{slag}} \quad (3.1)$$

$$\sum X^i = 1 \quad (3.2)$$

Equation (3.1) describes that the sum of oxide content in each phase was equal to the oxide content in slag, where X^i is the mass fraction of phase i , $(\text{mass\% MO})^i$ is the content of oxide MO in phase i measured by EPMA (shown in Table 3.3), and $(\text{mass\% MO})_{\text{slag}}$ is the content of oxide MO in slag. The contents of major oxides (CaO, SiO₂, Fe₂O₃, and P₂O₅) were used for

calculation, and the average of these calculations was defined as the mass fraction of each phase in slag. The calculated mass fractions of each phase are shown in Fig. 3.3. The mass fraction of solid solution in the quenched slag was approximately 25%. Decreasing cooling rate increased the mass fraction of solid solution, while that of matrix phase decreased due to the precipitation of magnesioferrite phase from the matrix phase. In the furnace-cooled slag, the mass fractions of solid solution and matrix phase were approximately 29% and 52%, respectively. Because of the similar composition of solid solution in these slags, it shows that slow cooling facilitated the enrichment of P_2O_5 in the solid solution.

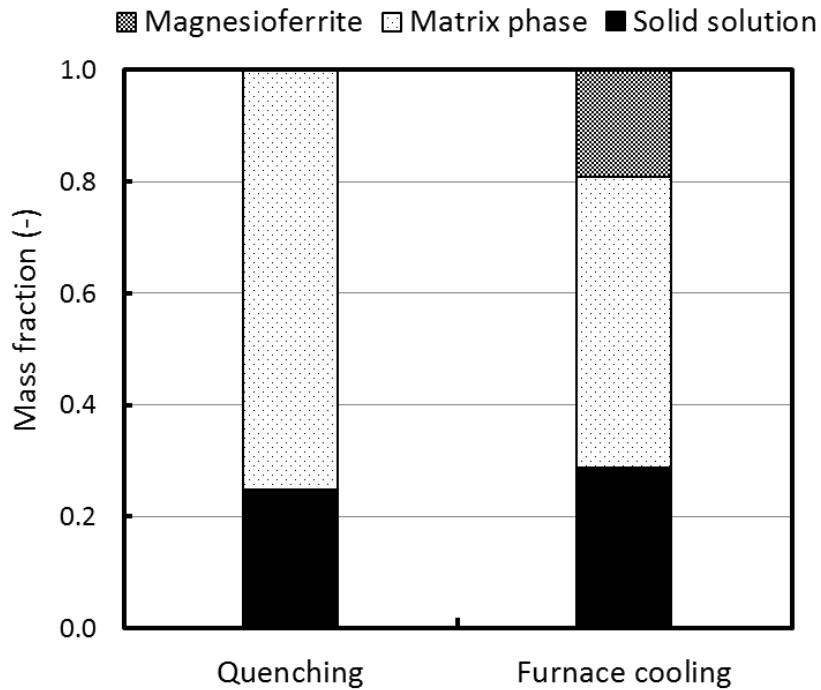


Fig. 3.3 Mass fractions of each phase in slags with different cooling rates

Using the above results, the mass fractions of each oxide distributed in each phase were evaluated as:

$$Y_{MO}^i = \frac{X^i \cdot (\text{mass\% MO})^i}{(\text{mass\% MO})_{\text{slag}}} \quad (3.3)$$

where Y_{MO}^i is the mass fraction of oxide MO distributed in phase i . The calculated results are shown in Fig. 3.4. Although the mass fraction of solid solution was not high, most of the P_2O_5 was concentrated in the solid solution because of its high P_2O_5 content. The majority of the CaO and SiO_2 were distributed in the matrix phase. As the cooling rate decreased, the mass fractions of CaO, SiO_2 , and P_2O_5 distributed in the solid solution increased, especially P_2O_5 . In the case of furnace cooling, more than 90% of the P_2O_5 was concentrated in the solid solution; the mass fractions of CaO and SiO_2 distributed in the solid solution were 45.5% and 21.2%, respectively.

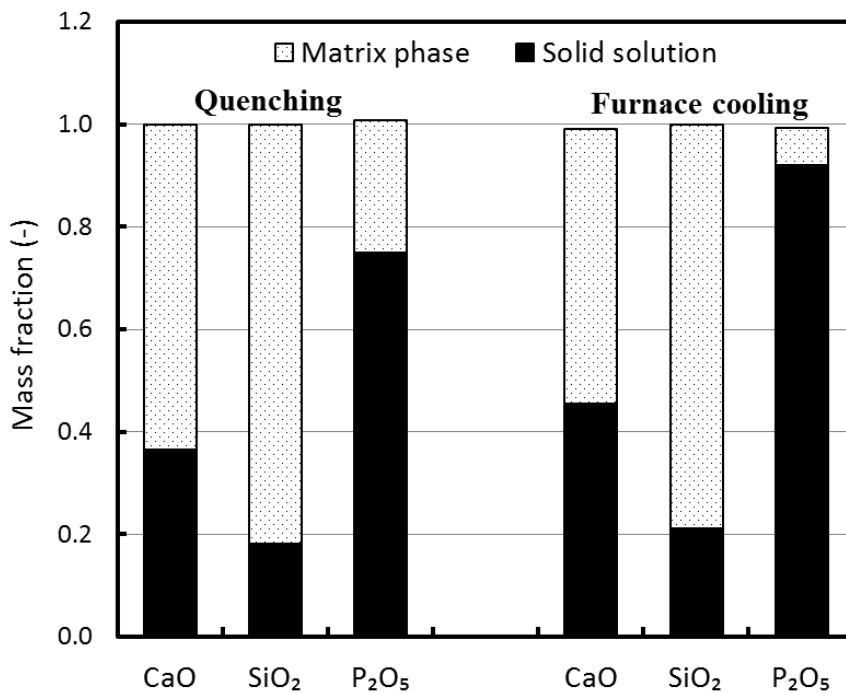
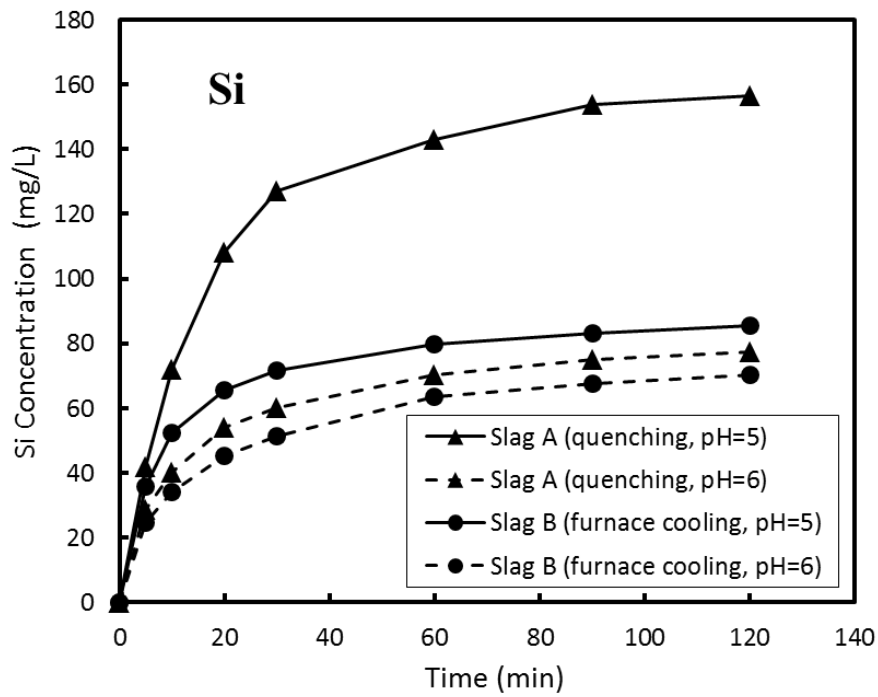
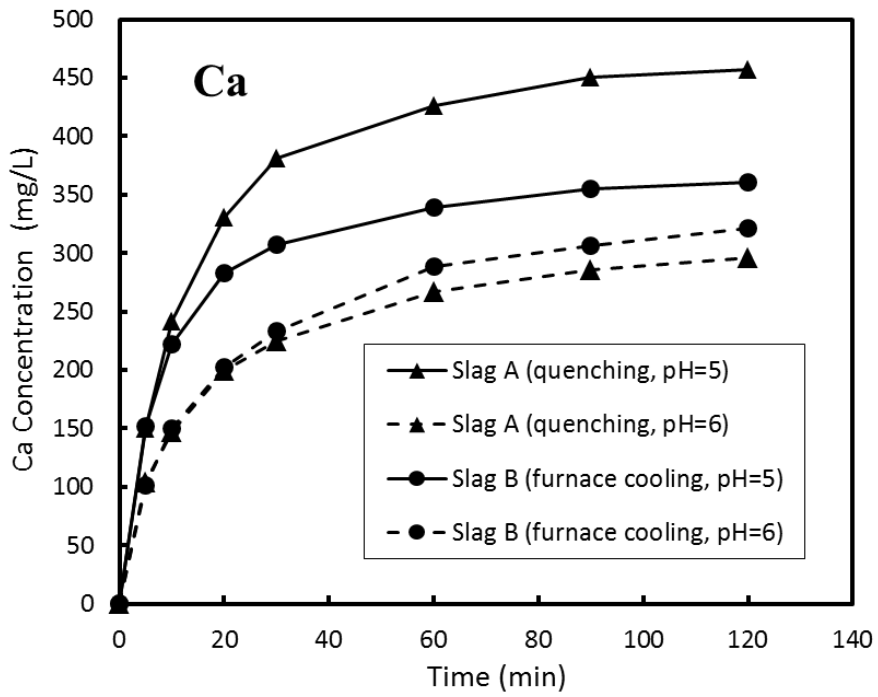


Fig. 3.4 Mass fractions of each oxide distributed in each phase

3.2.1.2 Dissolution behavior of slags with different cooling rates

The change in the concentrations of each element in the aqueous solution at pH 5 and 6 is shown in Fig. 3.5. For all the elements, the concentrations increased with leaching time. The

dissolution rates were initially fast, but after 60 min, the concentrations exhibited little change. According to Fick's First Law, the concentration gradient between the reaction interface and the aqueous solution decreased with the leaching time, resulting in a decrease in the diffusion flux. Therefore, the dissolution rate decreased. The Ca concentration was the highest among the dissolved elements. At pH 6, the Ca concentration of the furnace-cooled slag was a little higher than that of the quenched slag, reaching 320.8 mg/L after 120 min. The quenched slag showed higher Si and Fe concentrations. For each slag, the Fe concentration was far lower than those of other elements at pH 6. In the case of quenching, the Fe concentration was only 12.5 mg/L after 120 min. The P concentration of the furnace-cooled slag was higher than that of the quenched slag. It increased to 67.3 mg/L after 120 min. When the pH decreased to 5, the dissolution rate of slag increased, leading to higher concentrations of each element in a shorter time. In addition, the concentrations of each element were higher than those at pH 6. As the pH decreased, the dissolution of the quenched slag was significantly promoted compared to the furnace-cooled slag. The Ca concentration of the quenched slag increased from 296.2 mg/L to 456.6 mg/L. At pH 5, the Si and Fe concentrations of the quenched slag were 156.5 mg/L and 64.2 mg/L, respectively, after 120 min, which were far higher than those of the furnace-cooled slag. In the case of furnace cooling, the Fe concentration was still at a low level, but the P concentration was higher, reaching 74.2 mg/L.



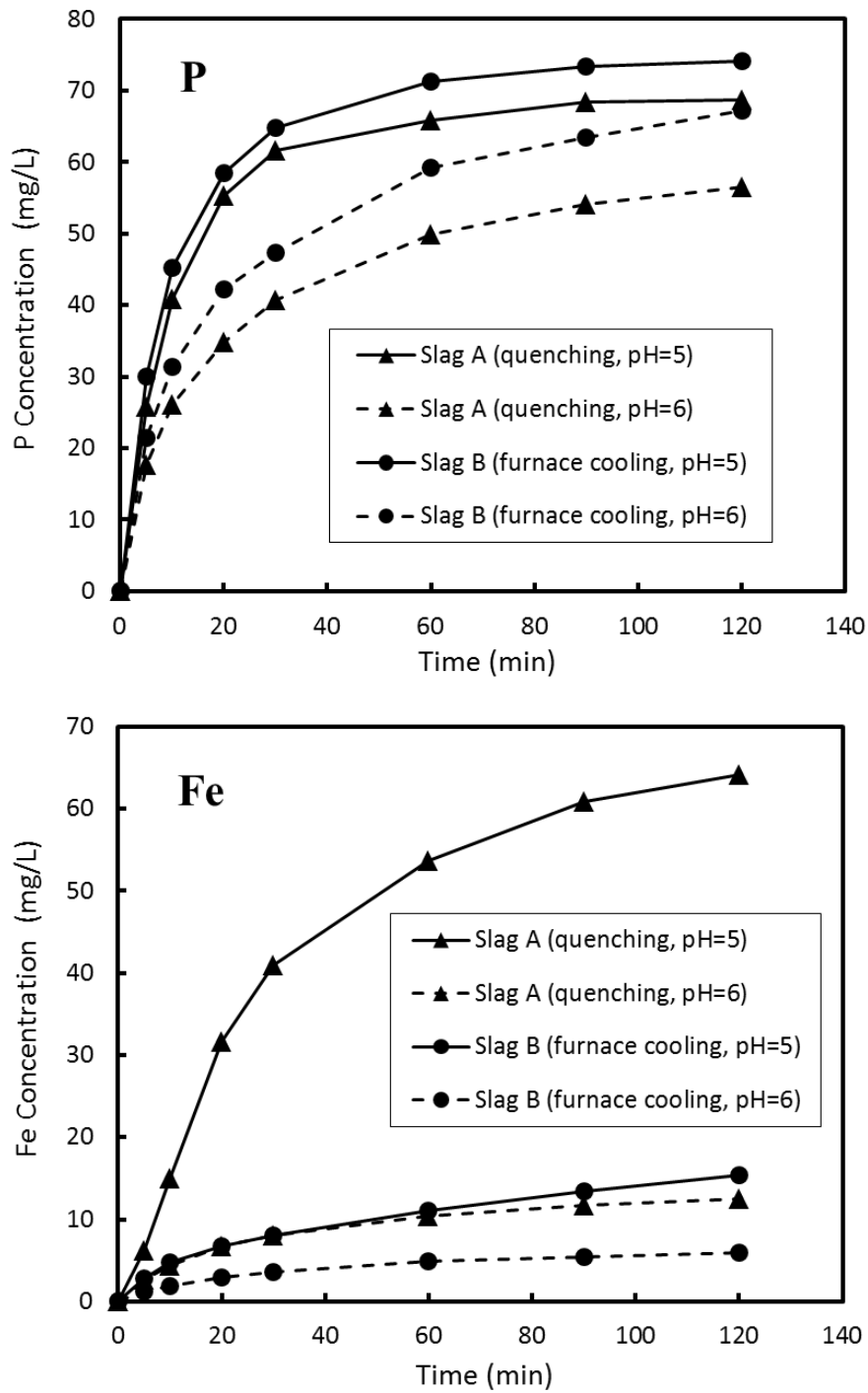


Fig. 3.5 Change in the concentrations of each element in the citric solution at pH 5 and 6

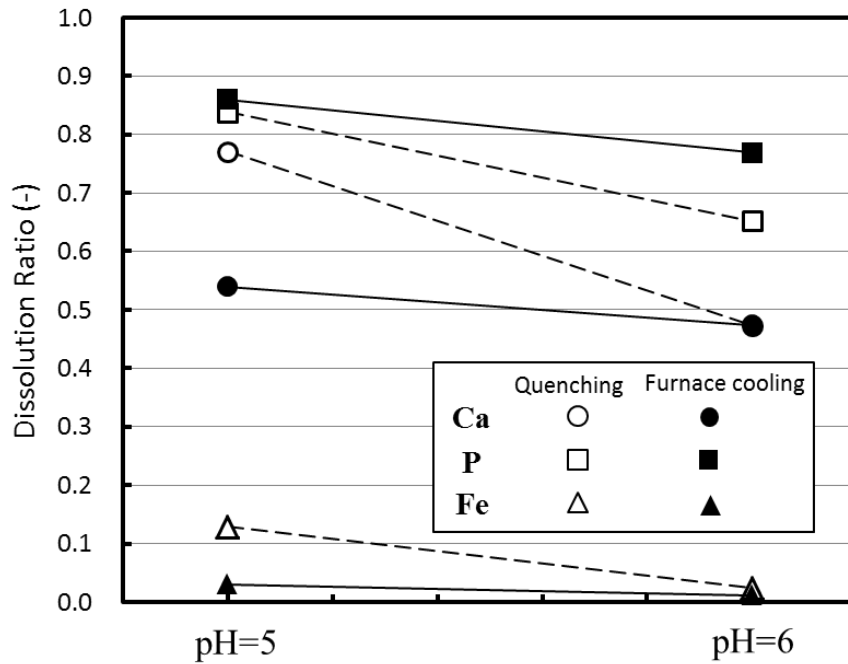


Fig. 3.6 Dissolution ratios of Ca, P, and Fe from slags with different cooling rates at pH 5 and 6

Table 3.4 Acid consumption during leaching of different slags at pH 5 and 6 (g)

pH	Sample	Slag A (quenching)	Slag B (furnace cooling)
	6		20.9
5		42.4	27.0

Table 3.4 lists acid consumption during leaching of different slags at pH 5 and 6. For the furnace-cooled slag, it consumed less citric acid during leaching compared to the quenched slag in each case. At pH 5, more citric acid was required to keep a constant pH value. In the case of the quenched slag, about 42.4 g of acid was consumed because of a large dissolution of slag.

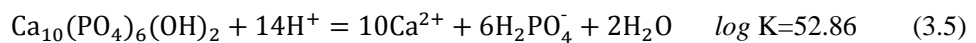
On the basis of leachate composition, the dissolution ratios of each element from slag were calculated using Eq. (3.4):

$$R_M = \frac{C_M \cdot V}{m_M} \quad (3.4)$$

where R_M is the dissolution ratio of element M from slag, C_M is the concentration of M after 120 min (mg/L), V is the final volume of the aqueous solution (L), and m_M is the mass of M in 1 g of the initial slag (mg). Figure 3.6 shows the calculated dissolution ratios of Ca, P, and Fe from slags with different cooling rates at pH 5 and 6. At pH 6, the dissolution ratios of Ca and Fe from each slag were almost the same, reaching 47.4%. The dissolution of Fe was difficult regardless of the cooling rate. A lower dissolution ratio of Fe indicated that the matrix phase was not dissolved. The dissolution ratio of P from the furnace-cooled slag was 76.9 %, which was higher than that from the quenched slag. When the pH decreased to 5, the dissolution of the quenched slag was promoted, resulting in higher dissolution ratios of Ca and Fe. The dissolution ratio of Fe was more than 10%, indicating that the dissolution of Fe-condensed phase occurred. In the case of furnace cooling, the dissolution ratios of each element increased slightly as the pH decreased. Only 3% of the Fe was dissolved from slag at pH 5. The dissolution ratio of P reached 85.9%, which was similar with that from the quenched slag. In summary, the furnace-cooled slag exhibited a higher dissolution ratio of P and a lower dissolution ratio of Fe than the quenched slag in each case. A decrease in the cooling rate was beneficial for the modified slag to achieve better selective leaching of P.

3.2.1.3 Discussion on the effect of cooling rate

As described in previous studies, Ca^{2+} and phosphate ions react easily and form $\text{Ca}_{10}(\text{PO}_4)_6(\text{OH})_2$ (hydroxyapatite, HAP) at higher pH condition (expressed in Eq. (3.5)), which determines the P concentration in the aqueous solution [8, 9].



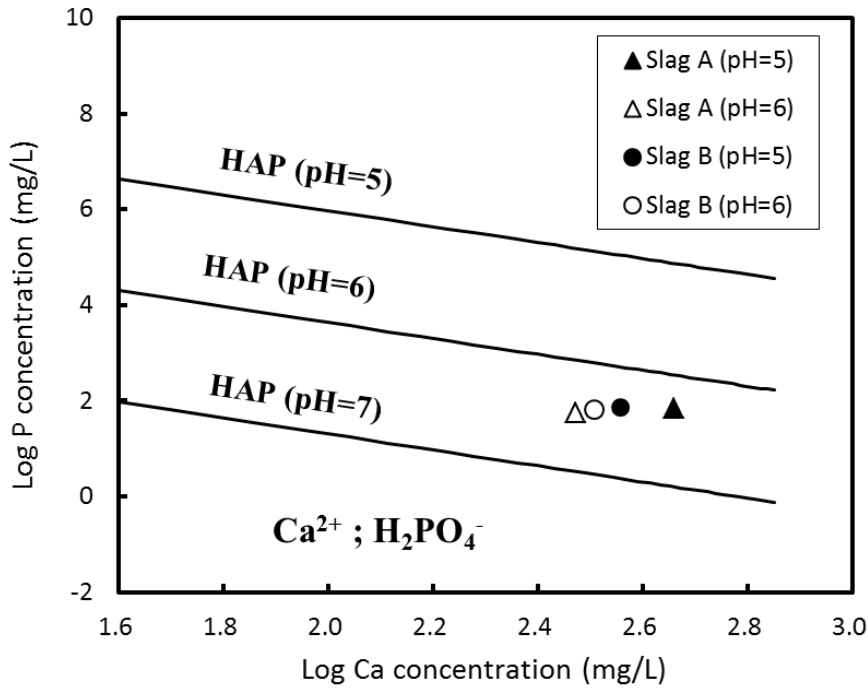


Fig. 3.7 Solubility lines of HAP and experimental results at various pH conditions

When the pH decreased to a lower level, the H^+ concentration increased, which facilitated dissolution of the solid solution. Figure 3.7 shows the solubility lines of HAP and experimental results at pH 5 and 6. Compared to that at pH 7, the solubility line of HAP at pH 6 moved to the region with higher Ca and P concentrations. The observed points of the present study (without considering the formation of $CaC_6H_5O_7^-$ complex) were located below this solubility line, indicating that P concentration did not reach saturation and HAP precipitate did not form in this case. Therefore, we did not consider phosphate precipitation in the following discussion.

To evaluate the dissolution behavior of solid solution, the presumed dissolution ratios of Ca and P from the solid solution were calculated using Eq. (3.6):

$$R_M^{SS} = \frac{C_M \cdot V}{m_M^{SS}} \quad (3.6)$$

where R_M^{SS} is the presumed dissolution ratio of element M from the solid solution, and m_M^{SS} is the original M mass in the solid solution (mg). Because most of the P was concentrated in the

solid solution, it was assumed that P dissolved only from the solid solution. On the basis of the above discussion, it was considered that the dissolved P from slag was measured in the aqueous solution without precipitates. Therefore, the presumed dissolution ratio of P from the solid solution (R_p^{SS}) could represent the dissolution ratio of solid solution. For Ca, if the presumed dissolution ratio (R_{Ca}^{SS}) exceeded unity, it indicated that the dissolution of Ca occurred not only from the solid solution but also from the matrix phase, because magnesioferrite was difficult to dissolve compared with other phases in the aqueous solution [10]. This value reflects the dissolution behavior of matrix phase. The larger this value, the more matrix phase was dissolved.

Figure 3.8 shows the presumed dissolution ratios of Ca and P from the solid solution under different cooling rates. In the case of furnace cooling, the presumed dissolution ratio of P (dissolution ratio of solid solution) was more than 85%, and that of Ca did not exceed unity largely at pH 5 and 6. It illustrates that almost all of the solid solution was dissolved from slag, and the matrix phase was barely dissolved. In the case of quenching, the presumed dissolution ratios of Ca and P were close to unit at pH 6, indicating that selective leaching of solid solution occurred. The practical dissolution ratio of P from the quenched slag was lower than that from the furnace-cooled slag. This was because the solid solution particles in the furnace-cooled slag aggregated and fine solid solution particles were not distributed in the matrix phase, which facilitated leaching of the solid solution. At pH 5, the presumed dissolution ratio of Ca was far greater than unity, indicating that a part of the matrix phase in the quenched slag was dissolved. The reason is explained as follows:

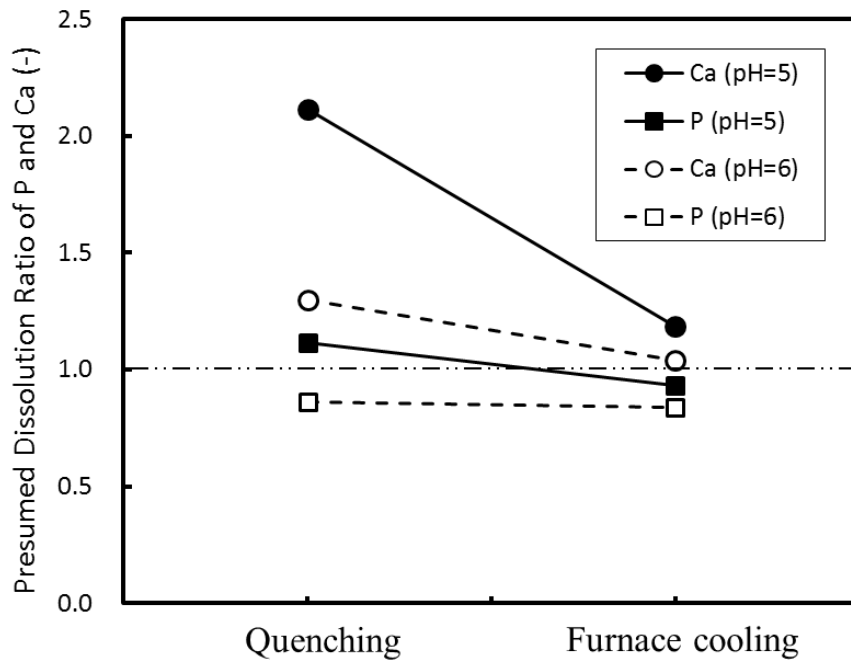


Fig. 3.8 Presumed dissolution ratios of Ca and P from the solid solution under different cooling rates

Matrix phase is a silicate glass of $\text{CaO-Fe}_2\text{O}_3\text{-SiO}_2$ system. As shown in Fig. 3.9, silicon forms a tetrahedral unit (SiO_4^{4-}) with four oxygen atoms, and complex network exists in silicate glass [11]. Shorter bond lengths and higher electric charges of the cation result in higher bond strengths [12]. The bond strength of Si-O is significantly higher than that of Metal-O. The dissolution of silicate minerals in acid solutions depends on the breaking of the weaker bond in structure [11]. In silicate glass, Fe^{3+} ions occupied both octahedral and tetrahedral sites [13, 14], as shown in Fig. 3.9. In the case of octahedrally coordinated, the Fe^{3+} ions, similar with Ca^{2+} ions, act as network modifier. In the case of tetrahedrally coordinated, Fe^{3+} ions act as network former, similar with SiO_4^{4-} . Because the bond length of Fe-O in the tetrahedral site is shorter than that in the octahedral site, it is considered that the bond strength of Fe-O in the tetrahedral site is higher. It has been reported that the fraction of Fe^{3+} ions in tetrahedral symmetry to the total Fe^{3+} ions decreased with increasing temperature [14]. The relative number of octahedral Fe^{3+} increased with increasing total ion content in the oxidized silicate glass [15]. Compared

with the matrix phase in the quenched slag, the matrix phase in the furnace-cooled slag was obtained at a lower temperature and the Fe_2O_3 content in it was lower because of the precipitation of magnesioferrite. Therefore, in the case of slow cooling, the fraction of Fe^{3+} ions in tetrahedral sites to total Fe^{3+} ions in the matrix phase was larger. The bond strength of Fe–O–Si in this matrix phase was higher, and thus the dissolution of matrix phase became difficult.

In summary, decreasing cooling rate could promote the dissolution of solid solution and suppress the dissolution of matrix phase. A better selective leaching of P from slag was performed in the case of slow cooling.

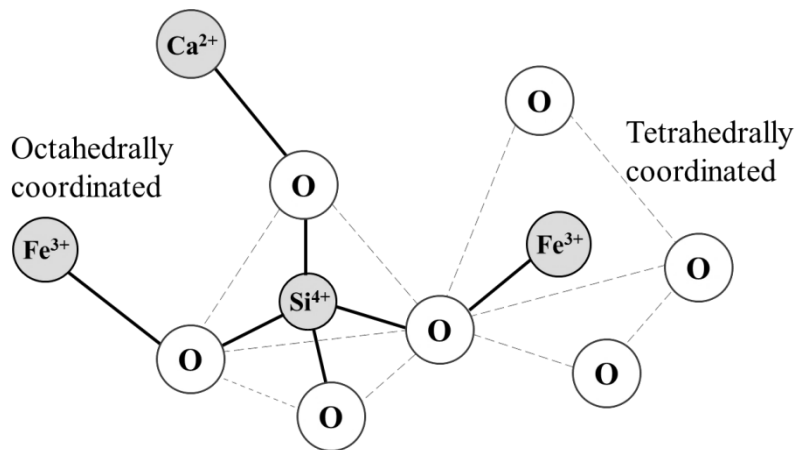


Fig. 3.9 Schematic illustration of the structure of silicate glass

3.2.2 Effect of Na_2O content on the dissolution behavior of slag

3.2.2.1 Mineralogical composition of slags with different Na_2O contents

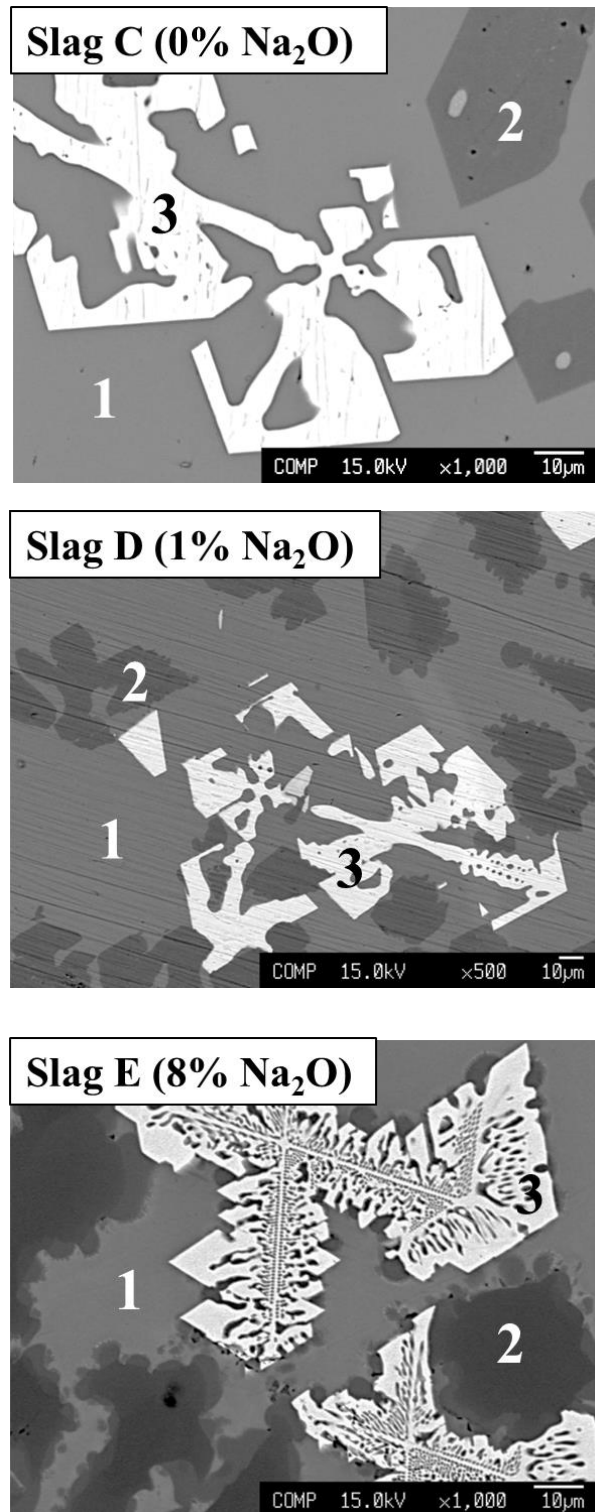


Fig. 3.10 Typical cross section of the slags with different Na₂O contents

Table 3.5 Compositions of each phase in slags with different Na₂O contents (mass%)

Phase	Sample	CaO	SiO ₂	P ₂ O ₅	Fe ₂ O ₃	MgO	Na ₂ O
1. Matrix phase	Slag C (0% Na ₂ O)	39.1	35.9	1.8	21.5	1.7	0
	Slag D (1% Na ₂ O)	40.1	34.0	2.3	20.8	1.0	1.7
	Slag B (4% Na ₂ O)	34.4	33.1	1.2	25.9	1.5	3.9
	Slag E (8% Na ₂ O)	24.5	29.3	0.5	34.6	1.2	9.9
2. Solid solution	Slag C (0% Na ₂ O)	54.2	12.6	31.7	0.8	0.7	0
	Slag D (1% Na ₂ O)	56.2	12.0	29.3	0.6	0.2	1.6
	Slag B (4% Na ₂ O)	51.4	15.6	25.4	0.9	0.3	6.4
	Slag E (8% Na ₂ O)	48.6	16.6	24.5	0.7	0.3	9.4
3. Magnesioferrite	Slag C (0% Na ₂ O)	1.2	0.1	0.0	88.1	10.6	0.0
	Slag D (1% Na ₂ O)	1.3	0.0	0.0	87.4	11.2	0.0
	Slag B (4% Na ₂ O)	1.8	0.0	0.0	86.8	11.1	0.3
	Slag E (8% Na ₂ O)	2.0	0.0	0.0	84.1	12.7	1.2

Figure 3.10 shows the typical cross section of the slags with different Na₂O contents. The average compositions of each phase in different slags are listed in Table 3.5. Three phases were clearly identified in each slag. The gray phase that consists of the CaO-SiO₂-Fe₂O₃ system was the matrix phase. The black phase containing a high P₂O₅ content was the solid solution. The white phase that was rich in iron oxide and magnesia was the magnesioferrite phase. The added Na₂O was distributed into the solid solution, and its content in the solid solution increased with an increase in Na₂O content in slag. For the slag with 8 mass% of Na₂O content, the Na₂O content in the solid solution reached 9.4 mass%; however, the distribution ratio of Na₂O between the solid solution and the matrix phase was lower than that in the slag containing 4 mass% of Na₂O. Na₂O addition led to a decrease in the P₂O₅ content in the matrix phase and in the solid solution. When the Na₂O content increased from 0 to 8 mass%, the P₂O₅ content in the solid solution decreased from 31.7 mass% to 24.5 mass%. For the matrix phase, the Fe₂O₃

content increased with an increase in the Na_2O content. The effect of the Na_2O content on the composition of magnesioferrite phase was not significant.

Using Eqs. (3.1) and (3.2), the mass fractions of each phase in slags with different Na_2O contents were calculated and shown in Fig. 3.11. With an increase in the Na_2O content in slag, the mass fraction of the solid solution increased, while that of the matrix phase decreased. The mass fraction of the magnesioferrite phase was about 20% in each slag. Without the Na_2O addition, the mass fraction of the solid solution in slag was 24.2%. When 8 mass% of Na_2O was added, the mass fraction of the solid solution increased to 34.0%, and that of the matrix phase was 49.1%.

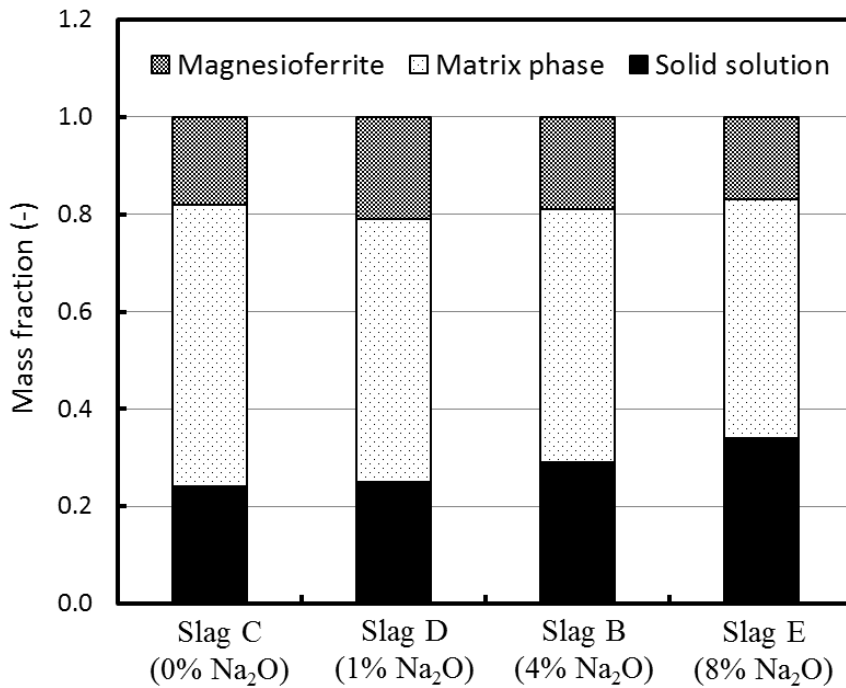


Fig. 3.11 Mass fractions of each phase in slags with different Na_2O contents

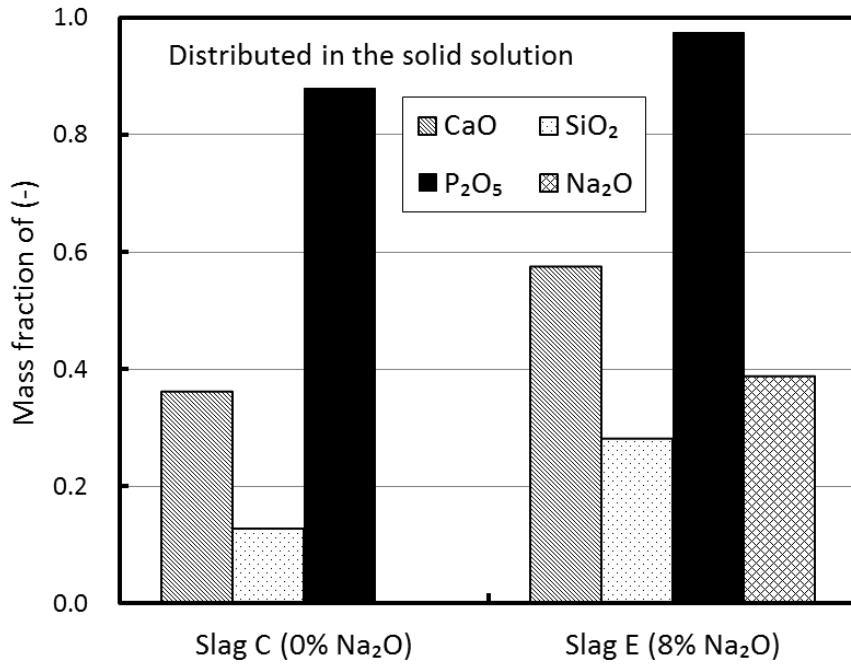


Fig. 3.12 Mass fractions of each oxide distributed in the solid solution

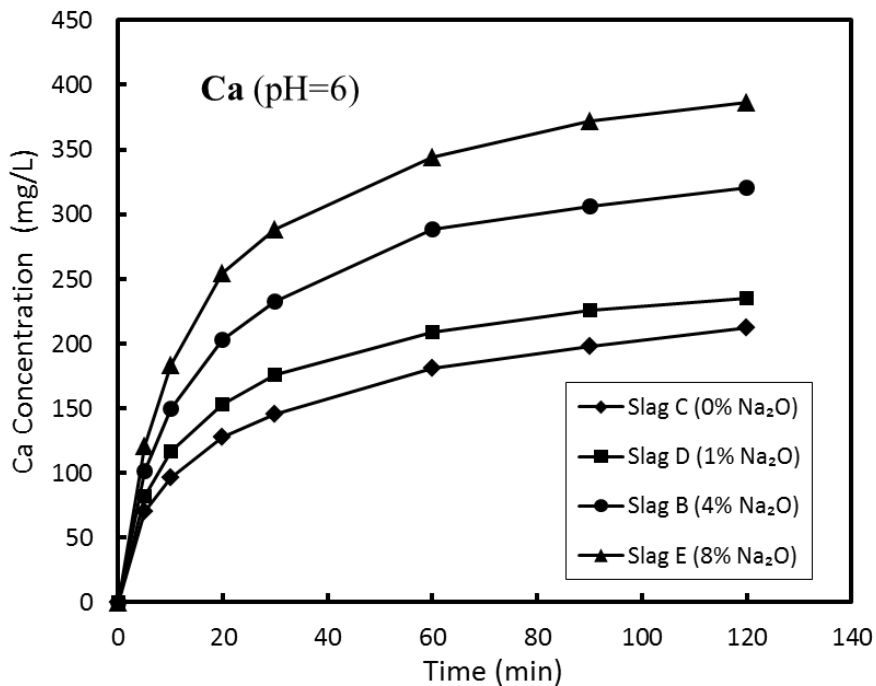
The mass fractions of each oxide distributed in the solid solution were calculated using Eq. (3.3), as shown in Fig. 3.12. After Na₂O addition, the mass fractions of CaO and SiO₂ distributed in the solid solution significantly increased because of the enlargement of solid solution. Although the P₂O₅ content in the solid solution was decreased by Na₂O addition, almost all of the P₂O₅ was concentrated in the solid solution. For the slag with 8 mass% of Na₂O, about 40% of the added Na₂O was distributed in the solid solution.

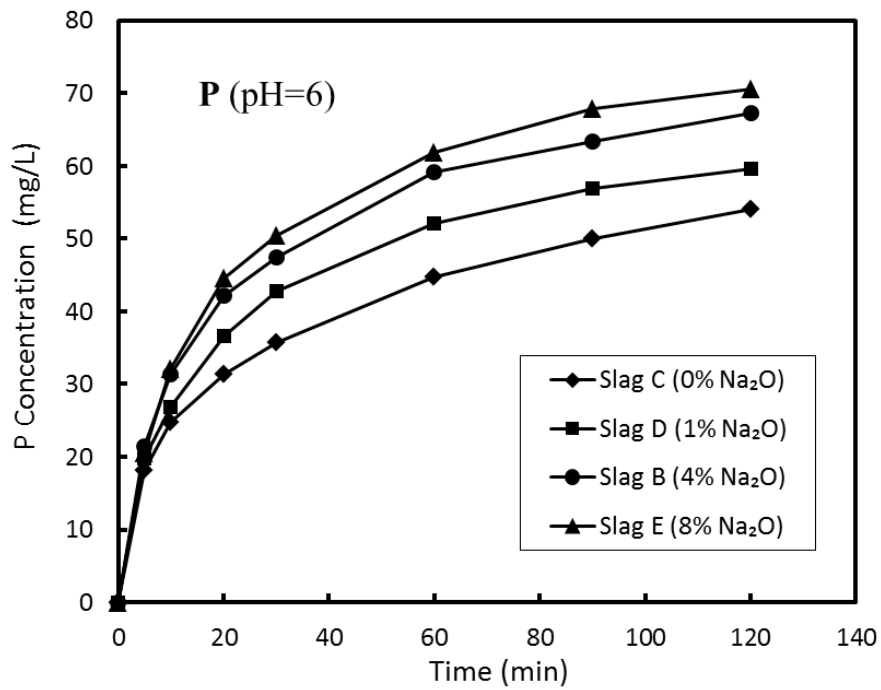
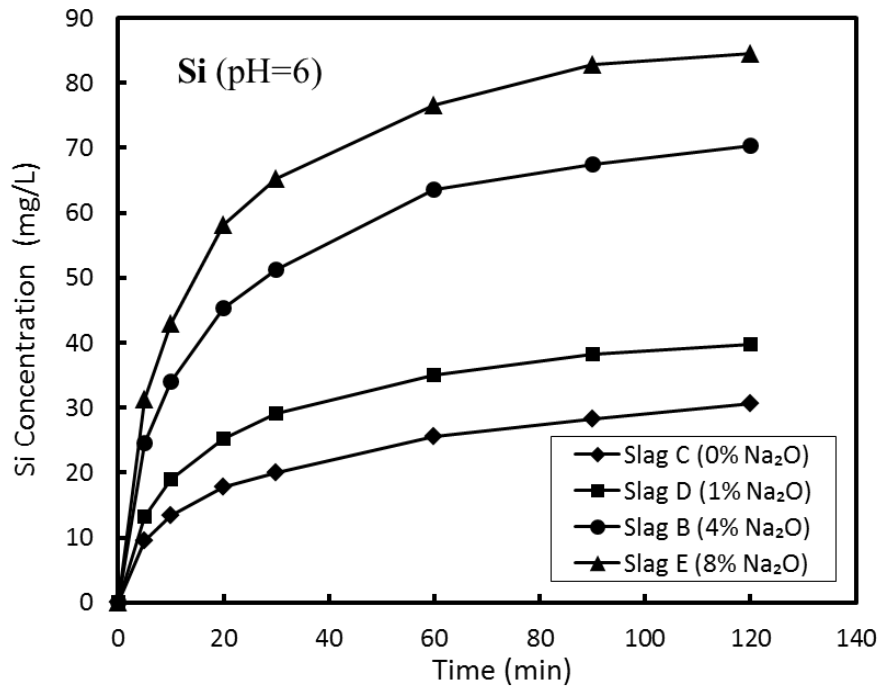
3.2.2.2 Dissolution behavior of slags with different Na₂O contents

The effect of Na₂O content on the change in the concentrations of each element in the citric solution is shown in Fig. 3.13. The concentration of each element increased with leaching time. The dissolution rate of slag gradually decreased owing to increased concentrations of each element in the aqueous solution. The Ca concentration was the highest among the dissolved elements, and it increased significantly with the increase in the Na₂O content in slag. For the

slag containing 8 mass% of Na_2O , the Ca concentration reached 386.2 mg/L after 120 min, which was about one time higher than that of the unmodified slag. Na_2O addition also resulted in higher Si and P concentrations. When the Na_2O content changed from 0 to 8 mass%, the Si concentration almost tripled, and the P concentration increased from 54.1 mg/L to 70.6 mg/L. The Fe concentration was the lowest in the aqueous solution: less than 10 mg/L in each case. The Na concentration increased with the Na_2O content in slag. It reached 63.4 mg/L in the case of slag containing 8 mass% of Na_2O .

Figure 3.14 shows the acid consumption during leaching of slags with different Na_2O contents. In the beginning, a large amount of acid was added to keep the pH at a constant value because the dissolution rate of slag was high. The change in the acid consumption was in good agreement with that in the Ca and Si concentrations during leaching. With the increase in the Na_2O content in slag, acid consumption increased. When 8 mass% of Na_2O was added, about 25.7 g of citric acid was consumed during leaching, which was two times higher than the unmodified slag.





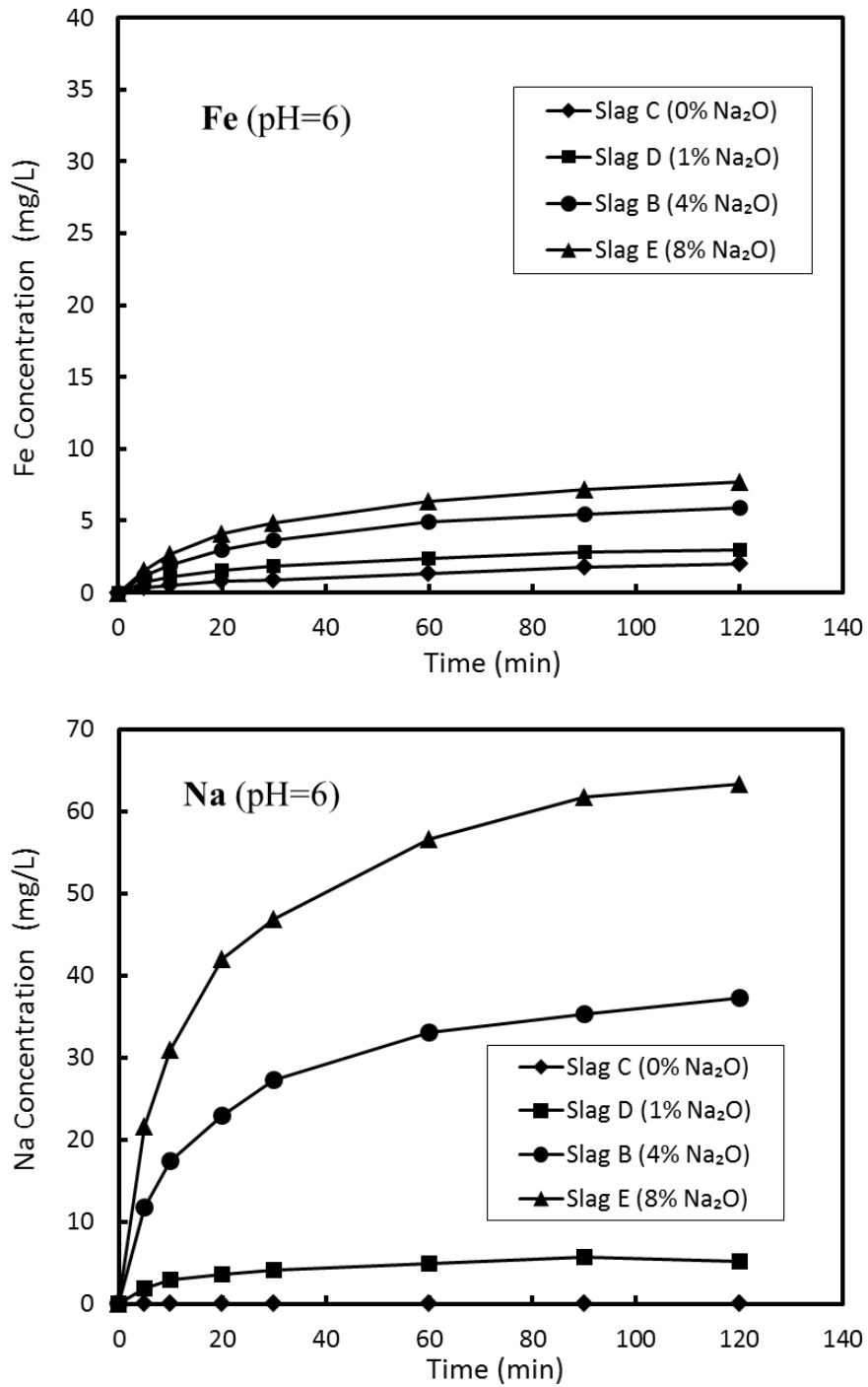


Fig. 3.13 Change in the concentrations of each element in the citric solution at pH 6

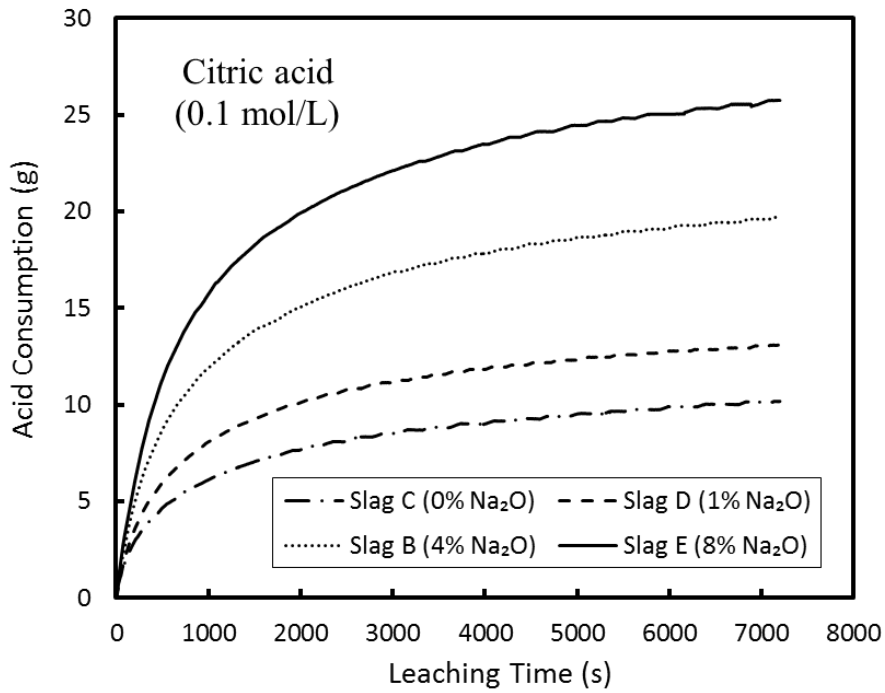


Fig. 3.14 Change in the acid consumption with leaching time under different Na₂O contents

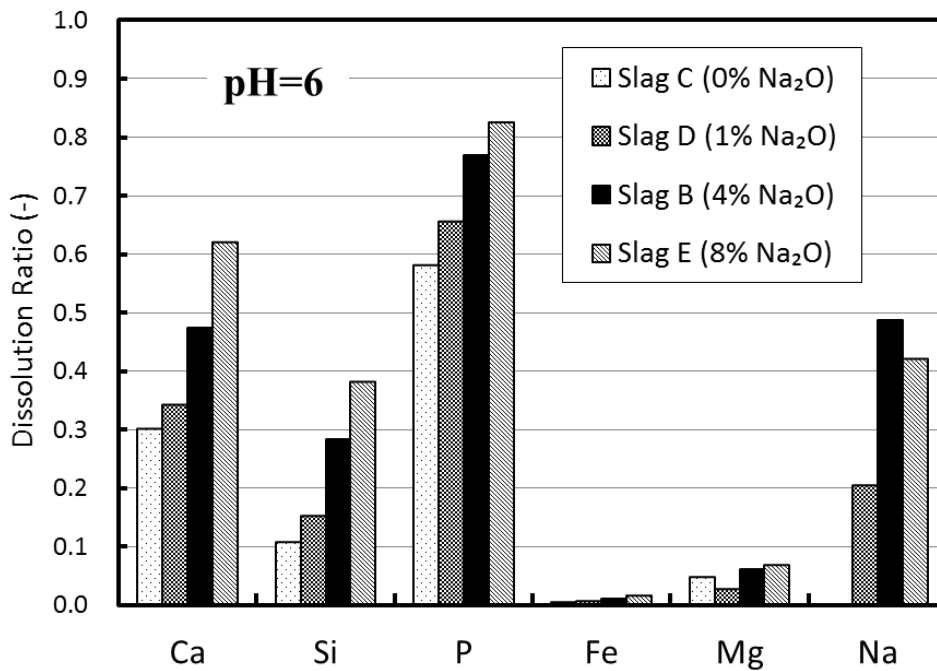


Fig. 3.15 Dissolution ratios of each element from slags with different Na₂O contents at pH 6

As discussed in the above studies, the dissolution ratios of each element from slag were calculated using Eq. (3.4). Figure 3.15 shows the calculated dissolution ratios of each element at pH 6. There were significant differences between the dissolution ratios of the elements. The dissolution ratio of P was the highest in each case. Fe was difficult to dissolve, and its dissolution ratio from different slags was negligible. With the increase in the Na₂O content, the dissolution ratios of Ca, Si, and P increased. Without Na₂O addition, only 58.2% of the P was dissolved from slag; the dissolution ratios of Ca and Si were 30.2% and 10.7%. When the Na₂O content in slag reached 8 mass%, the dissolution ratio of P increased to 82.3%, approximately 62.1% of the Ca and 38.1% of the Si were dissolved simultaneously. The dissolution ratio of Mg was lower compared to other elements in each case, less than 7%. For the slags containing more than 4 mass% of Na₂O, less than half of the Na was dissolved from slag. These results indicated that Na₂O addition promoted dissolution of the P-condensed solid solution without largely dissolving phases containing Fe and Mg. To obtain a higher dissolution ratio of P in the citric solution at pH 6, sufficient Na₂O addition to the slag was necessary.

3.2.2.3 Residue composition

The average compositions of residues after leaching were determined by ICP-AES analysis, as listed in Table 3.6. Due to selective leaching of solid solution, the P₂O₅ content in the residue reduced significantly compared with the original slags (listed in Table 3.1), and the Fe₂O₃ content increased. With the increase in the Na₂O content in the original slags, the CaO, SiO₂, and P₂O₅ contents in the residue decreased after leaching at pH 6; the Fe₂O₃ and MgO contents correspondingly increased. For the unmodified slag, its residue still contains 3.36 mass% of P₂O₅ because the dissolution of solid solution was poor. For the slag with 8 mass% of Na₂O, the P₂O₅ content in the residue decreased to 1.49 mass%, and the Fe₂O₃ content reached 50.70

mass%. In addition, some of the added Na₂O still remained in the residue. Overall, through selective leaching, a residue with a lower P₂O₅ content and a higher Fe₂O₃ content was obtained, which had the potential for recycling within the ironmaking and steelmaking process.

Table 3.6 Average compositions of residues of different slags (mass%)

Residue	pH	CaO	SiO ₂	Fe ₂ O ₃	P ₂ O ₅	MgO	Na ₂ O
Slag C (0% Na ₂ O)	6	34.22	22.37	36.29	3.36	3.75	0.00
Slag D (1% Na ₂ O)	6	30.71	21.37	39.93	2.79	4.19	1.01
Slag B (4% Na ₂ O)	6	26.17	19.20	44.85	2.09	4.59	3.10
Slag E (8% Na ₂ O)	6	18.32	16.30	50.70	1.49	5.14	8.06

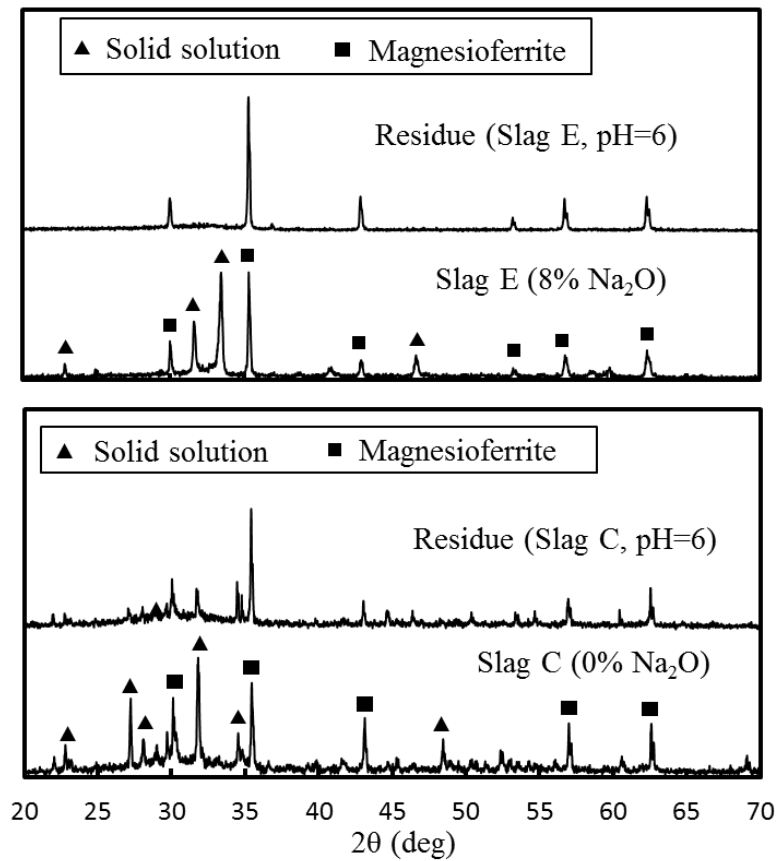


Fig. 3.16 XRD patterns of slags with and without Na₂O addition and their residues at pH 6

Figure 3.16 shows the XRD patterns of slags with and without Na₂O addition and their residues at pH 6. In each slag, the precipitated solid solution and magnesioferrite phase were observed. The crystal form of the solid solution was changed because of Na₂O modification. For the unmodified slag, the peaks associated with solid solution existed after leaching. However, for the slag with 8 mass% of Na₂O, the peaks associated with solid solution almost disappeared, and the intensity of the peaks associated with magnesioferrite phase increased. From the above findings, it demonstrated that the dissolution and separation of the solid solution from slag were enhanced by Na₂O addition.

3.2.2.4 Discussion on effect of Na₂O content

To estimate the dissolution behavior of solid solution and matrix phase, the presumed dissolution ratios of Ca and P from the solid solution were calculated using Eq. (3.6). As shown in Fig. 3.17, with the increase in the Na₂O content in slag, the presumed dissolution ratio of P (dissolution ratio of solid solution) increased. Without the Na₂O addition, only 68.0% of solid solution was dissolved from slag. When 4 mass% of Na₂O was added, the dissolution ratio of solid solution increased to 83.6%. However, a further Na₂O addition did not result in a significant improvement in the dissolution of solid solution. As discussed in the previous chapter, the dissolution of phosphate minerals in acid solutions depends on the breaking of the weaker bond in its structure. Because the bond strength of P–O is significantly higher than that of Metal–O, dissolution would favor the breaking of the Metal–O bond. Thus, the metal dissolves to form metal cations and the phosphorus dissolves to form phosphate, PO₄³⁻ [11]. When the Na₂O was distributed into the solid solution, some of the Ca–O–P bonds transformed into the Na–O–P bonds. Because the bond strength of Na–O was lower, the Na–O–P bond was easier to be broken during acid leaching [16]. Therefore, the solid solution containing Na₂O

shows good water solubility, and a higher dissolution ratio of P can be obtained. It has been reported that more than 0.2 mol of Na_2O addition to 1 mol P_2O_5 of calcium phosphate favored the formation of soluble phosphate [17]. In this study, for the slag containing 4 mass% of Na_2O , the molar ratio of Na_2O of P_2O_5 in the solid solution exceeded 0.5, and thus the dissolution of solid solution was promoted significantly.

The presumed dissolution ratio of Ca also increased with the Na_2O content in slag. When the Na_2O content was less than 4 mass%, this value was lower than unity. It also illustrated that the dissolution of solid solution was insufficient. When the Na_2O content was more than 4 mass%, this value exceeded unity, but not largely, indicating that the dissolution of matrix phase was not significant. A better selective leaching of solid solution was performed.

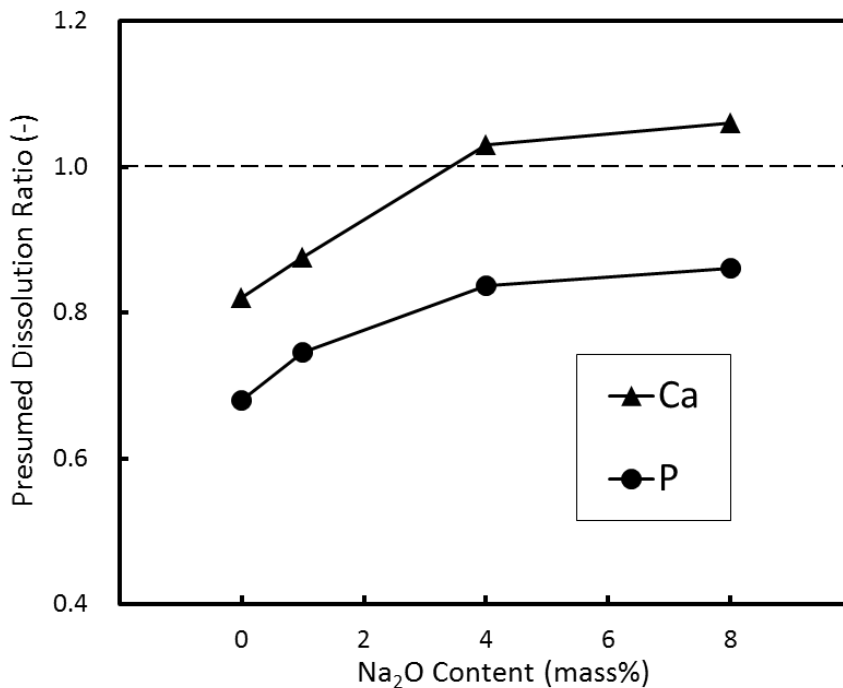


Fig. 3.17 Presumed dissolution ratios of Ca and P from the solid solution under different Na_2O contents

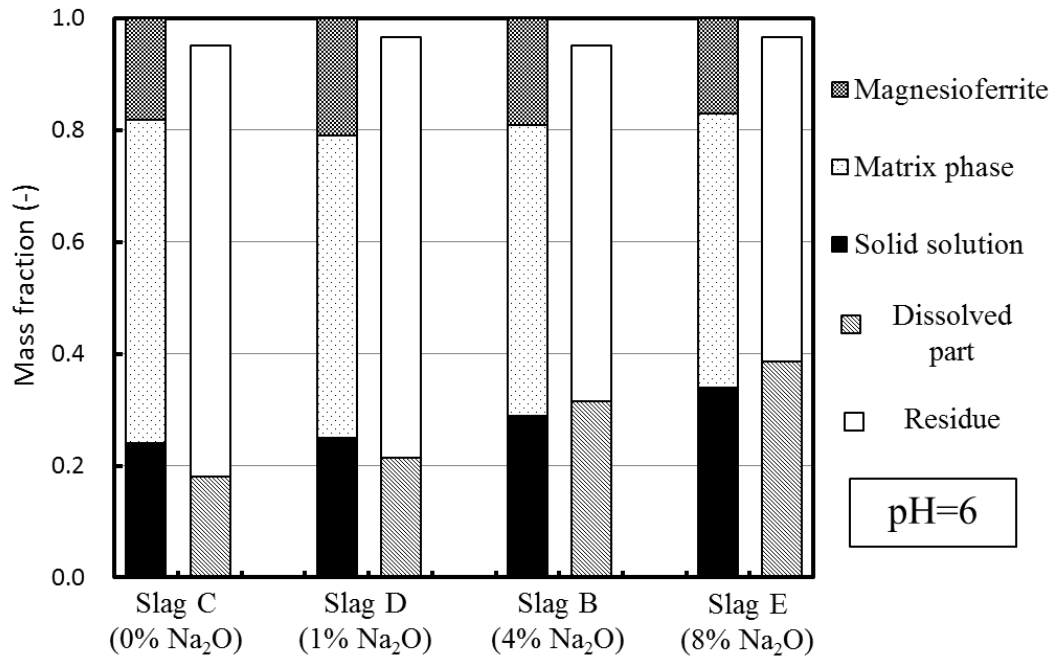


Fig. 3.18 Mass ratios of residue and dissolved part at pH 6, compared with the phase fractions of each slag

The phase fraction of slags with different Na₂O contents was compared with the mass ratios of the dissolved part and residue to estimate the dissolution behavior of each phase at pH 6. Figure 3.18 shows that with the increase in the Na₂O content, the mass fraction of the solid solution increased while that of the matrix phase decreased. In the case of unmodified slag, the mass ratio of the dissolved portion was lower than that of the solid solution, indicating that a part of the solid solution remained in the residue and did not dissolve. Because Na₂O addition promoted dissolution of Ca, Si, and P, the mass ratio of the dissolved part also increased by the increase in the Na₂O content. It was almost similar to the mass fraction of the solid solution when the Na₂O content was 4 mass%. The Fe-concentrated matrix phase and magnesioferrite were not dissolved because of the lower dissolution ratio of Fe. This result indicated that most of the solid solution was dissolved from slag. A further increase in the Na₂O content resulted in an increase in the dissolution of slag together with the mass fraction of the solid solution. The

mass ratio of the dissolved part was a little higher than that of the solid solution. It illustrated that solid solution could be dissolved and separated from slag by optimum Na_2O addition, without dissolving large amounts of other phases.

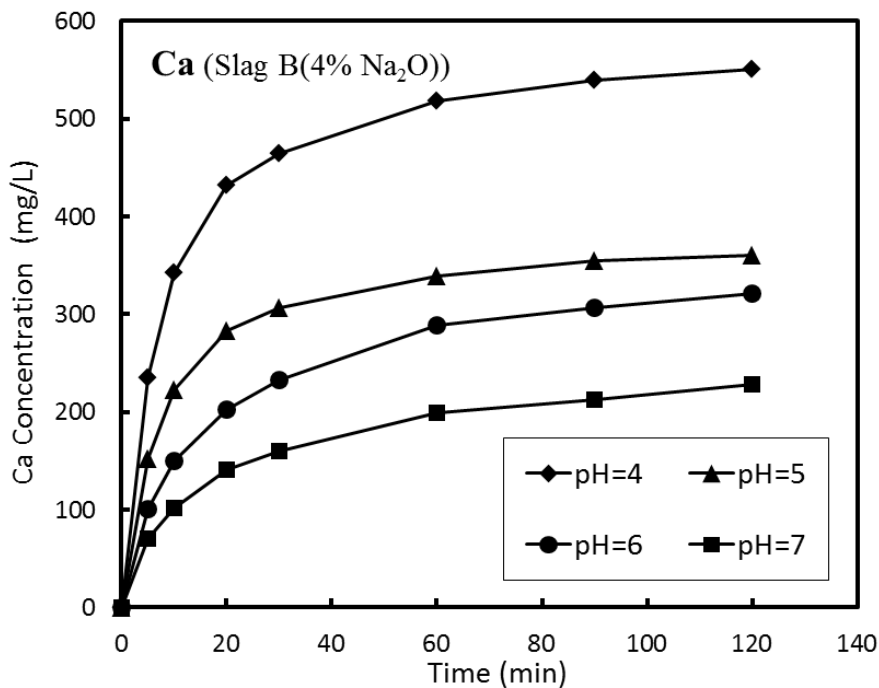
3.2.3 Effect of pH on the dissolution behavior of the modified slag

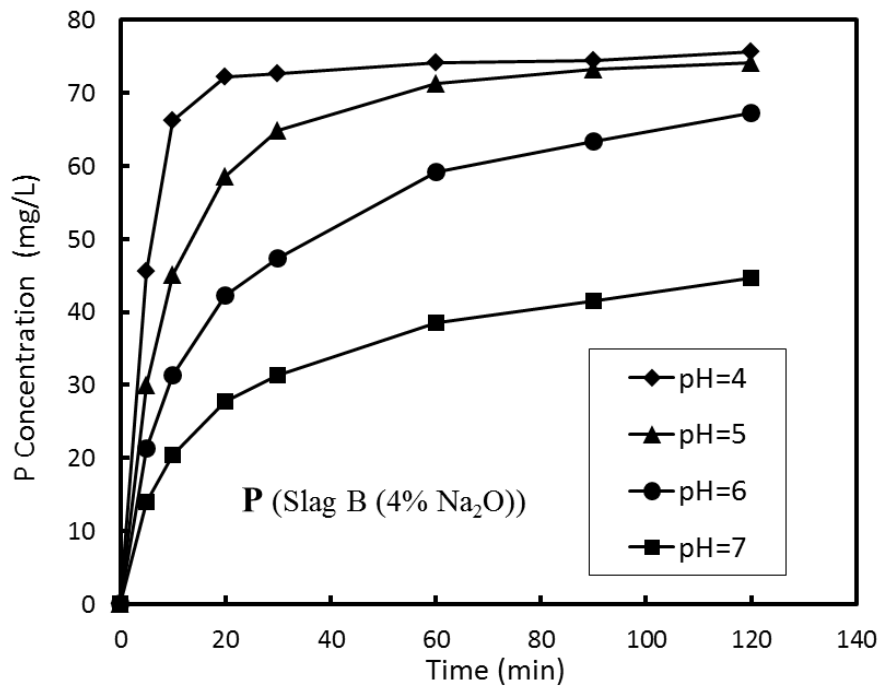
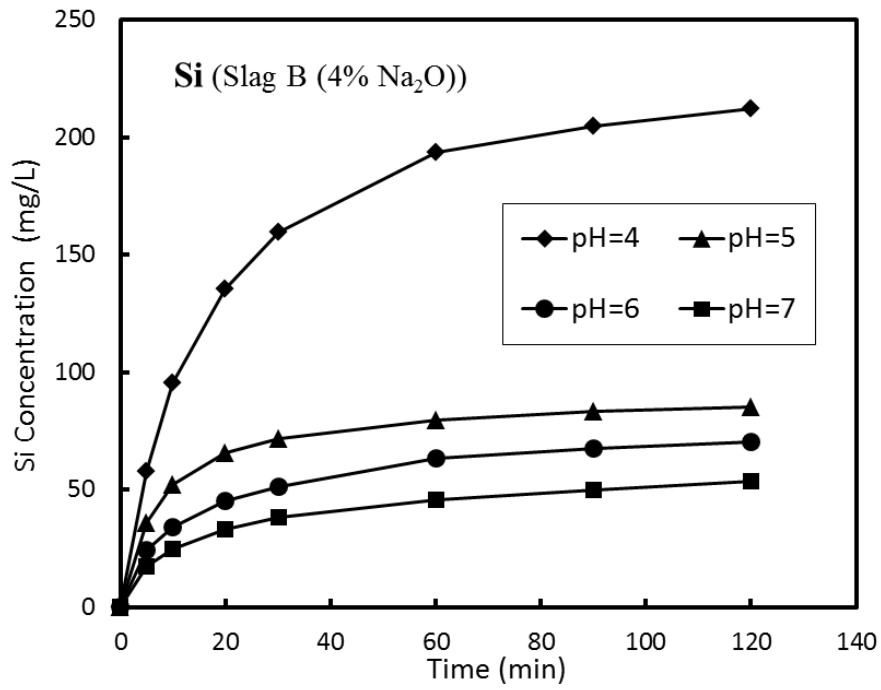
3.2.3.1 Dissolution behavior of slag under various pH values

Figure 3.19 shows the change in the concentrations of each element in the citric solution under various pH values for slag B (4% Na_2O). The concentrations of each element increased with leaching time in each case. Decreasing the pH increased the dissolution rate of each element, leading to higher concentrations in a shorter time. The Ca concentration increased from 227.8 mg/L to 550.9 mg/L as the pH decreased. When the pH decreased from 6 to 5, the Si and P concentrations increased slightly. However, when the pH decreased from 5 to 4, they increased many times. For example, the Si concentration increased from 85.5 mg/L to 212.4 mg/L. At pH 5, the Fe concentration was the lowest among these elements, only 15.3 mg/L. It sharply increased to 156.9 mg/L at pH 4, which was caused by significant dissolution of the Fe-containing phase. When the pH decreased from 7 to 6, there was a significant increase in the P concentration, and it reached 67.3 mg/L; however, further decrease in the pH changed the P concentration slightly. At pH 4, the P concentration was 75.6 mg/L, which was far lower than the Ca, Si, and Fe concentrations. These results also indicated that the P-concentrated phase dissolved preferentially compared to the Fe-containing phase.

Table 3.7 lists the acid consumption during leaching of the modified slag at various pH conditions. As the pH decreased, acid consumption increased because the dissolution of each element was promoted. A large amount of citric acid was consumed at pH 4, which was much more than the consumption at pH 5.

The dissolution ratios of each element from the modified slag at various pH values were calculated using Eq. (3.4), as shown in Fig. 3.20. Slag dissolution was promoted when the pH decreased, resulting in higher dissolution ratios of each element. The dissolution ratios of Fe and Mg were lower than those of other elements in each case, indicating that the phases rich in Fe and Mg were difficult to dissolve. The dissolution ratio of P increased from 49.7% to 76.9% when the pH varied from 7 to 6. A further decrease in the pH had little effect in promoting P dissolution. At pH 5 and 6, the dissolution ratio of P was far higher than those of Ca and Si, and the dissolution of Fe was little, showing a better selective leaching of P. There was a huge difference in the dissolution ratios of other elements between pH 5 and 4. Almost all of the Ca, Si, P, and Na were dissolved from slag at pH 4, and the dissolution ratio of Fe reached 31.6%. Large amounts of Fe and Mg dissolution deteriorated selective leaching, which was not beneficial for P recovery in the following processes. The pH of the aqueous solution should be controlled between 5 and 6 to achieve better selective leaching of P from slag.





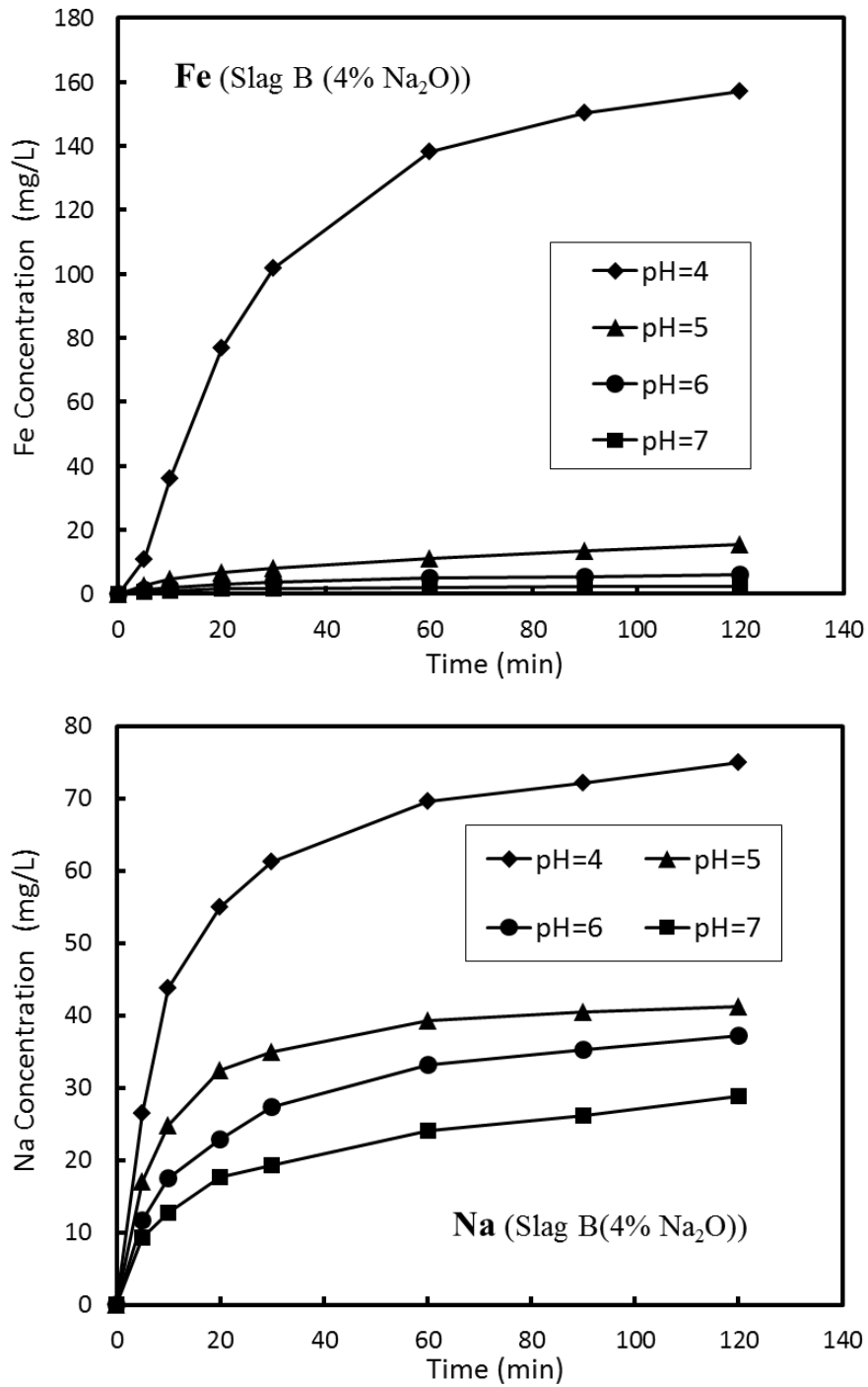


Fig. 3.19 Change in the concentrations of each element under various pH conditions

Table 3.7 Acid consumption during leaching at various pH conditions (g)

	pH=4	pH=5	pH=6	pH=7
Mass	45.0 (0.2mol/L)	27.0	19.7	13.2

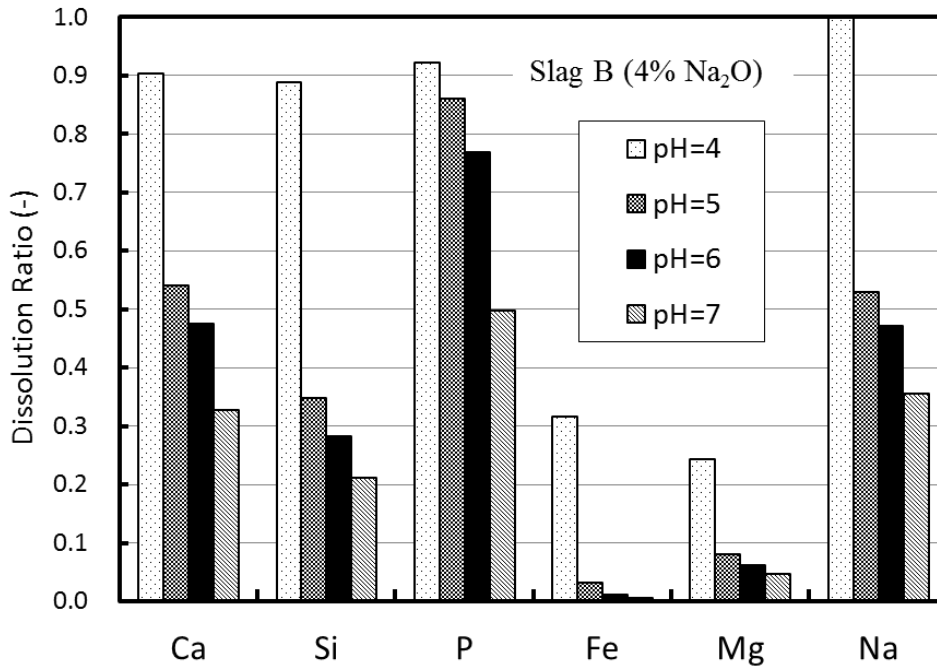


Fig. 3.20 Dissolution ratios of each element from the modified slag at various pH conditions

3.2.3.2 Residue composition

For the slag containing 4 mass% of Na_2O , the average compositions of residues after leaching under various pH conditions were listed in Table 3.8. As the pH decreased, the CaO and P_2O_5 contents in the residue decreased, while the Fe_2O_3 and MgO contents increased correspondingly. Because of a lower dissolution ratio of P at pH 7, the P_2O_5 content in the residue was 4.62 mass%. When the pH decreased to 5, the residue contained 0.93 mass% of P_2O_5 and 48.46 mass% of Fe_2O_3 , which can be used as flux or raw material in ironmaking and steelmaking process. The residue obtained by leaching at pH 4 mainly consisted of Fe_2O_3 and MgO , similar with the composition of magnesioferrite phase.

Figure 3.21 shows the XRD patterns of the modified slag and its residues under different pH conditions. The peaks associated with solid solution and magnesioferrite were observed in the original slag. After leaching, intensities of the peaks associated with solid solution weakened; in

contrast, the peaks associated with magnesioferrite intensified. When slag was leached at pH 7, the peaks associated with solid solution still existed, indicating that some of the solid solution did not dissolve. After leaching at pH 5 or 6, the peaks associated with solid solution almost disappeared, and only the peaks of the magnesioferrite phase were observed. These results indicated that the P-condensed solid solution was completely separated from slag.

Table 3.8 Average compositions of residues after leaching various pH conditions (mass%)

Residue	pH	CaO	SiO ₂	Fe ₂ O ₃	P ₂ O ₅	MgO	Na ₂ O
Slag B (4% Na ₂ O)	7	30.71	20.97	36.77	4.62	3.79	3.13
	6	26.17	19.20	44.85	2.09	4.59	3.10
	5	22.94	20.45	48.46	0.93	4.47	2.75
	4	8.93	2.01	78.39	0.21	9.44	1.02

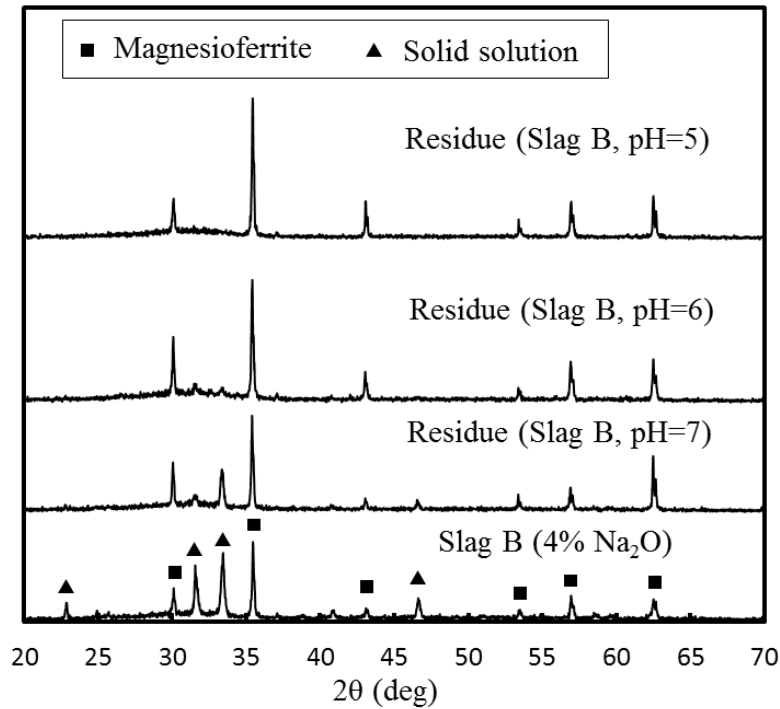


Fig. 3.21 XRD patterns of the modified slag and its residues under different pH conditions

After leaching of the modified slag at pH 5, the EPMA image and surface composition of the residue were shown in Fig. 3.22 and Table 3.9. Two main phases were identified in each residue.

The white area, rich in Fe_2O_3 and MgO , was considered the magnesioferrite phase. The grey phase, consisting of a $\text{CaO-SiO}_2\text{-Fe}_2\text{O}_3$ system, was considered the matrix phase. Compared with the results in Table 3.5, the compositions of these phases in the residue were almost identical to those in the slag prior to leaching. In the residue, it was difficult to detect the solid solution, indicating that the solid solution that contacted with the aqueous solution had dissolved. Selective leaching of the P-concentrated solid solution from slag was performed in this case.

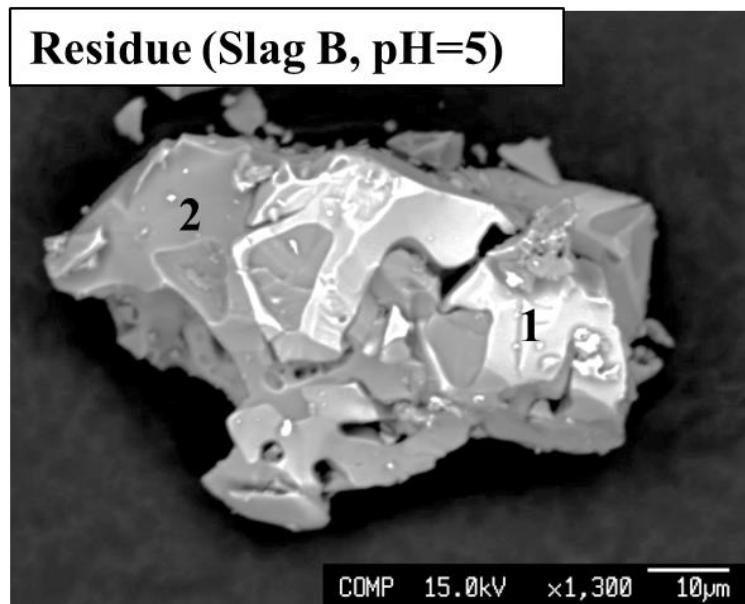


Fig. 3.22 EPMA images of the residue surface after leaching at pH 5

Table 3.9 Compositions of some phases on the residue surface after leaching at pH 5 (mass%)

Phase	CaO	SiO ₂	Fe ₂ O ₃	P ₂ O ₅	MgO	Na ₂ O
1	1.4	0.3	85.1	0.1	12.8	0.4
2	38.1	26.2	27.3	1.1	2	5.3

3.2.3.3 Discussion on the effect of pH

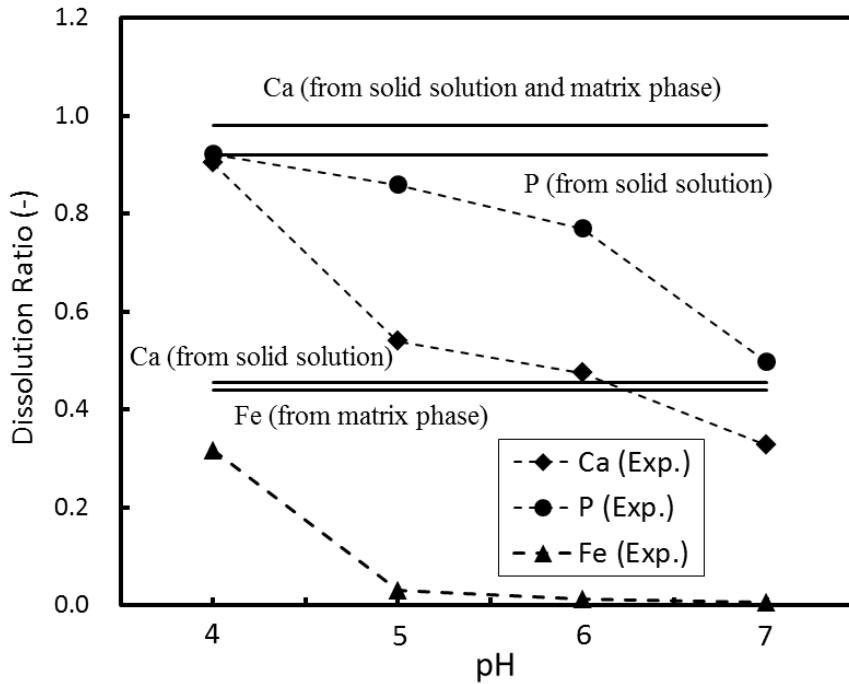


Fig. 3.23 Calculated dissolution ratios of some elements when each phase was dissolved, and the experimental results at various pH conditions

Assuming that each phase was individually dissolved from slag, the dissolution ratios of each element from slag could be calculated using the mass fraction of each phase (shown in Fig. 3.11) and phase composition (listed in Table 3.5). For example, when only solid solution was dissolved, the calculated dissolution ratio of element M from slag was equal to the mass fraction of MO distributing in solid solution (described in Eq. (3.3)). Figure 3.23 shows the calculated dissolution ratios of Ca, P, and Fe, and experimental results of slag with 4 mass% of Na_2O at various pH conditions. The dissolution ratios of P and Ca from slag reached 92% and 45.5%, respectively, when the solid solution was totally dissolved. At pH 7, the dissolution ratio of P was lower than the calculated value, indicating that the dissolution of solid solution was insufficient. When the pH was between 6 and 5, the dissolution ratio of P increased and approached the calculated value. The dissolution ratio of Ca was a little higher than the values calculated from solid solution. It illustrated that most of the solid solution was dissolved and the

dissolution of other phases was insignificant. When the pH decreased to 4, the dissolution ratio of Ca was higher than the value calculated from solid solution and lower when the solid solution and matrix phase were both dissolved. This result indicated that a portion of the dissolved Ca was from the matrix phase. The dissolution of Fe also went through similar conditions: when the pH varied from 5 to 4, the dissolution ratio of Fe gradually approached the value calculated from matrix phase. There was significant variation in the dissolution of matrix phase between pH 5 and 4.

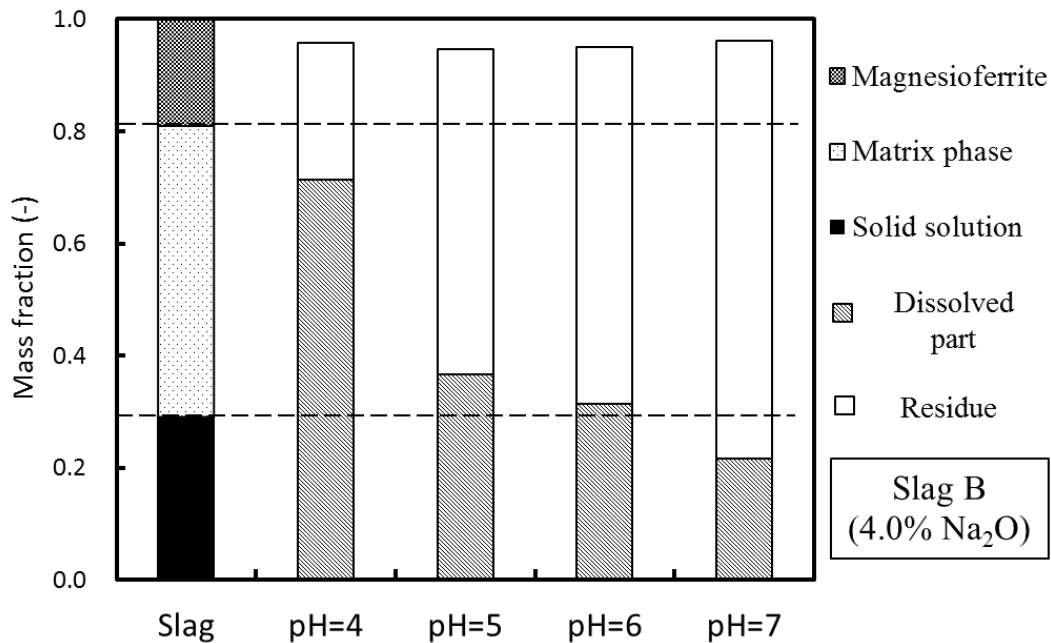


Fig. 3.24 Mass ratios of residue and dissolved part at various pH conditions, compared with phase fraction

Figure 3.24 shows the mass ratios of the dissolved portion and residue at various pH conditions, compared with phase fraction in the original slag. At pH 7, the mass ratio of the dissolved portion was lower than that of the solid solution. With the decrease in pH, the mass ratio of the dissolved portion increased and exceeded that of the solid solution at pH 6, indicating that a

majority of the solid solution was dissolved. When the pH decreased to 4, approximately 70% of slag was dissolved, which was almost equal to the mass fractions of the solid solution and a large proportion of the matrix phase. These results were consistent with the above discussion. To avoid dissolution of matrix phase and achieve selective leaching of solid solution, the pH should be controlled between 5 and 6.

3.2.4 Effect of the valency of Fe on the dissolution behavior of slag

3.2.4.1 Mineralogical composition of slags with different valency of Fe

Figure 3.25 shows the typical cross section of slags with different valency of Fe. The average compositions of each phase in these slags are listed in Table 3.10. In each slag, three domains corresponding to three phases are clearly identified. The white phase almost consists of Fe oxide. The grey phase was considered the matrix phase, because it mainly consisted of the CaO-SiO₂-Fe₂O system. The black phase rich in P₂O₅ was the solid solution. It shows that in the slag containing FeO, the size of solid solution particles was larger than that in the slag containing Fe₂O₃, while the size of Fe oxide was smaller. For the slag containing FeO, the P₂O₅ content in the solid solution was only 19.4 mass%, and far lower than that in the slag containing Fe₂O₃. In addition, the FeO content in the solid solution was a little high, reaching 7.0 mass%. The P₂O₅ content in the matrix phase was lower regardless of the valency of Fe in slag. The slag containing Fe₂O₃ had a higher CaO content and a lower Fe₂O content in the matrix phase compared to the slag containing FeO. The Na₂O content was higher in the solid solution than in the matrix phase in each case.

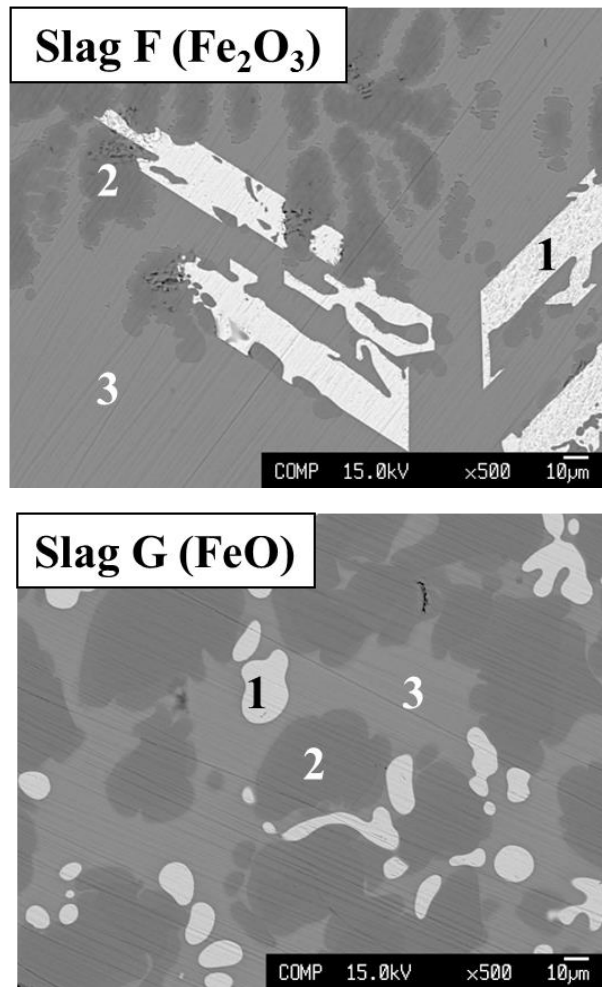


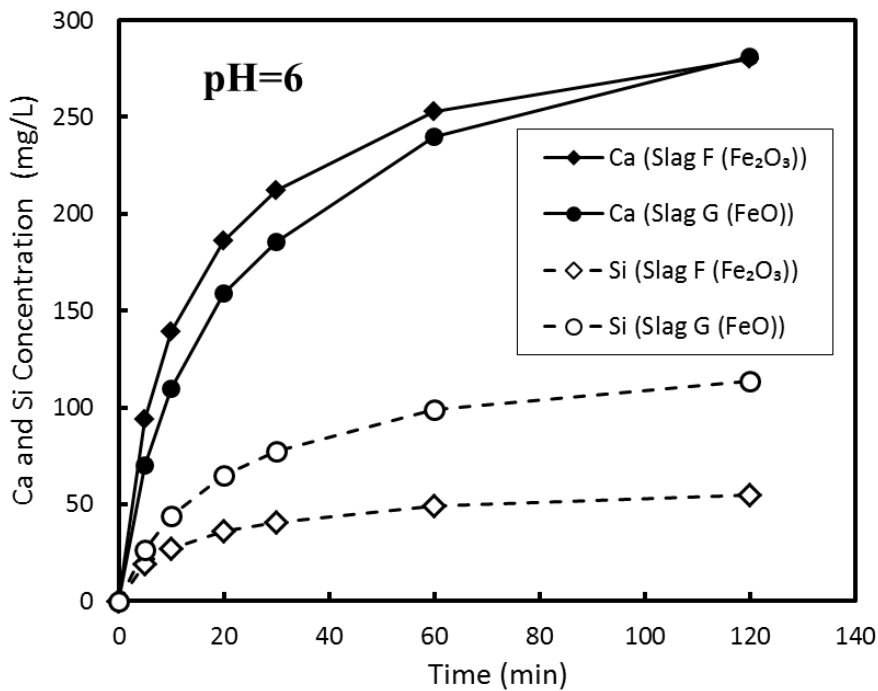
Fig. 3.25 Typical cross section of the slags with different valency of Fe

Table 3.10 Average compositions of each phase in slags with different valency of Fe (mass%)

Phase	Sample	CaO	SiO ₂	Fe ₁ O	P ₂ O ₅	Na ₂ O
1. Fe oxide	Slag F (Fe ₂ O ₃)	0.2	0	99.8	0	0
	Slag G (FeO)	0.5	0.1	99.4	0	0.1
2. Solid Solution	Slag F (Fe ₂ O ₃)	48.0	10.1	0.7	33.4	7.7
	Slag G (FeO)	47.4	20.7	7.0	19.4	5.6
3. Matrix phase	Slag F (Fe ₂ O ₃)	36.2	36.8	21.2	1.5	4.3
	Slag G (FeO)	27.9	36.0	30.7	1.6	3.9

3.2.4.2 Dissolution behavior of slags with different valency of Fe

The change in the concentrations of each element with leaching time at pH 6 is shown in Fig. 3.26. The concentrations of each element in the citric solution continuously increased with leaching time, but the dissolution rate gradually decreased. The Ca concentration was the highest among the dissolved elements. The Ca concentration of each slag was almost the same in each case, reaching approximately 280 mg/L after 120 min. When the Fe_2O_3 in slag changed to FeO, the Si concentration almost doubled. There was no decrease in the P concentration during leaching. The P concentration of the slag containing Fe_2O_3 was higher, reaching 71.7 mg/L. In the case of slag containing FeO, the P concentration was only 14.9 mg/L after 120 min, but the Fe concentration increased to 121.0 mg/L, which was far higher than that of the slag containing Fe_2O_3 . Overall, the dissolution behavior of Fe and P reversed when the Fe_2O_3 in the slag changed to FeO. The consumptions of citric acid during leaching of slag containing Fe_2O_3 and slag containing FeO were 18.2 mg/L and 26.1 mg/L, respectively.



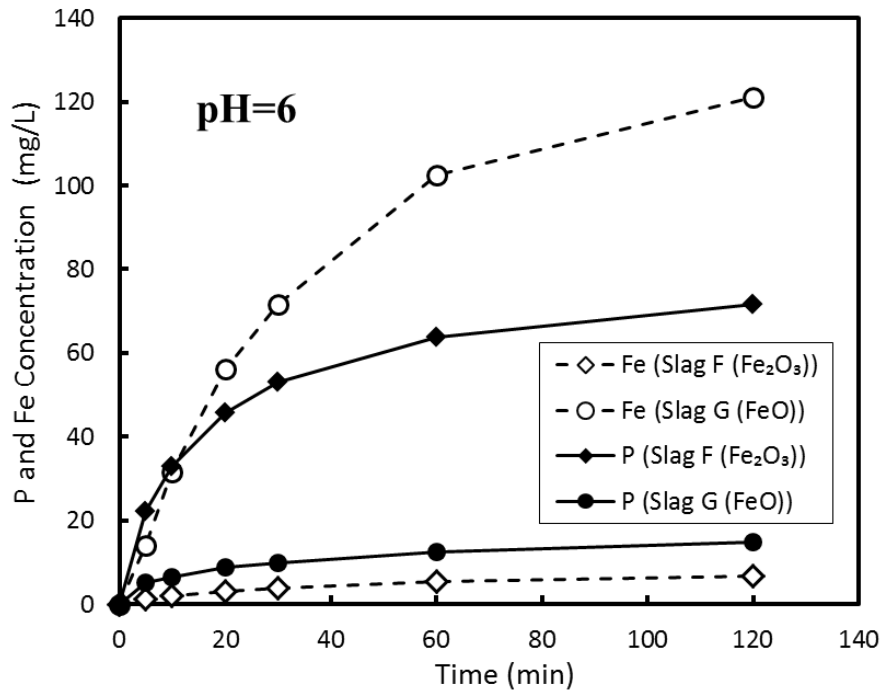


Fig. 3.26 Change in the concentrations of each element under different valency of Fe

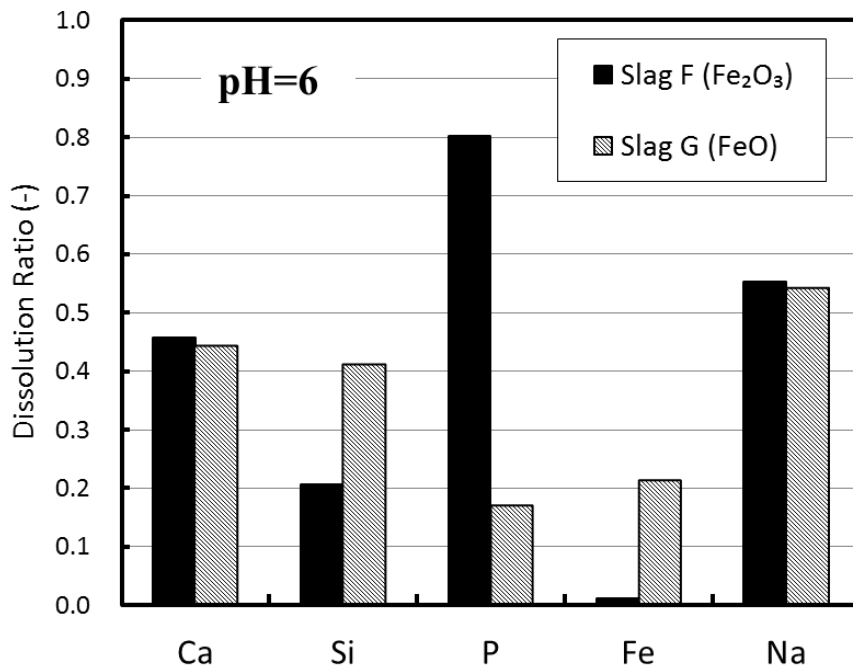


Fig. 3.27 Dissolution ratios of each element from different slags with different valency of Fe

The dissolution ratios of each element from slags with different valency of Fe at pH 6 were calculated using Eq. (3.4), as shown in Fig. 3.27. The dissolution ratio of Ca from these slags was almost the same, reaching 44%. About half of the Na was dissolved from each slag. For the slag containing Fe_2O_3 , the dissolution ratio of P was approximately 80%, which was higher than that of other elements. In this case, about one fifth of the Si was dissolved and the dissolution of Fe from slag was negligible. A better selective leaching of P from slag was performed. When the Fe_2O_3 in the slag changed to FeO, only 16.7% of the P was dissolved from slag, which was far lower than that from the slag containing Fe_2O_3 . However, the dissolution of Si and Fe was significantly promoted. The dissolution ratio of Si almost doubled, and that of Fe increased from 1.2% to 21.4%, which deteriorated selective leaching of P from slag.

3.2.4.3 Residue composition

The average compositions of residues after leaching at pH 6 are listed in Table 3.11. Compared with the original slag (listed in Table 3.1), in the case of slag containing Fe_2O_3 , the P_2O_5 content in the residue decreased to 1.71 mass% and the Fe_2O_3 content increased significantly due to selective leaching of P; however, in the case of slag containing FeO, the P_2O_5 content in the residue increased, reaching 9.91 mass%. Figure 3.28 shows the XRD patterns of slags with different valency of Fe and their residues after leaching at pH 6. The peaks associated with solid solution and Fe oxide were observed in each slag sample. The crystal form of Fe oxide changed slightly because of the difference in the valency of Fe. In the case of slag containing Fe_2O_3 , the peaks of solid solution almost disappeared after leaching, while that of Fe oxide remained and its intensity increased. It shows that the solid solution was dissolved and separated from slag after leaching. However, in the case of slag containing FeO, the peaks associated with solid solution still remained after leaching, indicating that the solid solution did not dissolve totally.

There were no peaks associated with phosphate precipitate in this residue. These results were in agreement with the above compositions of residues.

Table 3.11 Average compositions of residues after leaching at pH 6 (mass%)

Residue	CaO	SiO ₂	Fe ₂ O ₃	FeO	P ₂ O ₅	Na ₂ O
Slag F	24.73	22.35	48.51	-	1.71	2.70
Slag G	30.84	20.05	-	36.18	9.91	3.03

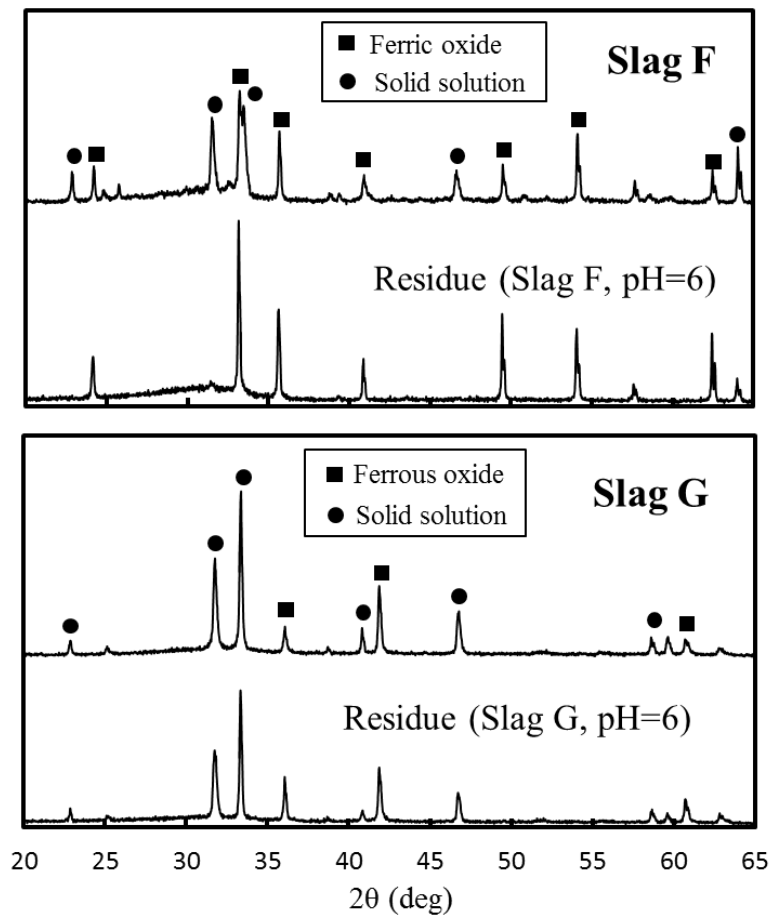


Fig. 3.28 XRD patterns of slags with different valency of Fe and their residues after leaching at pH 6

Figure 3.29 shows the EPMA images of the residue surface after leaching at pH 6. The compositions of the identified domains on the residue surface were listed in Table 3.12. Two phases which have the similar composition with matrix phase and Fe-rich phase were observed

on the residue surface of slag containing Fe_2O_3 . In this residue, it was difficult to detect the solid solution particles, indicating that the solid solution which contacted with the aqueous solution had dissolved selectively. In the case of slag containing FeO , besides Fe-rich phase and matrix phase, a domain with high P_2O_5 content was also observed. Its composition was similar with that of solid solution, demonstrating that solid solution did not dissolve sufficiently.

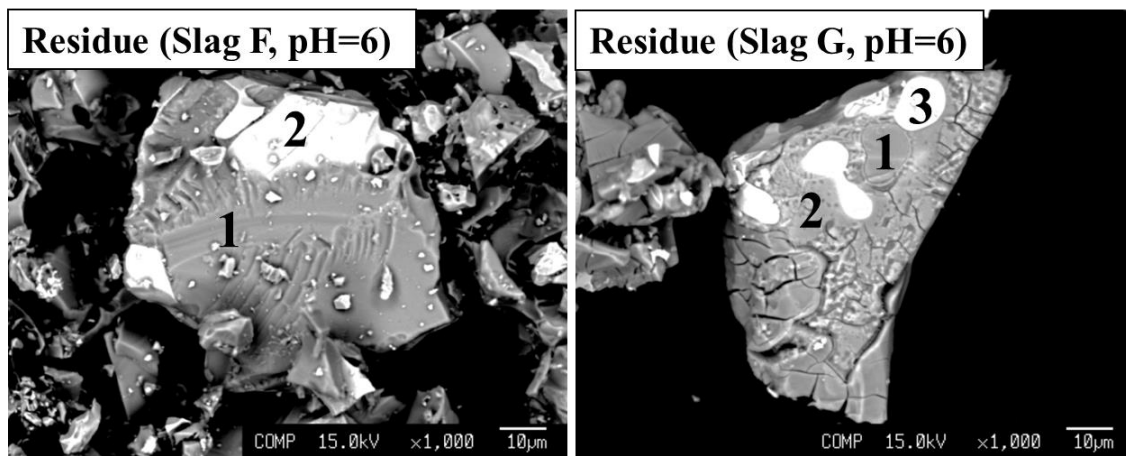


Fig. 3.29 EPMA images of the residue surface after leaching in the citric solution at pH 6

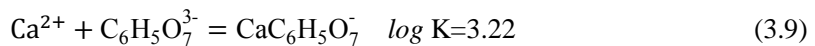
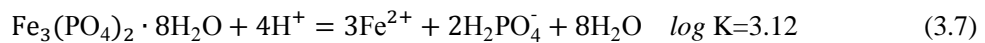
Table 3.12 Average compositions of some phases on the residue surface after leaching (mass%)

		CaO	SiO ₂	Fe _t O	P ₂ O ₅	Na ₂ O
Residue (Slag F)	1	36.7	38.6	19.9	1.7	3.2
	2	0.5	0.3	99.1	0.0	0.0
Residue (Slag G)	1	41.6	26.7	12.8	16.2	2.7
	2	19.4	42.6	33.3	4.1	0.5
	3	0.7	0.4	98.7	0.1	0.1

3.2.4.4 Discussion on the effect of the valency of Fe in slag

For the slag containing Fe_2O_3 , as the matrix phase was difficult to dissolve, the Fe concentration in the aqueous solution was very low. However, for the slag containing FeO , the Fe concentration was comparable with that of Si. Therefore, the possibility to precipitate iron

phosphate is discussed. As discussed in the previous studies, the predominant phosphate species in the aqueous solution are H_2PO_4^- at pH 6 [18, 19]. When Fe^{2+} and H_2PO_4^- exist in the aqueous solution, vivianite ($\text{Fe}_3(\text{PO}_4)_2 \cdot 8\text{H}_2\text{O}$) is possible to precipitate [20]. The dissolution reaction of vivianite and its equilibrium constant is described by Eqs. (3.7) [8, 20]. Based on these results, the relationship between the Fe^{2+} and P concentrations in the aqueous solution was calculated at pH 6, as shown in Fig. 3.30. In the citric solution, citrate ions ($\text{C}_6\text{H}_5\text{O}_7^{3-}$) can form complexes with Fe^{2+} . The formation reaction of $\text{FeC}_6\text{H}_5\text{O}_7^-$ complex is described by Eqs. (3.8) [20]. The remaining Fe^{2+} , which did not react with the citrate ions, were identified as free Fe^{2+} in the aqueous solution. Because Ca^{2+} can also form complex, as shown in Eq. (3.9) [21], the existence of $\text{CaC}_6\text{H}_5\text{O}_7^-$ was taken into consideration. The $\text{C}_6\text{H}_5\text{O}_7^{3-}$ concentration was determined by the final volume of the aqueous solution and the mass of the added citric acid. Using these equations, the concentration of free Fe^{2+} in the citric solution was calculated. The result is shown in Fig. 3.30. Although the total Fe concentration was high, the free Fe^{2+} concentration was very low, only 0.29 mg/L. The points for the concentration of P and free Fe^{2+} was located nearly the solubility line of vivianite. It shows that the dissolved P is possible to be restricted by the solubility of vivianite. Because the free Fe^{2+} concentration is too low, the amount of phosphate precipitate is negligible. As mentioned in the XRD results (Fig. 3.28), there were no peaks associated with phosphate precipitate in the residue. Therefore, most of the dissolved P could stably exist in the citric solution and did not precipitate in the case of slag containing FeO.



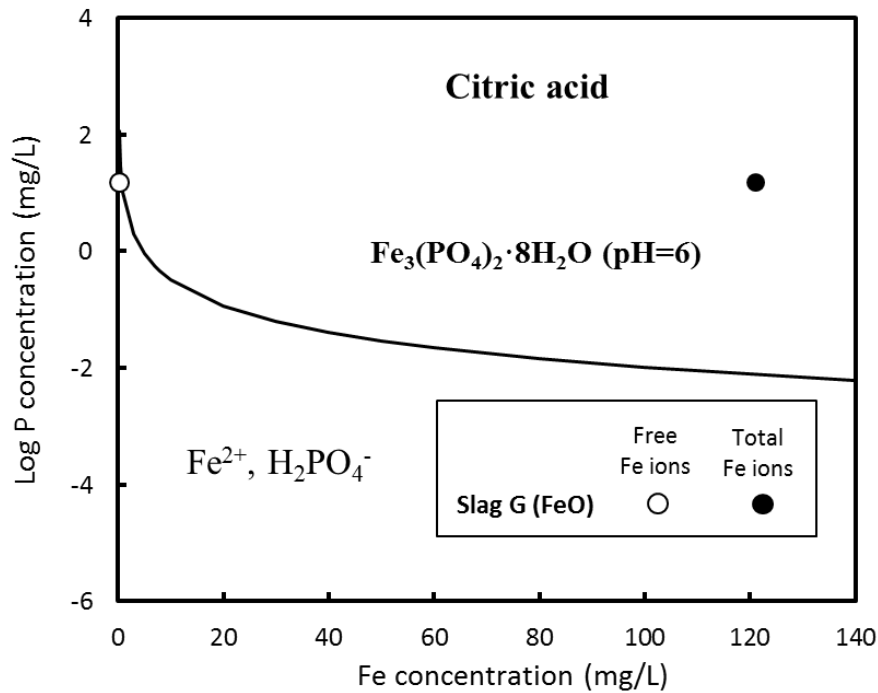


Fig. 3.30 Solubility line of phosphate precipitate and leaching results

Assuming that solid solution or matrix phase was individually dissolved, the dissolution ratios of P and Fe from slags with different valency of Fe were calculated using the mass fraction and composition of each phase. The calculated dissolution ratios were compared with the experimental results, as shown in Fig. 3.31. The calculated dissolution ratio of P from the slag containing Fe_2O_3 and slag containing FeO reached 91.1% and 95.0%, respectively, when the solid solution was totally dissolved. For the slag containing Fe_2O_3 , the practical dissolution ratio of P was close to the calculated value. The dissolution ratio of Fe was very low, same as that calculated from solid solution. It indicates that the majority of the solid solution was dissolved and the dissolution of other phases was insignificant. A better selective leaching of solid solution was performed.

In the case of slag containing FeO, the practical dissolution ratio of P was far lower than the calculated value, indicating that the dissolution of solid solution was poor. However, the dissolution ratio of Fe was higher than the value calculated from solid solution and lower when

the solid solution and matrix phase were both dissolved. It indicates that some of the dissolved Fe was supplied from the matrix phase. Gao *et al.* [10] has proved that Fe was easier to be dissolved in the aqueous solution from the CaO-FeO-SiO₂ phase than from the CaO-Fe₂O₃-SiO₂ phase. In summary, when FeO exists in slag, the dissolution of solid solution became difficult and the dissolution of matrix phase occurred obviously.

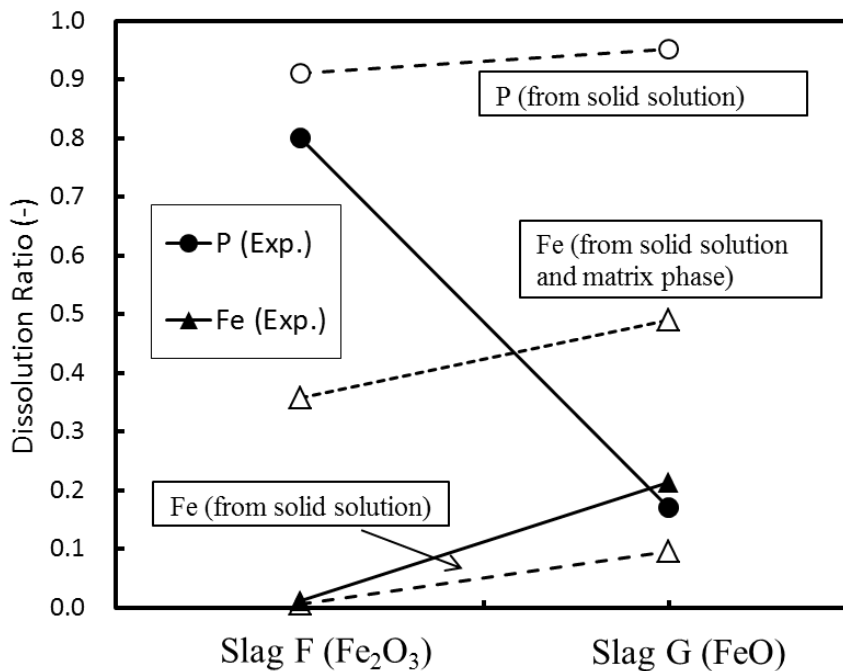


Fig. 3.31 Calculated dissolution ratios of P and Fe, and experimental results

The different dissolution behavior of these slags was attributed to the difference in their mineral structure and bond strength. As pointed by Hume-Rothery rule [22], if the radius of two different ions is near and they have the same ionic valence, these ions can be replaced with each other in the solid solution. As listed in Table 3.13 [12, 23], compared to Fe³⁺, Fe²⁺ has the same ionic valence as Ca²⁺, and the radius of Fe²⁺ is closer to that of Ca²⁺. Therefore, Fe²⁺ ions can replace with Ca²⁺ and are easier to enter into the C₂S-C₃P solid solution. This is the reason that some FeO existed in the solid solution in the slag containing FeO. For the solid solution

containing FeO, some Fe–O–P bonds are possible to exist, besides Ca–O–P bond. Because the ionization potential of Fe²⁺ is larger than that of Ca²⁺, the bond strength of Fe–O is higher than that of Ca–O [12]. The Fe–O–P bond is difficult to be broken than Ca–O–P bond during leaching. Therefore, for the slag containing FeO, the dissolution ratio of the solid solution containing FeO was lower.

Table 3.13 Effective ionic radius for cations and anions and their coordination number and ionization potential

Ion	Coordination number	Ionic radius (nm)	Z/r^2 (nm ⁻²)
Na ⁺	6	0.102	96.1
Ca ²⁺	6	0.100	200.0
Fe ²⁺	6	0.061	537.5
Fe ³⁺	6	0.055	991.7
Si ⁴⁺	4	0.026	5917.1
P ⁵⁺	4	0.017	17301.0
O ²⁻	-	0.140	102.0

Matrix phase in these slags is the silicate glass of CaO-Fe_tO-SiO₂ system. As discussed in Section 3.2.1.3, it has been reported commonly that Fe²⁺ ions in silicate glass act as network modifier, resulting in octahedral coordination [24], as shown in Fig. 3.32. However, in the case of CaO-Fe₂O₃-SiO₂ glass, Fe³⁺ ions are tetrahedrally and octahedrally coordinated [13, 14]. In tetrahedral site, Fe³⁺ ions act as network former, similar with SiO₄⁴⁻. As listed in Table 3.13, the ionization potential of Fe³⁺ is larger than that of Fe²⁺, and thus the bond strength of Fe(ferric)–O is higher. In addition, because the bond length of Fe–O in the tetrahedral site is shorter than that in the octahedral site, the strong Fe(ferric)–O bond exists in the tetrahedral site. It is concluded that the Fe(ferric)–O–Si bond is more stable than the Fe(ferrous)–O–Si bond in the silicate glass. Therefore, the dissolution of CaO-Fe₂O₃-SiO₂ phase in the aqueous solution was difficult compared with CaO-FeO-SiO₂ phase.

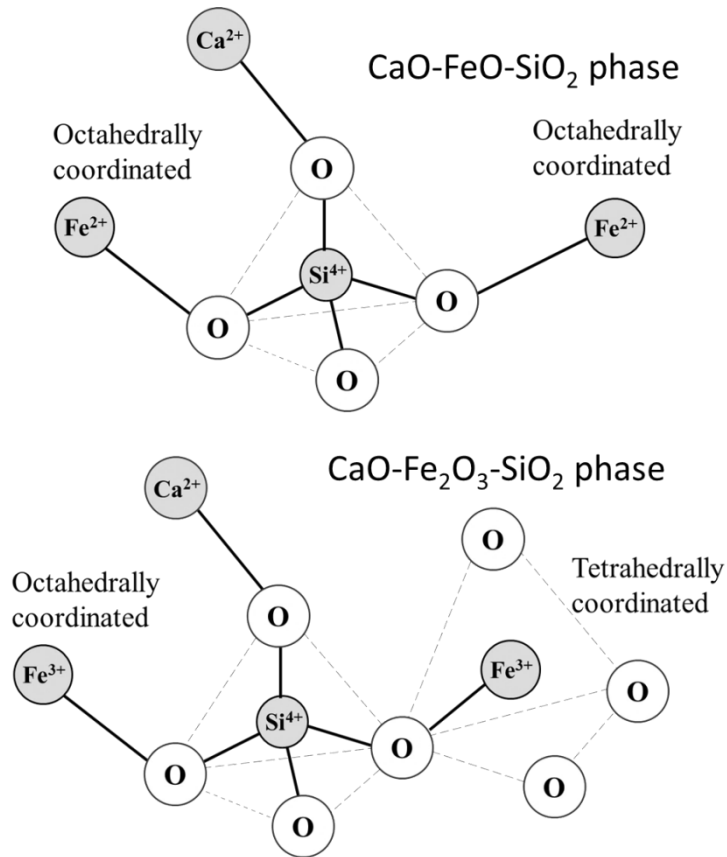


Fig. 3.32 Schematic illustration of the structure of CaO-FeO-SiO₂ and CaO-Fe₂O₃-SiO₂ phases

On the basis of mass balance, the phase fractions in slags with different valency of Fe were calculated and compared with the mass fractions of the dissolved part and residue in Fig. 3.33. When the Fe₂O₃ in slag changed to FeO, the mass fraction of the solid solution increased significantly, and those of the matrix phase and Fe oxide decreased correspondingly. For the slag containing Fe₂O₃, the mass fraction of the dissolved part was almost the same as that of the solid solution, showing that a better selective leaching of solid solution. For the slag containing FeO, the mass fraction of the solid solution was about 45%. Although the mass fraction of the dissolved part increased compared to the slag containing Fe₂O₃, it was lower than that of the solid solution. Considering that the dissolution of matrix phase occurred as mentioned above, this result also shows that the dissolution of solid solution was insufficient. This is because the

existence of FeO suppressed the dissolution of solid solution. Therefore, to promote the dissolution of solid solution and suppress the dissolution of matrix phase, the steelmaking slag should be oxidized to transform into the Fe₂O₃-containing slag.

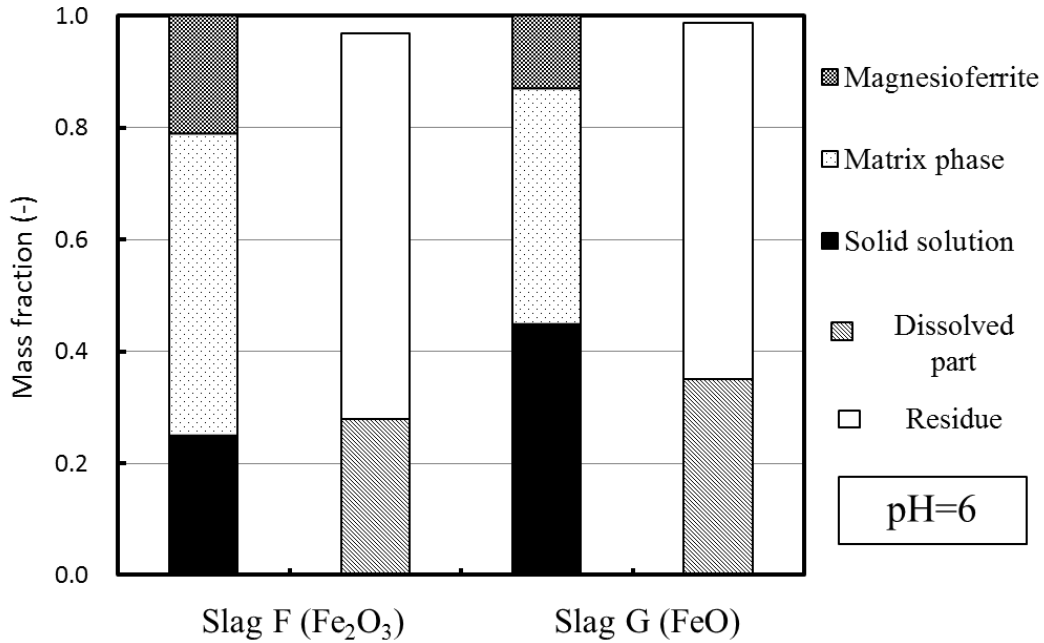


Fig. 3.33 Mass fractions of the dissolved part and residue, compared with phase fractions of slags with different valency of Fe

3.3 Summary

In order to achieve selective leaching of P from slag with high P₂O₅ content, the effects of the cooling rate of molten slag, Na₂O content, pH, and the valency of Fe in slag on the dissolution behavior of the modified slag were investigated. The results obtained are summarized below:

- (1) Decreasing cooling rate promoted the enrichment of P₂O₅ in the solid solution and the formation of magnesioferrite phase. Compared to the quenched slag, the furnace-cooled slag exhibited a higher dissolution ratio of P and a lower dissolution ratio of Fe, indicating that slow cooling was beneficial for selective leaching of solid solution from the modified slag.

- (2) Na_2O addition resulted in a higher mass fraction of the solid solution in slag. With the increase in the Na_2O content, the dissolution ratios of Ca, Si, and P from slag increased at pH 6, while Fe was barely dissolved. When the Na_2O content was 4 mass%, the majority of the solid solution was dissolved, showing a better selective leaching of P. Further increase in the Na_2O content did not increase P dissolution largely.
- (3) As the pH decreased, the dissolution of the modified slag was promoted, resulting in higher dissolution ratios of each element. The dissolution ratio of P increased significantly when the pH decreased from 7 to 5. Further decrease in the pH caused little improvement in P dissolution, and resulted in dissolution of large amounts of Fe. When the pH was controlled between 5 and 6, most of the solid solution was dissolved without a large dissolution of other phases.
- (4) The P_2O_5 content in the solid solution of the slag containing Fe_2O_3 was higher compared to that of the slag containing FeO, while the mass fraction of solid solution was lower. When the FeO in the slag changed to Fe_2O_3 , the dissolution ratio of P increased significantly at pH 6, and the dissolution of Si and Fe was suppressed. Oxidizing slag was necessary to achieve selective leaching of P from the modified slag.
- (5) Through selective leaching, the P_2O_5 content in the residue decreased compared to the original slag, and the Fe_2O_3 content increased correspondingly. Increasing the Na_2O content in the slag and decreasing the pH could further decrease the P_2O_5 content in the residue. Due to the dissolution and separation of the P-concentrated phase from slag, the residue had the potential for recycling within the ironmaking and steelmaking process.

References

1. M. Gautier, J. Poirier, F. Bodéan, G. Franceschini, E. Véron: *International Journal of Mineral Processing*, 123 (2013), pp. 94-101.
2. K. Maweja, T. Mukongo, R. K. Mbaya, E.A. Mochubele: *Journal of Hazardous Materials*, 183(2010), pp. 294-300.
3. H. Mizukami, M. Ishikawa, T. Hirata, T. Kamiyama, K. Ichikawa: *ISIJ International*, 44(2004), pp. 623-629.
4. T. Teratoko, N. Maruoka, H. Shibata, S. Kitamura: *High Temperature Material Process*, 31(2012), pp. 329-338.
5. S. Kitamura, F. Pahlevani: *Tetsu-to-Hagané*, 100(2014), pp. 500-508.
6. Y. Uchida, N. Sasaki, Y. Miki: *Tetsu-to-Hagané*, 102(2016), pp. 691-697.
7. M. Numata, N. Maruoka, S.J. Kim, S. Kitamura: *ISIJ International*, 54(2014), pp. 1983-1990.
8. T. Futatsuka, K. Shitogiden, T. Miki, T. Nagasaka and M. Hino: *ISIJ International*, 44 (2004), pp. 753-761.
9. A. L. Iglesia: *Estudios Geológicos*, 65 (2009), pp. 109-119.
10. X. Gao, N. Maruoka, S.J. Kim, S. Ueda, S. Kitamura: *Journal of Sustainable Metallurgy*, 1(2015), pp. 304-313.
11. F.K. Crundwell: *Hydrometallurgy*, 149(2014), pp. 265-275.
12. I. Sohn, D.J. Min: *Steel Research International*, 83(2012), pp. 611-630.
13. N. Iwamoto, Y. Tsunawaki, H. Nakagawa, T. Yoshimura, N. Wakabayashi: *Journal of Non-Crystalline Solids*, 29 (1978), pp. 347-356.
14. K. Nagata, M. Hayashi: *Journal of Non-Crystalline Solids*, 282(2001), pp. 1-6.
15. B. Hannoyer, M. Lenglet, J. Durr, R. Cortes: *Journal of Non-Crystalline Solids*, 151(1992), pp. 209-216.
16. R.D. Shannon: *Acta Crystallographica Section A*, A32(1976), pp. 751-767.
17. J. Ando: *Bulletin of the Chemical Society of Japan*, 31(1958), pp. 196-201.
18. S. Recillas, V. Rodríguez-Lugo, M.L. Montero, S. Viquez-Canoc, L. Hernandez, V.M. Castaño: *Journal of Ceramic Processing Research*, 13 (2012), pp. 5-10.
19. Kagakubinran, Kisohe, ed. by The Chemical Society of Japan, Maruzen Publishing, Tokyo, 1984.
20. S.J. Markich, P.L. Brown: *Thermochemical Data for Environmentally-relevant Elements*, ANSTO Environment Division, NSW, 1999.
21. J. Muus, H. Lebel: *Mathematisk-fysiske Meddelelser Danske Videnskabernes Selskab*, 13 (1936), pp. 1-16.

22. U. Mizutani: Hume-Rothery Rules for Structurally Complex Alloy Phases, Taylor & Francis, USA, 2010.
23. R.D. Shannon: Acta Crystallographica Section A, A32(1976), pp. 751-767.
24. L. Pargamin, C.H.P. Lupis, P.A. Flinn: Metallurgical Transactions, 3(1972), pp. 2093-2105.

4 Dissolution behavior of P from modified steelmaking slag with K₂O addition

K₂O has the similar chemical property with Na₂O, and is also an important fertilizer constituent. It was necessary to investigate the effect of K₂O addition on selective leaching of P from slag. In this study, the slag with high P₂O₅ content was modified by adding K₂O, and then leached in the citric solution at different pH conditions.

4.1 Experimental method

The method for synthesis of slag was similar with that described in Chapter 3. To prepare the steelmaking slag for a CaO-SiO₂-Fe₂O₃ system, reagent-grade SiO₂, Fe₂O₃, Ca₃(PO₄)₂, MgO and K₂CO₃, along with CaO (obtained by calcining CaCO₃ at 1273 K), were fully mixed and heated in a Pt crucible under air atmosphere. On the basis of the above results, Fe₂O₃ was used as the iron oxide because the dissolution ratio of P from this slag was higher than that from the CaO-SiO₂-FeO system slag [1]. The initial compositions of slags with different K₂O contents are shown in Table 4.1. Assuming that K₂CO₃ can decompose to K₂O, the target mass ratio of K₂CO₃ was added. In preliminary experiments, we confirmed that the vaporization of K₂O was negligible during slag synthesis. The P₂O₅ content in each slag was fixed as 8 mass%. Cooling method of these slags is furnace cooling. The heating pattern is the same as that shown in Fig. 3.1. These slags were first heated at 1823 K for 1 h to form a homogeneous liquid phase. Then, it was cooled to 1623 K at a cooling rate of 3 K/min and held at this temperature for 20 min to precipitate solid solution. Finally, the slag was cooled in furnace at a cooling rate of 5 K/min, and withdrew from the furnace at 1323 K. The composition of each phase in slag was measured

using electron probe microanalysis (EPMA). In addition, the precipitated phases were determined using X-ray diffraction (XRD) analysis.

The experimental procedure of leaching was the same as that used in the above studies. In this chapter, the synthesized slags with different K₂O contents were leached by citric acid (0.1 mol/L) at pH 5, 6, and 7, respectively. The concentrations of each element in the filtered aqueous solution were analyzed using inductively coupled plasma-atomic emission spectroscopy (ICP-AES), and the residue was weighted, and then analyzed by EPMA and XRD. The analysis method of residue composition is the same method described in Chapter 3.

Table 4.1 Compositions of slags with different K₂O contents (mass%)

Sample	CaO	SiO ₂	Fe ₂ O ₃	P ₂ O ₅	MgO	K ₂ O
Slag A	37.0	23.0	29.0	8.0	3.0	0
Slag B	34.5	21.5	29.0	8.0	3.0	4.0
Slag C	32.1	19.9	29.0	8.0	3.0	8.0

4.2 Experimental results

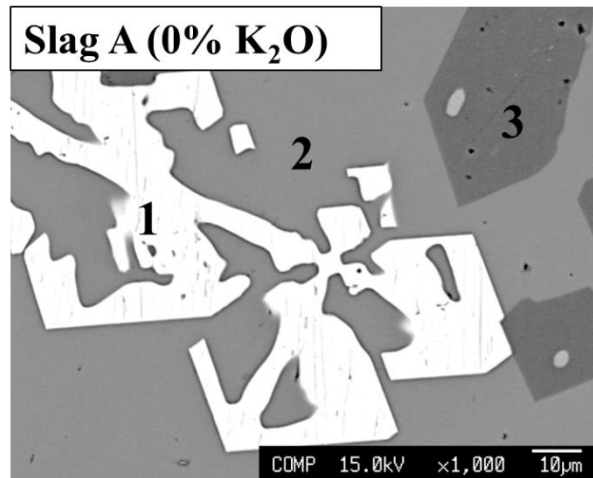
4.2.1 Mineralogical composition of slags

Typical mineralogical structure for each slag with different K₂O contents and the compositions of each phase analyzed by EPMA are shown in Fig. 4.1 and Table 4.2. In the slag without K₂O addition, three phases were observed. In addition to solid solution, magnesioferrite phase were precipitated from the matrix phase during slow cooling. There was a high distribution ratio of P between the solid solution and other phases. In contrast, Fe was mainly distributed in the matrix phase and magnesioferrite phase. Similar condition was also found in the slags with K₂O addition. Moreover, in these slags, some small solid solution particles, which had a lower P₂O₅ content than the large solid solution particles, surrounded magnesioferrite phase were observed. The added K₂O was distributed to the solid solution, but its content was lower than that in the

matrix phase. With the increase in the K_2O content in slag, the K_2O content in the solid solution increased, but the P_2O_5 content decreased. When 8 mass% of K_2O was added, the K_2O content in the solid solution reached 8.2 mass%, and the P_2O_5 content decreased from 31.3 mass% to 20.1 mass%. For the matrix phase, K_2O addition resulted in a decrease in the CaO and SiO_2 contents, corresponding to an increase in the Fe_2O_3 content.

Table 4.2 Average compositions of each phase in slags with different K_2O contents (mass%)

Sample		CaO	SiO ₂	Fe ₂ O ₃	P ₂ O ₅	MgO	K ₂ O	Phase
Slag A (0% K ₂ O)	1	1.3	0.1	88.1	0.0	10.5	0.0	Magnesianferrite
	2	40.0	34.8	21.5	1.8	1.9	0.0	Matrix phase
	3	54.9	11.8	1.1	31.3	0.9	0.0	Solid solution
Slag B (4% K ₂ O)	1	2.0	0.2	86.2	0.1	11.3	0.1	Magnesianferrite
	2	32.1	33.5	25.6	1.8	1.6	5.4	Matrix phase
	3	54.6	17.4	1.3	23.3	0.5	2.9	Solid solution
	4	54.0	27.0	3.2	10.9	1.1	3.9	
Slag C (8% K ₂ O)	1	1.6	0.2	85.4	0.0	12.4	0.3	Magnesianferrite
	2	23.0	31.4	32.8	0.6	1.2	11.0	Matrix phase
	3	51.6	18.8	1.1	20.1	0.3	8.2	Solid solution
	4	55.5	25.4	2.6	10.8	0.5	5.3	



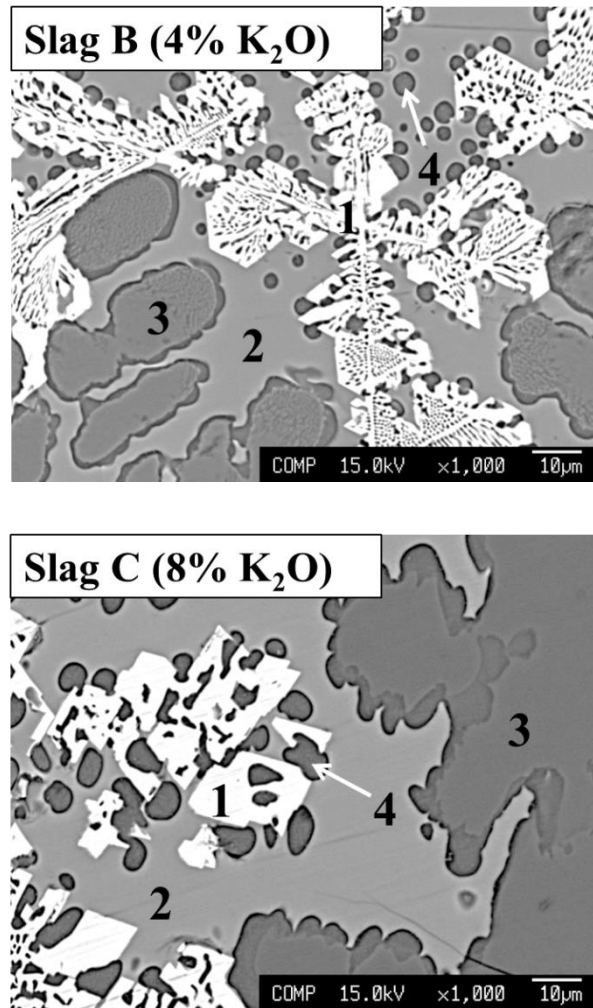


Fig. 4.1 Cross sections ($\times 1000$) of slags with different K_2O contents

The compositions of solid solution in slags with different K_2O contents were plotted in a $(CaO+K_2O)-SiO_2-P_2O_5$ pseudo-phase diagram, as shown in Fig. 4.2. The K_2O content in the solid solution was taken into consideration. The compositions of solid solution in this study are nearly located on the line between $2(CaO, K_2O)\cdot SiO_2$ and $3(CaO, K_2O)\cdot P_2O_5$. This would indicate that a part of CaO in the C_2S-C_3P solid solution was replaced by K_2O in the newly formed solid solution. The similar condition was also observed in the modified slag by Na_2O addition. A higher K_2O content in slag led to a lower P_2O_5 content in the solid solution. In

addition, the compositions of small solid solution particles with lower P_2O_5 content are also located on this line.

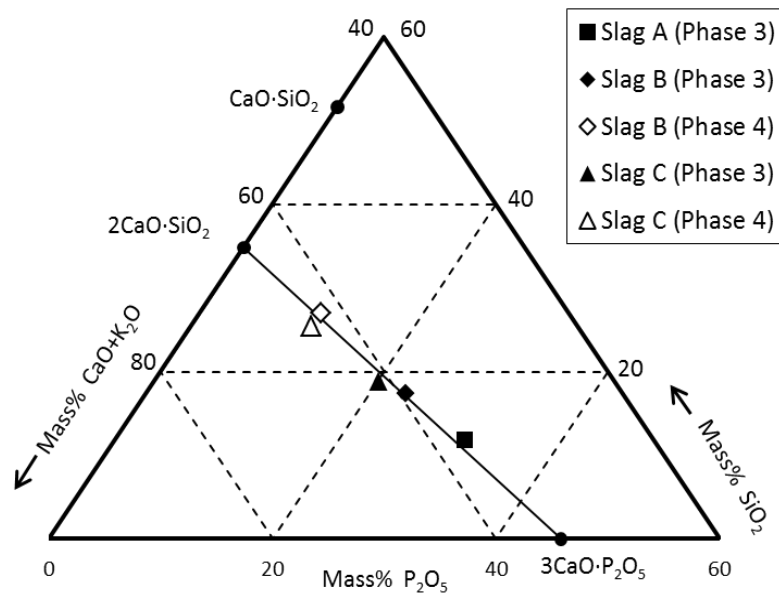


Fig. 4.2 Compositions of solid solution in the $(CaO+K_2O)-SiO_2-P_2O_5$ pseudo-phase diagram

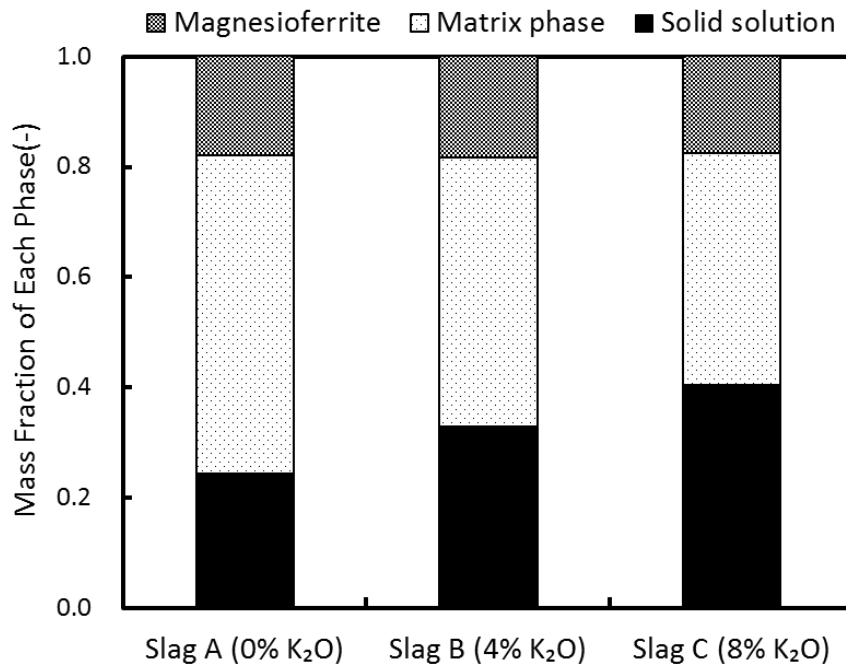


Fig. 4.3 Mass fractions of each phase in slags with different K_2O contents

The mass fractions of each phase in different slags were estimated using above EPMA results. To simplify calculation, we disregarded a small portion of the small solid solution particles with low P₂O₅ content. The mass balance of each oxide can be represented using Eq. (4.1)

$$N_{\text{MO}_n} = \alpha N_{\text{MO}_n}^{\alpha} + \beta N_{\text{MO}_n}^{\beta} + \gamma N_{\text{MO}_n}^{\gamma} \quad (4.1)$$

$$\alpha + \beta + \gamma = 1 \quad (4.2)$$

where α , β , and γ are the mass fractions of the magnesioferrite phase, matrix phase, and solid solution, respectively, N_{MO_n} is the MO_n content in slag, and $N_{\text{MO}_n}^{\alpha}$ is the MO_n content in phase α . The contents of major oxides (CaO, SiO₂, Fe₂O₃, and P₂O₅) were used for calculation, and the average of these calculations was defined as the mass fraction of each phase in slag. The calculated mass fractions of each phase are shown in Fig. 4.3. There was little change in the mass fraction of the magnesioferrite phase in different slags. With the increase in the K₂O content in slag, the mass fraction of the solid solution increased, and that of the matrix phase decreased correspondingly. When 8 mass% of K₂O was added, the mass fraction of the solid solution increased from 24.1% to 40.2%. As a result of the increase in mass fraction of the solid solution, the P₂O₅ condensed in the solid solution was “diluted”, and its content decreased; meanwhile, a part of CaO and SiO₂ in the matrix phase were used to enlarge the fraction of solid solution, which caused the decrease in their contents of the matrix phase.

On the basis of the above results, the mass fractions of each oxide distributed in the solid solution were evaluated as:

$$Y_{\text{MO}_n}^{\gamma} = \frac{\gamma \cdot N_{\text{MO}_n}^{\gamma}}{N_{\text{MO}_n}} \quad (4.3)$$

where $Y_{\text{MO}_n}^{\gamma}$ is the mass fraction of MO_n distributed in the solid solution. Figure 4.4 shows the calculated values of CaO, SiO₂, and P₂O₅. For the slag without K₂O addition, a small portion of the CaO and SiO₂ was distributed in the solid solution; most of the P₂O₅ was concentrated in the

solid solution. K_2O addition increased the mass fractions of CaO , SiO_2 , and P_2O_5 distributed in the solid solution, because of an increase in the mass fraction of the solid solution in slag. In the case of slag with 8 mass% of K_2O , although the P_2O_5 content in the solid solution decreased, more than 95% of the P_2O_5 was concentrated in the solid solution. Approximately 67.7% of the Ca and 36.9% of the Si was also distributed in this solid solution. Overall, K_2O addition was beneficial for the enlargement of solid solution and the enrichment of P_2O_5 in the solid solution.

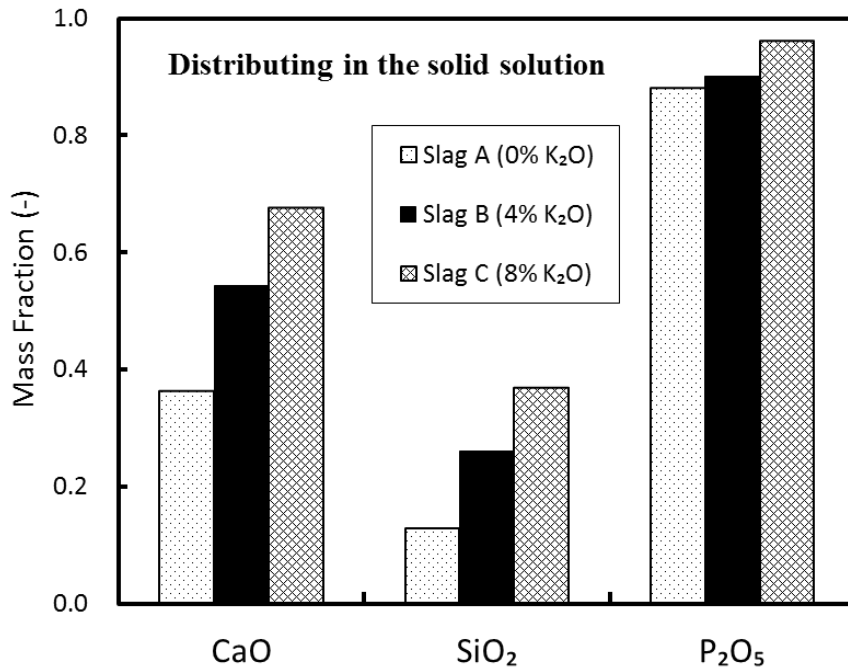
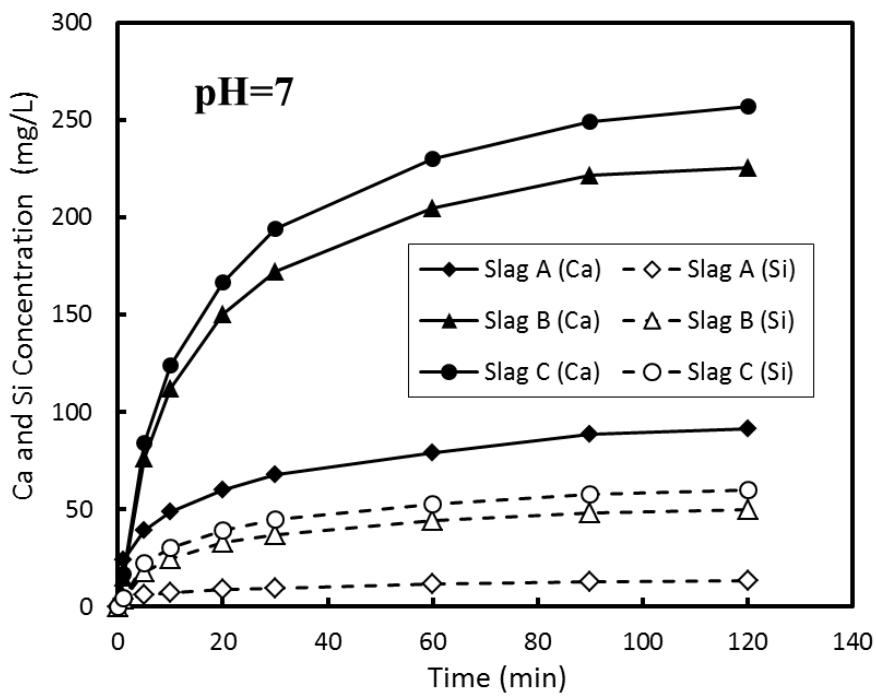


Fig. 4.4 Mass fractions of each element distributed in the solid solution

4.2.2 Dissolution behavior of slags at different pH conditions

Figure 4.5 shows the concentrations of each element as a function of leaching time in the citric solution at pH 7. As the leaching progressed, the concentrations of Ca, Si, and P increased, but after 60 min they exhibited a little change, showing that the dissolution rate of slag decreased. The Ca concentration was the highest among the dissolved elements. Fe was difficult to dissolve,

and its concentration was less 2.0 mg/L in each case. For the slag without K_2O addition, the concentrations of each element were lower. The Si and P concentrations reached 13.6 mg/L and 24.3 mg/L, respectively, after 120 min. When 4 mass% of K_2O was added to slag, the concentrations of each element increased significantly except Fe. The Ca concentration almost doubled, reaching 225.7 mg/L. The Si and P concentrations increased to 49.8 mg/L and 37.0 mg/L, respectively. However, further increase in the K_2O content had a little effect in increasing the Ca and Si concentrations. The P concentration of the slag with 8 mass% of K_2O was almost the same as that of the slag with 4 mass% of K_2O .



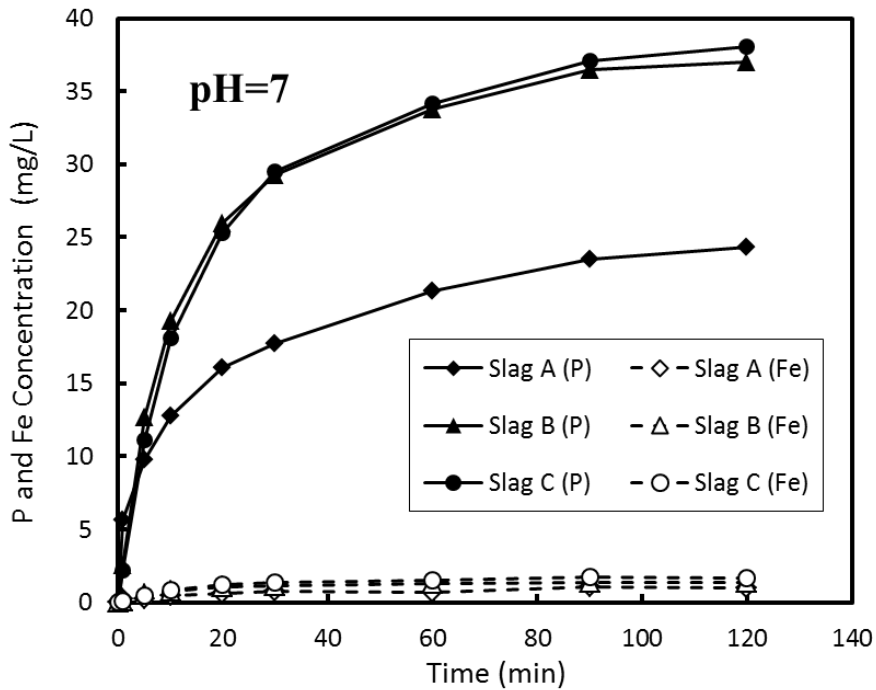


Fig. 4.5 Change in the concentrations of each element in the citric solution at pH 7

The dissolution ratios of each element from slags with different K_2O contents were calculated as:

$$R_M = \frac{C_M \cdot V}{m_M} \quad (4.4)$$

where R_M is the dissolution ratio of element M, C_M is the concentration of element M after 120 min (mg/L), V is the final volume of the aqueous solution (L), and m_M is the mass of element M in the initial slag (mg). The calculated dissolution ratios at pH 7 are shown in Fig. 4.6. P was easier to be dissolved from each slag compared to other elements, showing the highest dissolution ratio. The Fe dissolution was negligible in this case. Without K_2O addition, the dissolution of slag was difficult. The dissolution ratio of Ca was only 12.8%, and approximately 25.8% of the P was dissolved. K_2O addition promoted the dissolution of slag, resulting in higher dissolution ratios of each element. For the slag with 4 mass% of K_2O , the dissolution ratio of Ca increased to 31.5% and that of Si almost tripled compared to the slag without K_2O addition.

There was a significant improvement in the P dissolution. However, the improvement in P dissolution was little with a larger addition of K_2O at pH 7. The dissolution ratio of P from the slag with 8 mass% of K_2O was 43.0%. The dissolution ratio of Mg was lower, less than 5.5%. With the increase in the K_2O content in slag, the dissolution ratio of K increased. For the slag with 8 mass% of K_2O , it reached 30.4%. In summary, K_2O addition promoted the dissolution of P from slag, which had the same effect as the Na_2O addition.

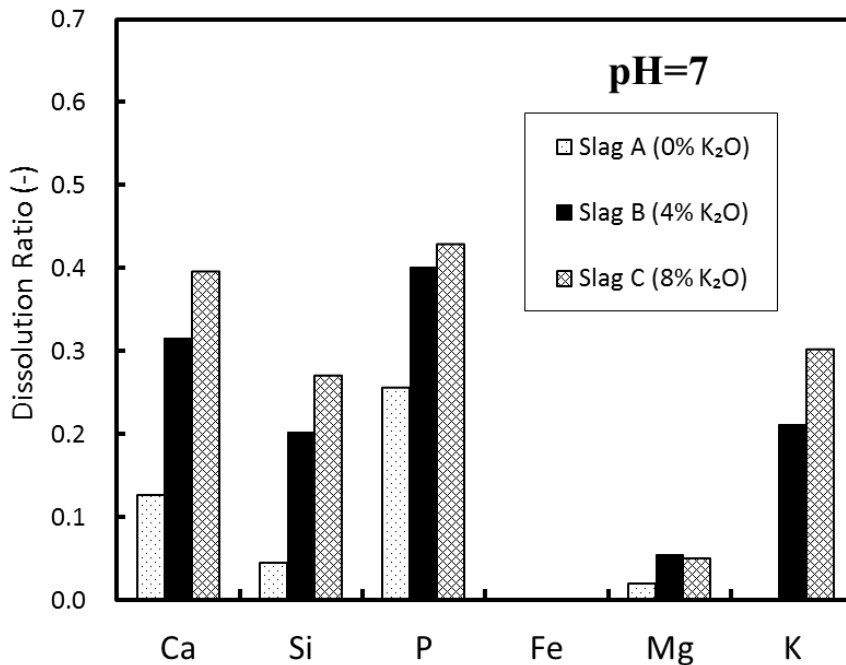
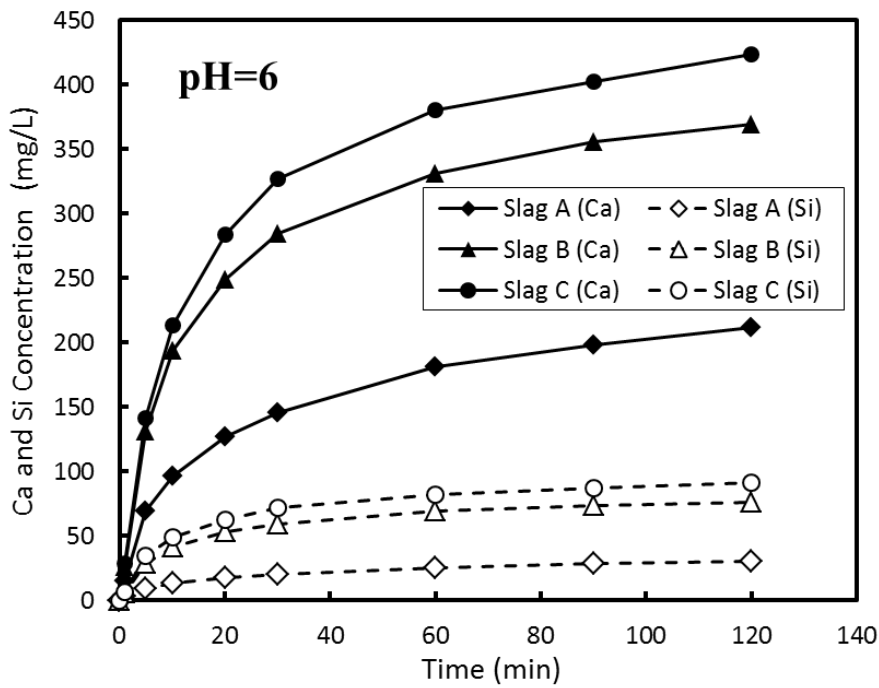


Fig. 4.6 Dissolution ratios of each element from slags with different K_2O contents at pH 7

The change in the concentrations of each element in the citric solution at pH 6 is shown in Fig. 4.7. Compared to the leaching results at pH 7, the concentrations of each element were higher; however, the difference among the slags exhibited almost the same trend. The concentrations of Ca, Si, and P increased rapidly in 20 min; however, following 60 min, the dissolution rate of slag decreased. The Fe and Mg concentrations were far lower than those of other elements, only several mg/L in each case. The Ca and Si concentrations of the slag without K_2O addition were

211.9 mg/L and 30.6 mg/L, respectively, after 120 min. When 4 mass% of K_2O was added, the concentrations of Ca and Si significantly increased, but a larger addition of K_2O resulted in a little increase in their concentrations. For the slag with 8 mass% of K_2O , the Ca concentration almost doubled compared to the slag without K_2O addition, and the Si concentration almost tripled. When 4 mass% of K_2O was added, the P concentration increased from 54.1 mg/L to 67.9 mg/L. If the K_2O content in slag increased continuously, it further increased, reaching 73.3 mg/L. The K concentration also increased with the K_2O content in slag. In the case of slag containing 8 mass% of K_2O , it reached 73.6 mg/L.



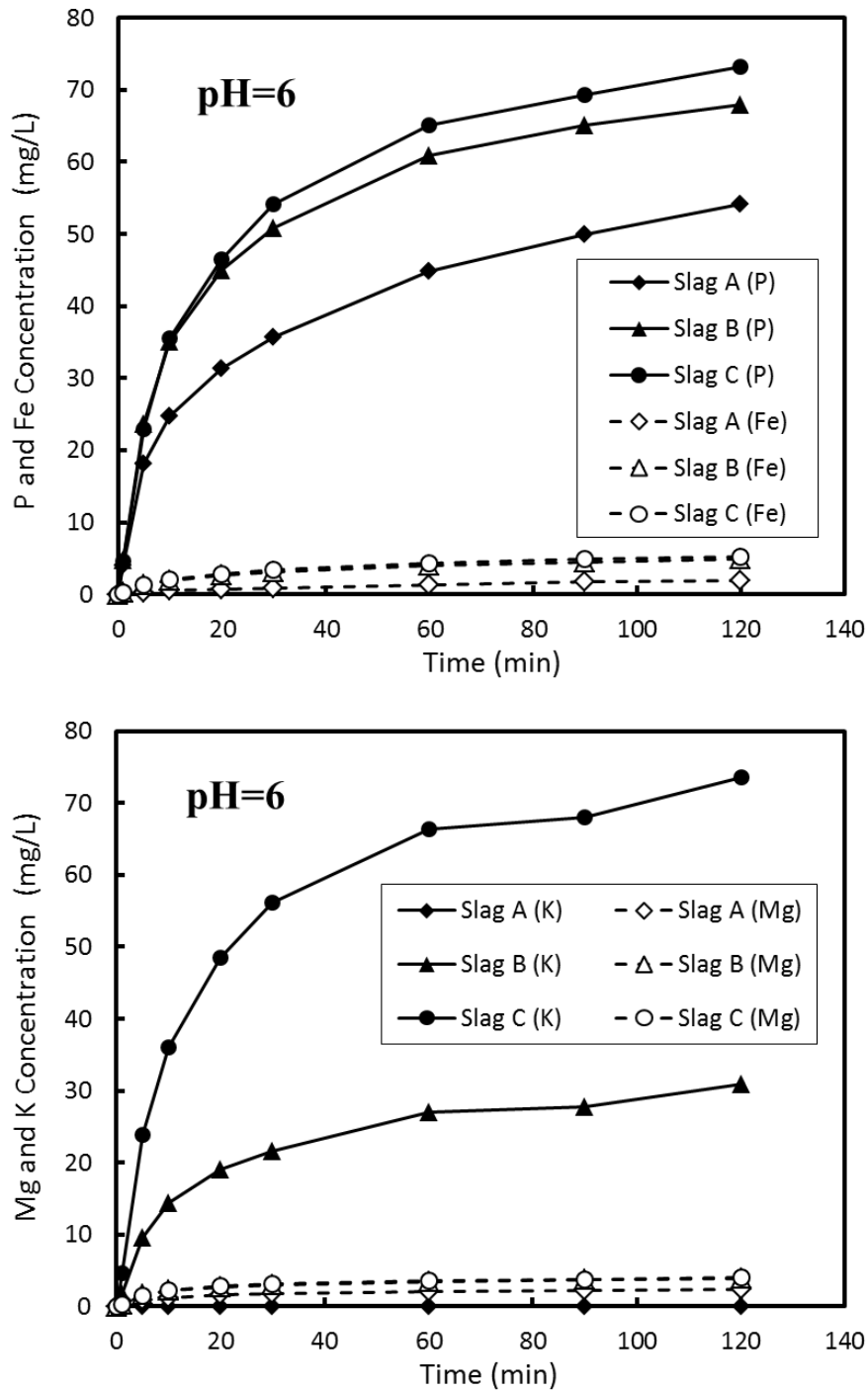


Fig. 4.7 Change in the concentrations of each element in the citric solution at pH 6

The dissolution ratios of each element from slags with different K_2O contents at pH 6 were calculated using Eq. (4.4), and are shown in Fig. 4.8. In each case, the dissolution ratio of P was

the highest, followed by those of Ca and Si, and the dissolution ratios of Fe and Mg were very low. Because Fe was mainly distributed in the magnesioferrite phase and matrix phase, it indicated that these two phases were difficult to be dissolved. In the case of the slag without K_2O addition, a selective leaching of P from slag was performed, but the dissolution ratio of P was insufficient, only 59.3%. With the increase in the K_2O content in slag, the dissolution of Ca, Si, and P was significantly promoted. For the slag with 8 mass% of K_2O , 72.0% of the Ca and 84.6% of the P were dissolved, while the Fe was hardly dissolved. The dissolution ratios of the added K and Mg were approximately 50% and 8%, respectively. In this case, a higher dissolution ratio of P and lower dissolution ratios of other elements demonstrated the superior selective leaching of P from slag.

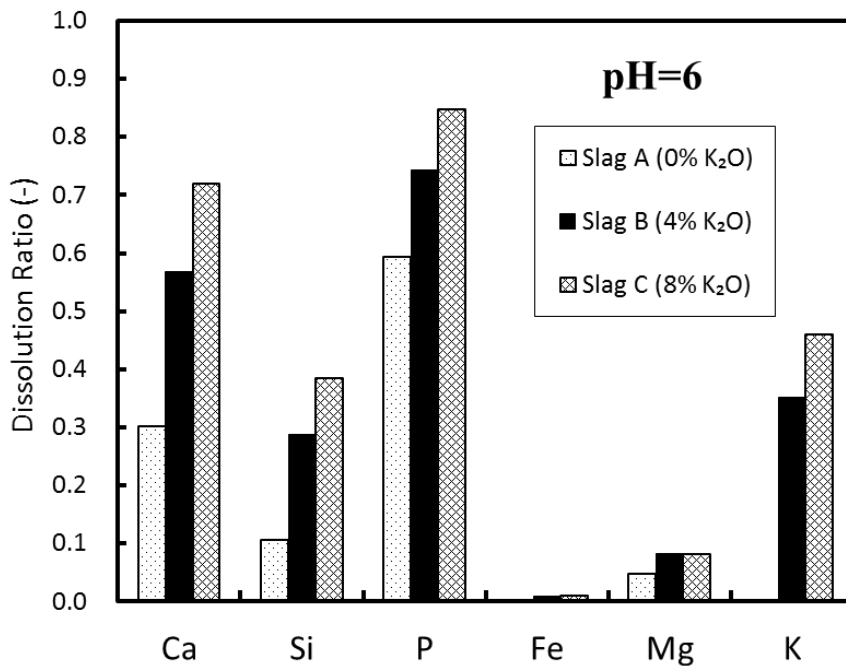


Fig. 4.8 Dissolution ratios of each element from slags with different K_2O contents at pH 6

The dissolution ratios of each element from slag at pH 5 were calculated using Eq. (4.4), and are shown in Fig. 4.9. A comparison with the results in Fig. 4.6 shows the significant increase in the

dissolution ratios of each element by the decrease in the pH. The dissolution of the slag without K_2O addition was large at pH 5, leading to higher dissolution ratios of each element. The dissolution ratio of P reached 82.2%, and approximately 20.4% of the Fe was also dissolved, which deteriorated selective leaching of P. When K_2O was added, the dissolution ratio of P had little change; however, the dissolution of other elements was significantly suppressed. In particular, the dissolution ratio of Fe decreased greatly, only 2.2%. Further increase in the K_2O content promoted dissolution of Ca, Si, and P, but did not affect dissolution of Fe and Mg. For the slag with 8 mass% of K_2O , the dissolution ratio of P reached 90.8%, which was far higher than those of Fe and Mg. These results show that the P-concentrated phase was preferentially dissolved compared with other phases. In summary, the modified slag with K_2O addition exhibited a better selective leaching of P at pH 5, because of a lower dissolution ratio of Fe.

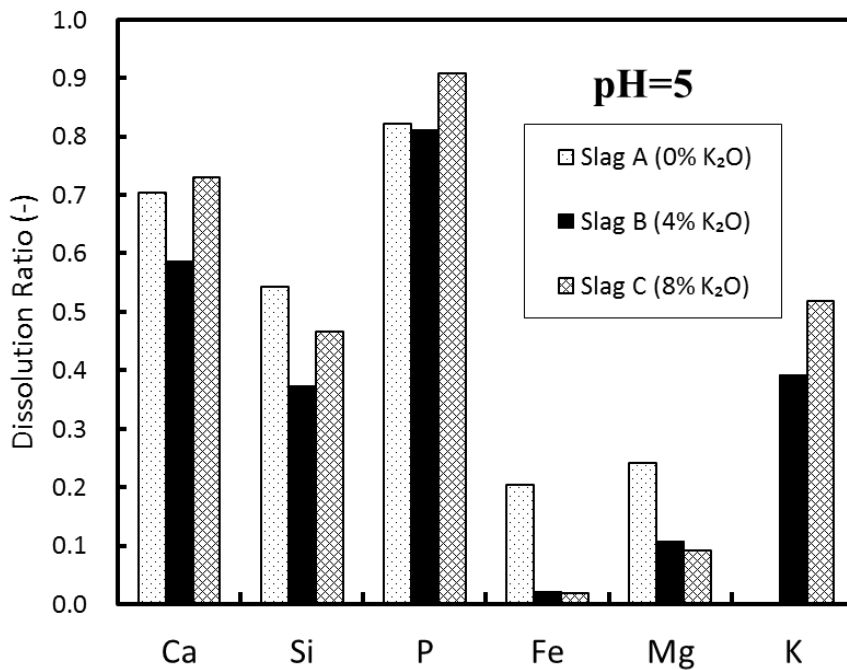


Fig. 4.9 Dissolution ratios of each element from slags with different K_2O contents at pH 5

Table 4.3 lists the acid consumption during leaching of slags with different K₂O contents at various pH conditions. With the increase in the K₂O content in slag, the consumption of citric acid increased at pH 6 and 7. For example, when 4 mass% of K₂O was added, acid consumption almost doubled. Decreasing pH also increased acid consumption because a larger portion of slag was dissolved. At pH 5, the slag without K₂O addition consumed the largest amount of acid. For the slags with K₂O addition, the consumption of citric acid decreased sharply. The change in the acid consumption was in good agreement with that in the Ca and Si concentrations during leaching.

Table 4.3 Acid consumption during leaching of slags with different K₂O contents (mL)

	Slag A (0% K ₂ O)	Slag B (4% K ₂ O)	Slag C (8% K ₂ O)
pH=7	4.6	12.1	15.5
pH=6	10.1	21.4	27.0
pH=5	39.9	28.1	33.8

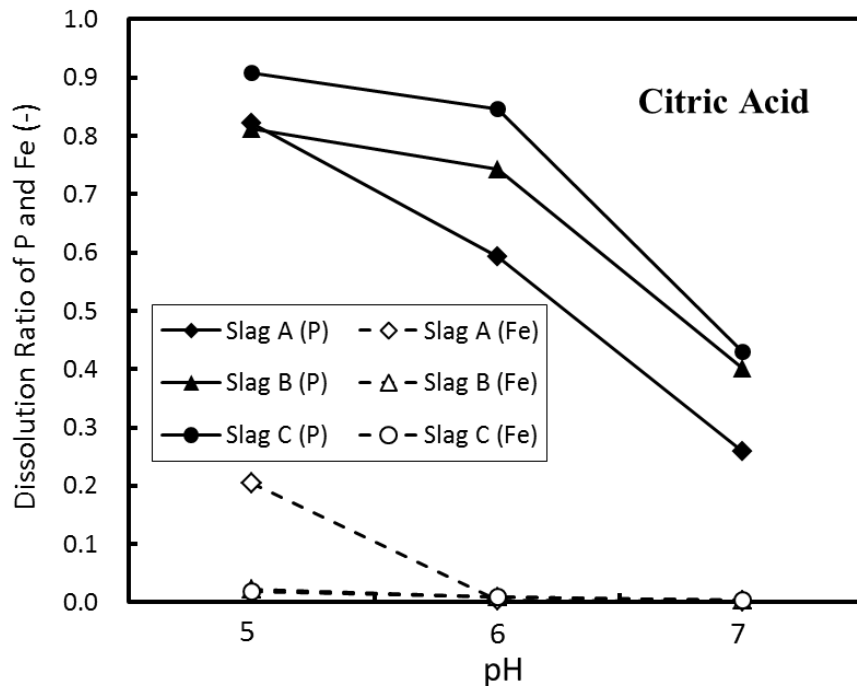


Fig. 4.10 Relationship between the dissolution ratios of P and Fe and the pH

According to the distribution of P and Fe in each phase, the dissolution ratios of P and Fe could represent the dissolution behavior of the solid solution and other phases, respectively. To determine the optimum conditions for selective leaching, these values at different pH conditions were summarized in Fig. 4.10. This figure shows that the dissolution ratio of P was far higher than that of Fe in each case. As the pH decreased, the dissolution ratios of P and Fe both increased; however, the associated trend differed for each slag. At pH 7, with a K₂O addition of 4 mass%, the dissolution ratio of P increased from 25.8% to 40.1%. However, a further increase in the K₂O content did not significantly promote the dissolution of P. When the pH decreased to 6, the concentration of H⁺ ions increased, which facilitated dissolution of the solid solution. In addition, as discussed in Chapter 3, higher concentrations of Ca and P could coexist in the aqueous solution and HAP precipitate was difficult to form at pH 6. Therefore, the dissolution ratio of P from each slag increased significantly. A larger addition of K₂O resulted in a higher dissolution ratio of P. In the case of the unmodified slag, the dissolution ratio of P exhibited a significant improvement when the pH decreased to 5; however, the dissolution ratio of Fe also increased sharply, reaching 20.4%. This illustrates that a part of the matrix phase also dissolved. In the case of the modified slags, the dissolution ratio of P increased slightly when the pH varied from 6 to 5, and the dissolution of Fe kept at low level; this indicates that the dissolution of matrix phase was suppressed. An excellent selective leaching of P from slag was performed.

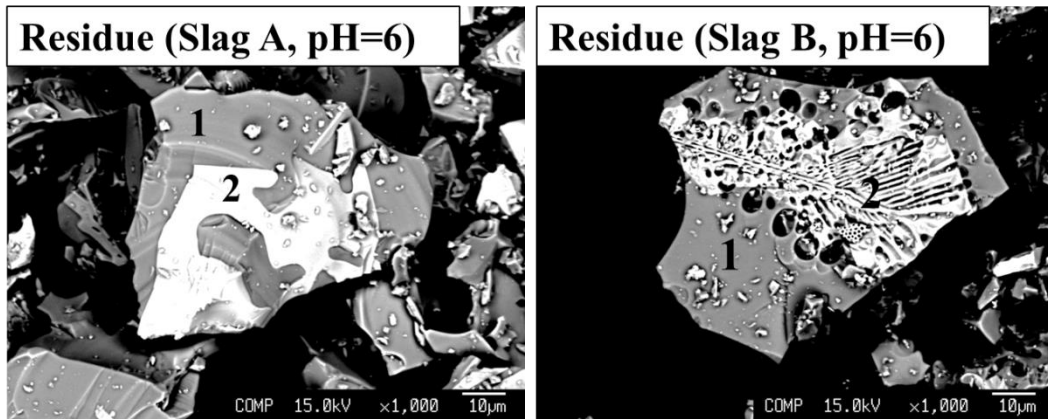
4.2.3 Residue composition

The average composition of the residue obtained after leaching was determined, as shown in Table 4.4. Compared with the initial slag prior to leaching (listed in Table 4.1), the CaO, SiO₂, and P₂O₅ contents in each residue reduced; however, the Fe₂O₃ and MgO contents increased. With the increase in the K₂O content in slag, the P₂O₅ content in the residue after leaching

decreased because of an increase in the dissolution ratio of P at pH 6. K₂O addition also resulted in lower CaO and SiO₂ contents in the residue. The undissolved Fe remained in the residue, and its content correspondingly increased. When the pH decreased to 5, the P₂O₅ and Fe₂O₃ contents in the residue further decreased and increased, respectively. When the slag with 8 mass% of K₂O was leached at pH 5, a residue containing 55.37 mass% of Fe₂O₃ and 0.66 mass% of P₂O₅ was obtained, which had the potential to be reused inside steelmaking process.

Table 4.4 Average compositions of residues obtained after leaching (mass%)

Residue	CaO	SiO ₂	Fe ₂ O ₃	P ₂ O ₅	MgO	K ₂ O
Slag A (pH=6)	34.22	22.37	36.29	3.36	3.75	0.00
Slag B (pH=6)	24.01	18.15	46.37	2.05	4.67	4.75
Slag C (pH=6)	16.12	17.99	51.06	1.47	5.16	8.21
Slag A (pH=5)	20.63	18.24	54.54	1.05	5.55	0.00
Slag B (pH=5)	21.98	18.35	48.84	1.29	4.87	4.68
Slag C (pH=5)	13.85	16.20	55.37	0.66	5.58	8.36



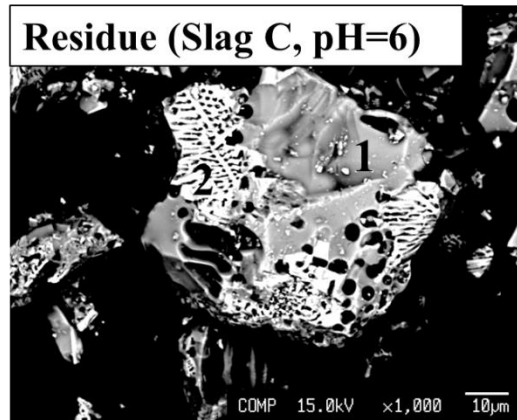


Fig. 4.11 EPMA images of residue surface after leaching of slags with different K_2O contents

Table 4.5 Compositions of each phase in the residue after leaching (mass%)

		CaO	SiO ₂	Fe ₂ O ₃	P ₂ O ₅	MgO	K ₂ O
Residue (Slag A, pH=6)	1	40.1	35.6	20.1	2.2	1.9	0.0
	2	1.3	0.3	87.6	0.0	10.8	0.0
Residue (Slag B, pH=6)	1	31.8	35.5	23.5	2.0	1.8	5.3
	2	1.7	0.7	85.3	0.1	12.1	0.1
Residue (Slag B, pH=6)	1	23.2	32.0	31.6	0.9	1.5	10.8
	2	0.9	2.8	83.0	0.1	13.0	0.2

The microstructure and compositions of the residue obtained after leaching at pH 6 are shown in Fig. 4.11 and Table 4.5. Two main phases were identified in each residue. The white area, rich in Fe_2O_3 and MgO , was the magnesian phase. The grey phase, consisting of a $CaO-SiO_2-Fe_2O_3$ slag system, was considered the matrix phase. Compared with the results in Table 4.2, the compositions of these phases in the residue were almost identical to those in the slag prior to leaching. There were no solid solution particles in each residue. It indicates that the solid solution that had contacted with the aqueous solution had dissolved. For the residue of the slags with K_2O addition, some holes could be observed near the magnesian phase. These areas are considered to be the small solid solution particles that were observed prior to leaching.

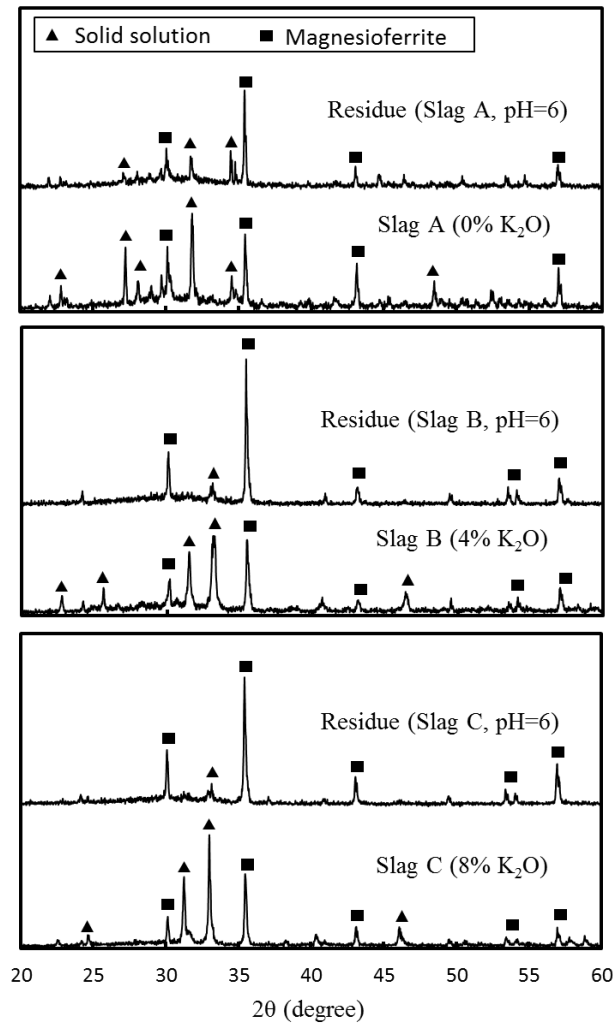


Fig. 4.12 XRD patterns of slags with different K_2O contents and their residue after leaching at pH 6

Figure 4.12 shows the XRD patterns of the slags and their residues after leaching at pH 6. In each slag, the precipitated solid solution and magnesioferrite phase were observed. The crystal form of the solid solution was changed because of K_2O addition. After leaching, the intensity of the peaks associated with solid solution weakened, and that of the magnesioferrite phase increased. In the case of the residue of the slag without K_2O addition, peaks associated with the solid solution still existed. However, for the slags with K_2O addition, the peaks associated with the solid solution almost disappeared, indicating that the dissolution of the solid solution was enhanced by K_2O addition. From the above findings, it can be determined that the P-condensed

solid solution was easily dissolved compared with other phases in the aqueous solution, and could be separated from slag via selective leaching.

4.3 Discussion on K₂O addition

First, the effect of K₂O addition on the mineralogical composition of slag was compared with that of Na₂O addition (shown in chapter 3). Na₂O and K₂O addition both enlarged the mass fraction of the solid solution and caused the decrease in the P₂O₅ content in the solid solution. When the same content of alkaline oxide was added, the P₂O₅ content in the solid solution of the slag with Na₂O addition was higher, but the mass fraction of the solid solution was lower. In the slag containing 4 mass% of K₂O, the distribution ratio of P₂O₅ between solid solution and matrix phase was about 13.0, lower than that in the slag containing Na₂O. Na₂O was easier to be distributed into the solid solution, and its content in the solid solution was higher. This is because the radius of Na⁺ ion (0.102 nm) is smaller than that of K⁺ ion (0.138 nm), and closer to the radius of Ca²⁺ (0.100 nm) [2]. The replacement between Na⁺ and Ca²⁺ in the solid solution occurs easily [3]. In the case of Na₂O addition, there was a higher distribution ratio of alkaline oxide between solid solution and matrix phase.

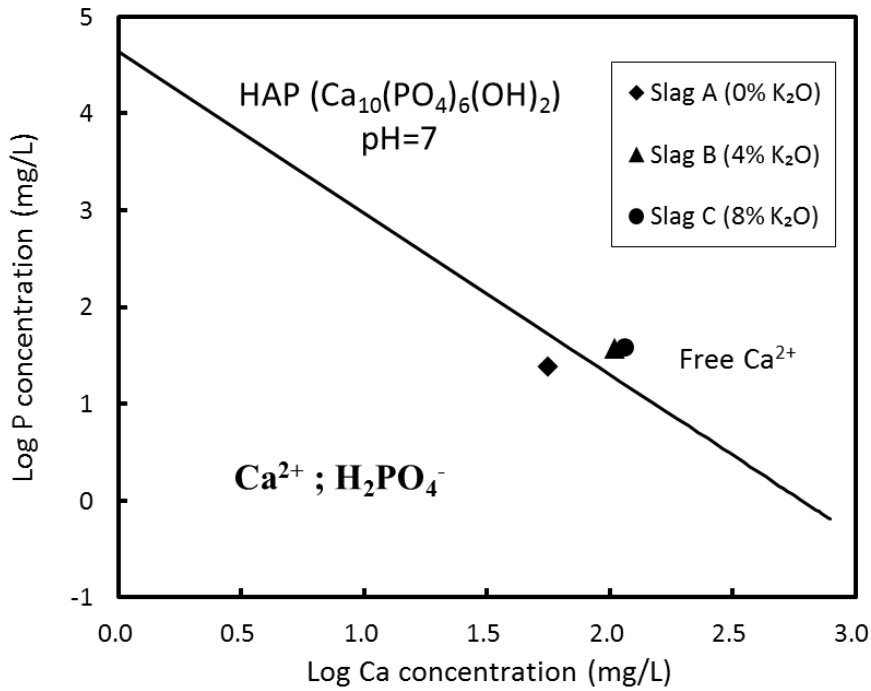


Fig. 4.13 Solubility line of the HAP precipitate and leaching results at pH 7

As discussed in the above Chapter, hydroxyapatite (HAP: $\text{Ca}_{10}(\text{PO}_4)_6(\text{OH})_2$) is easily formed at pH 7 [4]. Therefore, there is a high possibility that P concentration in the aqueous solution is controlled by the presence of HAP. The dissolution reaction of HAP and its equilibrium constant are described by Eq. (4.5) [5, 6].

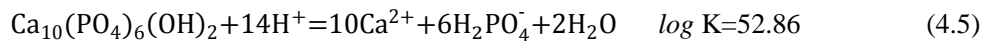


Figure 4.13 shows the relationship between the Ca and P concentrations in the aqueous solution at pH 7 determined by Eq. (4.5). The leaching results of different slags at pH 7 were also plotted in this Figure. Because of the existence of citrate ions ($\text{C}_6\text{H}_5\text{O}_7^{3-}$), the formation of $\text{CaC}_6\text{H}_5\text{O}_7^-$ complex was taken into consideration. The concentration of $\text{C}_6\text{H}_5\text{O}_7^{3-}$ ions in the aqueous solution was determined by the final volume of the aqueous solution and the mass of the added citric acid. The free Ca^{2+} concentration, which did not react with the citrate ions, was calculated using Eq. (4.6) [7]. The observed point for the free Ca^{2+} and P concentration of the slag without

K_2O addition was located below the HAP solubility line; this indicates that the P concentration did not reach saturation because of a lower Ca concentration, so the dissolved P did not precipitate. For the slags with K_2O addition, higher concentrations of Ca and P were obtained. The possible reason was that the newly formed solid solution containing K_2O had a high solubility. The observed points were located above the HAP solubility line, showing that the P concentration reached saturation and P dissolution was hindered by phosphate precipitation. Therefore, it was difficult to increase the dissolution ratio of P by further increasing the K_2O content in slag at pH 7.

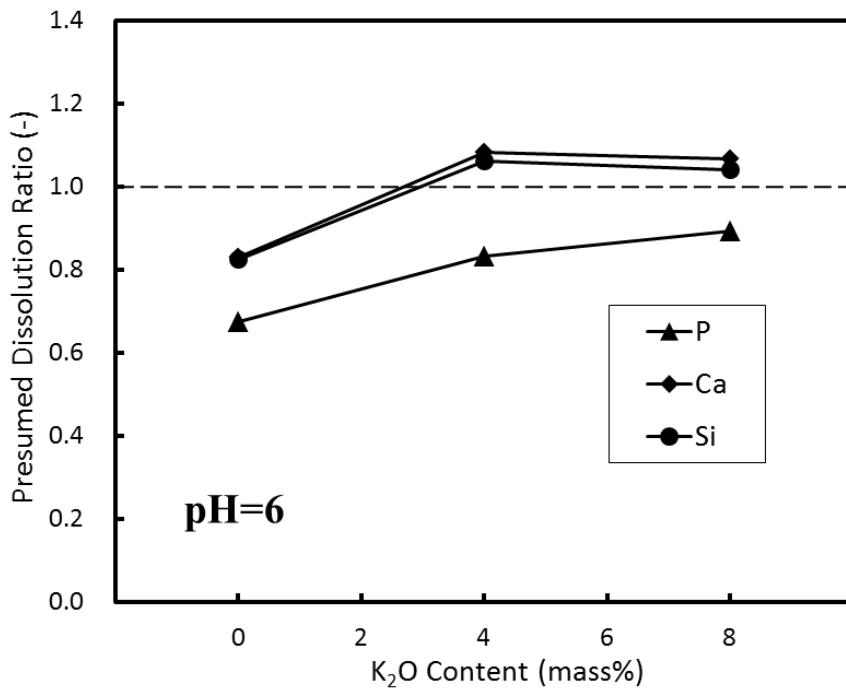


Fig. 4.14 Presumed dissolution ratios of Ca, Si, and P from the solid solution at pH 6

When the pH decreased to 6, higher concentrations of Ca and P could coexist in the aqueous solution, and the precipitates of calcium phosphate did not form in this case. To evaluate the dissolution behavior of each phase, the presumed dissolution ratios of element M (R_M^{SS}) from the solid solution were calculated using Eq. (4.7):

$$R_M^{SS} = \frac{C_M \cdot V}{m_M^{SS}} \quad (4.7)$$

where m_M^{SS} is the original mass of element M in the solid solution (mg). Because most of the P was concentrated in the solid solution, it was assumed that P dissolved only from the solid solution. The presumed dissolution ratio of P from the solid solution (R_P^{SS}) could represent the dissolution ratio of solid solution. For Ca and Si, if the presumed dissolution ratio is more than unity, it indicates that the dissolution of Ca and Si occurs not only from the solid solution but also from the matrix phase, because magnesioferrite was difficult to be dissolved compared with other phases in the aqueous solution [8]. The values of Ca and Si reflect the dissolution behavior of matrix phase. The larger these values, the more matrix phase are dissolved.

Figure 4.14 shows the presumed dissolution ratios of Ca, Si, and P from the solid solution at pH 6. In the case of slag without K₂O addition, the presumed dissolution ratio of P was only 67.3, indicating that the dissolution of solid solution was insufficient. With the increase in the K₂O content in slag, the presumed dissolution ratio of P increased. This shows that the dissolution of solid solution was promoted. In the previous chapter, it has been confirmed that the solid solution containing Na₂O shows higher water solubility than the C₂S-C₃P solid solution. Consequently, the introduction of K₂O is considered to enhance the solubility of solid solution. About 90% of the solid solution was dissolved from the slag containing 8 mass% of K₂O.

For the slag without K₂O addition, the presumed dissolution ratios of Ca and Si were both lower than unity. It also illustrated that the solid solution did not dissolve totally. However, these values were higher than that of P. This is because a small part of the dissolved Ca and Si was dissolved from the matrix phase. In the aqueous solution, phosphate and Fe³⁺ ions can easily form a precipitate of strengite (FePO₄·2H₂O) [9]. Another possible reason is that a small amount of P precipitated with the dissolved Fe³⁺ from the matrix phase. Because the dissolution of matrix phase was little and Fe concentration was very low, we generally ignored the

precipitation of iron phosphate in our discussion. A further addition of K_2O did not increase the presumed dissolution ratios of Ca and Si. These values exceeded unity, but not largely, indicating that the dissolution of matrix phase was not significant. The lower dissolution ratio of Fe would support this point.

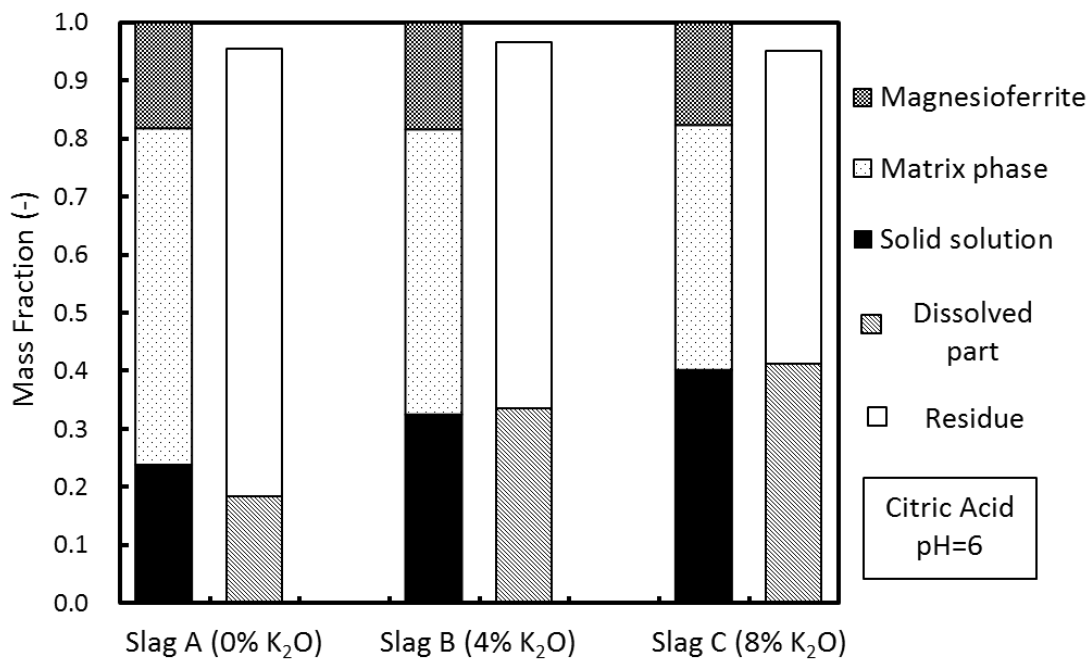


Fig. 4.15 Mass fractions of the residue and dissolved part at pH 6, compared with the phase fractions of different slags

After leaching, the mass of the residue and the dissolved portion, calculated using the dissolution ratio, were compared with the phase fractions of the initial slag in Fig. 4.15. In the case of the slag without K_2O addition, the dissolved mass was lower than the mass fraction of the solid solution, indicating that a portion of the solid solution remained in the residue. With the increase in the K_2O addition, the dissolved mass increased, and its value was almost identical to the mass fraction of the solid solution. Combined with above analysis, it could be concluded that the majority of the solid solution had dissolved, and little dissolution of other

phases occurred. Enhanced selective leaching of the P-condensed solid solution was achieved by K_2O addition.

Figure 4.16 shows the presumed dissolution ratios of Ca, Si, and P from the solid solution at pH 5. The presumed dissolution ratio of P was close to unity regardless of the K_2O content; this means that almost all of the solid solution was dissolved at pH 5. Nevertheless, K_2O addition had a significant influence on the dissolution of the matrix phase. For the slag without K_2O addition, the presumed dissolution ratios of Ca and Si were far greater than unity, indicating that a large amount of the matrix phase was dissolved. By K_2O addition, these values were reduced significantly, which shows that the dissolution of the matrix phase was suppressed. Because these values did not exceed unity largely, it is believed that the dissolution of the matrix phase from the modified slag was not significant at pH 5.

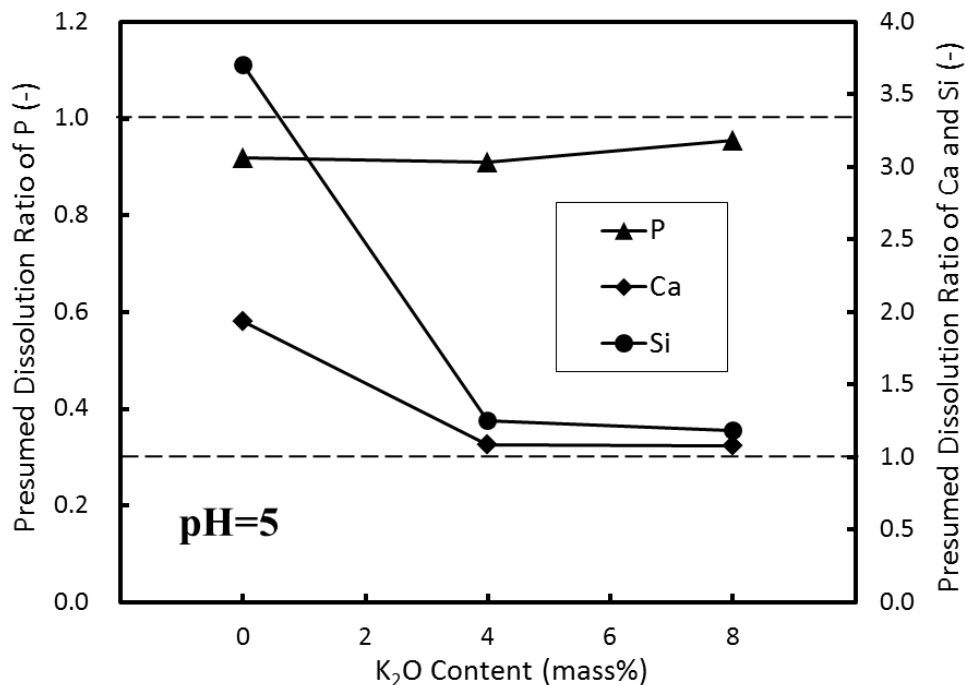


Fig. 4.16 Presumed dissolution ratios of Ca, Si, and P from the solid solution at pH 5

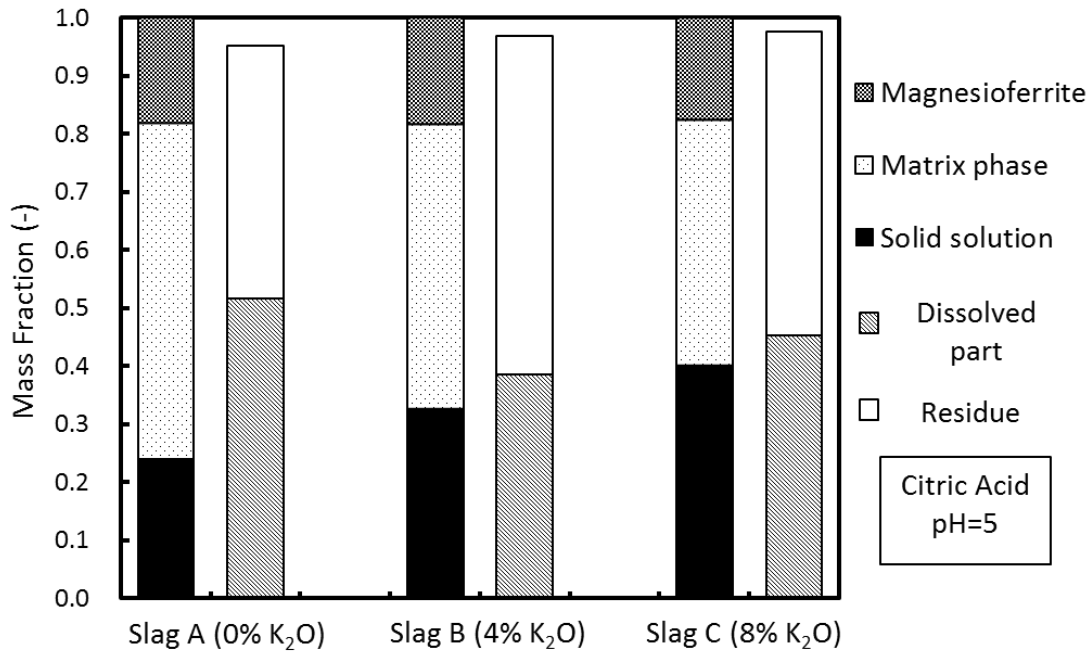


Fig. 4.17 Mass fractions of the residue and dissolved part at pH 5, compared with the phase fractions of different slags

The mass fractions of the residue and dissolved part at pH 5 were compared with the phase fractions of slags with different K₂O contents, as shown in Fig. 4.17. The dissolution ratio of the slag without K₂O addition was the highest, reaching 51%. This value was approximately equal to the sum of the total mass of the solid solution and half of the matrix phase, indicating that the matrix phase was easily dissolved in this case. When K₂O was added, the dissolution of slag became difficult. The mass fraction of the dissolved part reduced, and was slightly higher than that of the solid solution. This demonstrated that the dissolution of the matrix phase was little, which was consistent with the above analysis.

The mechanism to suppress the dissolution of glassy matrix phase by the addition of alkaline oxide (Na₂O or K₂O) was explained from the point of silicate structure. As discussed in Chapter 3, Fe³⁺ ions occupied both octahedral and tetrahedral sites in the silicate glass of CaO-Fe₂O₃-SiO₂ system [11, 12]. Pargamin *et al.* [13] reported that in the alkaline silicate glass,

$\text{Na}_2\text{O-Fe}_2\text{O}_3\text{-SiO}_2$, all of the Fe^{3+} cations was found to be tetrahedrally coordinated (network-former). Hayashi *et al.* [14] reported that the fraction of Fe^{3+} in tetrahedral sites is larger for the $\text{CaO-Na}_2\text{O-Fe}_2\text{O}_3\text{-SiO}_2$ system than that for the $\text{CaO-Fe}_2\text{O}_3\text{-SiO}_2$ system. Because alkaline oxides (Na_2O and K_2O) have the similar chemical properties, it is considered that the fraction of Fe^{3+} ions in tetrahedral sites to total Fe^{3+} ions in the matrix phase was increased by the addition of K_2O . As mentioned in the above chapter, the bond strength of Fe–O in tetrahedral site is higher than that in octahedral site. Consequently, for the modified slag with K_2O addition, the K_2O -containing matrix phase was more stable and its dissolution became difficult during leaching.

Finally, the effect of K_2O addition on the dissolution of slag was compared with that of Na_2O addition (shown in Chapter 3). In both cases, due to the formation of the solid solution containing Na_2O or K_2O , most of the solid solution was dissolved from the modified slag at pH 5. The dissolution ratio of P from the slag containing 4 mass% of alkaline oxide was almost the same, over 80%. In addition, the dissolution of the Fe-concentrated matrix phase was significantly suppressed by K_2O or Na_2O addition at pH 5. In summary, the addition of alkaline oxide has the same effect on the dissolution of slag with high P_2O_5 content. A better selective leaching of P from slag could be achieved.

4.4 Summary

To promote the dissolution of the P-concentrated solid solution and achieve selective leaching of P from slag, the effects of K_2O addition and pH on the dissolution behavior of steelmaking slag with high P_2O_5 content were investigated. The following results were obtained:

- (1) By K_2O addition, a portion of the K_2O was distributed into the P-concentrated solid solution, and the mass fraction of the solid solution in slag increased; however, the P_2O_5 content in the solid solution decreased.
- (2) K_2O addition promoted the dissolution of solid solution in the aqueous solution, resulting in higher dissolution ratios of Ca, Si, and P. However, at pH 7, further increase in the K_2O content in slag did not significantly increase the P dissolution ratio because of phosphate precipitation.
- (3) As the pH decreased, the dissolution of slag was promoted. With the increase in the K_2O content, the dissolution ratio of P increased at pH 6. The majority of the solid solution in the slag with 8 mass% of K_2O could be dissolved, and other phases remained in the residue, showing a better selective leaching of P from slag.
- (4) When the pH decreased to 5, more than 80% of the P was dissolved from each slag. For the slags with K_2O addition, the dissolution of the matrix phase was significantly suppressed, resulting in a lower Fe dissolution ratio. A residue with a higher Fe_2O_3 content and a lower P_2O_5 content was obtained after leaching, which had the potential to be reused inside steelmaking process.

References

1. T. Teratoko, N. Maruoka, H. Shibata, S. Kitamura: High Temperature Material Process, 31(2012), pp. 329-338.
2. R.D. Shannon: Acta Crystallographica Section A, A32(1976), pp. 751-767.
3. U. Mizutani: Hume-Rothery Rules for Structurally Complex Alloy Phases, Taylor & Francis, USA, 2010.
4. M. Bohner, J. Lemaitre, T. A. Ring: Journal of Colloid and Interface Science, 190(1997), pp. 37-48.
5. T. Futatsuka, K. Shitogiden, T. Miki, T. Nagasaka and M. Hino: ISIJ International, 44 (2004), pp. 753-761.
6. A. L. Iglesia: Estudios Geológicos, 65 (2009), pp. 109-119.
7. J. Muus, H. Lebel: Matematisk-fysiske Meddelelser Danske Videnskabernes Selskab, 13 (1936), pp. 1-16.
8. X. Gao, N. Maruoka, S.J. Kim, S. Ueda, S. Kitamura: Journal of Sustainable Metallurgy, 1(2015), pp. 304-313.
9. S.J. Markich, P.L. Brown: Thermochemical Data for Environmentally-relevant Elements, ANSTO Environment Division, NSW, 1999.
10. F.K. Crundwell: Hydrometallurgy, 149(2014), pp. 265-275.
11. N. Iwamoto, Y. Tsunawaki, H. Nakagawa, T. Yoshimura, N. Wakabayashi: Journal of Non-Crystalline Solids, 29 (1978), pp. 347-356.
12. K. Nagata, M. Hayashi: Journal of Non-Crystalline Solids, 282(2001), pp. 1-6.
13. L Pargamin, C.H.P. Lupis, P.A. Flinn: Metallurgical Transactions, 3(1972), pp. 2093-2105.
14. M. Hayashi, M. Susa: Proceedings of the 14th Japan-China symposium on science and technology of iron and steel, ISIJ, Sendai, (2016), pp. 114-122.

5 Distribution of P_2O_5 and Na_2O between the solid solution and liquid phase in slag with high P_2O_5 content

Na_2O addition to slag is considered an effective method for increasing dephosphorization efficiency [1-4]. In addition, Na_2O modification also facilitates dissolution of the solid solution from slag via selective leaching [5]. Therefore, it is necessary to investigate the distribution ratios of P_2O_5 and Na_2O between the solid solution and liquid phase in the slag of $CaO-SiO_2-Fe_2O_3-P_2O_5-Na_2O$ system.

5.1 Experimental method

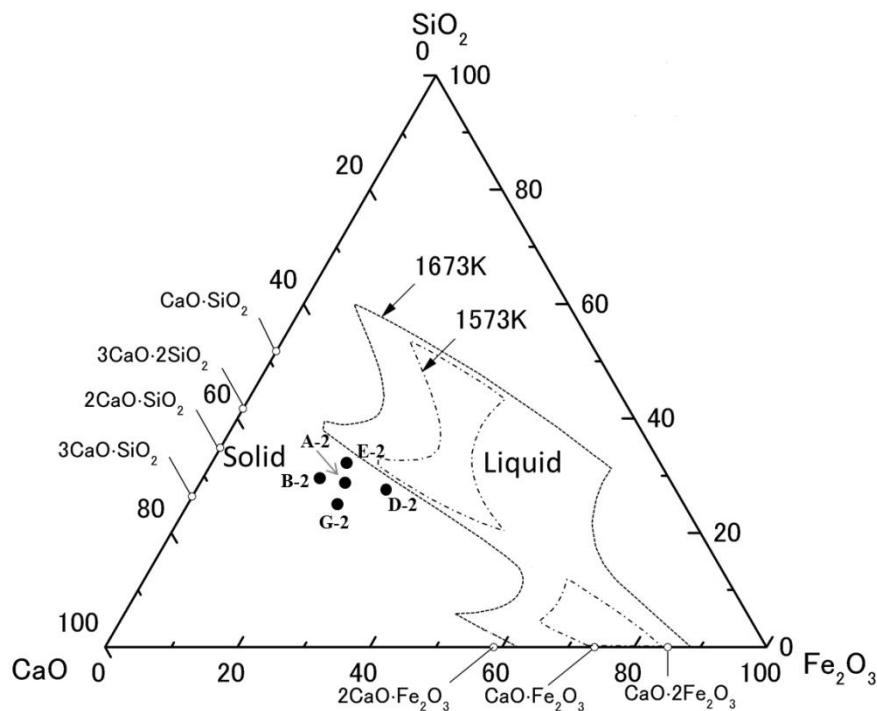


Fig. 5.1 Projection of slag composition in the $CaO-SiO_2-Fe_2O_3$ ternary phase diagram

Reagent-grade $CaCO_3$, SiO_2 , Fe_2O_3 , $Ca_3(PO_4)_2$, and Na_2SiO_3 were used to produce the $CaO-SiO_2-Fe_2O_3$ system slag. To reduce the vaporization of Na_2O at high temperatures,

Na_2SiO_3 was used in this study [6]. Fe_2O_3 was used as iron oxide, although in the steelmaking process, most of the iron oxide is in the form of FeO . This is because a better selective leaching of P from slag can be achieved in the case of slag containing Fe_2O_3 (shown in Chapter 3). In addition, the distribution of P_2O_5 between the solid solution and liquid phase underwent little change when the iron oxide was changed from FeO to Fe_2O_3 [7]; in the case of Fe_2O_3 , a Pt crucible can be used to avoid contamination by the crucible. CaCO_3 was calcined at 1273 K for 10 h in an Al_2O_3 crucible to prepare CaO . Each reagent was thoroughly mixed according to the slag composition (listed in Table 5.1). The slags with different P_2O_5 , Na_2O , Fe_2O_3 contents, and basicity were synthesized. The P_2O_5 content in slag varied from 7 mass% to 16 mass%; the Na_2O content varied from 2 mass% to 15 mass%. From the phase diagram of the $\text{CaO-SiO}_2\text{-Fe}_2\text{O}_3$ system [8], as shown in Fig. 5.1, it is determined that the compositions of these slags were located in a liquid region at 1823 K, and a $2\text{CaO}\cdot\text{SiO}_2$ precipitated during cooling to 1673 K. The heating pattern is shown in Fig. 5.2. First, 3 g of the mixed reagents was placed in a Pt crucible and heated to 1823 K in an electric resistance furnace under air. After holding at this temperature for 1 h, the sample was cooled to 1673 K and kept for 1 h. Based on the previous study [9, 10] and preliminary experiments, we considered the distribution of P_2O_5 and Na_2O between the solid solution and liquid phase reached equilibrium by this treatment. In the preliminary experiment, the Na_2O content in the synthesized slag was determined using chemical analysis (same method as the chemical analysis of slag and residue in Chapter 3). We confirmed that the vaporization of Na_2O was negligible when the Na_2O content was not high. After heating, the sample was quenched with water. Finally, the obtained slag sample was mounted and polished. The composition of many positions of each phase was analyzed with an electron probe micro analyzer (EPMA) and average compositions were calculated. The precipitated solid solution in slag was confirmed using X-ray diffraction (XRD) analysis.

Table 5.1 Mixing compositions of slags (mass%)

Sample	CaO	SiO ₂	Fe ₂ O ₃	P ₂ O ₅	Na ₂ O
A-1 (2% Na ₂ O)	42.9	26.7	21.4	7.0	2.0
A-2 (2% Na ₂ O)	41.5	25.8	20.7	10.0	2.0
A-3 (2% Na ₂ O)	40.0	25.0	20.0	13.0	2.0
A-4 (2% Na ₂ O)	38.6	24.1	19.3	16.0	2.0
A-1 (5% Na ₂ O)	41.5	25.8	20.7	7.0	5.0
A-2 (5% Na ₂ O)	40.0	25.0	20.0	10.0	5.0
A-3 (5% Na ₂ O)	38.6	24.1	19.3	13.0	5.0
A-4 (5% Na ₂ O)	37.2	23.2	18.6	16.0	5.0
A-2 (10% Na ₂ O)	37.7	23.5	18.8	10.0	10.0
A-3 (10% Na ₂ O)	36.2	22.6	18.2	13.0	10.0
A-3 (13% Na ₂ O)	34.8	21.7	17.5	13.0	13.0
A-2 (15% Na ₂ O)	35.4	22.0	17.6	10.0	15.0
B-2 (5% Na ₂ O)	43.1	26.9	15.0	10.0	5.0
C-2 (5% Na ₂ O)	37.0	23.0	25.0	10.0	5.0
D-2 (5% Na ₂ O)	30.8	19.2	35.0	10.0	5.0
E-2 (5% Na ₂ O)	37.9	27.1	20.0	10.0	5.0
F-2 (5% Na ₂ O)	41.8	23.2	20.0	10.0	5.0
G-2 (5% Na ₂ O)	43.3	21.7	20.0	10.0	5.0

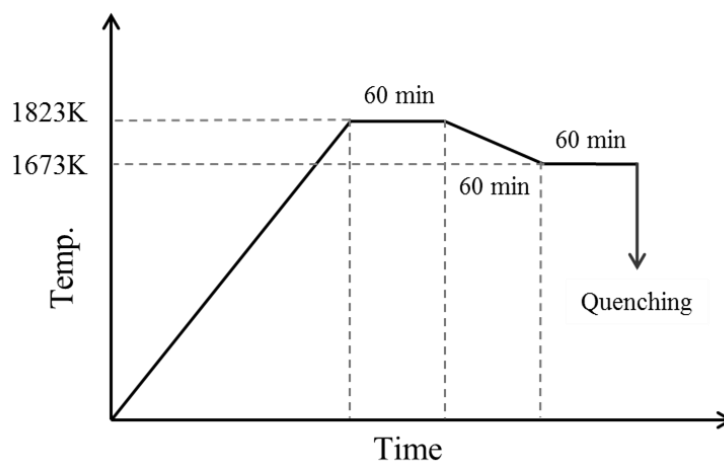


Fig. 5.2 Experimental condition for precipitation of solid solution

5.2 Experimental results

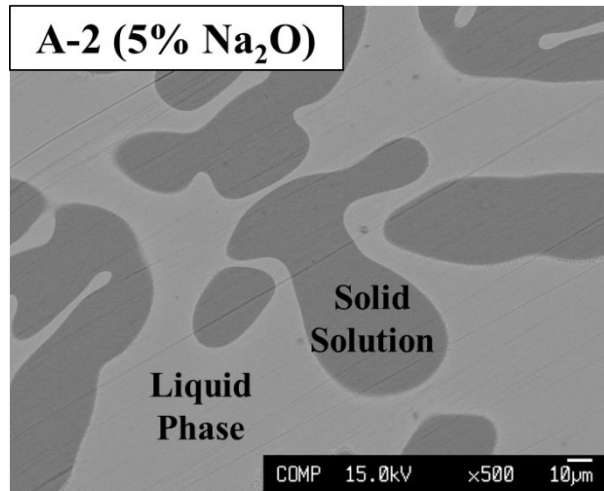


Fig. 5.3 Cross section (500 \times) of the typical slag (A-2 (5% Na₂O))

Precipitated solid solution particles and liquid phase were clearly observed in each slag, as shown in Fig. 5.3. The distribution ratios of P₂O₅ and Na₂O between the solid solution and liquid phase were calculated using Eqs. (5.1) and (5.2), respectively:

$$L_{P_2O_5} = \frac{(\%P_2O_5)_{SS}}{(\%P_2O_5)_L} \quad (5.1)$$

$$L_{Na_2O} = \frac{(\%Na_2O)_{SS}}{(\%Na_2O)_L} \quad (5.2)$$

where (%P₂O₅) and (%Na₂O) represent the P₂O₅ and Na₂O contents in each phase in mass%, and the subscripts *SS* and *L* denote the solid solution and liquid phase, respectively. The average compositions of the solid solution and liquid phase in each slag are listed in Table 5.2. This table also presents the calculated distribution ratios of P₂O₅ ($L_{P_2O_5}$) and Na₂O (L_{Na_2O}).

Table 5.2 Average compositions of the solid solution and liquid phase in each slag (mass%)

Sample	Phase	CaO	SiO ₂	Fe ₂ O ₃	P ₂ O ₅	Na ₂ O	L _{P2O5}	L _{Na2O}
A-1 (2% Na ₂ O)	solid solution	57.7	21.0	1.2	17.4	2.6	4.70	1.73
	liquid phase	37.7	28.8	28.3	3.7	1.5		
A-2 (2% Na ₂ O)	solid solution	54.3	14.6	1.2	26.8	3.0	4.79	1.58
	liquid phase	37.2	29.1	26.2	5.6	1.9		
A-3 (2% Na ₂ O)	solid solution	52.4	7.9	1.0	35.8	2.9	5.19	1.61
	liquid phase	35.1	31.6	24.7	6.9	1.8		
A-4 (2% Na ₂ O)	solid solution	52.0	4.3	0.9	39.8	3.0	4.68	1.76
	liquid phase	33.7	32.0	24.2	8.5	1.7		
A-1 (5% Na ₂ O)	solid solution	55.0	22.5	1.1	16.0	5.3	6.67	1.08
	liquid phase	33.6	28.3	30.8	2.4	4.9		
A-2 (5% Na ₂ O)	solid solution	51.9	15.2	1.1	25.0	6.7	5.10	1.49
	liquid phase	35.5	28.0	27.1	4.9	4.5		
A-3 (5% Na ₂ O)	solid solution	49.6	10.1	1.0	32.1	7.2	5.73	1.71
	liquid phase	34.2	29.1	26.9	5.6	4.2		
A-4 (5% Na ₂ O)	solid solution	48.0	5.8	0.9	38.4	6.9	5.49	1.57
	liquid phase	32.4	30.4	25.8	7.0	4.4		
A-2 (10% Na ₂ O)	solid solution	50.3	17.2	0.8	22.6	9.1	7.79	0.88
	liquid phase	27.5	26.1	33.3	2.9	10.3		
A-3 (10% Na ₂ O)	solid solution	47.0	12.8	0.8	29.2	10.1	9.13	1.10
	liquid phase	26.5	29.0	32.1	3.2	9.2		
A-3 (13% Na ₂ O)	solid solution	46.8	14.1	0.6	27.0	11.5	10.80	1.03
	liquid phase	19.3	26.8	40.2	2.5	11.2		
A-2 (15% Na ₂ O)	solid solution	51.5	19.0	0.5	20.1	9.0	11.17	0.56
	liquid phase	16.2	22.2	43.7	1.8	16.0		
B-2 (5% Na ₂ O)	solid solution	52.8	19.1	1.1	21.0	6.0	4.20	1.30
	liquid phase	36.2	29.7	24.5	5.0	4.6		
C-2 (5% Na ₂ O)	solid solution	48.0	12.6	1.1	30.5	7.7	6.49	1.71
	liquid phase	31.8	26.0	32.9	4.7	4.5		
D-2 (5% Na ₂ O)	solid solution	45.0	7.4	0.9	37.4	9.3	7.19	1.94
	liquid phase	27.3	21.0	41.6	5.2	4.8		
E-2 (5% Na ₂ O)	solid solution	50.7	12.0	1.1	29.3	6.9	4.37	1.57
	liquid phase	35.9	30.6	22.4	6.7	4.4		
F-2 (5% Na ₂ O)	solid solution	53.6	18.7	1.1	20.8	5.8	7.43	1.38
	liquid phase	33.0	26.4	33.7	2.8	4.2		
G-2 (5% Na ₂ O)	solid solution	55.9	19.8	1.0	17.7	5.7	10.41	1.06
	liquid phase	29.6	22.5	40.8	1.7	5.4		

5.2.1 Effect of P₂O₅ and Na₂O contents

Figure 5.4 shows the relationship between the P_2O_5 and Na_2O contents in slag and the distribution ratio of P_2O_5 . The distribution ratio of P_2O_5 between the solid solution and liquid phase was high in each case, indicating that P_2O_5 was mainly distributed in the solid solution. A linear relationship was found between the distribution ratio of P_2O_5 and the Na_2O content in slag, independent of the P_2O_5 content. When the Na_2O content increased from 2 to 10 mass%, the value of $L_{P_2O_5}$ approximately doubled, even in a slag with high P_2O_5 content. In the case of high Na_2O content, the distribution ratio of P_2O_5 exceeded 10, meaning that most of the P_2O_5 was concentrated in the solid solution.

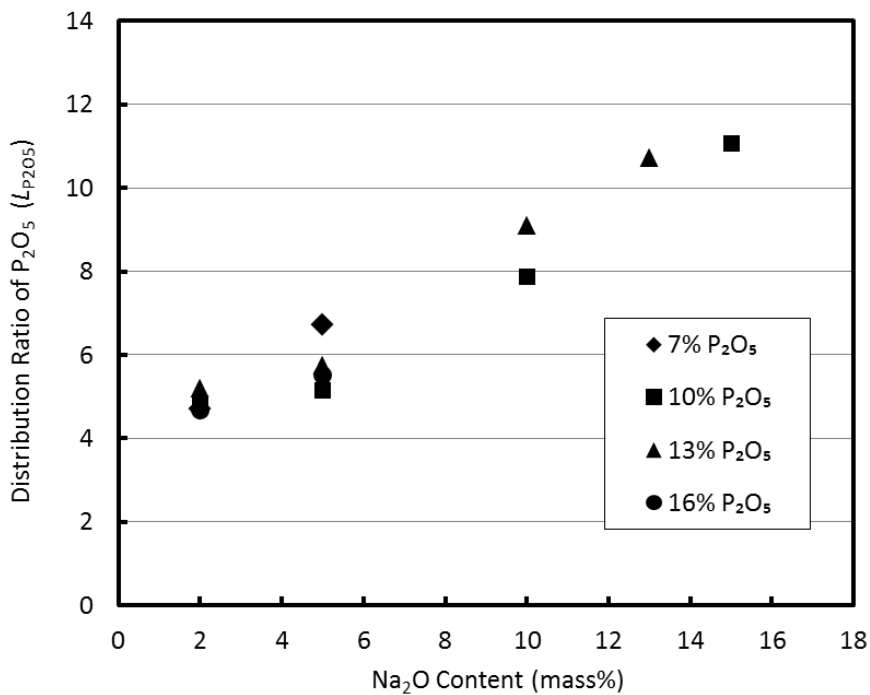


Fig. 5.4 Relationship between the Na_2O and P_2O_5 contents in slag and the distribution ratio of P_2O_5

The change in the distribution ratio of Na_2O with slag compositions is shown in Fig. 5.5. Compared with the distribution ratio of P_2O_5 , the distribution ratio of Na_2O was lower in each slag. With increase in the Na_2O content in slag, the distribution ratio of Na_2O decreased. In the low Na_2O content range, the Na_2O content in the solid solution was higher than that in the liquid

phase. In the high Na_2O content range, this value was less than unity, indicating that Na_2O was difficult to continue entering into the solid solution and mainly distributed in the liquid phase. The significant influence of the P_2O_5 content on the distribution ratio of Na_2O was not observed. These results show that Na_2O addition to a slag with high P_2O_5 content facilitated the enrichment of P_2O_5 in the solid solution, while it had the opposite effect on the distribution of Na_2O .

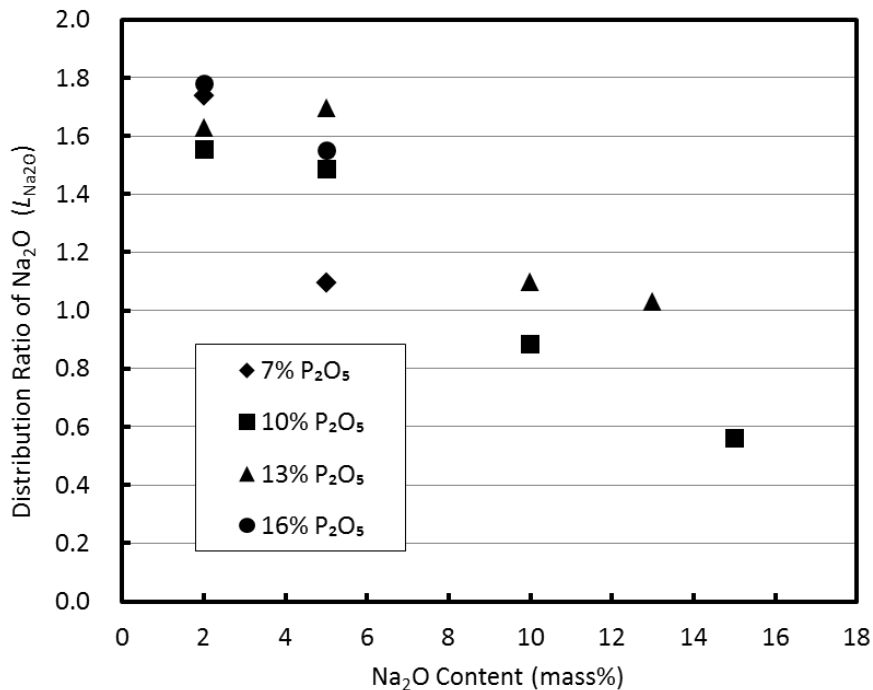


Fig. 5.5 Relationship between the Na_2O and P_2O_5 contents in slag and the distribution ratio of Na_2O

Figure 5.6 shows the change of the P_2O_5 and Na_2O contents in the solid solution with the P_2O_5 and Na_2O contents in slag. In the slag with 7 mass% of P_2O_5 , the P_2O_5 content in the solid solution was approximately 16 mass%. With an increase in the P_2O_5 content in slag, the P_2O_5 content in the solid solution increased, as reported by Shimauchi *et al.*[9]. In the case of the slag with 16 mass% P_2O_5 , the P_2O_5 content in the solid solution reached about 39 mass%. It shows that the majority of the solid solution consisted of $3\text{CaO}\cdot\text{P}_2\text{O}_5$. Na_2O addition resulted in a

decrease in the P_2O_5 content in the solid solution. When the Na_2O content in slag (containing 10 mass% of P_2O_5) increased from 2 to 10 mass%, the P_2O_5 content decreased from 26.8 to 22.6 mass%. The Na_2O content in the solid solution showed a slight increase with the increase of P_2O_5 content in slag. A larger addition of Na_2O in slag led to a high Na_2O content in the solid solution.

The compositions of the solid solution in slag with different Na_2O contents are plotted in a $(CaO+Na_2O)-SiO_2-P_2O_5$ pseudo-phase diagram, as shown in Fig. 5.7. The Na_2O content in the solid solution was taken into consideration. The tie-line between $2(CaO, Na_2O) \cdot SiO_2$ and $3(CaO, Na_2O) \cdot P_2O_5$ indicates the composition of C_2S-C_3P solid solution without considering Na_2O . The compositions of these solid solutions lay nearly on the composition line of pure C_2S-C_3P , indicating that the added Na_2O substituted CaO in the solid solution and a new solid solution similar to C_2S-C_3P was formed.

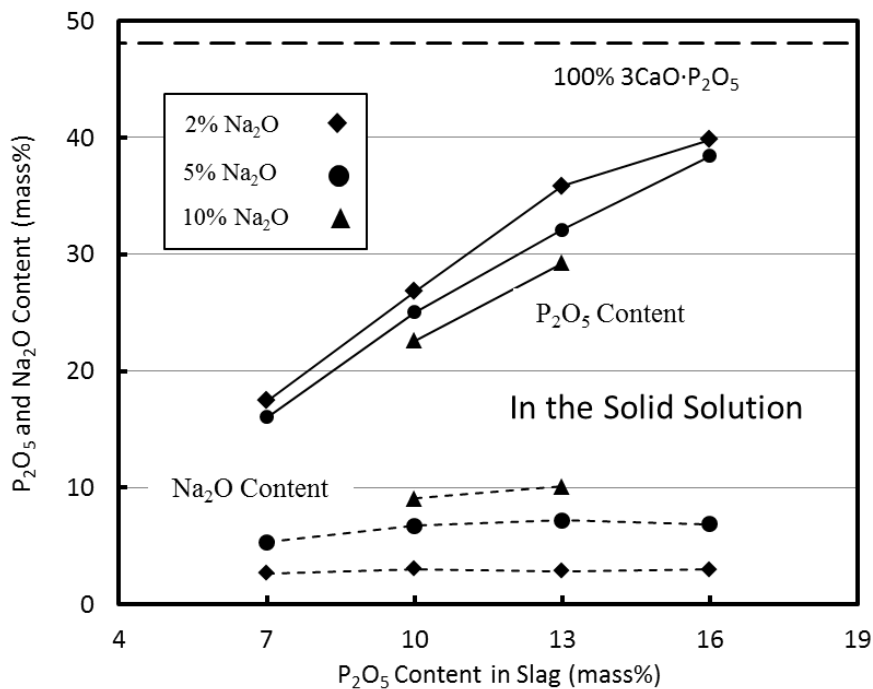


Fig. 5.6 Change in the P_2O_5 and Na_2O contents in the solid solution with the P_2O_5 and Na_2O content in slag

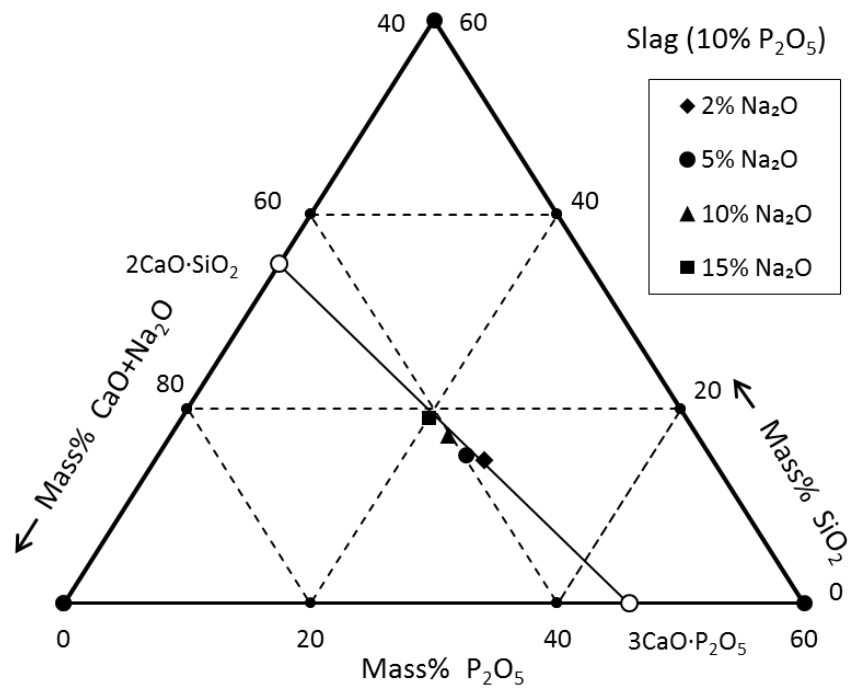


Fig. 5.7 Projections of the solid solution in the (CaO+Na₂O)-SiO₂-P₂O₅ pseudo-phase diagram under different Na₂O contents

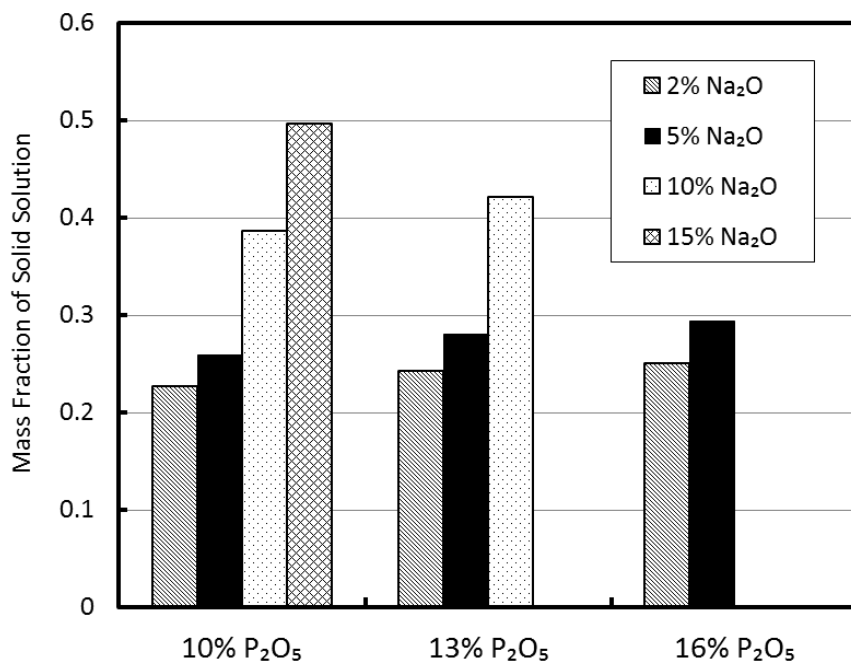


Fig. 5.8 Mass fraction of the solid solution in slags with different P₂O₅ and Na₂O contents

On the basis of mass balance, the mass fractions of the solid solution and liquid phase were estimated using the slag composition shown in Table 5.1 and the EPMA results in Table 5.2.

The mass balance of each oxide can be represented using Eqs. (5.3) and (5.4):

$$N_{\text{MO}_n} = \alpha N_{\text{MO}_n}^{\alpha} + \beta N_{\text{MO}_n}^{\beta} \quad (5.3)$$

$$\alpha + \beta = 1 \quad (5.4)$$

where α and β are the mass fractions of the solid solution and matrix phase, respectively, N_{MO_n} is the MO_n content in slag, and $N_{\text{MO}_n}^{\alpha}$ is the MO_n content in the solid solution. The mass fraction of the solid solution was defined as the average of the calculated mass fractions using the different combination of CaO , SiO_2 and Fe_2O_3 . Figure 5.8 shows the calculated mass fraction of the solid solution in slags with different P_2O_5 and Na_2O contents. With an increase in the Na_2O content in slag, the mass fraction of the solid solution increased. The reason is that slag basicity increased when Na_2O (basic oxide, has similar property with CaO) was added. According to the $\text{CaO-SiO}_2\text{-Fe}_2\text{O}_3$ phase diagram, increasing slag basicity results in a higher mass fraction of the solid solution. When the Na_2O content was the same, the slag with a higher P_2O_5 content showed a higher mass fraction of the solid solution. In the case of high Na_2O content, the mass fraction of the solid solution exceeded 40%. Enlargement of the solid solution mass and increase in the distribution ratio of P_2O_5 mean that the majority of the P_2O_5 in slag was concentrated in the solid solution.

Using the mass fraction of the solid solution, the mass fractions of P_2O_5 and Na_2O distributed in the solid solution were calculated using Eq. (5.5):

$$Y_{\text{MO}_n}^{\alpha} = \frac{\alpha \cdot N_{\text{MO}_n}^{\alpha}}{N_{\text{MO}_n}} \quad (5.5)$$

Figure 5.9 shows the calculated results for the slag with 10 mass% of P_2O_5 . With an increase in the Na_2O content in slag, although the P_2O_5 content in the solid solution decreased, the mass fraction of P_2O_5 distributed in the solid solution increased. Therefore, Na_2O addition facilitated

P_2O_5 enrichment. When the Na_2O content exceeded 10 mass%, more than 85% of the P_2O_5 was concentrated in the solid solution. However, the mass fraction of Na_2O distributed in the solid solution had little change with the Na_2O content in slag. Approximately 33% of the Na_2O was distributed in the solid solution. This result indicates that the increase of the Na_2O content in slag did not enrich the Na_2O in the solid solution, but a large amount of the Na_2O was distributed in the liquid phase.

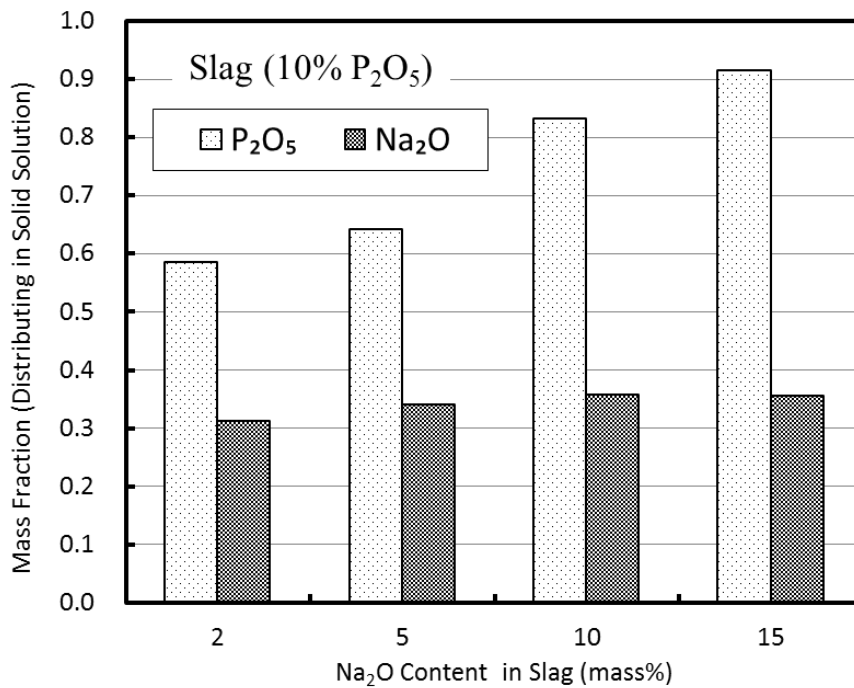


Fig. 5.9 Mass fractions of P_2O_5 and Na_2O distributed in the solid solution

5.2.2 Effect of Fe_2O_3 content

Figure 5.10 shows the relationship between the distribution ratio of P_2O_5 and the total Fe content (T.Fe) in the liquid phase for the slag containing 5 mass% of Na_2O . With increasing the T.Fe content in the liquid phase, the distribution ratio of P_2O_5 between the solid solution and liquid phase increased. The distribution ratio of P_2O_5 showed no dependence on the P_2O_5

content in slag. These results have the same trend as the results obtained by Ito *et al.* [7] (plotted in Fig. 5.10); however, the values of this study were higher. The difference was explained by the addition of Na₂O in slag, which resulted in a higher distribution ratio of P₂O₅. The change in the distribution ratio of Na₂O with the Fe₂O₃ content in slag is shown in Fig. 5.11. With the increase in the Fe₂O₃ content in slag, the distribution ratio of Na₂O increased. In the case of slag containing 35 mass% of Fe₂O₃, the value of $L_{\text{Na}_2\text{O}}$ reached about 2.0, indicating that a large amount of Na₂O was concentrated in the solid solution.

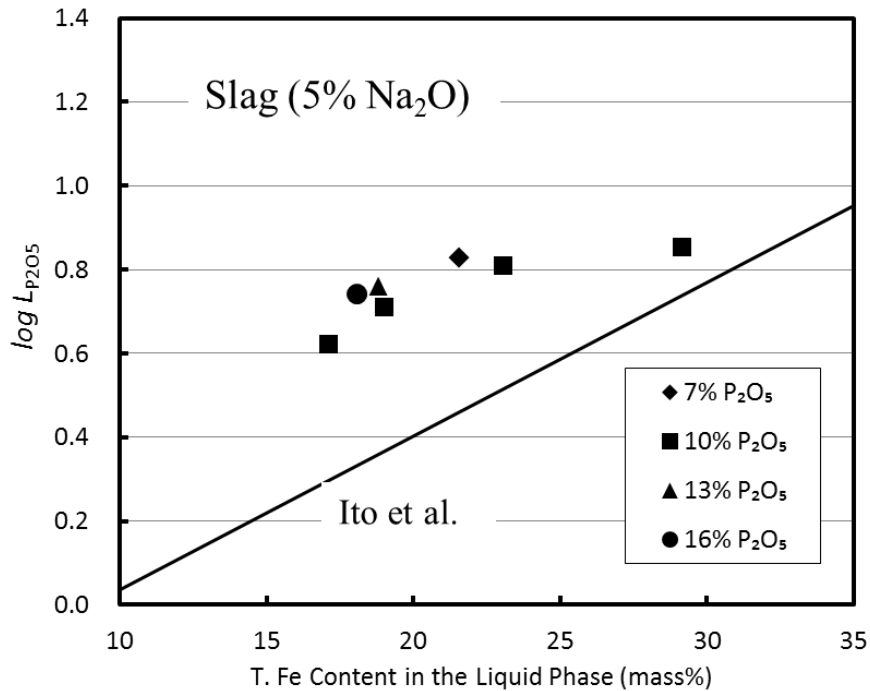


Fig. 5.10 Relationship between the distribution ratio of P₂O₅ and the T.Fe content in the liquid phase

The compositions of the solid solution in slags with different Fe₂O₃ contents are plotted in a (CaO+Na₂O)-SiO₂-P₂O₅ pseudo-phase diagram (Fig. 5.12). The tie-line between 2(CaO, Na₂O)·SiO₂ and 3(CaO, Na₂O)·P₂O₅ indicates the composition of C₂S-C₃P solid solution without considering Na₂O. The compositions of this study lay nearly on the composition line of pure

C_2S-C_3P , indicating that the added Na_2O substituted CaO in the solid solution and a new solid solution similar to C_2S-C_3P was formed. An increase in the Fe_2O_3 content in slag brought a significant increase in the P_2O_5 content in the solid solution. In the case of high Fe_2O_3 content, the composition of solid solution was closer to the $3(CaO,Na_2O) \cdot P_2O_5$ point, indicating that increasing the Fe_2O_3 content in slag facilitated P_2O_5 enrichment in the solid solution.

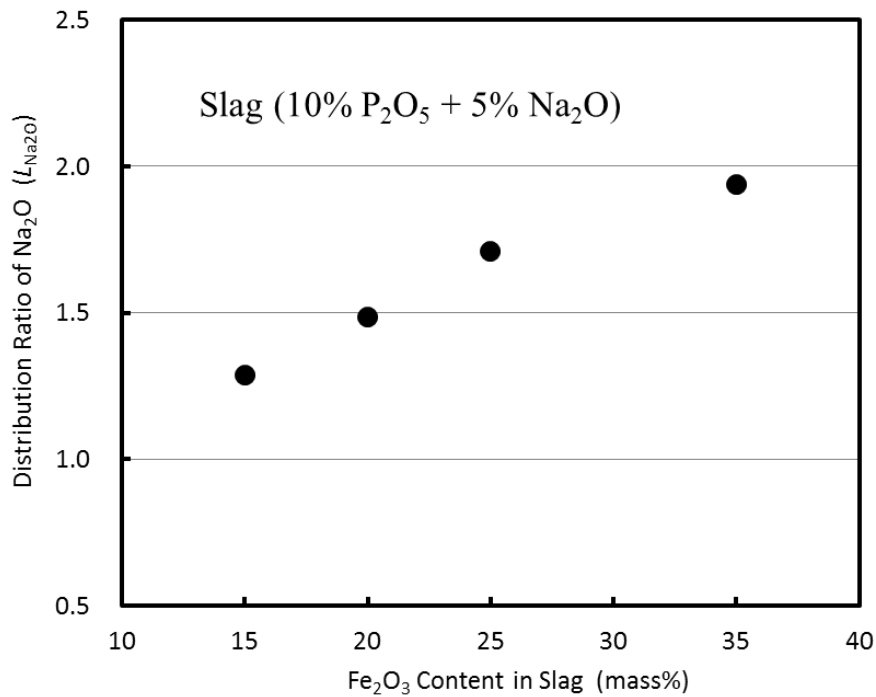


Fig. 5.11 Change in the distribution ratio of Na_2O with the Fe_2O_3 content in slag

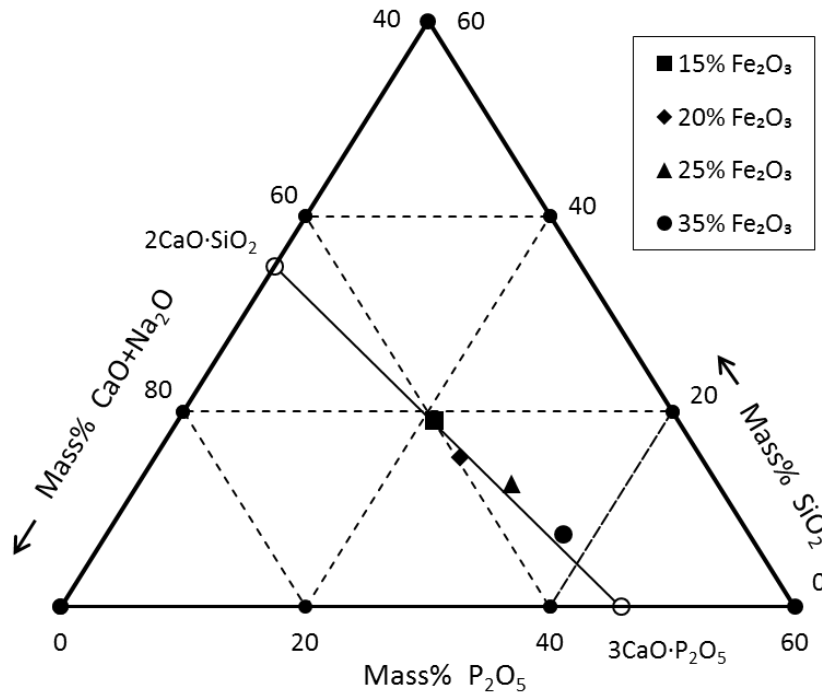


Fig. 5.12 Projections of the solid solution in the (CaO+Na₂O)-SiO₂-P₂O₅ pseudo-phase diagram under different Fe₂O₃ contents

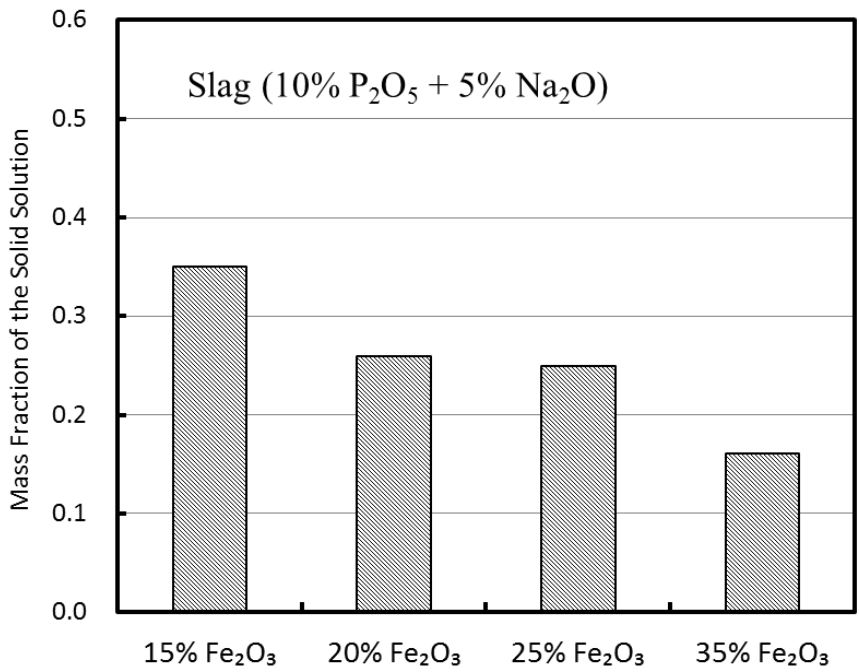


Fig. 5.13 Mass fraction of the solid solution in slags with different Fe₂O₃ contents

As mentioned above, the mass fraction of the solid solution in slags at different Fe_2O_3 contents were calculated using Eqs. (5.3) and (5.4), and shown in Fig. 5.13. The mass fraction of the solid solution decreased with an increase in the Fe_2O_3 content in slag. When the Fe_2O_3 content increased from 15 to 35 mass%, the mass fraction of the solid solution decreased from 34.9% to 16.1%.

5.2.3 Effect of slag basicity (CaO/SiO_2)

The relationship between slag basicity and the distribution ratios of P_2O_5 and Na_2O are shown in Fig. 5.14 for the slags containing 10 mass% of P_2O_5 and 5 mass% of Na_2O . In this study, slag basicity is defined as the mass ratio of CaO to SiO_2 in slag ($R = \text{mass\% CaO} / \text{mass\% SiO}_2$). With the increase in slag basicity, the distribution ratio of P_2O_5 increased significantly. When the basicity changed from 1.6 to 2.0, the value of $L_{\text{P}_2\text{O}_5}$ approximately doubled. However, the distribution ratio of Na_2O showed the reverse trend; higher slag basicity resulted in a lower distribution ratio of Na_2O .

Figure 5.15 shows the compositions of solid solution in the $(\text{CaO} + \text{Na}_2\text{O})\text{-SiO}_2\text{-P}_2\text{O}_5$ pseudo-phase diagram under different slag basicity. Although Na_2O existed in the solid solution, the composition of solid solution was close to the pseudo-binary relation of $2(\text{CaO}, \text{Na}_2\text{O})\cdot\text{SiO}_2$ and $3(\text{CaO}, \text{Na}_2\text{O})\cdot\text{P}_2\text{O}_5$. With the increase in slag basicity, the P_2O_5 content in the solid solution decreased.

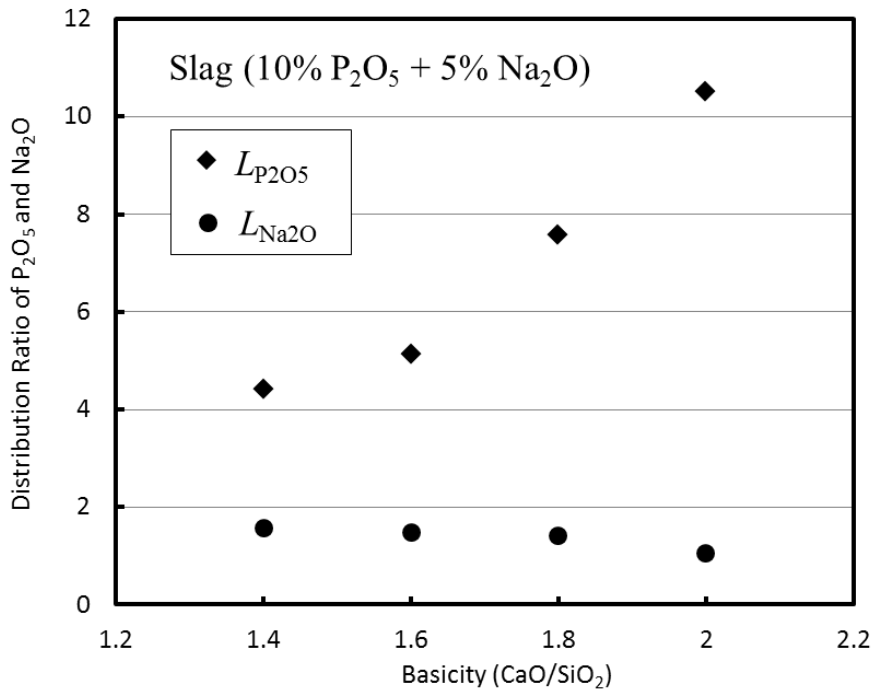


Fig. 5.14 Relationship between slag basicity and the distribution ratios of P₂O₅ and Na₂O

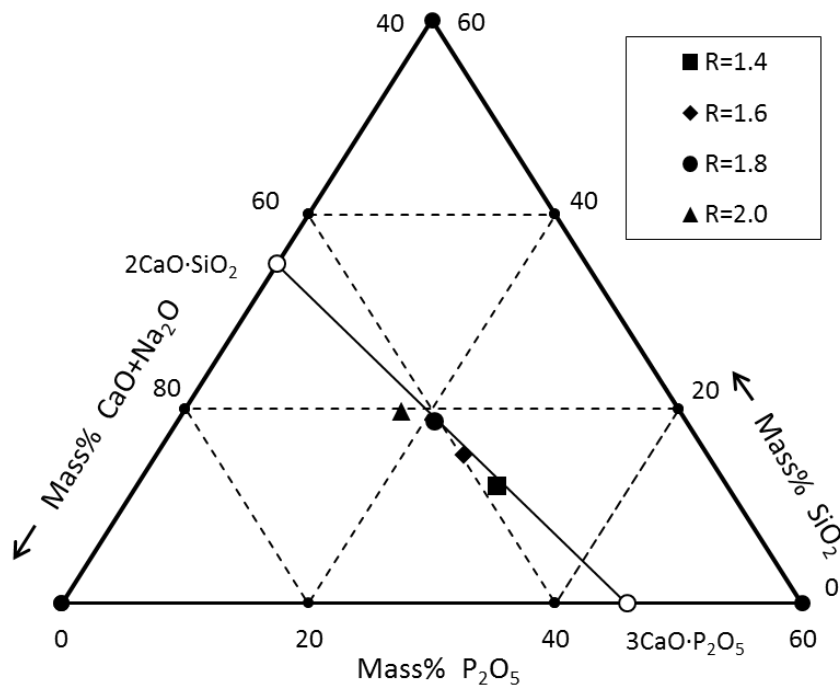


Fig. 5.15 Projections of the solid solution in the (CaO+Na₂O)-SiO₂-P₂O₅ pseudo-phase diagram under different slag basicity

Figure 5.16 shows the calculated mass fraction of solid solution in slags with different basicity. At low basicity, only a small amount of solid solution was formed. The mass fraction of the solid solution increased with increasing slag basicity. When the basicity increased to 2.0, about half of the slag consisted of solid solution.

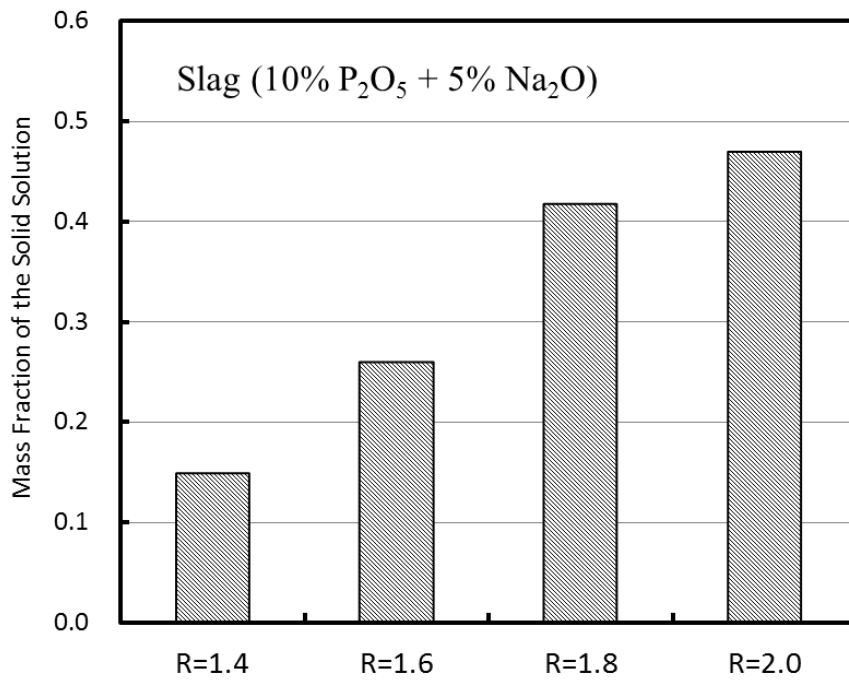


Fig. 5.16 Mass fraction of the solid solution in slags with different basicity

5.3 Discussion

5.3.1 Na₂O in the solid solution

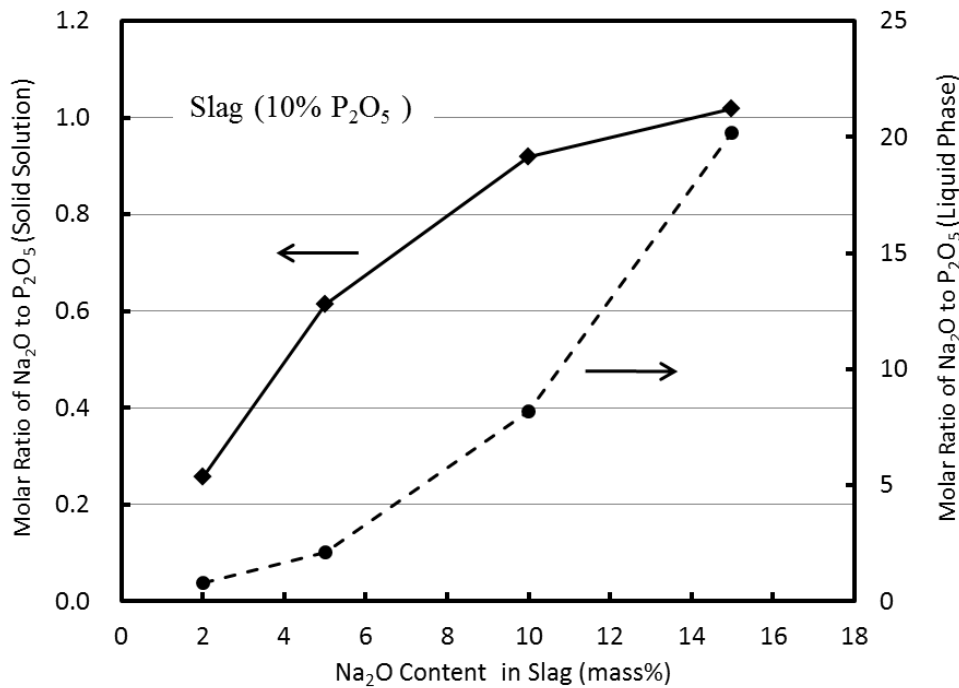


Fig. 5.17 Molar ratios of Na₂O to P₂O₅ in the solid solution and in the liquid phase

P₂O₅ is mainly concentrated in the solid solution with a certain molar ratio of CaO to P₂O₅. A part of the Na₂O was distributed in the solid solution. Previous studies [11, 12] clarified that Na₂O could substitute for CaO in the solid solution and combine with P₂O₅. To investigate the structure of the solid solution containing Na₂O, the molar ratio of Na₂O to P₂O₅ in the solid solution was calculated under various Na₂O contents. This value was also compared with that in the liquid phase to evaluate the distribution of Na₂O. Figure 5.17 shows that the molar ratios of Na₂O to P₂O₅ in the solid solution and in the liquid phase both increased with the increase in the Na₂O content in slag; however, they exhibited a different behavior. In the low Na₂O content range, the rate of increase of the molar ratio of Na₂O to P₂O₅ in the solid solution was higher than that in the liquid phase, indicating that the added Na₂O was preferentially distributed into the solid solution. When the Na₂O content in slag was further increased, the increasing rate of molar ratio of Na₂O to P₂O₅ in the solid solution became small, while that in the liquid phase increased sharply. This result indicates that the added Na₂O is difficult to continue entering the

solid solution, and the majority is distributed in the liquid phase. In the case of slag containing 15 mass% of Na_2O , the molar ratio of Na_2O to P_2O_5 in the solid solution was close to 1. It is considered that the Na_2O content in the solid solution approached saturation when the Na_2O content in slag increased to 10 mass% or more.

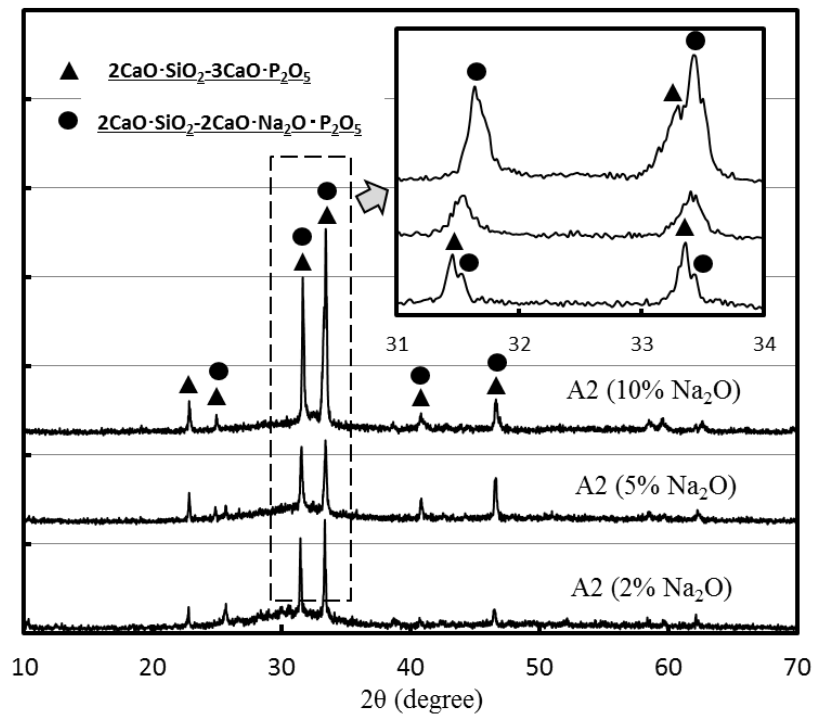


Fig. 5.18 XRD patterns of slags with various Na_2O contents

Figure 5.18 shows XRD patterns of slags with various Na_2O contents. The intensity of peaks associated with solid solution enhanced as the Na_2O content increased, which was consistent with the increase in the mass fraction of solid solution mentioned above. In addition to the $\text{C}_2\text{S}\text{-C}_3\text{P}$ solid solution, a new $2\text{CaO}\cdot\text{SiO}_2\cdot 2\text{CaO}\cdot\text{Na}_2\text{O}\cdot\text{P}_2\text{O}_5$ ($\text{C}_2\text{S}\text{-C}_2\text{NP}$) solid solution was observed in each slag. In the slag containing 10 mass% of Na_2O , the majority of the solid solution consisted of $\text{C}_2\text{S}\text{-C}_2\text{NP}$. According to the Hume-Rothery rule [13], when the radii of two different ions in the solute are similar, both ions in the molten system could be substituted

with each other to form solid solution. Because the ionic radius of Na^+ (0.102 nm) is very close to that of Ca^{2+} (0.100 nm), the Ca^{2+} and Na^+ ions can replace each other in the molten slag system [14]. In addition, because the electrostatic field of (PO_4^{3-}) is larger than that of (SiO_4^{4-}) , the Na^+ cations prefer combining with (PO_4^{3-}) in Na_2O -containing slags [15]. Therefore, it is concluded that the added Na_2O can substitute CaO in the solid solution, and combine with P_2O_5 to form a $\text{C}_2\text{S-C}_2\text{NP}$ solid solution. As more Na_2O was added, a larger amount of $\text{C}_2\text{S-C}_2\text{NP}$ was formed. The replaced CaO was distributed in the liquid phase. This reaction is described by Eq. (5.6).



5.3.2 Activity coefficient of P_2O_5

To better understand the distribution ratio of P_2O_5 between the solid solution and liquid phase, the activity coefficients of P_2O_5 in the solid solution and in the liquid phase were evaluated. As the liquid phase and the precipitated solid solution are in equilibrium, the activities of P_2O_5 in both phases are the same. The distribution ratio of P_2O_5 is proportional to the activity coefficient of P_2O_5 in each phase, as described in Eq. (5.7), where α is the activity; γ , the activity coefficient; and k , the coefficient for the conversion of mass percentage to mol fraction.

$$L_{\text{P}_2\text{O}_5} = \frac{(\% \text{P}_2\text{O}_5)_{\text{SS}}}{(\% \text{P}_2\text{O}_5)_{\text{L}}} = k \frac{\alpha_{\text{P}_2\text{O}_5(\text{SS})} \times \gamma_{\text{P}_2\text{O}_5(\text{L})}}{\alpha_{\text{P}_2\text{O}_5(\text{L})} \times \gamma_{\text{P}_2\text{O}_5(\text{SS})}} = k \frac{\gamma_{\text{P}_2\text{O}_5(\text{L})}}{\gamma_{\text{P}_2\text{O}_5(\text{SS})}} \quad (5.7)$$

The activity of P_2O_5 in the liquid phase was calculated using a regular solution model because it considers the interaction energies between the oxides in slag [16]. In a multi-component regular solution, the activity coefficient of component i is expressed by the following equation:

$$RT \ln \gamma_i = \sum_j \alpha_{ij} X_j^2 + \sum_j \sum_k (\alpha_{ij} + \alpha_{ik} - \alpha_{jk}) X_j X_k \quad (5.8)$$

where X_i is the molar fraction, and α_{ij} is the interaction energy between cations i and j . The reference state of the activity in this case is the hypothetical pure liquid that has a regular nature.

On the basis of the interaction energy between cations obtained by Ban-ya [17, 18] (listed in Table 5.3), the activity coefficient of $\text{PO}_{2.5}$ in regular solution was calculated in the $\text{CaO-SiO}_2\text{-Fe}_2\text{O}_3\text{-P}_2\text{O}_5\text{-Na}_2\text{O}$ slag system using Eq. (5.9). The conversion from the activity of $\text{PO}_{2.5}$ in regular solution to that of P_2O_5 in the liquid slag is shown in Eqs. (5.10) and (5.11) [17].

Table 5.3 Interaction energy between cations of major components in steelmaking slag, α_{ij} (J)

$i \backslash j$	Fe^{3+}	Ca^{2+}	Si^{4+}	P^{5+}	Na^+
Fe^{3+}	-	-95810	32640	14640	-74890
Ca^{2+}	-95810	-	-133890	-251040	15100
Si^{4+}	32640	-133890	-	83680	-111290
P^{5+}	14640	-251040	83680	-	-50210
Na^+	-74890	15100	-111290	-50210	-

$$RT \ln \gamma_{\text{PO}_{2.5}(\text{R.S.})} = -251040X_{\text{CaO}}^2 + 83680X_{\text{SiO}_2}^2 + 14640X_{\text{FeO}_{1.5}}^2 - 50210X_{\text{NaO}_{0.5}}^2 - 33470X_{\text{CaO}} \cdot X_{\text{SiO}_2} - 140590X_{\text{CaO}} \cdot X_{\text{FeO}_{1.5}} - 301250X_{\text{CaO}} \cdot X_{\text{NaO}_{0.5}} + 65680X_{\text{SiO}_2} \cdot X_{\text{FeO}_{1.5}} + 144760X_{\text{SiO}_2} \cdot X_{\text{NaO}_{0.5}} + 39320X_{\text{FeO}_{1.5}} \cdot X_{\text{NaO}_{0.5}} \quad (5.9)$$

$$\text{P}_2\text{O}_5(\text{L}) = 2\text{PO}_{2.5}(\text{R.S.}) \quad (5.10)$$

$$RT \ln \alpha_{\text{P}_2\text{O}_5(\text{L})} = 2RT \ln \alpha_{\text{PO}_{2.5}(\text{R.S.})} + 52720 - 230.706T \quad (5.11)$$

Figure 5.19 shows the change in the activity coefficient of P_2O_5 in the liquid phase with the basicity of the liquid phase. A higher basicity ((mass% CaO)/(mass% SiO_2)) of the liquid phase led to a lower activity coefficient of P_2O_5 in the liquid phase. As mentioned above, the mass fraction of solid solution increased with the Na_2O content in slag, causing a decrease in the CaO content in the liquid phase. In the case of high Na_2O content, as shown in Fig. 5.19, the basicity of the liquid phase was lower, and a higher activity coefficient of P_2O_5 in the liquid phase was performed. Figure 5.20 shows the change in the activity coefficient of P_2O_5 with the Fe_2O_3 content in the liquid phase. The activity coefficient of P_2O_5 had no dependence on the Fe_2O_3

content in the liquid phase. For the slags with high Na₂O content, the Fe₂O₃ content in the liquid phase and the activity coefficient of P₂O₅ were both higher.

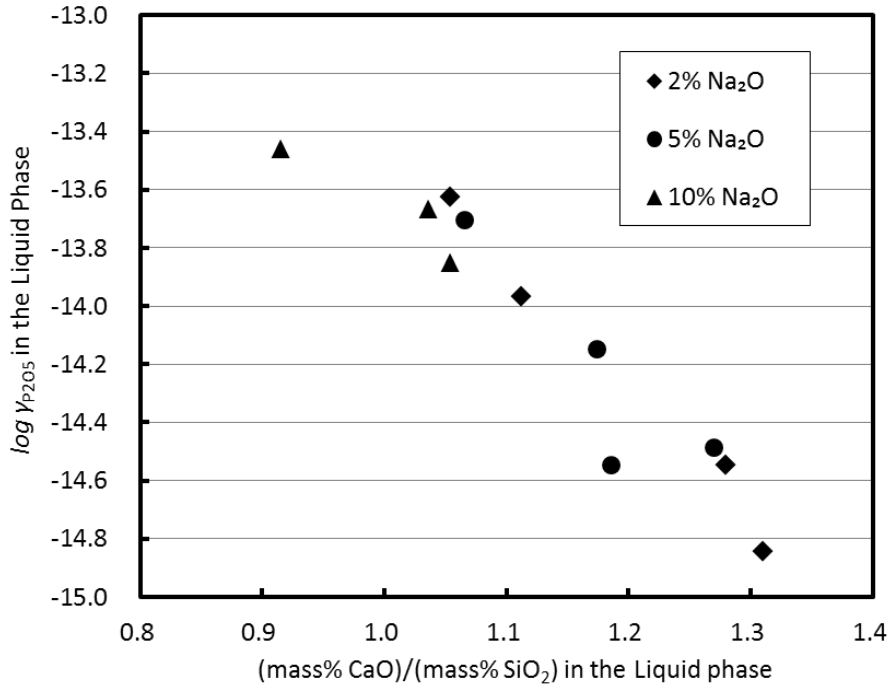


Fig. 5.19 Change in the activity coefficient of P₂O₅ with the basicity of the liquid phase

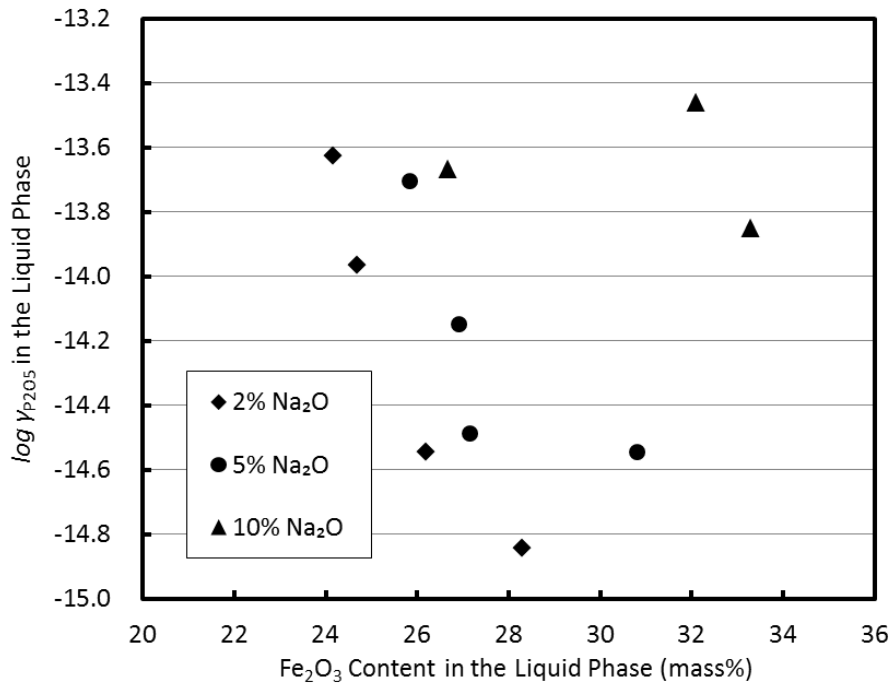
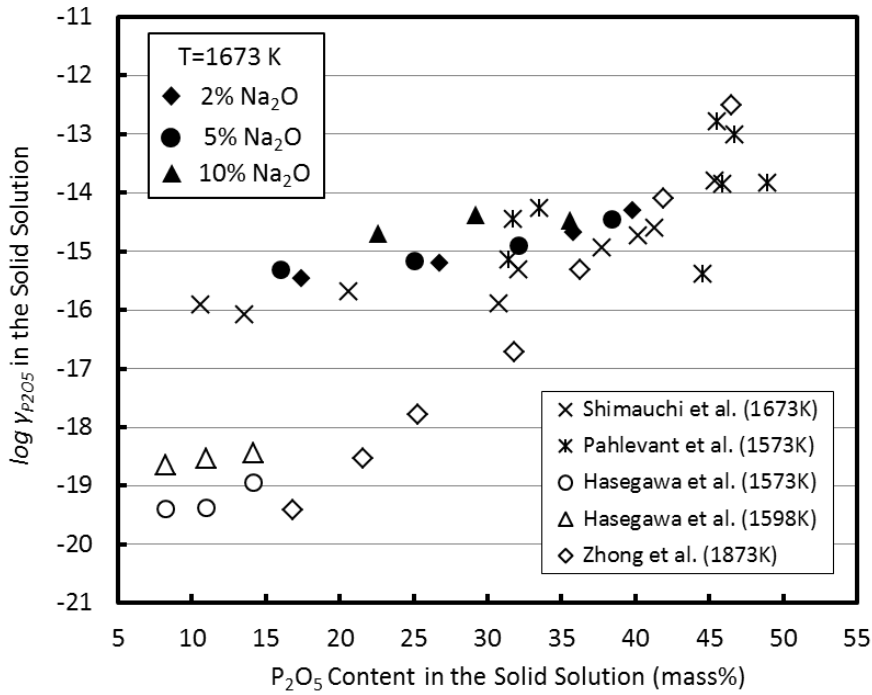
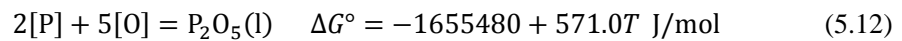


Fig. 5.20 Change in the activity coefficient of P_2O_5 with the Fe_2O_3 content in the liquid phaseFig. 5.21 Effect of P_2O_5 content on the activity coefficient of P_2O_5 in the solid solution

Because the activities of P_2O_5 in both phases are the same, the activity coefficient of P_2O_5 in the solid solution was calculated using the activity of P_2O_5 in the liquid phase obtained by the regular solution model. Figure 5.21 shows the change in the activity coefficient of P_2O_5 in the solid solution. The activity coefficient of P_2O_5 in the solid solution increased with the P_2O_5 content in the solid solution. The Na_2O content in slag had little influence on the activity coefficient of P_2O_5 in the solid solution. Because the distribution ratio of P_2O_5 was proportional to the activity coefficient of P_2O_5 in each phase, in the case of high Na_2O content, the higher activity coefficient of P_2O_5 in the liquid slag resulted in a higher distribution ratio of P_2O_5 .

The calculated activity coefficient of P_2O_5 in the present study was compared with the results obtained by other researchers, as shown in Fig. 5.21. Shimauchi *et al.* [9] and Pahlevani *et al.*

[10] estimated the activity coefficients of P_2O_5 in the solid solution in the $CaO-SiO_2-Fe_2O_3-P_2O_5$ slag system at 1673 K and in the $CaO-SiO_2-FeO-P_2O_5$ slag system at 1573 K, respectively. They also adopted a regular solution model to calculate the activity of P_2O_5 via the equilibrium between the solid solution and liquid phase. Zhong *et al.* [19] measured the activity coefficients of P_2O_5 by applying the equilibrium between liquid iron and C_2S-C_3P solid solution at 1873 K. Equation (5.12) [20] was used to calculate the activity of P_2O_5 , and the oxygen partial pressure was controlled with a $CO-CO_2$ gas atmosphere. Hasegawa *et al.* [21, 22] measured the activity of P_2O_5 in slag when slags containing $CaO-SiO_2$ and C_2S-C_3P solid solution were equilibrium with a $Cu-Fe-P$ liquid alloy. By measuring the equilibrium oxygen partial pressures with the aid of a zirconia electrolyte cell, the activities of P_2O_5 were obtained at 1573 K and 1593 K. Their results also show that the activity coefficient of P_2O_5 in the solid solution increased with the P_2O_5 content; however, the values were different. When applying a regular solution model, the calculated activity coefficient of P_2O_5 was almost of the same order of magnitude. The current values were approximately five orders of magnitude greater than those reported by Zhong *et al.* [19] and Hasegawa *et al.* [22].



5.4 Summary

To increase the efficiency of dephosphorization and to recover P from dephosphorization slag by selective leaching, it is necessary to determine the distribution ratios of Na_2O and P_2O_5 between the solid solution and liquid phase in slags with high P_2O_5 content. In this study, the change in composition and mass fraction of the solid solution with slag composition were investigated. The results obtained are summarized below:

- (1) A linear relationship was found between the distribution ratio of P_2O_5 and the Na_2O content in slag; the relationship was independent of P_2O_5 content. Further addition of Na_2O did not enrich Na_2O in the solid solution, because the Na_2O content in the solid solution became constant, and a new $2CaO \cdot SiO_2 \cdot 2CaO \cdot Na_2O \cdot P_2O_5$ solid solution formed.
- (2) With the increase in P_2O_5 content in slag, the P_2O_5 content in the solid solution also increased. Na_2O addition decreased the P_2O_5 content in the solid solution, while it increased the mass fraction of solid solution in slag, which facilitated P_2O_5 enrichment.
- (3) The distribution ratios of P_2O_5 and Na_2O both increased with increasing the Fe_2O_3 content in the liquid phase. In the case of high Fe_2O_3 content, a P_2O_5 -condensed solid solution was formed.
- (4) With the increase in slag basicity, the distribution ratio of P_2O_5 increased significantly, while that of Na_2O decreased. A higher basicity resulted in a larger mass fraction of the solid solution in slag.
- (5) The activity coefficient of P_2O_5 in the solid solution increased with the P_2O_5 content in the solid solution, which was independent of the Na_2O content in slag.

References

1. M. Muraki, H. Fukushima, N. Sano: Transactions of the Iron and Steel Institute of Japan, 25(1985), pp. 1025-1030.
2. J.J. Park, R. J. Frunhan: Metallurgical and Materials Transactions B, 22B(1991), pp. 39-46.
3. H. Suito, R. Inoue: Transactions of the Iron and Steel Institute of Japan, 24(1984), pp. 47-53.
4. K. Kunisada, H. Iwai: Transactions of the Iron and Steel Institute of Japan, 27(1987), pp. 263-269.
5. C. Du, X. Gao, S. Ueda, S. Kitamura: Journal of Sustainable Metallurgy, (2017), published online.
6. K. Kunisada, H. Iwai: Transactions of the Iron and Steel Institute of Japan, 26 (1986), pp. 121-127.
7. K. Ito, M. Yanagisawa, N. Sano: Tetsu-to-Hagané, 68 (1982), pp. 342-344.
8. Slag Atlas, Verein Deutscher Eisenhüttenleute, Dusseldorf, 1995.
9. K. Shimauchi, S. Kitamura, H. Shibata: ISIJ International, 49(2009), pp. 505-511.
10. F Pahlevani, S Kitamura, H Shibata, N Maruoka: ISIJ International, 50(2010), pp. 822-829.
11. L. Lin, Y. P. Bao, M. Wang, W. Jiang, H. M. Zhou: ISIJ International, 54(2014), pp. 2746-2753.
12. S. Xie, W. Wang, Y. Liu, H. Matsuura: ISIJ International, 54(2014), pp.766-773.
13. U. Mizutani: Hume-Rothery Rules for Structurally Complex Alloy Phases, Taylor & Francis, USA, 2010.
14. R.D. Shannon: Acta Crystallographica Section A, A32(1976), pp. 751-767.
15. P. Herasymenko, G.E. Speight: Journal of the Iron and Steel Institute, 166(1950), pp. 169-183.
16. S. Ban-ya, M. Hino: Chemical properties of molten slags, Iron and Steel Institute of Japan, Tokyo, 1991.
17. S. Ban-ya: ISIJ International, 33(1993), pp. 2-11.
18. S. Ban-ya, M. Hino, T. Nagasaka: ISIJ International, 33(1993), pp.12-19.
19. M. Zhong, H. Matsuura, F. Tsukihashi: ISIJ International, 55(2015), pp. 2283-2288.
20. E.T. Turkdogan: ISIJ International, 40(2000), pp. 964-970.
21. Y. Kaida, M. Hasegawa, Y. Kikuchi, K. Wakimoto, M. Iwase: Metallurgical and Materials Transactions B, 36B(2005), pp. 43-51.
22. R. Matsugi, K. Miwa and M. Hasegawa: ISIJ International, 57(2017), pp. 1718-1724.

6 P recovery from the leachate by precipitation

Chemical precipitation is a widespread approach for phosphate fertilizer production and P recovery from wastewater [1, 2]. To recover the dissolved P in the leachate, a process for extracting phosphate product by phosphate precipitation was explored. The effects of alkaline solution and pH on the P precipitation and the composition of the obtained phosphate product were investigated.

6.1 Experimental method

Based on the above studies, we determined the optimum conditions for selective leaching of P from slag. The leachate obtained under the optimum conditions was used to recover P. Table 6.1 lists the compositions of slags which were leached. These slags were modified by adding 4 mass% of alkaline oxide (Na_2O or K_2O) and were cooled in furnace. Then, these slags were leached by citric acid (0.1 mol/L) at pH 6 for 120 min. After leaching, the residue was filtered, and then the leachate was collected and stored in a beaker with a 2000 mL capacity. The concentration of each element was analyzed using inductively coupled plasma atomic emission spectroscopy (ICP-AES).

Table 6.1 Compositions of slags which were leached for P recovery (mass%)

Sample	CaO	SiO ₂	Fe ₂ O ₃	P ₂ O ₅	MgO	K ₂ O	Na ₂ O	Cooling method
Slag A	34.5	21.5	29.0	8.0	3.0	4.0	-	Furnace
Slag B	34.5	21.5	29.0	8.0	3.0	-	4.0	cooling

Calcium phosphate compounds have little solubility at higher pH [3], and this made it possible to precipitate the dissolved P in the leachate via the addition of the $\text{Ca}(\text{OH})_2$ or NaOH solution. The leachate was treated, via the following procedure, to recover P, as shown in Fig. 6.1. To

investigate the effect of alkaline solution, the $\text{Ca}(\text{OH})_2$ saturated solution and NaOH solution (1.0 mol/L) were added to the leachate to adjust the pH to approximately 11, respectively. To investigate the effect of pH, the pH of the leachate were adjusted to 9, 10, 11, and 12, respectively, by adding $\text{Ca}(\text{OH})_2$ saturated solution. The leachate became muddy with the increase in the pH, and some flocculent precipitate formed. Because this precipitate is difficult to be separated from the aqueous solution by the conventional filtration, gravity separation was adopted in this study. The muddy solution was settled for 24 h at room temperature to make the solution separate into two layers. After removal of the upper solution, the flocculent precipitate coexisting with a small amount of solution was obtained. Then, the flocculent precipitate with little water was dried at 373 K until solid precipitate formed. To remove crystal water and obtain a crystalline substance, the obtained precipitate was put in a Pt crucible and further calcined at 873 K for 2 h to produce phosphate product. The obtained phosphate product was weighted and its composition was analyzed using X-ray diffraction (XRD). To determine the contents of each component, a method, as the same as chemical analysis of residue (shown in Chapter 3), was adopted.

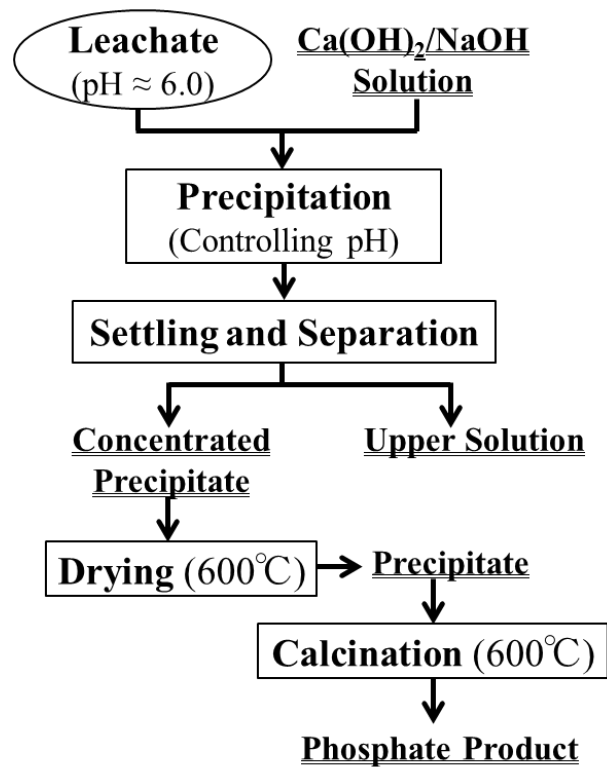


Fig. 6.1 Experimental procedure of abstracting phosphate product from leachate

To determine whether this phosphate product is used as a phosphate fertilizer, the available P content of phosphate product was evaluated by solubility tests. The laboratory evaluation of the available P content is generally made by determining either water-soluble or citrate-soluble P₂O₅ [4]. Slow-release phosphate fertilizers are often comparatively insoluble in water, but are soluble in citrate solutions. We used 2% citric acid as an extractant, a method first employed by Wagner [4]. The phosphate product was ground to pass 100 mesh sieves. One gram of sample was extracted with 100 mL of 2% citric acid or distilled water in a beaker, and the solution was stirred for 30 min at 291 K [5]. After filtration, the concentrations of each element in the aqueous solution were analyzed using ICP-AES.

6.2 Experimental results and discussion

6.2.1 Effect of alkaline solution on P precipitation

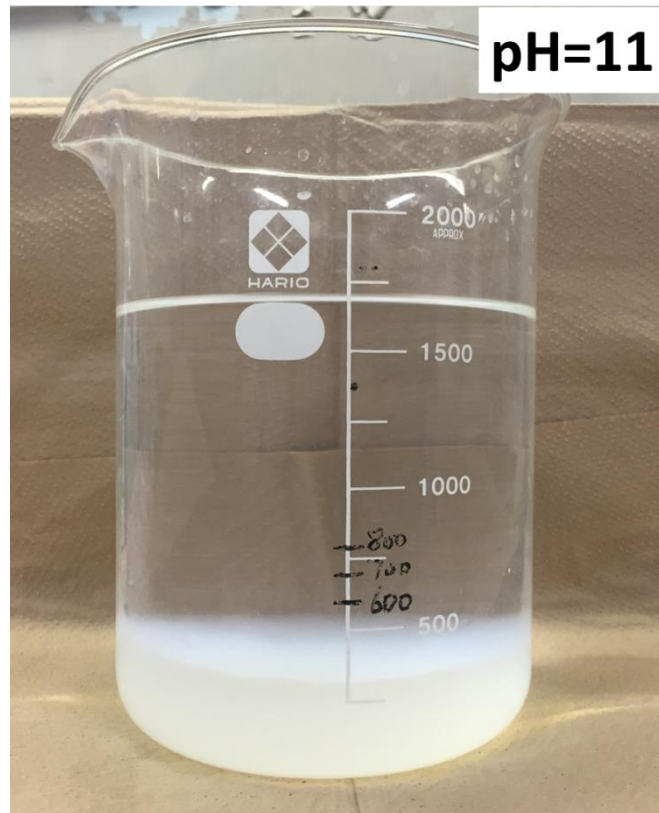


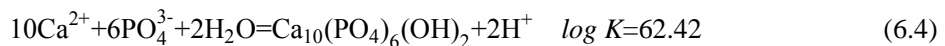
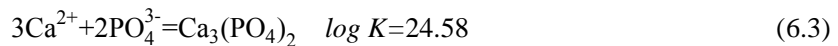
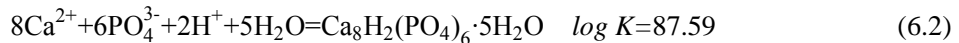
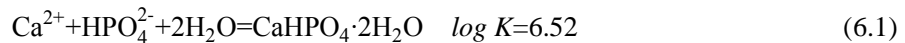
Fig. 6.2 Image of the leachate after adding $\text{Ca}(\text{OH})_2$ solution and settlement

The leachate A obtained by leaching of Slag A was used for the experiment of P recovery. The compositions of each element in the leachate are shown in Table 6.1. Owing to selective leaching of P from slag, the major ions in the leachate were those of Ca, Si, and P, which were the same elements consist of solid solution. The Ca concentration was the highest, reaching 328.4 mg/L. The P concentration was 65.2 mg/L, which was a little lower than the Si concentration. The Fe and Mg concentrations in the leachate were very low compared to other elements. The leachate also contains 25.1 mg/L of K. After adding alkaline solution and precipitation, the leachate was separated into two layers, as shown in Fig. 6.2. The flocculent precipitate was concentrated in the lower layer, and the upper solution became limpid.

The concentrations of each element in the upper solution were compared with those in the original leachate in Table 6.2. This shows that the concentrations of each element all decreased in each case, especially P. Adding Ca(OH)₂ solution could decrease the P, Si, and K concentrations in the upper solution to lower values. It indicates that P and Si were easily precipitated in this case. After precipitation, almost all of the P in the upper solution was removed; the P concentration was only 0.24 mg/L. The Ca concentration changed slightly because of the addition of Ca(OH)₂. In the case of NaOH addition, the P concentration in the upper solution decreased to 2.62 mg/L, and the Ca concentration decreased to half because of the precipitation of calcium phosphate. This upper solution contains a large amount of Na.

Table 6.2 Concentrations of each element in the leachate and in the upper solution after precipitation (mg/L)

	Ca	Si	P	Fe	Mg	Na	K
Leachate A	328.37	73.49	65.16	5.02	4.05	0.78	25.12
Upper Solution (adding Ca(OH) ₂)	307.50	49.20	0.24	0.10	1.38	0	19.60
Upper Solution (adding NaOH)	155.66	61.6	2.62	0.16	0.56	422.72	21.36



It is well known that in solutions containing Ca²⁺ and phosphate ions, a number of calcium phosphate precipitate such as dicalcium phosphate dihydrate (DCPD, CaHPO₄·2H₂O), octacalcium phosphate (OCP, Ca₈H₂(PO₄)₆·5H₂O), tricalcium phosphate (TCP, Ca₃(PO₄)₂), and HAP (Ca₁₀(PO₄)₃(OH)₂), may form depending on the pH and solution composition [6]. At

higher pH condition, the predominant phosphate species in the aqueous solution are PO_4^{3-} and HPO_4^{2-} [7]. The precipitation reactions of these calcium phosphates are described in Eqs. (6.1)-(6.4). On the basis of thermodynamic data of each species [8-10], as listed in Table 6.3, the equilibrium constants of precipitation reactions were calculated. The solubility curves of these calcium phosphates in the aqueous solution were calculated at pH 11 using these equilibrium constants, as shown in Fig. 6.3. The compositions of the original leachate and upper solutions after precipitation were also plotted in this Figure. The observed point for the original leachate was located above these solubility curves, indicating that the P concentration in the solution would reach saturation when the pH increased to 11. In the case of NaOH addition, the observed point for the upper solution was located near the solubility curve of DCPD; in the case of $\text{Ca}(\text{OH})_2$ addition, it was located between the solubility curves of DCPD and OCP. This shows that the precipitated calcium phosphate may consist of DCPD or OCP. Considering the thermodynamics, HAP is determined to be the most stable calcium phosphate, and the P concentration in the solution can be reduced to a much lower value. However, the precipitation of unstable compounds, as precursors, is commonly observed owing to the differences in the kinetic condition of nucleation [6]. In many natural environments, DCPD, along with OCP and TCP, plays a crucial role as a precursor or intermediate to HAP [11]. Therefore, the P concentration in the upper solution is considered to be determined by the solubility of DCPD and OCP.

Table 6.3 Thermodynamic data of each species in the aqueous solution (kJ/mol)

Species	$\text{Ca}_{10}(\text{PO}_4)_6(\text{OH})_2$	$\text{Ca}_3(\text{PO}_4)_2$	$\text{CaHPO}_4 \cdot 2\text{H}_2\text{O}$	$\text{Ca}_8\text{H}_2(\text{PO}_4)_6 \cdot 5\text{H}_2\text{O}$
ΔG^0	-12514.37	-3850.53	-2158.7	-12263.3
Species	$(\text{CaO})_5(\text{SiO}_2)_6(\text{H}_2\text{O})_{5.5}$	H_2O	H^+	Ca^{2+}
ΔG^0	-9880.31	-237.1	0	-553.07
Species	HSiO_3^-	PO_4^{3-}	HPO_4^{2-}	H_2PO_4^-
ΔG^0	-1015.6	-1025.55	-1094.17	-1135.17

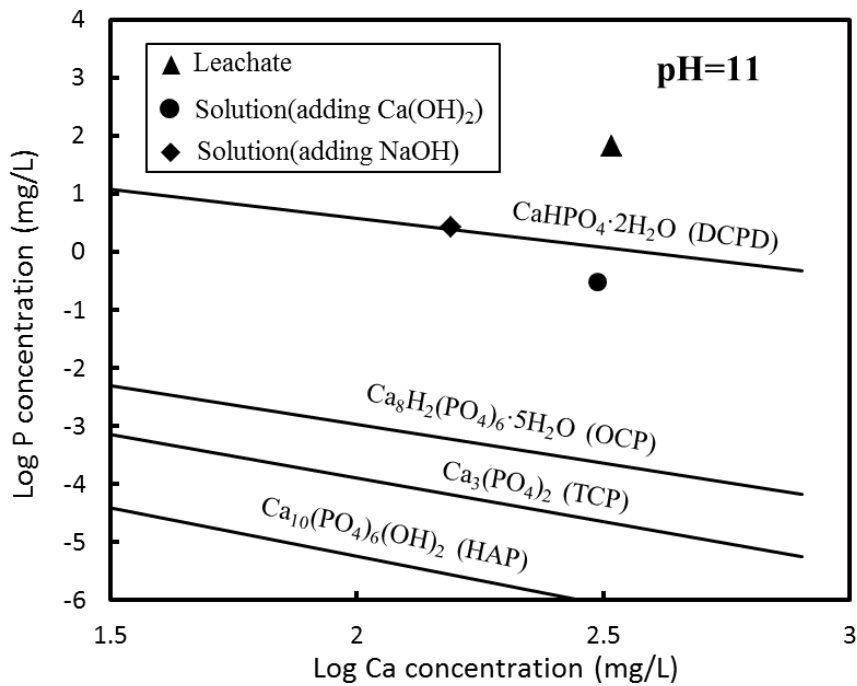


Fig. 6.3 Solubility curves for some calcium phosphates and the experimental results at pH 11

Figure 6.4 (A) shows an image of the precipitate when $\text{Ca}(\text{OH})_2$ was added. A white powder was obtained in this process. Table 6.4 shows the chemical composition of the obtained precipitates. These two precipitates mainly consist of CaO and P_2O_5 but K_2O content is very low. The precipitate also has SiO_2 and Fe_2O_3 contents of 3–5 mass% and 1.0% mass%, respectively. The CaO content in these precipitates are almost the same, reaching approximately 43 mass%. In the case of NaOH addition, the obtained precipitate had a higher P_2O_5 content and lower SiO_2 content. The P_2O_5 content in this precipitate was about 25 mass%, which was similar with that in the solid solution prior to leaching. According to the mass balance calculation, approximately 25 mass% of the precipitate was determined to be unknown. This constituent was considered to be crystal water and organic substance (calcium citrate).

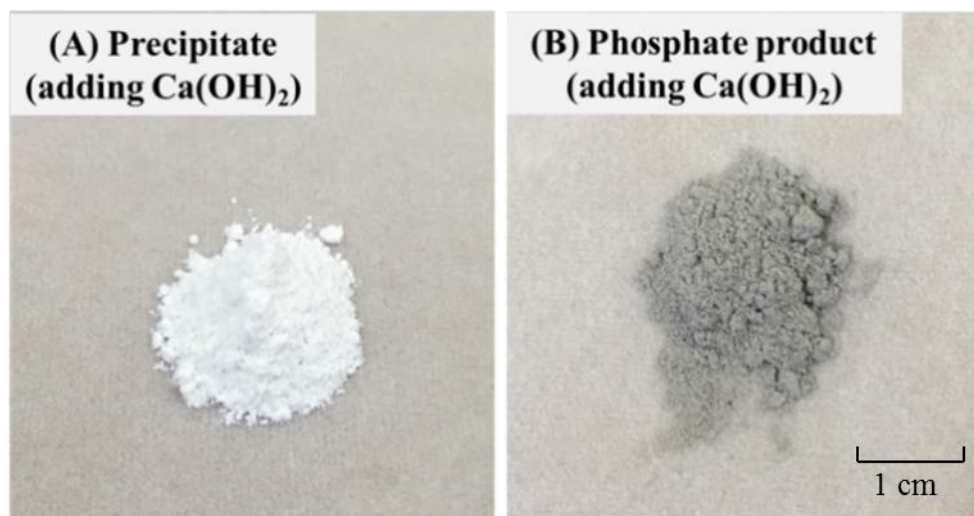


Fig. 6.4 Image of the precipitate and phosphate product when $\text{Ca}(\text{OH})_2$ was added

Table 6.4 Chemical composition of the obtained precipitates and phosphate products (mass%)

Sample		CaO	SiO ₂	P ₂ O ₅	Fe ₂ O ₃	Na ₂ O	MgO	K ₂ O	Others
Precipitate	adding $\text{Ca}(\text{OH})_2$	41.94	5.42	23.30	1.10	0.03	0.63	0.06	27.52
	adding NaOH	41.87	3.29	24.97	1.17	1.96	0.97	0.11	25.66
Phosphate product	adding $\text{Ca}(\text{OH})_2$	53.53	5.86	28.52	1.40	0.01	0.80	0.10	9.78
	adding NaOH	52.59	3.47	30.38	1.49	2.59	1.22	0.16	8.10

Figure 6.5 shows the XRD patterns of the obtained precipitate when different alkaline solutions were added. In the case of $\text{Ca}(\text{OH})_2$ addition, no obvious peaks were observed, indicating that crystalline substance did not form and this precipitate mainly consists of amorphous phases. In the case of NaOH addition, some peaks which were similar with those of silicon-substituted calcium hydroxyapatite ($\text{Ca}_5(\text{PO}_4)_{2.85}(\text{SiO}_4)_{0.15}(\text{OH})$) and HAP ($\text{Ca}_{10}(\text{PO}_4)_6(\text{OH})_2$) were observed, but not obviously. Amorphous phases still existed.

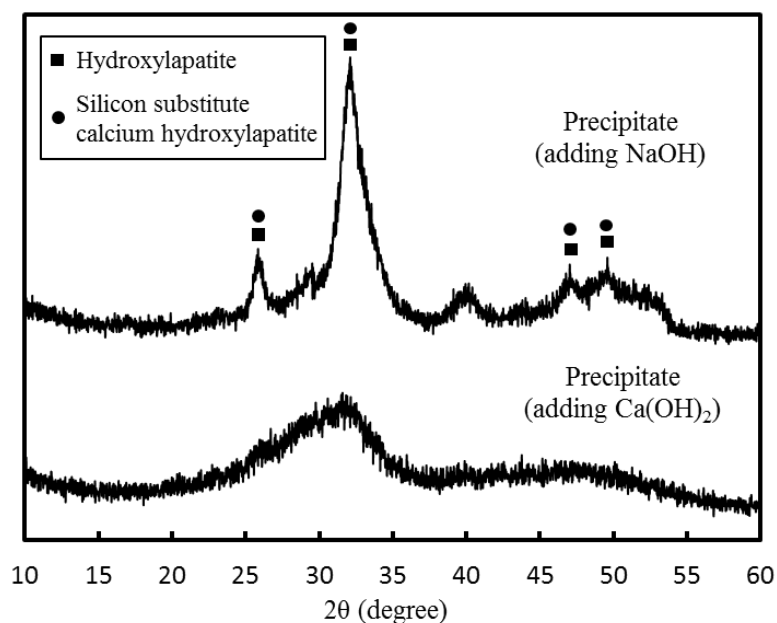


Fig. 6.5 XRD patterns of the obtained precipitates at pH 11

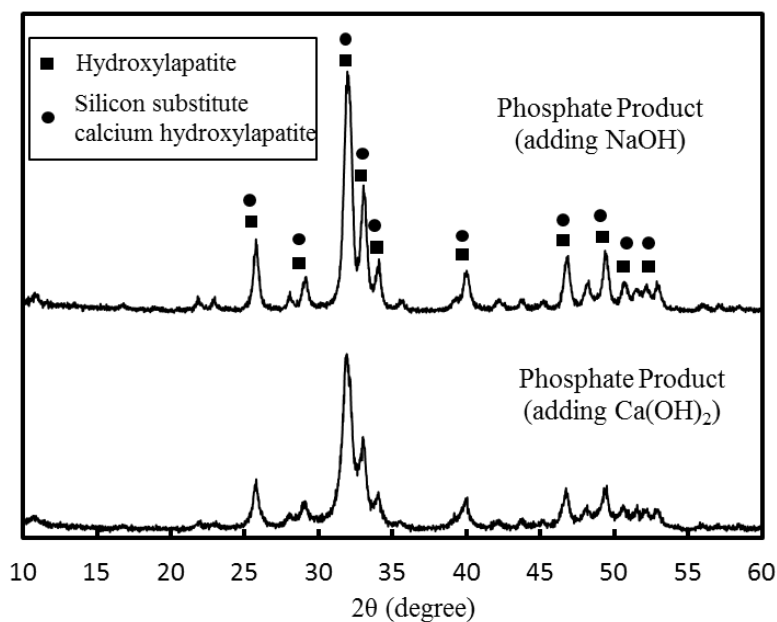


Fig. 6.6 XRD patterns of the phosphate products obtained by calcination

After calcination, the white precipitate transformed into a grey phosphate product, as shown in Fig. 6.4 (B). The compositions of these phosphate products are also listed in Table 6.4. Compared with those of the precipitate, the contents of each constituent all increased because of

the removal of the crystal water and the decomposition of the organic substance. The CaO content in these phosphate products was more than 50 mass%. The Fe₂O₃ content was about 1.4 mass%. About 8 mass% of these products were still unknown. It is considered that this part consists of the hydroxyl (OH) which did not remove during heating and the carbide which came from the decomposition of the organic substance. In the case of NaOH addition, the P₂O₅ content in the phosphate product reached 30.4 mass%, and the SiO₂ content was lower.

Figure 6.6 shows the XRD patterns of the phosphate products obtained by calcination. Obvious peaks were observed in each case. The main peaks of these two products are almost identical. The peaks were consistent with those of silicon-substituted calcium hydroxyapatite and HAP. This shows that, following calcination, the phosphate that was precipitated from the leachate finally existed in the form of HAP. As shown in Fig. 6.3, the most stable calcium phosphate is HAP. There is also evidence to show that ultimately, any calcium phosphate that is precipitated will probably transform into the thermodynamically more stable HAP [12].

In summary, the addition of Ca(OH)₂ or NaOH solution into the leachate had similar effects on phosphate precipitation, and a HAP product was obtained. Adding NaOH solution could produce a higher quality of phosphate product (a higher P₂O₅ content and lower SiO₂ content); however, some P still existed in the upper solution, indicating that the precipitation of phosphate in the leachate was insufficient. The addition of Ca(OH)₂ solution not only increased the pH but also supplied some Ca²⁺ ions which are involved in the precipitation of calcium phosphate. As shown in 6.3, the P concentration in the aqueous solution decreased with the increase in the Ca concentration. As a result, almost all of the P was precipitated in this case, which was beneficial for the P recovery. In this process, the obtained precipitate or phosphate product has the potential to be used as a fertilizer, because they have the same components (CaO and P₂O₅) as phosphate fertilizer and a high enough P₂O₅ content [13].

6.2.2 Effect of pH on P precipitation

Table 6.5 Concentration of the leachate and the upper solution after precipitation (mg/L)

Solution	Ca	Si	Fe	P	Mg	Na
Leachate B	301.01	69.60	6.25	63.03	2.51	35.54
Upper Solution (pH=9)	230.61	64.33	2.38	4.14	2.00	30.09
Upper Solution (pH=10)	233.49	56.25	0.32	0.91	1.86	28.99
Upper Solution (pH=11)	247.13	51.44	0.04	0.24	1.50	28.38
Upper Solution (pH=12)	295.52	37.69	0.03	0.20	0.37	24.69

The leachate B obtained by leaching of Slag B (shown in Table 6.1) was used to investigate the effect of pH on P precipitation. As shown in Table 6.5, the concentrations of each element in this leachate were similar with those in the leachate A. The Ca concentration was the highest, reaching 301 mg/L. The P and Si concentration were almost the same, more than 60 mg/L. The concentrations of other element were lower because of selective leaching of P. Following the addition of $\text{Ca}(\text{OH})_2$ solution to adjust the pH, the leachate was separated into two layers via settling: the upper solution and the precipitate. Table 6.5 lists the compositions of the upper solution at various pH conditions. The concentration of each element in the upper solution decreased relative to the original leachate. With the increase in the pH of the leachate, the concentrations of Si, Fe, and P further decreased because of the precipitation of some substances. The Ca concentration in the upper solution increased because of $\text{Ca}(\text{OH})_2$ addition. When the pH was adjusted to 10, the P concentration varied from 63 mg/L to less than 1 mg/L. The Si concentration reduced by approximately half when the pH increased to 12.

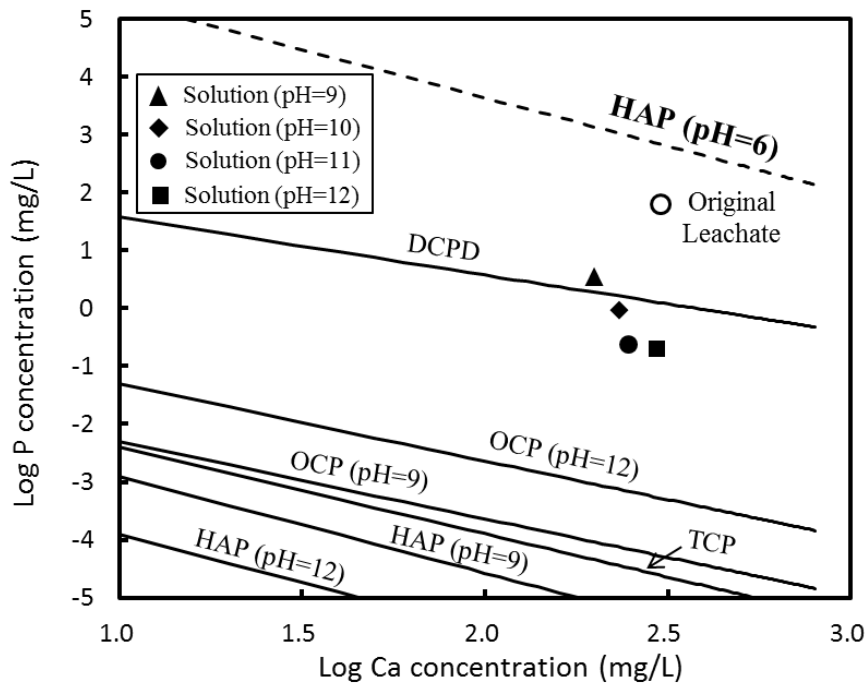


Fig. 6.7 Solubility curves of calcium phosphates and the experimental results at various pH conditions

The solubility curves of calcium phosphates (DCPD, OCP, TCP, and HAP) were calculated using Eqs.(6.1)–(6.4) at various pH conditions. Figure 6.7 shows the solubility curves of calcium phosphates (the solubility of OCP and HAP was influenced by the pH) and the experimental results. With the increase in the Ca concentration, the saturated concentration of P in the aqueous solution decreased in each case. In the present study, the solubility of calcium phosphate decreases in the order of DCPD, OCP, TCP, and HAP. The Ca and P concentrations in the original leachate were lower than those required for HAP precipitation at pH 6, but were higher than the saturated concentration of calcium phosphates at higher pH conditions. It was thus possible to precipitate P in the leachate via adjusting the pH. After precipitation, the observed points for the upper solution were located around the solubility curves of DCPD. At pH 11 and 12, they lay between the solubility curves of DCPD and OCP. Therefore, DCPD was

considered the major constituent of the precipitate and its solubility determined the Ca and P concentrations in the upper solution.

In the solution rich in Ca^{2+} and silicate ions, $\text{CaO-SiO}_2\text{-H}_2\text{O}$ gel in the form of $(\text{CaO})_5(\text{SiO}_2)_6(\text{H}_2\text{O})_{5.5}$ generally precipitates in alkaline conditions [14]. The reaction for the formation of calcium silicate hydrogel is given by Eq. (6.5) [10]. Its equilibrium constant was calculated using the thermodynamic data in Table 6.3.

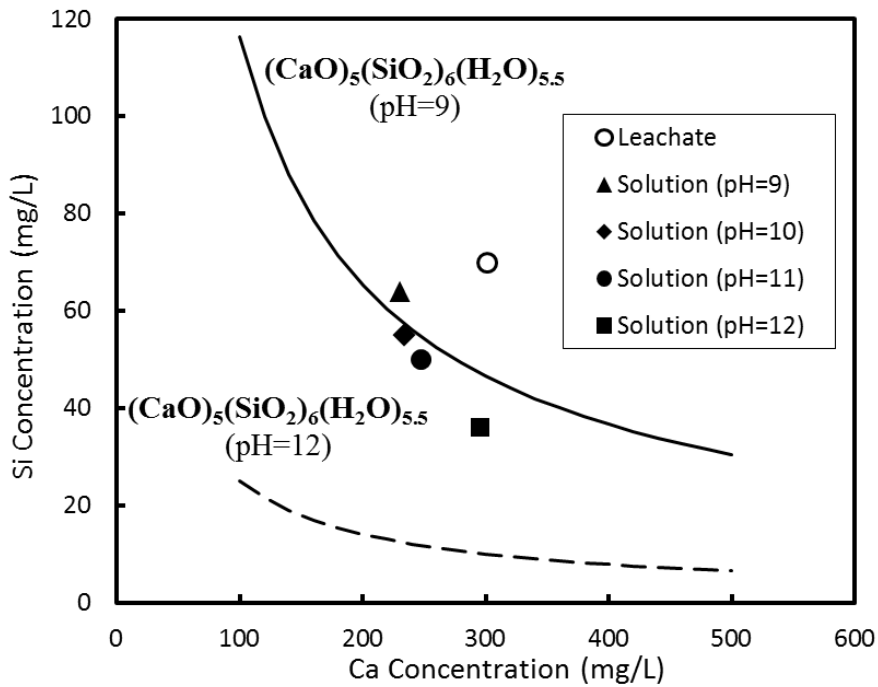


Fig. 6.8 Solubility curves of calcium silicate hydrogel and the experimental results under different pH conditions

Figure 6.8 shows the solubility curves of calcium silicate hydrogel and the experimental results under various pH conditions. With the increase in the Ca concentration, the Si concentration in the aqueous solution decreased. High pH suppressed dissolution of this gel. The observed point for Ca and Si concentrations at pH 9 was located near the solubility line at pH 9, indicating that

the solubility of calcium silicate hydrogel determined the Si concentration. As the pH decreased, the observed points moved to the solubility line at pH 12. However, the experimental values were far higher than the values determined by the solubility of the gel at pH 12. The reason is not clear.

Table 6.6 Chemical compositions of the precipitates under various pH conditions (mass%)

	CaO	SiO ₂	Fe ₂ O ₃	P ₂ O ₅	MgO	Na ₂ O	Others
Precipitate (pH=9)	41.39	0.30	1.21	27.29	0.15	0.13	29.52
Precipitate (pH=10)	40.59	1.58	1.48	25.02	0.17	0.10	31.06
Precipitate (pH=11)	41.06	3.16	1.51	23.84	0.25	0.10	30.07
Precipitate (pH=12)	40.15	5.34	1.25	19.68	0.48	0.09	33.02

Table 6.7 Chemical compositions of the phosphate products under various pH conditions (mass%)

	CaO	SiO ₂	Fe ₂ O ₃	P ₂ O ₅	MgO	Na ₂ O	Others
Phosphate product (pH=9)	54.28	0.51	1.65	34.48	0.21	0.26	8.61
Phosphate product (pH=10)	53.12	2.25	1.95	31.27	0.22	0.26	10.95
Phosphate product (pH=11)	53.71	3.91	2.00	30.18	0.35	0.24	9.61
Phosphate product (pH=12)	54.94	5.71	1.73	26.05	0.72	0.15	10.70

A white precipitate was obtained through separation and drying. The chemical compositions of the precipitates under various pH conditions were listed in Table 6.6. CaO and P₂O₅ are the major components in these precipitates. The P₂O₅ content in these precipitates exceeded 20 mass%, and it increased further with a decrease in the pH. Approximately 30 mass% of the precipitate was unknown, which maybe consist of crystal water and organic substances. After calcination, the white precipitate changed into a gray phosphate product. Table 6.7 lists the chemical compositions of the phosphate products under various pH conditions. Compared with precipitate composition in Table 6.6, the contents of each constituent in the phosphate product increased. The CaO content was almost identical in each product, approximately 54 mass%. The P₂O₅ content in the product obtained at pH 12 was 26.05 mass%. When the pH decreased to 9, a

product containing 34.48 mass% of P_2O_5 was obtained. With the increase in the pH, the SiO_2 content in the phosphate product increased because of the precipitation of calcium silicate hydrogel. At pH 12, the obtained product contains 5.71 mass% of SiO_2 . The Fe_2O_3 content in each product was less than 2.0 mass%.

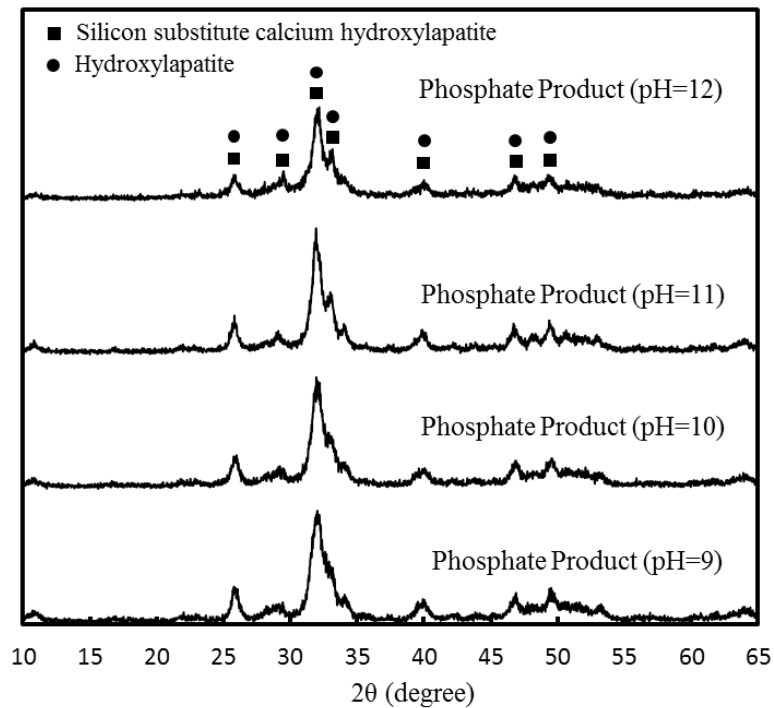


Fig. 6.9 XRD patterns of the phosphate products under various pH conditions

Figure 6.9 shows the XRD patterns of the phosphate products under various pH conditions. Similar peaks associated with hydroxylapatite (HAP) and silicon substituted calcium hydroxylapatite were observed in each product, indicating that the same substance was formed after calcination of the precipitates. As discussed above, HAP was the most stable calcium phosphate. The precipitation of phosphate from leachate depended on nucleation and growth [6]. The precipitation kinetics of DCPD was fast and DCPD precipitated instead of HAP, which

determined the P concentration in the upper solution. Through calcination, DCPD contained in the precipitate was transformed to thermodynamically stable HAP [12].

In the solubility test, as shown in Table 6.8, the phosphate product obtained at pH 11 was difficult to dissolve in water. The dissolution ratio of P was only 0.004, indicating that these P was poorly water-soluble. In the 2% citric acid solution, almost all of the phosphate product was dissolved. The dissolution ratio of P reached 0.971, indicating that these P was citrate-soluble and available in the soil. Therefore, the phosphate product obtained had a high content of citrate-soluble P_2O_5 and could be used as a fertilizer.

Table 6.8 Dissolution ratio of each element from the phosphate product obtained at pH 11 in different solutions

Element Solvent	Ca	P	Si	Fe	Mg	Na
Distilled water	0.045	0.004	0.225	0	0.170	0.158
2% citric acid	0.994	0.971	1.000	0.904	0.947	0.917

Table 6.9 Precipitation ratio of P from leachate and total recovery ratio of P from slag in this process

	Precipitation at various pH condition			
	pH=9	pH=10	pH=11	pH=12
Dissolution Ratio (pH=6)	0.769			
Precipitation Ratio	0.879	0.950	0.972	0.988
Total Recovery Ratio	0.676	0.731	0.748	0.760

The precipitation ratio of P in the leachate ($R_{\text{precipitation}}$), and the total recovery ratio of P from the modified steelmaking slag (R_{total}) via selective leaching and precipitation were calculated using Eqs. (6.6) and (6.7), where m is the mass of precipitate obtained (g), $w_{P_2O_5}$ is the mass ratio of P_2O_5 in the precipitate, M is the molar mass (g/mol), V is the volume of the original leachate (L), C_p is the P concentration in the original leachate (g/L), and $R_{\text{dissolution}}^P$ is the dissolution ratio of P from slag. As shown in Table 6.9, most of the P in the leachate was

concentrated in the precipitate after precipitation. The precipitation ratio of P in the leachate increased from 87.9% to 98.8% when the pH changed from 9 to 12. Figure 6.10 shows the change in the composition of phosphate product and the precipitation ratio of P with pH. With the increase in the pH, the precipitation ratio of P in the leachate increased, while the quality of the obtained phosphate product decreased because the P_2O_5 content in it decreased and the SiO_2 content increased. The dissolution ratio of P from the slag with 4 mass% of Na_2O was 76.9% in this case. Most of the P in the steelmaking slag was thus recovered in the form of phosphate product. The total recovery ratio of P from slag exceeded 73% when the pH exceeded 10.

$$R_{\text{precipitation}} = \frac{m \cdot w_{P_2O_5} \cdot 2M_P}{V \cdot C_P \cdot M_{P_2O_5}} \quad (6.6)$$

$$R_{\text{total}} = R_{\text{dissolution}}^P \cdot R_{\text{precipitation}} \quad (6.7)$$

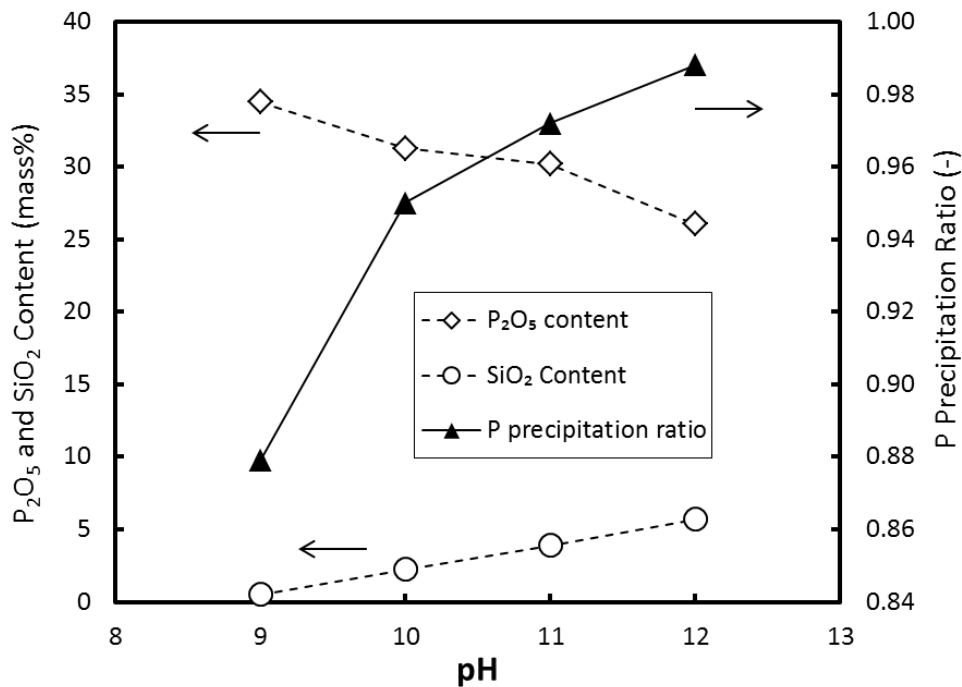


Fig. 6.10 Change in the composition of phosphate product and the precipitation ratio of P with pH

6.3 Overall process outline

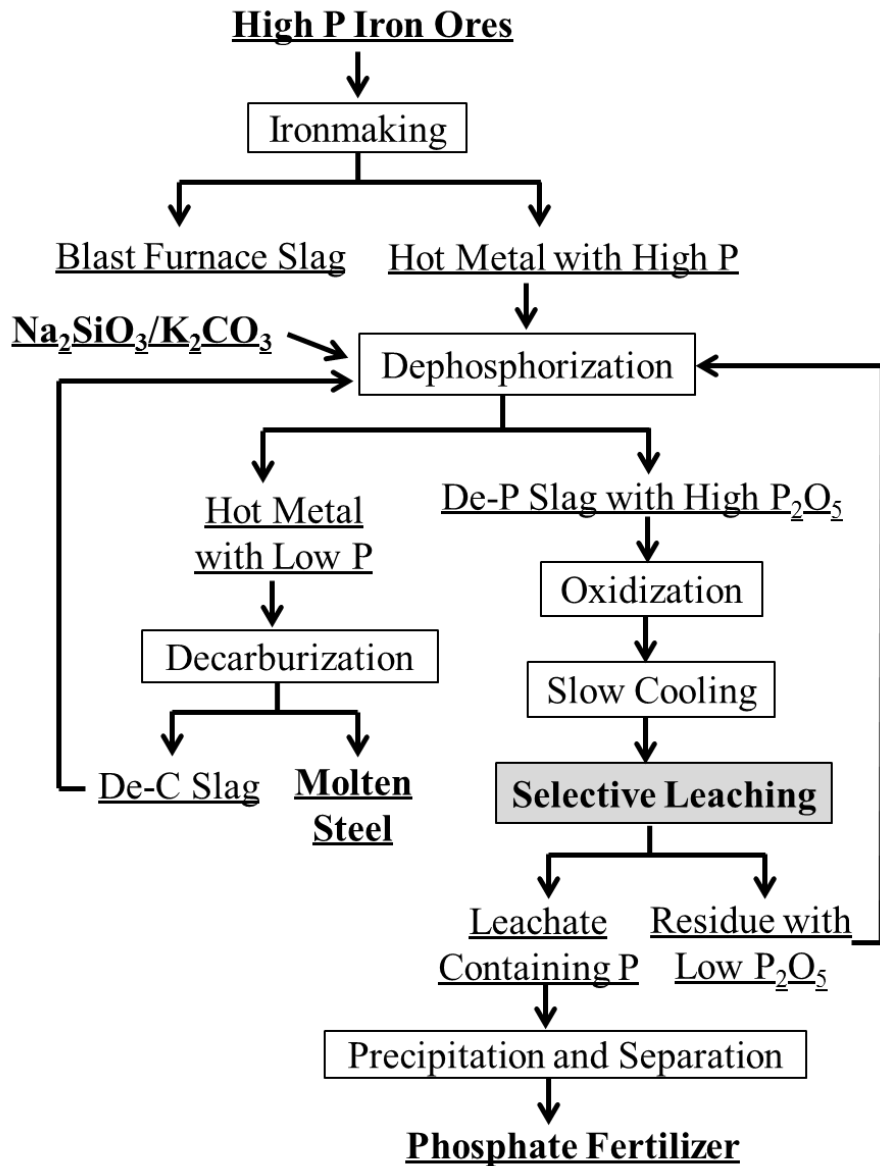


Fig. 6.11 A process for the comprehensive utilization of slag with high P_2O_5 content

In this study, a process for the comprehensive utilization of slag with high P_2O_5 content and waste-free steelmaking was proposed, which is outlined in Fig. 6.11. During a conventional ironmaking process, hot metal with high P content will be generated because of the reduction of high-P iron ores. First, it is dephosphorized in a converter. During this process, alkaline oxide (Na_2O or K_2O) is added as a flux to increase the phosphate capacity of slag [15]. Following

dephosphorization, the hot metal is decarburized with a smaller amount of slag, and molten steel is produced. The slag with high P_2O_5 content is oxidized to transform into a Fe_2O_3 -containing slag. Then, this slag was cooled slowly, and treated via selective leaching. The P in steelmaking slag is dissolved and concentrated in the leachate. The leaching residue and decarburization slag, with a lower P_2O_5 content and higher Fe_2O_3 content can be returned to the dephosphorization process. The soluble phosphate in the leachate is precipitated in the form of calcium phosphate, which can be used as a fertilizer. No extra slag is discharged during this steelmaking process.

6.4 Summary

Following selective leaching of P from slag, to recover the dissolved P in the leachate, a process for extracting phosphate product by phosphate precipitation was explored. The effects of alkaline solution and pH on the P precipitation and the composition of the obtained product were investigated. The results obtained are summarized below:

- (1) When the pH of the leachate increased by the addition of $Ca(OH)_2$ or NaOH solution, the dissolved P in the leachate precipitated, and the P concentration in the upper solution decreased to a low value. Through separation and calcination, a HAP product, which mainly consists of CaO and P_2O_5 , was obtained.
- (2) Adding $Ca(OH)_2$ or NaOH solution into the leachate had similar effects on phosphate precipitation. The P_2O_5 content in these phosphate products exceeded 28.0 mass%.
- (3) With the increase in the pH of the leachate, the precipitation ratio of P in the leachate increased, while the P_2O_5 content in the obtained phosphate product decreased and the SiO_2 content increased. Through selective leaching and precipitation, approximately 70% of the P in steelmaking slag was recovered in the form of the phosphate product in this process.

- (4) Most of the P in the obtained phosphate product was citrate-soluble and available in the soil, indicating that this phosphate product has the potential to be used as a phosphate fertilizer. On the basis of this study, a process for the comprehensive utilization of high-P iron ores, and waste-free steelmaking, was proposed.

References

1. G.K. Morse, S.W. Brett, J.A. Guy, J.N. Lester: Science of the total environment, 212 (1998), pp.69-81.
2. N.C. Bouropoulos, P.G. Koutsoukos: Journal of Crystal Growth, 213(2000), pp.381-388.
3. S. Markich, P. Brown: Environmentally-Relevant Thermochemical Data, ANSTO Environment Division, 1999.
4. W.H. Pierre, A.G. Norman: Soil and Fertilizer Phosphorous in Crop Nutrition, Academic Press, London, New York, 1953.
5. R.P. Gunawardane, F.P. Glasser: Journal of Materials Science, 14(1979), pp.2797-2810.
6. E. Valsami-Jones: Mineralogical Magazine 65(2001), pp.611-620.
7. S. Recillas, V. Rodríguez-Lugo, M.L. Montero, S. Viquez-Canoc, L. Hernandez, V.M. Castaño: Journal of Ceramic Processing Research, 13 (2012), pp. 5-10.
8. T. Futatsuka, K. Shitogiden, T. Miki, T. Nagasaka and M. Hino: ISIJ International, 44 (2004), pp. 753-761.
9. A. L. Iglesia: Estudios Geológicos, 65 (2009), pp. 109-119.
10. D.A. Kulik, M. Kersten: Journal of the American Ceramic Society, 84(2001), pp.3017-3026.
11. P.G. Koutsoukos, G.H. Nancollas: Journal of Crystal Growth, 53 (1981), pp.10-19.
12. W. Kibalczyk: Crystal Research and Technology, 24 (1989), 773-778.
13. www.maff.go.jp/j/kokuji_tuti/kokuji/pdf/k0000977.pdf. Ministry of Agriculture, Forestry and Fisheries, 2017.
14. C.S. Walker, S. Sutou, C. Oda, M. Mihara, A. Honda: Cement and Concrete Research, 79(2016), pp.1-30.
15. J.J. Park, R. J. Frunhan: Metallurgical and Materials Transactions B, 22B(1991), pp.39-46.

7 Conclusions and future works

7.1 Conclusions

In order to separate and recover P from steelmaking slag with high P_2O_5 content, selective leaching of P from slag and P precipitation in the leachate was adopted in this study. The dissolution behavior of the P-condensed solid solution and the modified slags with Na_2O or K_2O addition, the distribution of P_2O_5 and Na_2O between the solid solution and liquid phase in slag, and P recovery from the leachate via precipitation were investigated in this thesis. The conclusions of this study are as follows:

7.1.1 Conclusions of the dissolution of solid solution

To promote the dissolution of P, the effects of acid (leaching agent), Na_2SiO_3 modification, and pH on the dissolution behavior of the C_2S-C_3P sample in the aqueous solution were investigated.

Firstly, it was determined that when nitric acid was used as leaching agent, the dissolution ratio of P was not high at pH 7 because of phosphate precipitation. When oxalic acid or citric acid was used as leaching agent, Ca^{2+} ions were removed by the formation of CaC_2O_4 precipitate or $CaC_6H_5O_7^-$ complex, respectively. Phosphate precipitation in the aqueous solution was suppressed, and thus the dissolution ratio of P from the C_2S-C_3P sample increased significantly.

Secondly, when the C_2S-C_3P sample was modified by adding Na_2SiO_3 at high temperatures, the solid solution containing Na_2O was formed. A $2CaO \cdot SiO_2 - 2CaO \cdot Na_2O \cdot P_2O_5$ phase was detected by XRD analysis, which indicated that Na_2O substituted for the CaO in C_3P . By Na_2SiO_3 modification, the dissolution of P in the oxalic and citric solutions was promoted. With an increase in the Na_2SiO_3 content, the dissolution ratio of P increased. As the acid consumption to keep pH was increased by the Na_2SiO_3 modification, the solid solution of

$2\text{CaO}\cdot\text{SiO}_2\cdot 2\text{CaO}\cdot\text{Na}_2\text{O}\cdot\text{P}_2\text{O}_5$ would have better water solubility than $\text{C}_2\text{S}\cdot\text{C}_3\text{P}$. However, at pH 7, the dissolution ratio of P from the modified solid solution containing about 20 mass% of Na_2SiO_3 reached only 43.9% in the oxalic solution.

Finally, we found that as the pH decreased, the dissolution ratio of P significantly increased in the citric solution. At pH 5, the dissolution ratio of P from the modified solid solution containing about 20 mass% of Na_2SiO_3 reached 85.7%. However, in the oxalic solution, the precipitated CaC_2O_4 prevented the further dissolution of P by decreasing the pH; the dissolution ratio was not high enough to extract P from slag. Therefore, citric acid was an optimal leaching agent for extracting P from solid solution at pH 5.

7.1.2 Conclusions of the dissolution of slag with high P_2O_5 content

To achieve selective leaching of P from slag with high P_2O_5 content, the effects of the cooling rate of molten slag, Na_2O or K_2O content, pH, and the valency of Fe in slag on the dissolution behavior of the modified slag were investigated.

Firstly, it was found that decreasing cooling rate promoted the enrichment of P_2O_5 in the solid solution and the formation of magnesioferrite phase. Compared to the quenched slag, the furnace-cooled slag exhibited a higher dissolution ratio of P and a lower dissolution ratio of Fe, indicating that slow cooling was beneficial for selective leaching of solid solution from the modified slag.

Secondly, with the increase in the Na_2O or K_2O content in slag, the mass fraction of the solid solution in slag increased. Na_2O and K_2O addition had the same effect on promoting dissolution of the solid solution from slag, and thus higher dissolution ratios of Ca, Si, and P was obtained. A further addition of Na_2O or K_2O resulted in a higher dissolution ratio of P at pH 6. When the

Na₂O or K₂O content in slag exceeded 4 mass%, the majority of the solid solution was dissolved, and other phases remained in the residue, showing a better selective leaching of P.

As the pH decreased, the dissolution of the modified slag was promoted, resulting in higher dissolution ratios of each element. At pH 7, further increase in the K₂O content in slag did not significantly increase the dissolution ratio of P because of phosphate precipitation. The dissolution ratio of P increased significantly when the pH decreased from 7 to 5. Further decrease in the pH caused little improvement in P dissolution, and resulted in dissolution of large amounts of Fe. When the pH was controlled between 5 and 6, most of the solid solution was dissolved without a large dissolution of other phases.

The P₂O₅ content in the solid solution of the slag containing Fe₂O₃ was higher compared to that of the slag containing FeO, while the mass fraction of solid solution was lower. When the FeO in the slag changed to Fe₂O₃, the dissolution ratio of P increased significantly at pH 6, and the dissolution of Si and Fe was suppressed. Oxidizing slag was necessary to achieve selective leaching of P from the modified slag.

Finally, after leaching, the P₂O₅ content in the residue decreased compared to the original slag, and the Fe₂O₃ content increased correspondingly. Increasing the Na₂O or K₂O content in the slag and decreasing the pH could further decrease the P₂O₅ content in the residue. Due to the dissolution and separation of the P-concentrated phase from slag, the residue had the potential for recycling within the ironmaking and steelmaking process.

7.1.3 Conclusions of the distribution of P₂O₅ and Na₂O

To increase the efficiency of dephosphorization and to recover P from dephosphorization slag by selective leaching, it is necessary to determine the distribution ratios of Na₂O and P₂O₅ between the solid solution and liquid phase in slags with high P₂O₅ content. In this study, the

change in composition and mass fraction of the solid solution with slag composition were investigated.

Firstly, a linear relationship was found between the distribution ratio of P_2O_5 and the Na_2O content in slag; the relationship was independent of P_2O_5 content. Further addition of Na_2O did not enrich Na_2O in the solid solution, because the Na_2O content in the solid solution became constant, and a new $2CaO \cdot SiO_2 \cdot 2CaO \cdot Na_2O \cdot P_2O_5$ solid solution formed. With the increase in P_2O_5 content in slag, the P_2O_5 content in the solid solution also increased. Na_2O addition decreased the P_2O_5 content in the solid solution, while it increased the mass fraction of solid solution in slag, which facilitated P_2O_5 enrichment.

Secondly, it was determined that the distribution ratios of P_2O_5 and Na_2O both increased with increasing the Fe_2O_3 content in the liquid phase. In the case of high Fe_2O_3 content, a P_2O_5 -condensed solid solution was formed. With the increase in slag basicity, the distribution ratio of P_2O_5 increased significantly, while that of Na_2O decreased. A higher basicity resulted in a larger mass fraction of the solid solution in slag.

Finally, the activity coefficient of P_2O_5 in the liquid phase was calculated using regular solution model. It was determined that the activity coefficient of P_2O_5 in the solid solution increased with the P_2O_5 content in the solid solution, which was independent of the Na_2O content in slag.

7.1.4 Conclusions of P recovery from the leachate

Following selective leaching of P from slag, a process for extracting phosphate product in the leachate by phosphate precipitation was explored. The effects of alkaline solution and pH on the P precipitation and the composition of the obtained product were investigated.

Firstly, it was found that when the pH of the leachate increased by the addition of $Ca(OH)_2$ or NaOH solution, the dissolved P in the leachate precipitated, and the P concentration in the upper

solution decreased to a low value. Through separation and calcination, a HAP product, which mainly consists of CaO and P₂O₅, was obtained.

Secondly, adding Ca(OH)₂ or NaOH solution into the leachate had similar effects on phosphate precipitation. The P₂O₅ content in these phosphate products exceeded 28.0 mass%. With the increase in the pH of the leachate, the precipitation ratio of P in the leachate increased, while the P₂O₅ content in the obtained phosphate product decreased and the SiO₂ content increased.

Finally, it was determined that through selective leaching and precipitation, approximately 70% of the P in steelmaking slag was recovered in the form of the phosphate product in this process. Most of the P in the obtained phosphate product was citrate-soluble and available in the soil, indicating that this phosphate product has the potential to be used as a phosphate fertilizer. On the basis of this study, a process for the comprehensive utilization of high-P iron ores, and waste-free steelmaking, was proposed.

7.2 Future works

(1) Efficient dephosphorization of hot metal with high P content

In the case of the hot metal with high P content, a highly efficient dephosphorization process with less slag was essential to meet the demand for low P steel and to ease the environmental burden. This is also the key point of utilization of high-P iron ore. It has been reported Na₂O addition to steelmaking slag significantly increased the distribution ratio of P between the slag and hot metal and the phosphate capacity of slag. However, they did not consider the existence of C₂S-C₃P solid solution in steelmaking slag. Therefore, in the case of Na₂O addition, it was necessary to investigate the distribution ratio of P between hot metal, liquid phase, and solid solution in steelmaking slag. Meanwhile, we also need to

promote the enrichment of P_2O_5 in the solid solution, which was beneficial for the selective leaching of P from slag.

(2) Effect of slag composition on dissolution of P from slag

In this thesis, we had determined that effects of treatment condition of slag, leaching condition, and modification on the dissolution behavior of P from steelmaking slag. To determine whether selective leaching can be achieved in a wide range of slag composition, it was necessary to study the effect of slag composition on the dissolution behavior of P under the above mentioned conditions. It is well known that the Fe_2O_3 content and slag basicity has a significant influence on the dephosphorization of hot metal; the P_2O_5 content in slag varied with the dephosphorization process and the P content in hot metal. Consequently, the effects of the P_2O_5 content, the Fe_2O_3 content, and slag basicity on the dissolution behavior of the modified slag should be further investigated.

In addition, we will also investigate the saturation concentration of P in the aqueous solution and obtain the optimum mass ratio of slag to water during leaching.

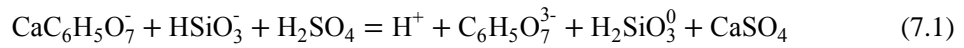
(3) Dissolution kinetics of slag

To enhance productivity, the dissolution kinetics of slag is necessary to be investigated systematically. The effects of particle size, temperature, and stirring intensity on the dissolution behavior of slag will be studied.

(4) Treatment of the leachate after P separation and Re-produce of acid

To recover P by precipitation, the pH of the leachate was increased to a high level. After P precipitation and separation, how to deal with these upper solutions with high pH will be a problem. In addition, organic acid (citric acid) was used as a leaching agent in this process. Because its price is high, we should consider how to re-produce and recycle them to reduce production cost. The upper solution mainly consists of Ca, Si, Na, and citrate ions. Sulfuric

acid (H_2SO_4) is an important by-product in industry. If sulfuric acid is added to the upper solution, the following reactions (7.1) are possible to occur:



The added H^+ from sulfuric acid will substitute for the Ca in the citrate complex ($\text{CaC}_6\text{H}_5\text{O}_7^-$), and the insoluble Ca_5O_4 will precipitate. After filtration, this solution is condensed by using the exhaust heat in iron and steel industry, and thus a citric acid solution is produced and it can be used as the leaching agent to dissolve slag. Therefore, it is necessary to explore this kind of process to recycle organic acid during P recovery from steelmaking slag.

Achievements

Peer Reviewed Paper and Proceeding:

1. **C. Du**, X. Gao, S. J. Kim, S. Ueda and S. Kitamura, "Effects of acid and Na_2SiO_3 modification on the dissolution behavior of $2\text{CaO}\cdot\text{SiO}_2\text{-}3\text{CaO}\cdot\text{P}_2\text{O}_5$ solid solution in aqueous solutions", *ISIJ International*, 56 (2016), 1436-1444.
2. **C. Du**, X. Gao, S. Ueda and S. Kitamura, "Effects of cooling rate and acid on extracting soluble phosphorus from slag with high P_2O_5 content by selective leaching", *ISIJ International*, 57 (2017), 487-496.
3. **C. Du**, X. Gao, S. Ueda and S. Kitamura, "Effect of Na_2O addition on phosphorus dissolution from steelmaking slag with high P_2O_5 content", *Journal of Sustainable Metallurgy*, 3 (2017), 671-682.
4. **C. Du**, X. Gao, S. Ueda and S. Kitamura, "Distribution of P_2O_5 and Na_2O between solid solution and liquid phase in the $\text{CaO-SiO}_2\text{-Fe}_2\text{O}_3\text{-P}_2\text{O}_5\text{-Na}_2\text{O}$ slag system with high P_2O_5 content", *Metallurgical and Materials Transactions B*, 2017, published online.
5. **C. Du**, X. Gao, S. Ueda and S. Kitamura, "Recovery of phosphorus from modified steelmaking slag with high P_2O_5 content via leaching and precipitation", *ISIJ International*, 58 (2018), accepted.
6. **C. Du**, X. Gao, S. Ueda and S. Kitamura, "Optimum Conditions for Phosphorus Recovery from Steelmaking Slag with High P_2O_5 Content by Selective Leaching", *ISIJ International*, 58 (2018), accepted.

7. T. Iwama, **C. Du**, X. Gao, S. J. Kim. S. Ueda and S. Kitamura, “Extraction of phosphorus from steelmaking slag by selective leaching using citric acid”, *ISIJ International*, 2017, submitted.
8. **C. Du**, X. Gao, S. J. Kim. S. Ueda and S. Kitamura, “Improving the dissolution of phosphorus from $2\text{CaO}\cdot\text{SiO}_2\text{-}3\text{CaO}\cdot\text{P}_2\text{O}_5$ solid solution in aqueous solutions”, *Proceedings of The 10th International Conference on Molten Slags, Fluxes and Salts*, Seattle, USA, 2016, 909-916.
9. X. Gao, **C. Du**, M. Numata, T. Iwama, S. Kim, S. Ueda and S. Kitamura, “Separation of phosphorus from synthetic steelmaking slag by selective leaching”, *Proceedings of 1st International Conference on Energy and Material Efficiency and CO₂ Reduction in the Steel Industry*, Kobe, Japan, 2017, 158-161.

Engineering Report:

1. 杜传明, 高旭, 植田滋, 北村信也, 高リン酸含有製鋼スラグからのリンの選択浸出, 日本學術振興會製鋼第 19 委員會, 19 委-12826, 反応プロセスVII-117, 京都, 日本, 2016.10.

International Conference:

1. **C. Du**, X. Gao, S. J. Kim. S. Ueda and S. Kitamura, Improving the dissolution of phosphorus from $2\text{CaO}\cdot\text{SiO}_2\text{-}3\text{CaO}\cdot\text{P}_2\text{O}_5$ solid solution in aqueous solutions, *Molten 2016*, (Seattle, USA, 2016/5).

2. **C. Du**, X. Gao, S. J. Kim, S. Ueda and S. Kitamura, Extraction of phosphorus from steelmaking slag made by high phosphorus iron ore using leaching technology, *Melbourne-Tohoku Symposium on Advanced Materials*, (IMRAM, Sendai, Japan, 2016/9).
3. X. Gao, **C. Du**, M. Numata, T. Iwama, S. Kim, S. Ueda, S. Kitamura, Separation of phosphorus from synthetic steelmaking slag by selective leaching, *EMECR 2017*, (Kobe, Japan, 2017/10).
4. T. Iwama, X. Gao, **C. Du**, S. Kim, S. Ueda, S. Kitamura, Selective leaching of phosphorus from steelmaking slag by citric acid, *EUROMAT 2017*, (Thessaloniki, Greece, 2017/9).

Domestic Conference (in Japan):

1. **C. Du**, X. Gao, S. J. Kim, S. Ueda and S. Kitamura, Effect of Na_2SiO_3 modification and acid on the dissolution behavior of $2\text{CaO}\cdot\text{SiO}_2\cdot 3\text{CaO}\cdot\text{P}_2\text{O}_5$ solid solution in aqueous solution, 日本鉄鋼協会第 170 会秋季講演大会, (福岡, 2015.9)
2. **C. Du**, X. Gao, S. Ueda and S. Kitamura, Improving the dissolution of phosphorus from $2\text{CaO}\cdot\text{SiO}_2\cdot 3\text{CaO}\cdot\text{P}_2\text{O}_5$ solid solution in aqueous solution, 第 15 回多元物質科学研究所研究発表会, (仙台, 2015.12)
3. **C. Du**, X. Gao, S. Ueda and S. Kitamura, Improving the dissolution of phosphorus from $2\text{CaO}\cdot\text{SiO}_2\cdot 3\text{CaO}\cdot\text{P}_2\text{O}_5$ solid solution in aqueous solution, 日本鉄鋼協会第 171 会春季講演大会, (東京, 2016.3)
4. **C. Du**, X. Gao, S. Ueda and S. Kitamura, Effect of acid and pH on phosphorus recovery from the slag with high P_2O_5 content by selective leaching, 日本鉄鋼協会第 172 会秋季講演大会, (大阪, 2016.9)

5. **C. Du**, X. Gao, S. Ueda and S. Kitamura, Effect of Na₂O addition on phosphorus dissolution from steelmaking slag with high P₂O₅ content by leaching, 日本鉄鋼協会第 173 会春季講演大会, (東京, 2017.3)
6. **C. Du**, X. Gao, S. Ueda and S. Kitamura, Effect of Na₂O on the distribution of P₂O₅ between solid solution and liquid phase in slag with high P₂O₅ content, 日本鉄鋼協会第 174 会秋季講演大会, (札幌, 2017.9)
7. **C. Du**, X. Gao, S. Ueda and S. Kitamura, Recovery of phosphorus from steelmaking slag with high P₂O₅ content by K₂O modification, 日本鉄鋼協会第 175 会春季講演大会, (千葉, 2018.3) 予定

Academic Award:

1. 多元物質科学研究奨励賞 受賞 仙台, 日本 2015 年 12 月
2. 科学計測振興基金 受賞 仙台, 日本 2017 年 12 月

Acknowledgement

First and foremost, I would like to express the deepest appreciation to my supervisor, Professor Shin-ya Kitamura, for his constant encouragement, guidance, and help. He has always been a great inspiration and motivator for me. Without his creative ideas, patient instruction, and insightful advice, the completion of my study and this thesis would not have been possible.

I would like to express appreciation to Associate Professor Shigeru Ueda, Assistant Professor Xu Gao and Assistant Professor Sun-joong Kim (Chosun University) for their patient supervision and support during the span of this research. They are very experienced professors, who taught me various experimental methods, which are essential for my study. Thanks to their great help, I could finish this study successfully.

I would like to thank Professor Tetsuya Nagasaka, Professor Hongmin Zhu, and Professor Hiroyuki Shibata to become the committee in my oral dissertations. Through discussions, I could review my research results thoroughly from various points of view, and hence, my thesis has been greatly improved.

Especially, I would like to express a deep appreciation to Ministry of Education, Culture, Sports, Science and Technology, Japan (MEXT) for funding me to finish my doctoral course. Many thanks also to China Scholarship Council.

Extended gratitude is also addressed to the rest of staffs and members in Kitamura laboratory; Jiang Liu, Junpei Suzuki, Masaaki Kageyama, Ryoustake Sasaki, Motomi Yagi, Hiroki Yoshida, Dongjun Shin, Takayuki Iwama, Shouhei Koizumi, Kengo Sugiyama, Masanori Tanno, Shinsuke Oku, Zuoqiao Zhu, Akihiro Hatayama, Isshi Hosoi, Chunyang Liu, Lichun Zheng, Ryo Yamashina, Satoshi Nakagawa, Yosuke Baba, Megumi Obara, Hiroyuki Hashimoto for direct or indirect helps during my research and daily life. Meanwhile, I would like to thank Takumi Akiyama, Takashi Kamaya, Masaya Hino, and Yuki Dohi for helping me analyze experimental samples.

I also extend my gratitude to my previous supervisor, Professor Jingkun Yu at Northeastern University. Without his encouragement and support, I would not study for a doctorate and have a chance to study abroad. I will be forever thankful.

Finally, I would like to thank my parents and my sister, for their love, selfless support and encouragement to finish my studies. I also thank my girlfriend Jiangnan Xu, for accompanying me to go through this difficult period.